2020

Lab-scale bioremediation technology: the development of environmental biotechnology for the ex situ bioremediation of cadmium-contaminated freshwater

Jebril, Nadia

.

UNIVERSITY OF
PLYMOUTH

Lab-scale bioremediation technology: the development of environmental biotechnology for the *ex situ* bioremediation of cadmium-contaminated freshwater

By

Nadia Mahmoud Tawfiq Jebril

A thesis submitted to the University of Plymouth in partial fulfilment for the degree of

DOCTOR OF PHILOSOPHY

School of Biological and Marine Sciences

August 2020

Grant Statement

The research work disclosed in this thesis was funded by the Ministry of Higher Education and Scientific Research, Iraq (2014).

Lab-scale bioremediation technology: the development of environmental biotechnology for the *ex situ* bioremediation of cadmium-contaminated freshwater

Nadia Jebril

Cadmium (Cd) is one of the most common contaminates in freshwater. Among freshwater remediation techniques, bioremediation – the use of bacteria to extract Cd from water – is an eco-friendly technique. Cd-resistant bacteria evolve in the natural environment and can be used to develop a bioremediation process for Cd. However, gaining an adaptive strain is usually difficult. This research aimed to find an alternative bioremediation process for Cd from freshwater using Cd-resistant bacteria. To increase the Cd-resistance of the isolated *Brevibacillus agri* C15, UV-light mutagenesis was used to generate the mutant *B. agri* C15 Cd^R with a minimum inhibitory concentration (MIC) of 21 ± 0.4 mM Cd, which was approximately 0.25 – fold higher than that of the wild type *B. agri* C15 (MIC:16 ± 0.7 mM Cd). Laboratory bench-scale column reactors were operated for 28 days to investigate the effectiveness of the mutant *B. agri* C15 Cd^R entrapped in calcium alginate gel, as a bioremediation process for Cd from artificial groundwater (AGW) at different Cd concentrations (4.4, 8.8, 13.4 and 17.4 μM). A new process for the purpose of attaining high Cd removal rates from AGW was achieved using the mutant in this study. Scanning electron microscopy (SEM) observations enabled a detailed description of the beads, and the detection of Cd within the beads supported the Cd accumulation mechanism using a dithizone histochemical method. The interactions of Cd, cation/anion, and humic acid competing for ion exchange sites on Ca-alginate beads containing the mutant cells in addition to the effect of pH were investigated. The efficient removal of Cd was achieved from AGW at pH 4.00. The constituents were found to hinder Cd uptake due to the formation of Cd complexes. The preferential removal of Cd using the mutant from AGW (pH 4.00 and 7.50), as well as from natural river water (NRW, Walkham River), reflects its ability to remove Cd from freshwater in general. The hazard classification and risk assessment of the products of this study's new bioremediation process was not hazardous substances and did not represent a risk to humans. From a biotechnology standpoint, this thesis presents new prospects for this maintainable water bioremediation technique and the knowledge assembled in this study may provide a basis for the development of other bacteria for metal remediation and for further research in investigating and applying this technique.

Acknowledgements

It is a great pleasure to express my profound gratitude to Dr Rich Boden, Associate Professor, School of Biological and Marine Sciences, Faculty of Science and Engineering, and Dr Charlotte Braungardt, Associate Professor, School of Geography, Earth and Environmental Sciences, Faculty of Science and Engineering, the University of Plymouth for their guidance, valuable help, and consistent inspiration throughout this research. I would also like to express my gratitude to the Ministry of Higher Education and Scientific Research, Iraq, for sponsoring me for the PhD programme at Plymouth University. I give special thanks to the Cultural Attaché/Iraqi Embassy in London, for their unflinching cooperation during my study. I am also thankful to Matthew Emery, Senior Microbiology Technician, and Sarah Jamieson, Microbiology Media Technician, School of Biological and Marine Sciences, for their microbiological assistance and friendly suggestions. I wish to express my appreciation to Dr Andrew Fisher, Dr Rob Clough, and Dr Alex Taylor, School of Geography, Earth and Environmental Sciences, for providing me with the ICP facility. Many thanks to Dr Joceline Triner, Senior Technician (Histology and Microscopy), School of Biological and Marine Sciences, for her provision of histology facilities. I am grateful to the team at the Plymouth Electron Microscopy Centre (PEMC). I would like to especially thank Dr Roy Moate, Mr Peter Bond, and Mr Glenn Harper for providing the scanning electron microscope and transmission electron microscope facilities.

Finally, I give special thanks to who helped me, my children, Hind, Mazin, and Haitham, for their support during the time I have studied for my PhD programme.

Author's Declaration

At no time during the registration for the degree of Doctor of Philosophy has the author been registered for any other University award without prior agreement of the Doctoral College Quality Sub-Committee.

Work submitted for this research degree at the University of Plymouth has not formed part of any other degree either at the University of Plymouth or at another establishment.

This study was financed through a scholarship from the Ministry of Higher Education and Scientific Research, Iraq (2014).

Nadia Mahmoud Jebril confirms that the studies presented in this thesis were her work except for the 16S rRNA analysis; Rich Boden also carried out the phylogenetic tree for the work in Chapter Three.

Presentation and conferences attended

- Jebril, N, Boden, R, and Braungardt, C. (2018). Bioremediation of cadmium for protecting human health, and ecosystem. Third Scientific Conference (Degradation of the Environment in Iraq, and its Impact on Public Health). The Iraqi Environment and Health Society, London-UK.
- Jebril, N, Boden, R, and Braungardt, C. (2017). *In situ* bioremediation simulation for cadmium contaminated artificial groundwater using a bed reactor. 9th Annual Biogeochemistry Conference, School of Geography, Earth, and Environmental Sciences, Plymouth University, Plymouth, UK.
- Jebril, N, Boden, R, and Braungardt, C. (2017). Heavy metal biogeochemistry, and removal by microbial biotechnology, Second Annual Conference on Environ Pollut in Iraq. The Iraqi Environment, and Health Society, London-UK.

- Jebril, N, Boden, R, and Braungardt, C. (2017). Microbial contamination of Iraqi water resources, and their effects on social health. Second Annual Conference on Environ Pollut in Iraq. The Iraqi Environment, and Health Society, London-UK.
- Jebril, N, Boden, R, and Braungardt, C. (2016). Elemental analysis of metal contaminated soils using ICP-MS, XRF techniques, and CHNS analyser, 8th Annual Biogeochemistry Conference, School of Geography, Earth, and Environmental Sciences, Plymouth University, Plymouth, UK.
- Jebril, N, Boden, R, and Braungardt, C. (2017). Heavy metal biogeochemistry and removal by microbial biotechnology. School of Biological and Marine Sciences Poster Presentation and Networking Event. Plymouth University, Plymouth, UK.

Word count of the thesis: 79,694

Signed: Nadia Jebril

Date: August 2020

Table of Contents

List of Figures

List of Tables

List of Abbreviations

Abbreviation	Glossary
AGW	Artificial groundwater
ATSDR	Agency for toxic substances and disease registry
ATP	Adenosine triphosphate
ABC	ATP-binding cassettes
CPx	Cysteine-proline-xsequence
CDF	Cation-diffusion facilitator
CFU	Colony-forming unit
CRM	Certificated reference material
ddH_2O	Deionised water
DOC	Dissolved organic carbon
DNA	Deoxyribonucleic acid
EBS	E-Basal salts
EDTA-Na_2	Ethylene Diamine Tetraacetic Acid Di-Sodium
EPS	Extracellular polymeric substances
GSH	Glutamyl L-cysteinyl glycine
HRT	Hydraulic residence time
ICP-MS	ICP-MS Inductively coupled plasma – mass spectrometry
ICP-OES	ICP-OES Inductively coupled plasma – optical emission spectrometry
K_{sp}	Constant stability
M	Molar
MIC	Minimum inhibitory concentration
NRAMP	Natural resistance-associated macrophage protein
NRW	Natural river water
OD_x	Optical density
R2A	Reasoner's 2A

RND	Resistance-nodulation-cell division
ROS	Reactive oxygen species
PBS	Phosphate buffered saline
p*K*a	Acid dissociation constants
PolyP	Polyphosphate
P*β*HB	Poly-*β*-hydroxybutyrate
SEM	Scanning electron microscopy
TEM	Transmission electron microscopy
US EPA	United State Environmental Protection Agency
UV	Ultraviolet
WHO	World health organisation

Chapter 1. General Introduction

1-1 Introduction

Human and industrial activities have led to a marked increase in the level of Cd in the environment across the globe. The estimated global average level of Cd in uncontaminated soil is 0.36 mg/kg, in soil water is 5 μg/L and in unpolluted groundwater less than 1 μg/L (Kubier *et al*., 2019). Cadmium groundwater contamination is a widespread problem that causes severe environmental and health concerns. An average Cd level of 0.2 μg/L was determined in Irish groundwater (Tedd *et al*., 2017). Nokes and Weaver (2014) reported that health risks are associated with Cd in groundwater. Therefore, Cd is listed as a priority hazardous substance in the European Water Framework Directive (2000). Thus, Cd treatment is needed for water and more effective methods. Water treatment through physical, chemical, and biological techniques is an important aspect of water cleansing, and many studies have been undertaken to identify and develop treatment technologies.

1-1-1 Groundwater

Most of the water on the Earth's surface is saline (96.5%) and is present in oceans, glaciers, and ice caps, the remainder being freshwater (3.5%). Saline waters are unusable by humans, while the usable water comes from freshwater resources such as groundwater, lakes, and rivers. Groundwater represents 99% of the Earth's freshwater US Geological Survey (US GS, 2011) and is a significant source of drinking water for humans, who require at least 2 litres of water per day.

Groundwater is considered an essential stage in the hydrologic cycle, formed where surface water leaks into the subsurface, into vast reservoirs of water in aquifers and subterranean rivers. In its natural state, the quality of groundwater is high, being almost free from pathogens and water were drawn from uncontaminated aquifers does not usually require complex treatment. However, pollution present in the soil or the

catchment of an aquifer, in general, can be transferred into the groundwater (UK Groundwater Forum, 2011). The importance of groundwater to human endeavour can be illustrated with some examples: In England and Wales, one-third of the domestic water supplies (2,400 million L per year) comes from groundwater (Holman *et al*., 2010) and in the Middle East, groundwater is a significant source of domestic supplies owing to having just two rivers, Tigris (Turkey and Iraq) and Euphrates (Turkey, Syria, and Iraq). The geochemistry of groundwater varies depending on the local mineralogy present above and throughout the aquifer, the contact time of groundwater with the rock holding the water, and the local biogeochemical processes. Usually, groundwater is high in calcium, magnesium, bicarbonates, calcium chlorides, and magnesium sulphates, contributing to its alkalinity, making it 'hard' (Boyd, 2020). This hardness is, for example, due to the biological process of the organic matter, which is present in the soil zone, producing carbon dioxide, which leads to the formation of carbonic acid and biocarbonate ion:

$CO_2 + H_2O \rightleftharpoons H_2CO_3 \rightleftharpoons H^+ + HCO_3$, which gives a pH of groundwater between 6.0 and 8.5 (Van Nguyen *et al*., 2020).

Additionally, the occurrences of minor ions such as: borate, nitrate, potassium, strontium, fluoride, iron, and trace ions such as: aluminium, cadmium, arsenic, barium, chromium, copper, lead, manganese, lithium, phosphate, selenium, silver, uranium and zinc dissolved in groundwater at concentrations below 0.1 mg/L, contribute to the minerals content of groundwater. Elevated metal contents in groundwater are generally linked to the abundance of clay minerals, organic matter, carbonates, and hydrous oxides, as well as physicochemical conditions, such as pH, and/or anoxic conditions. For example, differences in arsenic concentration in groundwater were previously documented because of constant redox conditions (Du Laing *et al*., 2009).

It was found that the metal mobility increased with the decrease of groundwater pH (due to seasonal change in pH or pollution), while the hardness and salinity cause the immobilisation metals (Mulligan *et al*., 2001). For instance, high pH in the soil immobilises Cd, thus forming $CdCO_3$ and Cd $(OH)_2$ precipitate (Liang *et al*., 2014).

1-1-2 Groundwater contamination

Pollution is defined as the condition in which substances that are not normally found or where they occur are above the natural background levels that lead to pollution, causing damage to living resources and risks to human health (Chapman and Anderson, 2005). Population increase, urbanisation, industrialisation, and agricultural activities have led to the deterioration of the quality and the chemistry of groundwater in many areas of the world. While undoubtfully important, assessment and monitoring of aquifer parameters can be expensive, and therefore numerical methods are increasingly applied to groundwater quantity, movement, and quality (Batu, 2005). For example, different models can be used to predict element concentrations in water systems. Recently, Locatelli *et al*. (2019) have estimated the risk to groundwater by modelling the fate of contaminants and their transport. Rader *et al*. (2019) used the tableau-input coupled kinetic equilibrium transport–unit world model (TICKET–UWM) for evaluating of copper in surface water. A study performed by Ramachandran *et al*. (2018) to assess the environmental impact on groundwater, using Piper's diagram and Gibbs plot, showed that the interaction between rock, water, and the anthropogenic activity were the most critical processes that controlled groundwater chemistry.

Notably, due to human activities, approximately two-thirds of groundwater bodies in England and one-third of those in Wales are at risk due to pollution from nitrate and other pollutants, such as phosphate, oil, pesticides, solvents, and cadmium (Zhang and Hiscock, 2011). High concentrations of nitrate, fluoride, and arsenic have

increased groundwater risk in India and Bangladesh (Alagumuthu and Rajan, 2008). Globally, most groundwater is contaminated with some elements, which can affect human health and the overall health of the ecosystem. For example, groundwater contamination in 59 out of 64 regions in Bangladesh has been reported with 300 µg/L of arsenic (Chakraborti *et al*., 2010) exceeded the maximum recommended concentration for As in drinking water (10 µg/L, World Health Organisation- International Agency for Research on Cancer (WHO-IARC, 2004).

1-1-3 Contamination and human health

Arsenic is commonly used in the manufacturing of herbicides, insecticides, fungicides, and insecticides, which increases its level in the environment. US EPA (2018) reported that wood treatment with arsenic was estimated to release 48.9 million metric tons in 2015. In addition to the agricultural arsenic applications, arsenic has also been used in veterinary medicine to eradicate tapeworms in sheep and livestock and the medical field in the treatment of syphilis, trypanosomiasis, amoebic and dysentery. Furthermore, the Food and Drug Administration (FDA) recently stated that arsenic trioxide might be used in the treatment of acute leukemia in localised cells. These applications have increased the concentrations of arsenic to 5 mg/kg in soil, 10 µg/L in surface and groundwater, and between 1–2 µg/L in seawater (Ghosh *et al*., 2018). Lead is commonly used in many applications such as industrial, agricultural, and domestic products and processes. Lead-acid batteries were estimated to account for 83% of the 152,000 metric tons of lead used in various industries in the United States in 2004. The assessment of metals in the UK recorded that the annual mean concentrations of lead emission in rural locations reached 7.58 ng/mL in 2003 and more contamination of lead (102.88 ng/mL) was recorded in an industrial location, Brookside Bilston Lane (Ireland *et al*., 2006).

Mercury is used in the manufacture of fungicides, batteries, thermostats, and dental amalgams. In Iraq, the use of treated wheat with methyl mercury as a fungicide in 1955 caused poisoning to livestock and humans a dire consequence, which is referred to as the Iraq poison grain disaster (Al-Damluji, 1976). Because of this, the agricultural demand for mercury began to decline after this disaster suddenly. However, the total mercury consumption by industrial sectors such as artisanal gold mining, vinyl chloride monomer production, batteries, lamps was increased from 3000 metric tonnes in 2005 to 6027 metric tonnes in 2015 in which East and Southeast Asia were the highest consumers of mercury with 2882 metric tonnes (United Nations Environment Programme [UNEP], 2017). In water, the dominant form of mercury is methylmercury (MeHg). This strong neurotoxin bioaccumulates easily in the food chain and poses a major risk to human health, primarily through fish consumption (Morway *et al*., 2017).

1-1-4 Cadmium chemistry and geochemistry

Cadmium is a post-transition metal of the d-block, with an atomic number of 48 and a relative atomic mass of 122.411 g/mol. Under surface environmental conditions (temperature, pressure, redox), its chemistry is dominated by the Cd (II) oxidation state, and Cd (I) is sometimes also observed (Corbett *et al*., 1961). Redox potential (*E*h) does not affect the solubility of Cd directly, as Cd (II) is the stable oxidation state, Cd mobility is indirectly related to the redox conditions when forms redox-sensitive aqueous complexes. The impact of *E*h changes on Cd reduction or oxidation in natural environments has not been observed (Rinklebe *et al*., 2016). Depending on the composition of the groundwater, free Cd^{2+} comprises 55 % to 90 % of the total soluble Cd, while the remaining forms of Cd are inorganic complexes (Wilkin, 2007).

In the Earth's crust, Cd occurs in association with zinc minerals, mostly in sphalerite (ZnS) in the form of greenockite (CdS), owing to their similar electron configuration

(Clark *et al*., 2001). Production figures for Cd vary between years in the range of 20,000 to 28,000 metric tons. For example, the US GS (2019) estimated 23,520 metric tons of Cd were produced in 2017 by China (the top producer), South Korea, Japan, Canada, Mexico, Kazakhstan, Russia, Peru, Netherlands, and Poland. The British Geological Survey reported that more than 26,500 metric tons of Cd were produced in 2016 by the countries listed above and in addition: Bulgaria, Germany, Norway, Turkey, USA, Argentina, Brazil, and India (Brown *et al*., 2018). Secondary Cd minerals include cadmoselite (CdSe), cadmium metacinnabar (Hg, Cd)S), monteponite (CdO), and otavite ($CdCO_3$), which are rare and not used commercially (Clark *et al*., 2001). These natural forms of Cd in the Earth's crust have an average of 890 nmol/kg (Tchounwou *et al.*, 2012). In anaerobic environments, anaerobic, sulfate-reducing microorganisms (SRM) contribute in the biogeochemical cycling of Cd, forming CdS:

$Cd^{2+} + H_2S \rightarrow CdS + 2H^+$

These microorganisms use sulfate as their terminal electron acceptor, producing hydrogen sulfide (Pagnanelli *et al*., 2010). In addition to SRM, *Geobacillus* species may also immobilise Cd to carbonate precipitation ($CdCO_3$) at pH ≥7 (Hetzer *et al*., 2006).

CdS and CdSe are also chemically produced from mined greenockite and used as CdS and Cd_2SSe for the production of pigments for use in inks, paints, and plastics. Such pigments are becoming a human health concern in common household products, as high levels of cadmium have been found in paints on enamel drinking glasses, ceramics, and children’s toys (Turner, 2019). Cd has wide-ranging applications in the production of nickel-cadmium batteries, plating metals, and as a neutron absorber in nuclear reactors (Scoullos *et al.*, 2012). Rechargeable, nickel-cadmium batteries contribute to 85% of the total cadmium consumption

globally; however, the use of Cd has risen with the increase of the expenditure on coatings, pigments, stabilisers, alloys and electronic compounds (Agency for Toxic Substances and Disease Registry [ATSDR], 2012). Like all metals, Cd cannot be degraded biologically after being released into the environment. Cadmium-containing mining waste, products, and compounds have to be recycled or treated before safe storage or disposal into the environment. The majority of waste Cd is found in coal ash, cement production waste, and sewage sludge (Scoullos *et al*., 2012). For example, in the 1980s, Cd in coal fly ash contributed more than 26% of total Cd globally released into landfills, from where it entered treated landfill leachate, subsequently reached wastewater treatment plants and river systems (Nriagu, 1989). Anthropogenic sources contribute 85% – 90% of the total yearly emission of Cd to the air (19,700 tonnes/year in 2000), while natural sources were estimated at 150-2,600 tonnes/year in 2000 (WHO, 2008). The forms of Cd in the atmosphere predominantly consist of Cd, CdO, CdS, and CdCl. The typical atmospheric residence time of Cd is about 1 – 10 days, which is sufficient for it to be transported up to a thousand kilometers before the deposit occurs. The continuous volcanic emissions, smelting, fossil fuel combustion, and refuse incineration leads to levels of Cd in the air, which exceed the Cd inhaled daily (5 ng/mL), resulting in concern about annual production levels and their consequent impact on human health. The average Cd concentrations which are discharged from the effluents of metal plating industries were 0.13 – 0.17 μM, whereas the highest concentration (8.8 μM) was discharged from lead-acid mine drainage (Bar and Das, 2016). United States Environmental Protection Agency (US EPA, 2011) estimated that 0.15 metric tons of Cd was released into surface water in 2009. The concentration of Cd in the flow of rainwater in urban areas ranges from 0.8 μM to 1.2 μM (Cole *et al*., 1984). Due to the pollution from the Orinoco and the

Amazon rivers, Cd concentration in the Gulf of Mexico is higher, exceeding 4.4 μM (Hernández-Candelario *et al.*, 2019).

Excessive concentrations of Cd, which contaminate water, have been detected in several countries, have consequently attracted attention, and raised significant concern. Cd concentrations in various freshwater types, many of which exceed environmental quality standards (e.g., 4.4 μM in Irish groundwater in the UK, Tedd *et al*., 2017), are listed in Table 1. High concentrations in rivers and aquifers are possible due to the activities of mining industries and leaching from soil contamination, as reported by Vaessen and Brentführer (2014). Aquifers impacted by past or present mining activities have been reported to contain the highest Cd concentrations by sources collected in Table 1 (e.g., Portugal, 622 μM (Neiva *et al*., 2015)) and the UK, 427 μM (Banks, 1997)), but also show more modest contamination (< 5 μM, e.g., USA (Davis *et al*., 2010; Sims *et al*., 2017)). High concentrations of Cd were also recorded in areas within proximity to industrial activities, such as brass manufacture, metal-working, automotive engineering, jewellery making, armaments, and brewing in Birmingham, UK (61 μM (Shepherd *et al.,* 2006)). Landfill appears to contribute to contamination of the aquifer with Cd in Vision, Denmark (60 μM Cd, Christensen, 1996), but less so in Gazipur, India (0.14 μM, Mor *et al*., 2006). The groundwater in rural areas, is usually less contaminated with Cd, for example, in India (0.08 to 1.0 μM Cd (Buragohain *et al*., 2010)).

Table 1. Total concentrations of Cd in different freshwater bodies reported in the literature. The standard guideline concentration for Cd in drinking water is 3 µg/L (WHO, 2011), equivalent to 0.027 µM.

Freshwater	Average (range) of concentration of Cd (µM)	pH	Reference
Aquifer impacted by landfill, Gazipur, Delhi, India	0.13 (0.10-0.17)	6.3-6.9	Mor *et al.,* 2006
Aquifer impacted by mining, Dhanbad, India	22 (20-24)	**	Prasad *et al.,* 2014
Aquifer impacted by mining, Phoenix, Nevada, USA	3.8 (3.2-4.4)	6.5-7.9	Davis *et al*., 2010
Aquifer impacted by mining, Techatticup, Nevada, USA	4.7 (4.1-5.3)	**	Sims *et al.,* 2017
Rural aquifer, Qatar	7.6 (6.8-8.4)	7.8-7.9	Kuiper *et al*., 2015
Pigeon spring, Snake Gulch, Kanab Creek, USA	124.5 (120-128)	6.7-8.0	Beisner *et al.,* 2017
Aquifer impacted by mining, Antiquary, Bolivian Altiplano	36.4 (31-42)	7.8-9.4	Ramos *et al.,* 2014
Aquifer impacted by mining, Sorval Guarda, Portugal	622 (603-642)	**	Neiva *et al*., 2015
Aquifer impacted by industries, Birmingham, UK	61 (5.8-6.4)	**	Shepherd *et al.,* 2006
*Aquifer impacted by Landfill, Vejen, Denmark	60 (55-63)	**	Christensen *et al*.,1996
Aquifer impacted by mining, North-western Arizona, USA	1.4 (1.1-1.6)	**	Rösner, 1998
Rural aquifer, Reading, Berkshire, UK	2.1 (1.8-2.4)	6-6-8.4	Edmunds *et al*., 2003

Freshwater	Average (range) of concentration of Cd (μM)	pH	Reference
Rural aquifer, Dhemaji, Assam, India	0.5 (0.08-1.0)	**	Buragohain *et al.,* 2010
Aquifer impacted by a river, Washington state	45 (42-48)	**	Twarakavi and Kaluarachchi, 2005
Aquifer impacted by River Ubeji River, Delta State, Nigeria	1.2 (0.75-1.5)	**	Etchie *et al*., 2012
Aquifer impacted by River Basin, Seini, Romania	0.21 (0.12-0.31)	7.8-8.5	Dippong *et al*., 2019
Aquifer impacted by mining, Yorkshire, UK	472 (423-432)	**	Banks, 1997
Glacial aquifer, Alaska, USA	1.2 (0.45-25)	**	Groschen *et al.*, 2009

* No control of reference site established except for aquifer impacted by Landfill, Vejen, Denmark was 6.3-6.6 μM
** No pH established.

These differences in Cd contamination relate not just to the source strength but also to the pathways whereby the Cd transfer to and transport within aquifers depends on its mobility, for which pH is an important parameter. The pH range varied from 6.6 to 8.5. Cd speciation and mobility is strongly affected by pH, with the highest movement in the pH range of 4.5 to 5.5, and likely precipitation occurring at a pH > 7.5 (Mulligan *et al*., 2001).

1-1-5 Effects of cadmium on human health

Some metals are essential for living organisms in trace amounts, such as cobalt, copper, iron, manganese, molybdenum, and vanadium. In contrast, others, such as cadmium, chromium, mercury, lead, arsenic and antimony, are non-essential. Both essential and non-essential metals cause toxic effects, depending on the dose an organism is experiencing (Bernard, 2008). Cadmium is a non-essential element for life, and it is toxic to *Homo Sapiens*. The United States Environmental Protection Agency (US EPA) and the International Agency for Research on Cancer (IARC) classified some elements, including Cd, As, Hg, and Pb, as human carcinogens (ATSDR, 2012). Furthermore, chronic exposure to low levels of Cd is associated with several diseases, such as deranged blood pressure regulation, osteoporosis, early onset of diabetic renal complications, and end-stage renal failure.

Humans may be exposed to Cd by drinking polluted water, ingesting contaminated food, and inhaling polluted air, which causes diseases. For example, end-stage renal disease was reported in a Swedish population, living near a Cd battery plant, and using renal replacement therapy (Hellström *et al.*, 2001). Skin exposure to Cd is rare, and it occurs mainly as an occupational hazard through contact with Cd-contaminated workplaces (ATSDR *et al.*, 2012). After absorption, the blood transfers Cd into different organs, such as the liver, kidney, testis, lungs, heart, prostate, and bone, potentially with harmful consequences. One of the biggest concerns about the presence and accumulation of Cd in the human organs is that the Cd can persist for many years, as it has a long biological half-life of 30 years (ATSDR *et al.*, 2012).

Standard and guidelines for Cd in various media include (ATSDR *et al.*, 2012):

- Soils with concentrations of > 1 mg/kg Cd are considered contaminated with Cd
- Drinking water standard guideline concentration is 3 µg/L (WHO, 2011).
- Daily intake through food of Cd is 7 µg Cd/kg body.
- Air pollution exposure is > 5 ng/mL.

The mechanism of Cd toxicity is associated with reactive oxygen species (ROS), despite the Cd not being observed as a Fenton metal. Cd is capable of protein depletion and glutathione-bound sulfhydryl groups, resulting in an oxidant, such as the hydroxyl radical species, in cellular environments. These ROS lead to the peroxidation of the lipid to evolve until the DNA is damaged (Waisberg *et al*., 2003).

Animal, molecular, and epidemiological models have shown that exposure to Cd causes remarkable health effects upon humans. Interestingly, the depletion of glutathione, which is the dominant form of Cd-induced hepatic toxicity, was observed in the liver of a rat (Liu *et al*., 2009).

Cd toxicity is usually determined by measuring its concentration and its biologically effective dose at the target organ. A study on Australian people between the ages of 41 to 50 years, who died of accidental causes, showed Cd concentrations in the kidney cortex and liver were 26 and 1 µg Cd/g wet weight, respectively (Satarug *et al.*, 2002). The use of a biomarker for exposure is the best way to determine the biologically effective dose when it is impossible to decide the dosage of Cd at the target tissue. Commonly, the biomarker of exposure to Cd is determined by quantifying Cd levels in urine or blood. The level of Cd in urine reflects the accumulation of Cd in the body or, more commonly, the kidney load of Cd, while the level of Cd in blood indicates possible recent exposure to Cd (Wittman, 2002).

Most epidemiological studies for Cd exposure in humans showed that the main target organs for Cd toxicity are the liver and the kidney, due to having a high concentration of metallothionein protein (Waalkes and Klaassen, 1985). Biomarker studies for assessing Cd-induced kidney damage in the general population have provided indications of the association between Cd and critical renal impairment concentrations between 100 and 200 μg/g Cd, which links to a urinary threshold limit of 5 – 10 μg Cd/g creatinine (Satarug *et al*., 2009). The Food and Agriculture Organization/World Health Organization (FAO/WHO, 2010) guideline for a provisional tolerable daily intake of Cd is 1 μg Cd/kg body.

Several studies have shown differing kidney effects at urinary Cd levels below the urinary threshold limit of 5-10 μg Cd/g creatinine. The elevation of protein markers, beta-2 macroglobulin, albumin, and retinol-binding protein, in a population with urinary Cd contamination, living in an area near a zinc smelter, have presented with > 2 μg Cd/g creatinine (Trzcinka-Ochocka *et al.*, 2004). Women living in an area contaminated with low Cd also revealed a positive association between Cd concentration and renal damage, which showed that the protein marker at a lower concentration (0.67 μg Cd/g creatinine, Åkesson *et al.*, 2005).

Several studies have reported an increase in lung cancer (increased excretion of creatinine) from chronic Cd exposure (0.01 μg Cd/m^3 ≥ 1 year). A very small study in a silver soldering company reported that 90% of ten workers who were exposed to Cd contaminated air from 0.006 to 0.015 mg/m^3, were found to have urinary Cd contamination, 63.0 μg/g creatinine, having urine protein (beta coefficient 10.27) (Choi *et al*., 2018). Therefore, due to the high association between Cd intake and carcinogenic effects, the standard guideline concentration for Cd in drinking water is 3 μg/L (WHO, 2011).

1-1-6 Ecotoxicity of cadmium

The ecotoxicity of Cd has been established for different organisms, including invertebrates, vertebrates, alga, plants, and bacteria (Table 2). Pavlaki *et al.* (2016) studied acute toxicity (lethal concentration, LC_{50}) in relation to different marine species. *Daphnea magna*, *Lemna minor,* and fish eggs (*Solea seegalensis*) were found to be most sensitive to Cd, for a day with LC_{50} values around 0.03 mg Cd/L (Clément and Lamonica, 2018; Pavlaki *et al.* 2016; Santos *et al.*, 2018). The cyanobacteria *Synechocystis* sp. PCC6803 is more tolerant to Cd for 5 h with a mean LC_{50} of 8.2 mg Cd/L (Du *et al.*, 2019). It is well-known that Cd inhibits soil microalga, for example, *Chlorococcum* sp. MM11 showed a mean LC_{50} of 2.85 mg Cd/L for 4 days (Subashchandrabose *et al.*, 2015). More Cd tolerant organisms include the earthworm, *Eisenia fetida*, for seven days with a mean LC_{50} value of 129.4 (91.6-202.8) mg Cd/L (Du *et al.*, 2014).

Table 2. The values of LC_{50} of Cd for some organisms.

Organism	Duration	Average (range) LC_{50} (mg Cd/L)	Reference
Solea senegalensis eggs	A day	0.03	Pavlaki *et al.*, 2016
Synechocystis sp. PCC6803	5 h	8.2 (2.8 – 13.6)	Du *et al.*, 2019
Escherichia coli	4 h	14.3 (4.35 – 29.50)	Lv *et al*., 2019
Chlorococcum sp. MM11	4 d	2.85 (3.09 – 4.71)	Subashchandrabose *et al.*, 2015
Muliercula inexpectata	28 d	7.57 (5.40 – 10.60)	Owojori *et al.*, 2019
Eisenia fetida	7 d	129.4 (91.6 – 202.8)	Du *et al.*, 2014
Ceriodaphnia dubia	4 d	0.029 (0.024 – 0.036)	Naddy *et al*., 2015
Pseudokirchneriella subcapitata *Lemna minor*	7 d 7 d	0.04 0.03	Clément and Lamonica, 2018

1-2 Remediation techniques for cadmium contaminated groundwater

In order to make contaminated groundwater suitable for drinking, agriculture, or domestic and industrial purposes, remediation techniques need to be applied. The selection of the remediation techniques depends on a number of factors: the type of pollutant, the purpose of the remediation project, the financial plan, the period, and the required removal efficiency.

In water, Cd occurs in the dissolved state as the hexaaquacadmium (II) complex ($[Cd(H_2O)_6]^{2+}$) and inorganic complexes (e.g., chloro or slufate). Within the water column Cd also occurs and is transported in combination with colloids, either inorganic (clay, oxides) or organic (humic substances) or with biological cells (viruses, bacteria, phytoplankton) (Li and Zhou, 2010). The chemistry of these colloids varies according to their origin, functional groups at the surface, and within their structures, which affects the strength of complexes they form with different elements. In rivers and aquifers, Cd transport by colloids can be important and is affected by the water flow rate, pH, presence of competing cations, dissolved organic matter, and the ionic strength of the water (Zhang *et al*., 2019). Therefore, the design of remedial treatment requires the consideration of both dissolved and colloidal transport of Cd.

As Cd is an element that cannot be chemically or biologically degraded or oxidised and has low volatility, a range of treatment techniques can be excluded from consideration:

- Air sparging and soil vapour extraction (SVE) techniques are only suitable for volatile and semi-volatile compounds. The air sparging technique (also known as air stripping) involves the injection of compressed air into the saturated zone of groundwater to evaporate compounds, which depends on their Henry's law constant, in the unsaturated area of groundwater (Fetter, 1999).

- Chemical oxidation techniques involve the addition of strong oxidising chemicals to degrade oxidisable organic compounds.
- Bioventing and bioslurping techniques involve the aerobic biodegradation of other compounds, such as fuel residuals and volatile organic compounds, by increasing the activities of indigenous microbes, which are present in groundwater and soil, and releasing oxygen or air to improve the process of biodegradation (Philp and Atlas, 2005).

1-2-1 Pump and treat technique

The pump and treat technique is suitable for volatile and non-volatile compounds, including Cd contamination. It involves pumping groundwater to the surface, where it is treated before returning. Examples of surface treatment options include chemical precipitation, ion exchange, adsorption, and bioremediation (Sepa and Oswer, 2001), some of which will be covered in more detail below.

1-2-2 Permeable reactive barrier techniques

Permeable reactive barrier techniques contribute to the prevention of contaminants from reaching the aquifer by the installation of gates or barriers in the flow path of groundwater. The barriers are installed as a vertical wall, within which groundwater contamination is treated by precipitation or absorption within the barrier materials. The barrier materials can be physical, chemical, or biological, or a combination of these materials (Asokbunyarat *et al*., 2017). Elementary iron has shown efficient Cd removal, such as nanoscale zero-valent iron (nZVI), which is used to remove cadmium by the isolation of the Cd^{2+} ions on nZVI through an adsorption process (Soto-Hidalgo and Cabrera, 2018).

1-2-3 Adsorption techniques

Cd adsorption techniques have been applied using a variety of adsorbent materials, such as agricultural wastes, granular activated carbon, and industrial wastewater with specific properties (Table 3). The adsorption process involves the concentration of cadmium on the surface of the surfactants via the van der Waals force (such as hydrogen bonds), which occurs between the adsorbates (i.e., Cd ions) and molecules of the adsorbents (Kazemipour *et al*., 2008). In addition, chemical sorption contributes by forming new chemical compounds.

Table 3 shows the capabilities of some adsorbent materials, which have been used for Cd adsorption in the range of 0.009 to 0.87 mmol Cd/g surfactant. Surfactants differ in their abilities to bind Cd, whereby the availability of sufficient functional groups with reliable and stable binding characteristics is critical for effective Cd adsorption. For example, bagasse carbon is widely used for Cd adsorption, for which a reasonable adsorption rate (0.04 mmol Cd/g) is recorded, due to having carboxylic and lactonic groups (Mohan and Singh, 2002). Agricultural waste sorbents showed better adsorption rates, for example, *Cocos nucifera* L. adsorbed 0.38 mmol Cd/g, and sunflower stalks adsorbed 0.37 mmol Cd/g. The adsorption process of these sorbents occurs by Cd binding to various functional groups, such as hydroxyl, carboxyl, amino, sulphate, and phosphate groups.

Table 3. Cadmium adsorption capacities of some adsorbent materials of different studies.

Adsorbent materials	Adsorption capacity (mmolCd/g surfactant)	Reference
Carbon nanotubes	0.009	Li *et al*., 2003
Ceiba pentandra L. (Gaertn hulls)	0.17	Rao *et al*., 2006
Cocos nucifera L.	0.38	Kadirvelu and Namasivayam, 2003
Radix luteola Lamarck	0.17	Hossain *et al*., 2015
Zea mays L. (raw corn stalk)	0.02	Zheng *et al*., 2010
Sunflower stalks	0.37	Sun and Shi, 1998
Olea europaea (stone carbon)	0.04	Mohan and Singh, 2002
Prunus persica (stone carbon)	0.04	
Limonia acidissima (wood apple) shell	0.24	Sartape *et al*., 2013
Olea europaea (stone carbon)	0.05	Azouaou *et al*., 2008
Zea mays L. (corncob)	0.04	Leyva-Ramos *et al*., 2005
Juglans regia L. (walnut tree sawdust)	0.05	Bulut, 2007
Acidosasa edulis (bamboo charcoal)	0.1	Wang *et al*., 2010

1-2-4 Biosorption techniques

In addition to the surfactants mentioned above, plants, algae and microorganisms have been used as biosorbents for Cd. Biosorption involves the adsorption of molecules or elements on the surface of biosorbents, which may be inactive, dead, or living biomass. Adsorption occurs via the functional groups on the surface wall of the biomass, including carboxyl, ketones, and aldehyde groups. Biosorption can be more

effective in dormant (inactive) organisms than live ones because the inactivation process may increase the number of anionic ligands at the cell surface (Katırcıoğiu *et al.*, 2008). Different processes are involved in the biosorption, in addition to the adsorption process, which includes ion exchange, chelation, complexation, and surface precipitation. Ion exchange is well-known for being the central part of the biosorption, which involves the exchange of elements existing on the surface of the organism, with dissolved Cd (Vijayaraghavan and Balasubramanian, 2015). Following the adsorption or ion exchange processes, chelation and complexation can occur, whereby stable bonds between an adsorbed Cd ion and the ligand(s) on the organism`s surface are formed.

The specific process and capacity of biosorption generally depend upon the composition of the biosorbent, in particular, the type of molecules in the cell walls and density of available functional groups that act as ligands. Table 4 shows the wide range (spanning seven orders of magnitude) of biosorption capacities of some plants, algae, fungi, yeasts, and bacterial species that have been used previously for the removal of Cd. Alga recorded high biosorption rates, ranging from 117 to 810000 nmol Cd/g dry biomass. Cell walls of algae are mainly composed of alginate ($C_{12}H_{20}O_{12}P_2$, Figure 1A), which makes up about 40% of dry biomass. The central character of the alginate enables it to absorb ions and has high availability (70%) of binding sites (Davis *et al*., 2003). Some fungi also recorded high biosorption rates, reaching up to 730 μmol Cd /g dry biomass, facilitated by chitin in their cell wall (Figure 1B). Chitin contains two molecules of beta-1, 4-linked *N*-acetylglucosamine, which provides enough groups for binding Cd (Salvadori *et al.*, 2014).

Table 4. Biosorption capacities for Cd of some plants, algae, fungi, yeasts and bacterial species derived biomass, used as biosorbents for the removal of cadmium.

Species	Removal capacity (nmol Cd/g dry biomass)	Reference
Plant		
Luffa cylindrica	0.038	Chen *et al*., 2014
Techtona grandis	88	Rao *et al*., 2010
Triticum aestivum	133	Nouri *et al*., 2007
Algae		
Chlorella coloniales	40000	Jaafari and Yaghmaeian, 2019
Scenedesmus obliquus	338	Chen *et al*., 2014
Parachlorella sp.	810000	Dirbaz and Roosta, 2018
Mucor rouxii	117	Yan and Viraraghavan, 2003
Padina sp.	530	Kaewsarn and Yu, 2001
Chlorella vulgaris	765	Aksu, 2001
Spirulina platensis	622	Rangsayatorn *et al*., 2004
Sargassum glaucescens	200	Naddafi *et al*., 2007
Fungi		
Aspergillus terreus	10856	Massaccesi *et al*., 2002
Trichoderma koningii	729653	
Tetraselmis suecica	70284	Pérez-Rama *et al*., 2002
Phanerochaete chrysosporium	622	Pakshirajan and Swaminathan, 2006
Lentinus sajor-caju	1094	Bayramoglu *et al*., 2002
Trametes versicolor	106	Arıca *et al*., 2001
Agaricus bisporus	61	Nagy *et al*., 2014
Lactarius piperatus	58	

Species	Removal capacity (nmol Cd/g dry biomass)	Reference
Yeast		
Saccharomyces cerevisiae	7.6	Marques *et al*., 2007
Saccharomyces cerevisiae pYD1-T68CadR	5.3	Tao *et al*., 2016
Bacteria		
Bacillus subtilis	2233	Ahmad *et al*., 2014
Bacillus cereus RC-1	275	Huang *et al*., 2013
Bacillus circulans	231	Yilmaz and Ensari, 2005
Pseudomonas putida	71	Pardo *et al*., 2003
Halomonas BVR 1	106	Rajesh *et al*., 2014
Streptococcus equisimilis	560	Costa and Tavares, 2016
Bacillus cereus S5	662	Wu *et al*., 2016
Streptomyces lunalinharesii	195	Veneu *et al*., 2012
Caulobacter crescentus JS4022/p723	142	Patel *et al*., 2010
Corynebacterium glutamicum	391	Mao *et al*., 2013
Pantoea TEM18	462	Ozdemir *et al*., 2004
Brevundimonas ZF12	435	Masoudzadeh *et al*., 2011
Lactarius scrobiculatus	472	Anayurt *et al*., 2009
Escherichia coli JM109	560	Deng *et al*., 2007
Pseudomonas sp.	2473	Ziagova *et al*., 2007
Staphylococcus xylosus	2224	
Enterobacter J1	409	Lu *et al*., 2006
Brevibacterium jeotgali U3	1138	Green-Ruiz *et al*., 2008

Plants and bacteria have recorded biosorption capacities ranging from 0.038 to 133 and 101 to 2473 (nmol Cd /g dry biomass), respectively. The main binding sites on plant cell walls are hemicellulose ($C_5H_{10}O_5$), pectin ($C_6H_{10}O_7$), and cellulose ($C_6H_{10}O_5$) (Figure 1C). Bacterial cell walls are mainly composed of peptidoglycan ($C_9H_{17}NO_7$), which contains two molecules of *N*-acetylglucosamine (NAG) and *N*-Acetylmuramic acid (NAM), which provide ligands for binding Cd.

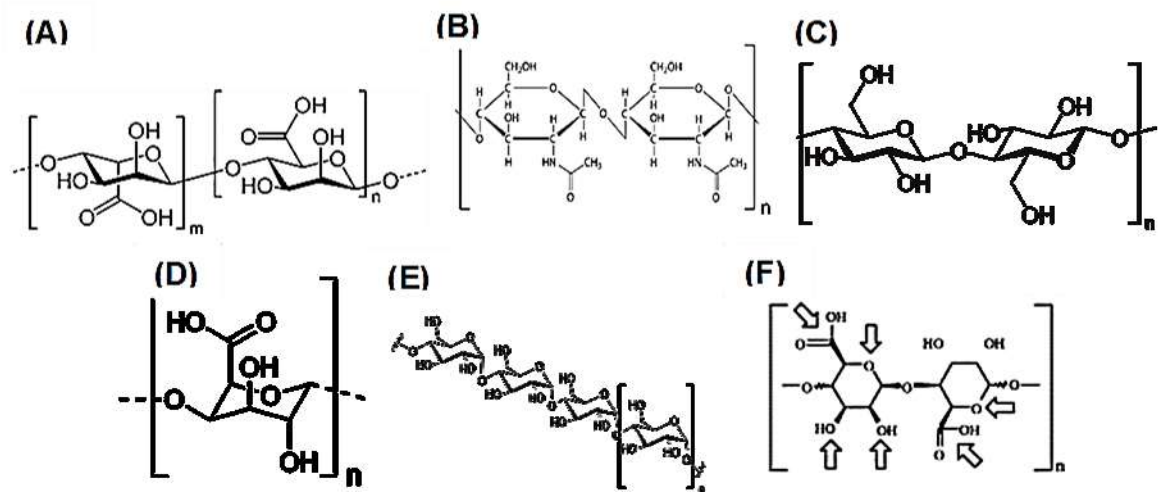

Figure 1. Chemical structures of **(A)** alginate (António *et al*., 2016), **(B)** chitin (Salvadori *et al*., 2014), **(C)** cellulose (Moon *et al*., 2011), **(D)** pectin (Mohnen, 2008). **(E)** Polysaccharides (Aspinall, 2014) and **(F)** possible Cd binding sites on functional groups.

Cellulose or hemicelluloses makes up 20 – 30 % of the dry biomass of plants, while pectin contributes more than 30% (Figure 1D). The main property of pectin enables it to adsorb ions, and Cd is less powerfully bound to pectin. The limited number of yeasts that have been investigated show a relatively low biosorption capacity (<10 nmol Cd/g biomass) compared to algae, fungi, and bacteria. Polysaccharides ($C_6H_{10}O_5$) (Figure 1E) are the main component of their cell walls, and these contain molecules of alkali-insoluble *β*-glucans, mannan, alkali-soluble *β*-glucans and minor chitin, providing the groups to bind with Cd ions (Figure 1F).

1-2-5 Electrochemical technique

The electrochemical technique involves using an electrode for the collection of the Cd ions by applying low electricity or potential gradient into the groundwater zone. There are four methods involved in the electrochemical technique: electro-osmosis; diffusion; electrophoresis, and electro-migration. Electro-migration is reported as the primary electrochemical technique for Cd treatment due to the transfer efficiency of Cd ions towards the anode, which has a negative charge, OH^-. The electro-migration technique involves the gradual movement of Cd ions and electrons in a conductor or electrolyte due to the momentum transfer caused by an electric field between electrodes. The efficacy of this reaction depends on the pH. Under acidic conditions, the H^+ increases, and the cadmium speciation is dominated by the Cd^{2+} ion in solution, which readily transfers toward the anode (Grau and Bisang, 2001).

1-2-6 Precipitation technique

The precipitation technique is a common technique used to treat Cd contaminated groundwater due to its high efficiency of removal. This is a chemical process that involves the creation of a solid mineral or oxide by controlling the Cd solubility through the addition of chemical precipitants. The efficiency of this technique in the precipitation of Cd is generally determined by the solubility constant (K_{sp}), pH, and the presence of other substances. Groundwater is mostly anoxic, and its pH is 6 – 7. The change of pH is the most common procedure of modifying Cd solubility limits with the addition of alkali, such as quicklime (CaO), slaked lime ($Ca(OH)_2$) or limestone ($CaCO_3$). The reaction of precipitation is reversible, as shown in the following reaction:

$Cd^{2+} + 2OH \rightleftharpoons Cd(OH)_2$, ΔG^o = -138.7 kJmol^{-1} of Cd^{2+} (Okinaka, 1985).

This formation of cadmium hydroxides at pH ≥ 10 occurs with a K_{sp} of 7.2 X10^{-15}, lower than the K_{sp} of $CdCO_3$ (1.0 X10^{-12}) (Rumble, 2018). The addition of limestone or slaked

lime was found to be very useful for Cd hydroxide precipitation at pH 8.5 (Wang *et al*., 2005). The reduction of pH <4 remobilises the precipitated Cd.

The presence of an additional ion was also found efficient for the precipitation of Cd. For example, high concentrations of calcium in the presence of Cd results in the precipitation of cadmium calcite. Calcium minerals, such as hydroxyapatite ($Ca_{10}(PO_4)_6(OH)_2$), have also been used for the precipitation of Cd (Mobasherpour *et al*., 2011). As a result of this, the mechanism of cadmium precipitation consequences from the formation of hydroxypyromorphite [$Cd_{10}(PO4)_6(OH)_2$] as shown in the following reaction:

$Cd^{2+} + 9Ca^{2+} + 6HPO_4^{2-} + 2H_2O \rightarrow Ca_9Cd_x(PO_4)_6(OH)_2 + 8H^+$

$Cd_3(PO_4)_2$, $K_{sp} = 2.53 \text{ X} 10^{-33}$.

Similarly, the precipitation of Cd as cadmium sulphide (CdS) has shown reasonable precipitation rates due to the K_{sp} of CdS is $1 \text{ X } 10^{-28}$ (Rumble, 2018). Sulfide minerals, such as pyrite (FeS_2), have been used for precipitation of cadmium due to the formation of CdS, as shown in the following reaction:

$FeS_2 + 4HCl \rightarrow FeCl_2 + 2H_2S + 2Cl^-$

$Cd^{2+} + H_2S \rightarrow CdS + 2H^+$, $\Delta G^o = -45.33$ kJmol^{-1} of Cd^{2+} (Zhdanov, 1985).

This reaction occurs at relatively low pH (3 – 6) due to the generation of H_2S. Alternatively, chelating precipitants such as potassium/sodium thiocarbonate, trimercaptotriazin, and sodium dimethyldithiocarbamate have been used to precipitate Cd from water at low pH (3.5 – 4.5) (Matlock *et al*., 2002). Polettini *et al*. (2006) used EDTA, nitrilotriacetic acid (NTA), citric acid and H_2S, and an *S*-isomer of ethylenediamine succinic acid ([S-S]-EDDS) to precipitate Cd. The mechanism for Cd precipitation results from the formation of a Cd complex, for example, Cd(EDTA), as shown in the following reaction:

$Cd^{2+}+H_4EDTA \rightleftharpoons [Cd(EDTA)]^- + 4H^+$

Cd(EDTA) is a stable complex with log *K* = 5.93 (Munataka *et al*., 1986), and is readily soluble, preventing Cd precipitation. This is also the case for precipitation of Cd in groundwater due to complex formation with ligands, which are naturally present in the groundwater. These include chloride, sulfate, carbonate, and bisulfide anions, have relatively high stability constants with Cd (log *K*: 1.98, 3.5, 6.4, and 20.9, respectively) (Rumble, 2018) and may be present at sufficient concentrations.

1-2-7 Ion exchange technique

The ion exchange technique involves exchanging cations (e.g., Cd^{2+}) in the electrolyte solution with cations (e.g., H^+) at an insoluble electrolyte in the solid (resin) component, which fills the column reactor (Al Sadat Shafiof and Nezamzadeh-Ejhieh, 2020) and provides a polyanion surface. Resins may be natural, such as inorganic zeolites, or synthesised, organic resins, such as dolamite, amberlite IR120, amberlite IRC 718, and dowex 50 W. Artificial resins are the most common type used, due to their optimised characteristics for particular applications.

In this technique, two mechanisms could occur, firstly exchange of Cd^{2+} from the water with the cations bound to the polyanions, and secondly, the coordination between Cd^{2+} with functional groups (hydroxyl groups) of the polyanions. These mechanisms are affected by the Cd solubility, where Cd^{2+} is the species that can be exchanged or coordinated by polyanions, compared with other species of Cd, due to its high affinity (Boparai *et al*., 2013).

The cadmium exchange efficiencies of different solid polyanions vary depending on their acidic ability, resulting from varied acid groups. The stronger or weaker properties of the functional group of polyanions are determined by their acid dissociation constant (p*K*a). If the functional group has a strong p*K*a, it is referred to as a strong ion

exchange polyanion, while if it has a weak p*K*a, it is referred to as a weak ion exchange polyanion. The functional groups have been classified according to their p*K*a from strong to weaker acid, such as hydrochloric acid (p*K*a = - 8), carboxylic acids (p*K*a = 5), protonated amines (p*K*a = 10), water (p*K*a = 14), alkyne (p*K*a = 25), amine (p*K*a = ~35), and alkane (p*K*a = ~50) (Shriver and Atkins, 1999).

The most common cation exchangers are strongly acidic resins with sulfonic acid groups (SO_3H) and weak acid resins with carboxylic acid groups (COOH). Hydrogen ions in the sulfonic group or carboxylic group of the resin can provide exchangeable ions for metal cations, as shown in the following reactions (Fu and Wang, 2011):

$$nR\text{-}SO_3H + Cd^{2+} \rightarrow (R\text{-}SO_3^-)_nCd^{2+} + nH^+$$

$$nR\text{-}COOH + Cd^{2+} \rightarrow (R\text{-}COO^-)_nCd^{2+} + nH^+$$

The pH of an aqueous solution affects the chemistry of Cd, the activity of the functional groups on the polyanions and the competition of Cd ions in the solution. Free Cd^{2+} ions dominate in the pH of the range of 4.5 to 5.5, and its solubility decreases significantly at a pH > 7.5 (Taty-Costodes *et al.*, 2003). The pH also affects the acidic properties of various functional groups on the polyanions, alkaline ligand groups, such as carboxyl, imidazole, phosphate, and amino groups (negative charge). At more acid pH, these alkaline ligand groups will combine with H^+ in a process called protonation, resulting in changing their charge, progressively, from negative, to neutral, and, in some instances, to positive. Therefore, Kocaoba (2007) found that ion exchange enables the uptake of Cd from a solution at a low pH, mainly 3 to 4.

The efficiency of the ion exchange process may be reduced due to the formation of competitive complexes on ion exchange resins. For example, in a study by Vilensky *et al*. (2002), the resins duolite GT73 and amberlite IRC-748 were used in the remediation of cadmium-contaminated groundwater, the presence of high

concentrations of elements, especially those responsible for hardness (magnesium, calcium, sodium, chloride, and potassium), in addition to organic matter, reduced the efficiency of the process.

1-2-8 Bioremediation technique

Bioremediation techniques utilise living organisms, such as microorganisms and plants, for the removal, transformation, or immobilisation of contaminants, such as hydrocarbons, agrochemicals, other organic toxicants or metals from soils or aquatic environments (Dixit *et al*., 2015).

Bioremediation is an eco-friendly process through the use of materials and organisms that are not toxic or pathogenic. Plants and microorganisms have evolved different strategies to survive in environments that present stress factors (e.g., extremes of pH, salinity, temperature, desiccation, toxic substances, etc.). These include detoxifying mechanisms for metals, such as biosorption, bioaccumulation, biotransformation and biomineralisation, all of which can be utilised in bioremediation techniques (Gupta and Prakash, 2020). Bioremediation (also known as bioremoval) efficiencies of organisms vary, depending on their detoxification mechanisms (e.g., active bioaccumulation or passive adsorption) and concentration or density of active sites or cells, which result in different affinities to Cd (Romera *et al*., 2007). As covered in the previous section, the biosorption capacity of microbial cells is afforded by their constituents being mainly polysaccharides, lipids and proteins, which provide functional groups for metal binding, such as carboxylate, hydroxyl, amino and phosphate groups (Dixit *et al*., 2015).

The type of genus and species of the organism and their tolerant capacity are important parameters. For example, specific species that belong to the same family may have a different bioremoval efficiency, due to their different tolerant capacities, which result in different bioremoval mechanisms (Nanda *et al*., 2019). The biomass

concentration is an important factor in the process, which motivates bioremoval efficiency. Generally, it has been observed that the efficiency of Cd bioremediated by bacterial biomass from aqueous solutions was noticeably enhanced by increasing the amount of active biomass surface or binding sites, which available for Cd bioremoval (Khan *et al*., 2016).

In addition to the character and concentration of biomass, the characteristics and concentrations of Cd and the environmental conditions affect the bioremoval efficiency. The speciation of Cd, which depends on pH and other constituents in the water, is key to obtain the binding of Cd that leads to efficient bioremoval (Taty-Costodes *et al*., 2003). The ionic strength of the water is the critical parameter influencing the Cd bioremediation process. At high ionic strengths, Cd tends to complex with anions and free Cd ions in solution, are rare; however, at lower ionic strength, this complex tends to dissociate due to an increase in their electrophoretic mobilities, providing free ions in solution (Yee *et al*., 2004). Similarly, environmental conditions, such as pH and temperature, are abiotic factors influencing the efficiency of the cadmium bioremediation process. The pH of an aqueous solution affects the chemistry of Cd, the activity of the functional groups on the biomass cell surfaces, and the competition of Cd ions in the solution. Cd is predominantly mobile (free ions, inorganic complexes) in the pH of the range of 4.5 to 5.5, and its solubility decreases at a pH > 7.5 (Taty-Costodes *et al.*, 2003). The pH also affects the acidic properties of various functional groups on the microorganism. Alkaline ligand groups, such as carboxyl, imidazole, phosphate, and amino groups (negative charge), which are on the microorganism cell wall, are more common. At more acid pH, these alkaline ligand groups will combine with hydrogen ions in a process called protonation, resulting in changing their charge, progressively, from negative, to neutral and, in some instances,

to positive. The functional groups of the cell wall of *Shewanella putrefaciens* under different pH values are shown in Figure *2* (Haas *et al*., 2001).

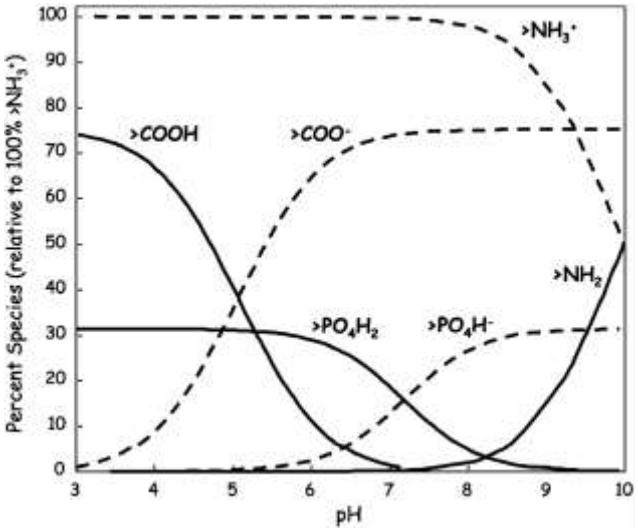

Figure 2. The relative proportion of species of the main functional groups of the wall in *Shewanella putrefaciens* at different pH values (Haas *et al*., 2001).

Usually, Cd bioremoval occurs under thermodynamic control (Dirbaz *et al*., 2018), the nature of which depends on the type of binding between the Cd ions and other functional groups on the cell wall of the microorganism. Mainly, the interactions of Cd ions with carboxyl groups are endothermic, while the interactions with amine groups are exothermic. Therefore, high temperatures enhance the Cd bioremoval if the binding is endothermic. Yu *et al.* (2006) reported that an increase in temperatures from 4.85, 14.85, and 24.85 to 39.85 ^{o}C increases Cd adsorption.

1-2-9 Advantages and disadvantages of some remediation technologies of cadmium from groundwater

The advantages and disadvantages of the techniques mentioned above are listed in Table 5 in order to assist the selection of a suitable technology in a groundwater remediation project. Bioremediation is a common remediation strategy used with low Cd concentrations due to the ability of the bacterial cells to bioremediate Cd.

Table 5. The advantages and disadvantages of some remediation technologies of cadmium removal.

Technique	Advantages	Disadvantages
Pump and treat	• An efficient technique for removal of Cd-contaminated groundwater from the aquifer, controlling the spread of the contaminant.	• It is an expensive technique due to the cost of the construction and operation and the combination with aboveground treatment techniques for the removal of Cd. • Technique efficiency can be affected by the precipitation of other minerals in the withdrawal wells (Brusseau, 2019).
Permeable reactive barriers	• Cost-effective subsurface barrier. • Highly efficient technique.	• The effectiveness of the reactive wall can be affected by constraints such as pH, minerals, in addition to biological activity (Henderson and Demond, 2007).
Electrochemical technique	• Efficient technique.	• It is an expensive technique due to the cost of the construction and operation of the equipment. • Its combination with below-ground treatment techniques for the removal of Cd. • In order to solubilise the Cd hydroxide, the pH must be controlled, which adds more cost. • It needs an electricity supply.
Adsorption	• High Cd holding capacity. • Cost-effective materials.	• Desorption of Cd under high acidic conditions could happen, leading to the leaching of Cd. • The Cd-loaded adsorbent is finally removed and landfilled, increasing the risk of hazard compounds in the environments. • Adsorption efficiency decreases due to the blockage of the permeability of adsorbent materials by solids, which are present in the groundwater constituents, and possibly the biofilm formation (Al-Rashdi *et al*., 2011).
Precipitation	• The cost-effective technique for the removal of Cd at a high concentration. • The stable technique for the removal. • Efficient technique.	• The not cost-effective technique for the removal of Cd at a low concentration • It produces a waste product.

Technique	Advantages	Disadvantages
Ion exchange	• A useful technique for the removal of Cd at low concentrations. • A suitable technique for the final treatment after the application of other techniques.	• Resins are expensive. • Eventually, Cd-resins are disposed into landfills. • Ion exchange efficiency can be affected by the high concentration of Ca ions in the water, resulting in increasing the ion exchange of Ca instead of Cd; therefore, it is not a suitable technique for removing Cd in hard water, groundwater (Bedessem *et al.*, 2009).
Bioremediation	• Cost-effective technology, simple to install and uses available biomaterials. • Lowest energy requirement.	• Immobilisation of biomaterials. • The selective technique requires preliminary studies to confirm the applicability of biomaterials and is dependent on water conditions. • Treatment is slow, requiring long term monitoring and maintenance. • Biomaterials efficiency decreases due to the inhibition of biomaterials by certain chemicals. • Require conditioning of conditions such as nutrient and pH. • Desorption of the Cd under high acidic condition. • Cd-loaded biomaterials are lastly removed and landfilled, increasing the risk of hazard compounds in the environments, depending on their hazard assessment (Jain and Arnepalli, 2019)

1-3 Interaction of cadmium with bacteria

1-3-1 Transporters of cadmium to a cell and bacterial toxicity

Although some metals are essential for cellular metabolism in bacteria, high concentrations of metals can have fatal effects on bacteria. Some elements present in nature at low concentrations, such as Cd, are not necessary for bacteria (Schirawski *et al.*, 2002). Nevertheless, organisms, including bacteria, have mechanisms to take up Cd into their cells (Palmer and Skaar, 2016). Mainly, there are two main categories of carriers of Cd in a cell:

Firstly, the proteins, which are involved in the absorption of essential micronutrients, such as Zn^{2+} and Mn^{2+}, can also transfer Cd across the cell wall. Cd is the structural equivalent of Zn^{2+} and Mn^{2+} and is handled by Zn^{2+} or Mn^{2+} carriers in most bacteria (Palmer and Skaar, 2016). Two transmitters, the inner membrane ATP-ABC (ATP-binding cassette) ZnuACB and ZIP (Zrt, Irt-like Protein, ZRT/IRT), facilitate the absorption of Zn^{2+} in the cell. ZnuACB shows the carrier for Zn^{2+} absorption in *Yersinia pseudotuberculosis* (Figure 3A). ZIP carriers are the dominant carrier, which allows Cd to enter a cell (Binet and Poole, 2000). ABC carriers facilitate the transport of Mn^{2+} across the outer membrane. The SitABCD vector (an example of ABC transport protein) is predominantly a Mn^{2+} transporter (Figure 3B) and also facilitates the entrance of Cd into cells (Kehres *et al.*, 2002). Secondly, specific ligands, such as siderophores, located on the cell surface, can transfer Cd to a cell. Siderophore is a protein with low molecular weight and a significant affinity to Fe^{2+}. The proteins FecA, FepA, and FhuA, mediate the absorption of iron, resulting in ferrisiderophore. The protein substrate is ferrous like FhuD, located in the space between the cell wall membranes, which carries a ferrisiderophore complex from the outer layer to the internal membrane (Figure 3C; Palmer and Skaar, 2016). Similarly, the

ferrisiderophore appears to contribute to the uptake of Cd^{2+} in the cell (Winkelmann, 2002).

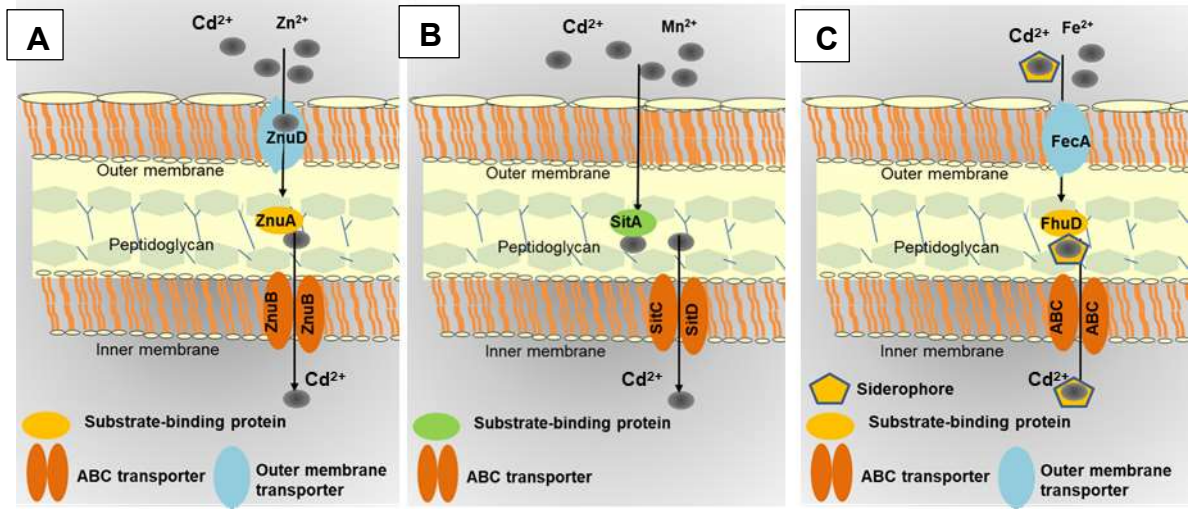

Figure 3. Schematic representation of Cd transposition into a cell (Palmer and Skaar, 2016). **(A)**Transposition of Zn^{2+} in the bacterial cell. Bacteria translocate Zn^{2+} from the extracellular spaces to the cytoplasm by ZnuACB transporters. This Figure is based on the structure of ABC transporter to transport Zn^{2+} into *Yersinia pseudotuberculosis*. **(B)**Transposition of Mn^{2+} in Gram-stain-negative bacteria by SitABCD transporters. **(C)** Fe^{2+} transporter by ABC transporter via siderophore. This structure is based on the structure of ABC transporter to transport Zn^{2+} into *Pseudomonas aeruginosa*.

After Cd entered the cell, its toxicity appears mainly due to oxidation reactions with biological macromolecules. Fenton`s reaction summarises the oxidative stress of metals, generally, on the bacterial cells and the production of reactive oxygen species (ROS) as shown in the reactions below (Fenton, 1894):

$$M^{(n)} + O_2^{\cdot -} \rightarrow M^{(n-1)} + O_2$$

$$2O_2^{\cdot -} + 2H^+ \rightarrow H_2O_2 + O_2$$

$$M^{(n-1)} + H_2O_2 \rightarrow M^{(n)} + HO^{\cdot} + OH^-$$

Hydrogen peroxide (H_2O_2) can be reduced in the presence of metals, thus creating one of the most powerful oxidising reagent, the hydroxyl radical ($OH^{\cdot}$). Although Cd does not appear to be working immediately on ROS production, it has been speculated that Cd generates ROS, leading to cell damage (Stohs and Bagchi, 1995). Several

other mechanisms enable Cd to damage bacteria (Nies, 2013). The first mechanism is replacing Cd with other ions that occur in functional groups, which are located on the surface of an organism. This substitution is mainly performed with sulfhydryl groups, which are a part of the proteins, or with hydroxyl groups, the main groups of phospholipids, leading to protein damage and lipid oxidation (Chrestensen *et al*., 2000). Therefore, the toxicity of Cd on the cell is dependent on fatty acids and protein compositions of its cell wall, in addition to the Cd concentration. The second mechanism involves Cd binding with cellular thiols groups, which are part of the proteins, leading to the oxidation of thiols. This oxidation sequentially reduces ATP and NADPH, leading to cell destruction. The third mechanism is DNA damage through $OH^{\cdot}$ oxidation, which occurs when $OH^{\cdot}$ attacks DNA, causing DNA to have permanent reductions in its structure and function. The destruction of the DNA leads to the inhibition of gene expression to proteins and prevents the growth of the cell. The high affinity of Cd with thiol groups is the main chemical basis of Cd toxicity. The superfamily proteins thioredoxin, which has Cys-Gty-Pro-Cys linkage in an active position, such as Dsb (disulfide bond proteins), are placed in the periplasm (Missiakas and Raina, 1997). Most organisms encode mechanisms that protect the proteins from the oxidative damage, and the thioredoxin protein plays an important role in this process (Khairnar *et al*., 2013). During severe conditions of oxidative stress, these thioredoxin proteins become depleted or overloaded, so the cysteine residues become susceptible to oxidation. The proteins DsbA (disulfide bond A) and DsbB (disulfide bond B) were studied in *E. coli* (Rensing *et al*., 1997; Stafford *et al*., 1999) under severe conditions of oxidative stress.

1-3-2 Mechanisms of cadmium resistance in bacteria

Some bacteria have a variety of protection mechanisms that increase their tolerance to very high concentrations of Cd without any effect on their growth and metabolism. The protective mechanisms include efflux of the Cd out of the cell, extracellular sequestration, biosorption, precipitation, and bioaccumulation within cells (Bruins *et al*., 2000). Generally, Cd resistance is defined by the minimum inhibitory concentration (MIC), which is the lowest concentration of a chemical that inhibits the visible growth of a bacterium (Wiegand *et al*., 2008). The MIC of bacteria is determined by incubating cultures with increasing concentrations of the chemical solution of interest on agar (well-known agar dilution) or in broth (well-known broth dilution) and respectively, evaluating the results by observing the number of bacterial colonies or by determining the biomass of the bacterial growth (Wiegand *et al*., 2008). Microbes are assumed to be tolerant to Cd if their MIC values exceed 0.8 mM Cd (Matyar *et al*., 2008). Table 6 illustrates some cadmium strains with their classifications and their natural MIC resistance levels. According to this table, the bacterial phyla *Actinobacteria*, as well as *Firmicute* and *Acidobacteria,* can resist Cd. In addition, strains that belong to *Proteobacteria* phylum have been reported to have a promising Cd-resistance compared to the other phyla (200 – 700 mM Cd, Ghosh *et al*., 1997; Mahapatra and Banerjee, 1996). *Proteobacteria* is a major phylum of Gram-stain-negative bacteria, while *Firmicutes* and *Actinobacteria* phyla are the Gram-stain-positive bacteria. Gram-stain-negative bacteria are commonly known to be more resistant to metals compared to Gram-stain-positive bacteria, due to their cell wall composition. Gram-stain-negative bacteria have a compound wall layer, consisting of the outer membrane, the plasma membrane, and the peptidoglycan layer. The outer membrane is a wall through which undesirable elements move from the inside to the outside the

cell. The outer membrane consists of an exclusive molecule, LPS (lipopolysaccharide), proteins, lipoproteins, and porins. The plasma membrane, which forms up to 40% of the cell wall, is the high region, separating the outer membrane and the peptidoglycan layer. The peptidoglycan layer is a thin layer of about 3 nm and comprises 10% of the cell wall.

In comparison, Gram-stained-positive bacteria contain a single wall layer, consisting of 30 – 90% of the peptidoglycan layer with an estimated thickness of 25 – 30 nm. In addition, secondary polymers, such as teichoic and lipoteichoic acids are formed from cell wall components. Gram-stain-negative bacteria occur in metal-rich environments, and it is reported that, under similar conditions, absorbs less than 10% of the amount of metals that Gram-stain-positive bacteria absorb (Konhauser, 2009). This low absorption rate is due to the metal associated with the functional groups of the outer membrane of Gram-stain-negative bacteria, LPS. Carboxyl groups in the LPS of the cell wall provide binding sites of sufficient electrical charge to bind metal cations to the cell surface effectively. LPS provides enough electrical charge, which can respectively bind with more minerals to the cell surface. LPS consists of three sections: lipid A, a core oligosaccharide, and an O-antigen polysaccharide. Lipid A is the most hydrophobic section, which is composed of glucosamine associated with acyl chains (fatty acids). Chemically, glucosamine and fatty acids are abundant with the carboxylic groups. The second part of LPS is the core, which is linked to the lipid contribution, contains the distinctive sugars of 3-deoxy- D-mannooctulosonate and L-glycerol-D-mannoheptose, in addition to *N*-acetylglucosamine, galactose and a number of additional sugars, which vary between the bacterial species. These acids and sugars provide large numbers of carboxyl groups, which are the main groups in LPS cores, providing a negative charge for COOH-Cd assembly. The O-antigen

polysaccharide is a glycan polymer containing monosaccharides, resulting in a large number of carboxyl groups (Raetz and Whitfield, 2002).

The production of extracellular polymeric substance (EPS) by Gram-satin positive/negative bacteria allows the binding of metal cations to anionic carboxyl groups. The types of EPS vary in terms of the nature of their association with the cells, including C-EPS (capsular), S-EPS (slime), LB-EPS (loosely bound), and TB-EPS (tightly bound) (Żur *et al*., 2016). EPS consists of carbohydrates, homopolysaccharides, such as either cellulose and dextran or heteropolysaccharides (xanthan, gellan, and alginate) or proteins. Similarly, Poly-L-Lysine and poly-gamma-glutamate act as proteins in EPS (More *et al.*, 2014). These carbohydrates and EPS proteins provide sufficient hydroxyl groups for binding Cd, preventing Cd from cytotoxicity and increasing the cell resistance to Cd.

Table 6. Minimum inhibitory concentration value of some cadmium resistant strains with their classifications. *No strain code established

Class	Order	Family	Genus and species	Strain code	MIC (mM)	Reference
Phylum: "*Acidobacteria"*						
Acidimicrobiia	*Actinomycetales*	*Actinomycineae*	*Actinomyces turicensis*	AL36Cd	10	Oyetibo *et al*., 2010
Phylum: "*Actinobacteria"*						
Actinobacteria	*Micrococcales*	*Micrococcaceae*	*Arthrobacter ramosus*	AY509238	2.5	Abou-Shanab *et al*., 2007
			A.rhombi	AY509239	5.0	
			Arthrobacter sp.	D9	0.6	Aiking *et al*., 1985
		Microbacteriaceae	*Clavibacter xyli*	AY509235	5.0	Abou Shanab *et al*., 2007
			C.xyli	AY509236	5.0	
			C.xyli	AY509237	5.0	
			Microbacterium arabinogalactanolyticum	AY509224	2.5	

Class	Order	Family	Genus and species	Strain code	MIC (mM)	Reference
			M.arabinogalactanolyticum	AY509226	2.5	
			M.arabinogalactanolyticum	AY509220	0.5	
			M.arabinogalactanolyticum	AY509219	1.0	
			M.arabinogalactanolyticum	AY509221	2.5	
			M.arabinogalactanolyticum	AY509222	5.0	
			M.arabinogalactanolyticum	AY509223	1.0	
	Actinomycetales	*Corynebacteriaceae*	*Corynebacterium ulcerans*	CA56Co	2.0	Oyetibo *et al.,* 2010
			C.kutscheri	FL108Hg	10	
	Actinomycetales	*Streptomyceetaceae*	*Streptomyces*	CdTB01	50	Zhou *et al*., 2016
Phylum: *"Firmicutes"*						
Bacilli	*Bacillales*	*Bacillaceae*	*Bacillus circulans*	ATCC11778	1.0	Baligarx, 2012
			B. cereus	ATCC11778	1.0	
			B. cereus	S5	10	Wu *et al*., 2016

Class	Order	Family	Genus and species	Strain code	MIC (mM)	Reference
			B.subtilis	BNi11	2.5	Ndeddy and Babalola, 2017
			B. cereus	BCr26	0.2	
			B.cereus	BNi12	0.1	
			B.cereus	BNi22	2.5	
			B. pumulis	BCd2	5.0	
			B. safensis	BCr7	0.5	
			B.thuringiensis	DM55	0.25	El-Helow *et al*.,2000
			B.cereus	RC-1	0.98	Huang *et al.,* 2013
			B.flexus	AY509229	5.0	Abou-Shanab *et al*., 2007
			B.niacini	AY509227	0.1	
			B. psychrosaccharolyticus	AY509230	5.0	
			B. megaterium	H3	0.9	Li *et al*., 2017
		Paenibacillaceae	*Brevibacillus agri*	C15	16 ± 0.7	This study

Class	Order	Family	Genus and species	Strain code	MIC (mM)	Reference
			B. agri	C15 Cd^R	21 ± 0.4	This study
			Geobacillus stearothermophilus	DSM 6453		Hetzer
				DSM 5507	0.6	*et al*., 2006
			G.thermocatenulatus		0.05	
		Moraxellaceae	*Acinetobacter junni*	CA109Cr	1.0	Oyetibo *et al.*, 2010
Phylum "*Proteobacteria*"						
Alphaproteobacteria	*Rhodobacterales*	*Acetobacteraceae*	*Acidiphilium cryptum*	Lhet 2	700	Mahapatra and Banerjee, 1996
			A.symbioticum	KM2	700	
			A.symbioticum	H8	700	
			A.multivorum	JCM	700	
			A.multivoram	GS19h	400	Ghosh
			Acidocella facilis	*	200	*et al*., 1997

Class	Order	Family	Genus and species	Strain code	MIC (mM)	Reference
	Rhizobiales	*Rhizobiaceae*	*Rhizobium etli*	AY509210	0.1	Abou-Shanab *et al*., 2007
			R. etli	AY460185	5.0	
			R.galegae	AY509213	0.1	
			R. galegae	AY509214	2.5	
			R. galegae	AY509216	0.1	
			R. galegae	AY509215	0.1	
			R. gallicum	AY509211	0.1	
			R.mongolense	AY509212	0.1	
			R.mongolense	AY509209	0.1	
			Sinorhizobium fredii	AY509217	2.5	
	Sphingomonadles	*Sphingomonadaceae*	*Sphingomonas alaskensis*	AY509242	0.1	Abou-Shanab *et al*., 2007
			S.asaccharolytica	AY509241	0.1	
			S.macrogoltabidus	AY509243	0.5	

Class	Order	Family	Genus and species	Strain code	MIC (mM)	Reference
	Parvularculaceae	*Caulobacteraceae*	*Caulobacter crescentus*	AY512823	0.1	Abou-Shanab *et al*., 2007
Betaproteobacteria			*Alcaligenes feacalis*	BCd33	7.5	Ndeddy Aka and Babalola , 2017
			A. feacalis	BCr32	2.0	
			A.eutrophus	X58441	10	Abou-Shanab *et al*., 2007
		Comamondaceae	*Acidovorax avenae*	AY512827	2.5	Abou-Shanab *et al*., 2007
			A.delafieldii	AY512826	0.1	
			Variovorax paradoxus	AY512828	5.0	
Gammaproteobacteria	*Pseudomonadales*	*Pseudomonadaceae*	*Pseudomonas putida*	KT2440	0.8	Miller *et al*., 2009
			P.aeruginosa	CA207Ni	10	Oyetibo *et al*., 2010
			P. aeruginosa	AL80Ni	2.0	
			P.aeruginosa	B237	8.0	Baligarx, 2012

Class	Order	Family	Genus and species	Strain code	MIC (mM)	Reference
			P. aeruginosa	BCr3	1.5	Ndeddy and Babalola, 2017
			P.aeruginosa	EP-Cd1	0.45	Muneer *et al*., 2016
			P.riboflavina	AY512822	5.0	Abou-Shanab *et al*., 2007
			P.stutzeri	MTCC101	0.7	Halder and Basu, 2016
			P. aeruginosa	CW-96-1	5.0	Wang *et al.*, 1997
Betaproteobacteria	*Burkholderiales*	*Burkholderiaceae*	*Cupriavidus metallidurans*	DSM 2839T	4.5	This study
	Lysobacterales	*Lysobacteraceae*	*Stenotrophomonas minatitlanensis*	AY512829	0.5	Abou-Shanab *et al*., 2007
	Enterobacteriales	*Enterobacteriaceae*	*Enterobacter cloacae*	CMCB-Cd1	1.90	Haq *et al*., 1999

Class	Order	Family	Genus and species	Strain code	MIC (mM)	Reference
			Escherichia coli	ATCC25922	1.0	Baligarx, 2012
			Klebsiella aerogenes	NCTC 418	0.6	Aiking *et al*., 1985
			Klebsiella sp.	CMBL-Cd2	0.97	Haq
			Klebsiella sp.	CMBL-Cd3	1.97	*et al*., 1999
			K. yangling	12	1.51	Hou
						et al., 2015
			K. planticola	Cd-1	15	Sharma
						et al., 2000
			Proteus mirabilis	BNi6	2.5	Ndeddy and Babalola, 2017
			Salmonella enterica	43C	13.3	Khan *et al*., 2016
Acidothiobacillia	*Acidothiobacilales*	*Acidothiobacillaceae*	*Acidithiobacillus*	DDSM583	500	Baillet *et al*., 1997

Bacteria utilise a range of effective survival mechanisms to assist them in stressful conditions. The mechanisms of bacterial resistance to Cd are shown in Figure 4A.

(A)

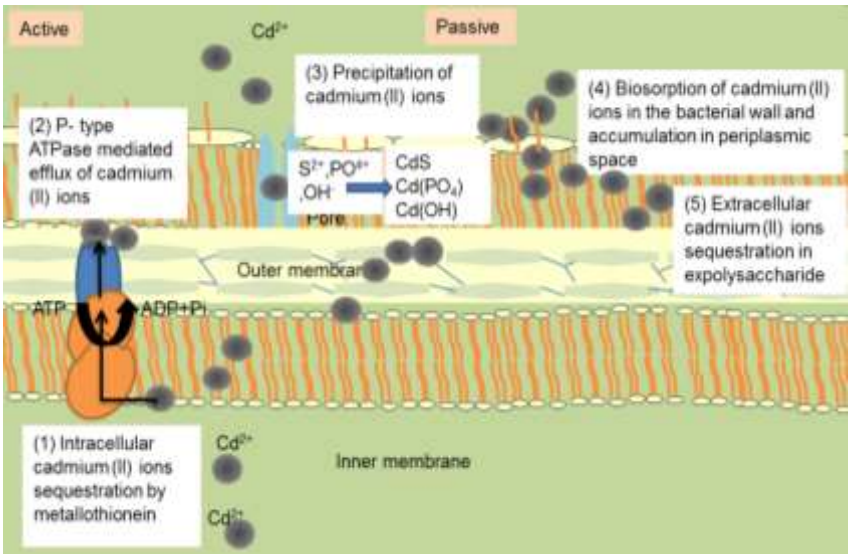

(B)

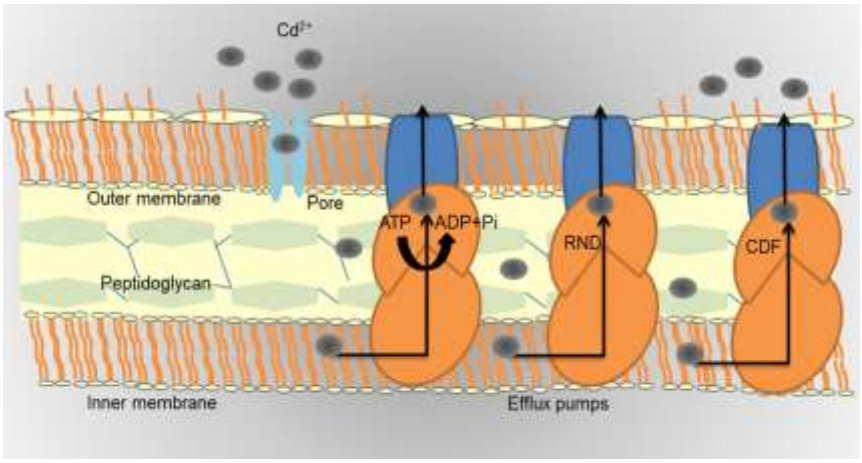

Figure 4. Schematic representation of the bacterial resistance mechanisms to Cd. **(A)** Bacterial defence against Cd. **(1)** Bacteria can deactivate Cd through binding with metallothionein for facilitating the sequestration. (2) The transport of Cd from the cytoplasm to extracellular spaces by efflux pumps. **(3)** Cd can be deactivated via binding with either S, OH, or PO_4 for facilitating precipitation of Cd or **(4)** extracellular substances outside cells for facilitating adsorption of Cd on the bacterial wall (ion exchange, complexation, and physical adsorption). **(5)** Extracellular polymeric substance serves the binding of Cd. The structure was adopted and redrawn according to Prasad *et al*. (2006); Sochor *et al*. (2011); Das and Dash (2017); and Abbas *et al*. (2018). **(B)** Efflux-mediated Cd resistance in bacteria. Cd enters the cell through a transporter. Upon the presence of efflux transporters: P-type ATPase, RND, and CDF, transporters start to pump Cd ions to the out cell. Abbreviations: ATPase (Adenosine triphosphate), RND (resistance-nodulation-cell division) and CDF (cation-diffusion facilitator). The scheme was adopted and redrawn, according to Nies (2003); Rensing and Mitra (2007) and Hynninen (2010).

1-3-2-1 Surface biosorption mechanism

Surface biosorption is an independent metabolism process. Several mechanisms are mediated by surface biosorption such, chelation, complexation, and surface precipitation (Vieira and Volesky, 2000). These mechanisms involve the binding of cadmium to functional groups in the microbial cell wall via electrostatic interactions. As mentioned earlier, the cell walls of the bacteria consist of peptidoglycan, which contains two molecules of NAG (*N*-acetylglucosamine) and NAM (*N*-Acetylmuramic acid), LPS (lipopolysaccharide) and proteins, lipoproteins, porins, and EPS. These components provide several functional groups such as -OH (hydroxyl), -COOH (carboxyl), $-PO_3$ (phosphate), $-NH_2$ (ammonia) and -SH (sulfhydryl), which generally have a negative charge, and concurrently a great binding attraction to Cd cation via van der Waals force or covalent bonding (chemisorption). In the adsorption mechanism (Bruins *et al*., 2000), Cd coordinates with the functional groups, forming cadmium complex, sorbed on the bacterial surface. For example, the reaction of Cd with sulphur bonding is (Xiao *et al*., 2020):

$$Cd + S + 2e^- \rightarrow CdS$$

Following this process, the chelation process could occur (Bruins *et al*., 2000). As the cells are resistant to Cd exposure, they have evolved their chelation mechanism, such as the extracellular production of substances that can complex with Cd, and eventually, cover its occurrence. The chelation (also well-known as complexation) is a firm binding of Cd with a ligand such as EPS, resulting in a stable cadmium complex. The cadmium chelation is the formation of the coordinate bonds, and it is distinguished from a ligand, which forms a complex compound between the ligand and a single central atom of cadmium. EPSs in bacterial cells are related to their roles in the initial attachment of a cell to different unwanted molecules and Cd biosorption. The carboxyl

groups of EPS contribute significantly to the Cd binding site at the bacterial wall of Gram-stain-positive bacteria; whereas, the phosphate groups, which are in the form phospholipids, contribute to Gram-stain-negative bacteria. Recently CadR binding protein, which is responsible for the biosorption of Cd, was found in *E.coli* BL21 (DE3), and the *capB* gene, responsible for Cd adsorption, was present in this strain (Qin *et al*., 2017).

1-3-2-2 Precipitation of cadmium on the bacterial cell surface

The positive charge at cell surfaces resulting from protonation of functional groups at low pH leads to a limitation of Cd cation sorption and their ensuing precipitation on the cell surface, and cadmium remains in solution. Conversely, at a high pH, the functional groups of the cell walls are associated with anions, permitting the approach of Cd cation, resulting in an adequate bond force for sorption to take place. Cell surface precipitation independent of metabolism involves the production of certain compounds when the cells are exposed to Cd, resulting in Cd precipitation. Bacterial cells produce a variety of compounds that react with Cd ions, forming cadmium compounds with different properties. Some of these cadmium compounds have low solubility constants. Some of the theoretical solubility constant in the water at 25 °C are 2.53 $X10^{-33}$ for $Cd_3(PO_4)_2$, 1 $X10^{-28}$ for CdS, 7.2 $X10^{-15}$ for $Cd(OH)_2$, 1.0 $X10^{-12}$ for $CdCO_3$, 2.6 $X10^{-4}$ for CdO and 4.3 $X10^{-1}$ for $CdSO_4$ (Rumble, 2018). With reduced solubility of Cd, the bioavailability and toxicity of the metal are reduced, and precipitation occurs.

Macaskie and Dean (1982) studied the first biological precipitation of Cd by *Citrobacteria* sp. with phosphate, which was mediated by phosphatase to accumulate Cd as $CdHPO_4$. Whereas later, Cunningham and Lundie (1993) suggested the precipitation of Cd in *Clostridium thernoaceticum* as CdS, which was formed by active metabolism of the cells that were able to produce sulfide in a growth culture containing

EDTA. It has been reported that sulfides can be produced biologically by several mechanisms, for example, the engineered *E. coli* produced sulfide by heterologous expression of the thiosulfate reductase gene (Bang *et al*., 2000a). The gene responsible for the surface precipitation of Cd is the thiosulfate reductase gene (*phsABC*), which represents the production of hydrogen sulphide, in *Salmonella enterica* (Bang *et al*., 2000b).

1-3-2-3 Bioaccumulation of cadmium within the cells

Bioaccumulation is a complex detoxification process that involves either the localisation of metal within specific organelles or the enzymatic transformation of the metal within specific enzymes (Bruins *et al*., 2000). The bioaccumulation of Cd involves the intracellular accumulation of Cd, rather than including the enzymatic pathway, which is the possible transformation for the transmission of metals such as Hg, Se, and Cr.

A metal-binding protein, such as the metallothionein can bind with cadmium ions, thereby aiding the accumulation of free-cadmium ions. Metallothioneins are cysteine-rich proteins that are capable of forming stable complexes with different metal cations, such as Cd, Zn, and Cu, to the thiol groups of cysteine (R-SH). Cadmium-metallothioneins sequester Cd within the cell, leading to bioaccumulation and facilitating Cd detoxification by prevention the interaction of Cd with other crucial proteins of cellular metabolism. The first report of bacterial cadmium metallothionein (in *Pseudomonas putida*) was in the early 1980s (Higham *et al*., 1984), and metallothionein was found to be responsible for the sequestration of Cd in *Synechococcus* spp (Li *et al*., 2020). The bioaccumulation of Cd in *Arthrobacter* sp. and *Pseudomonas* sp. has been documented by Scott and Palmer (1990) and Velásquez and Dussan (2009) reported that more ions accumulated in living cells than

dead ones, due to two processes occurring: (1) the adhering of Cd onto the cell surface and (2) the accumulation of Cd inside the cell. Heterologous protein, LamB, which was obtained from gene cloning of *E. coli*, enables binding with Cd (Kotrba, 1999). Proteomic approaches showed that SBP`s (selenium binding protein) overexpression protects *Arabidopsis* from the toxic effects of Cd (Hugouvieux *et al*., 2009).

1-3-2-4 Efflux pumps

The transport of Cd from the outer membrane to the cytoplasm of the cells is a dynamic process. The transporters (either proteins or siderophores) are present at the cell surface, transferring the Cd and concentrating it within the cell. The basic strategy for reducing Cd concentrations within the cell is to pump Cd outside the cell (Wood and Wang, 1983). The efflux pumps are the central detoxification systems of divalent metal ions, including Cd. The P-type ATPase transporter is the primary efflux pump transporter, which is required for Cd resistant microbes to export Cd from their cytoplasm to periplasm. P-type ATPase transporter belongs to the transmembrane transporter family, the superfamily 1B-2 subgroup (Tsai and Linet, 1993). Three cadmium resistant transporters for the efflux pumps are shown in Figure 4 B: the resistance-nodulation-cell division (RND), the cation-diffusion facilitator (CDF), and the ATP-binding cassettes (ABC), (Leedjärv *et al*., 2008). These transporters can be divided further into two classes, CzcCBA, and Czn systems, which are categorised depending on the mechanism they use to pump Cd out of the cell (Stähler *et al*., 2006). Cd transport in Gram-stain-positive bacteria are similar to those of the Gram-negative bacteria, but their transport functions vary. The cation-proton antiporter in the Gram-stain-negative bacteria CDF is a transporter rather than a cation-transporting ATPase, which is the primary transporter in Gram-stain-positive bacteria (Nies, 2003). The proteins CDF, DmeF, and FieF in *Wautersia metallidurans* CH34 (Munkelt *et al*.,

2004), and FrnE protein in *Deinococcus radiodurans* (Khairnar *et al.*, 2013) were found to be the efflux proteins for Cd. RND proteins are the leading Cd exporters in Gram-stain-negative bacteria, as it has been found in *Ralstonia metallidurans* CH34 (Nies, 2003).

1-3-2-5 Molecular mechanisms of cadmium regulation in bacteria

Gesturing proteins, transcriptional regulators, and metabolites are the main mediators of the cell`s response to cadmium. Glutathione, glutamyl- cysteinyl-glycine (GSH) is the significant ligand of Cd ions in *E. coli* K-12. GSH contributed to gain resistance against Cd by using a GSH biosynthetic pathway (Suzuki *et al*., 2005). The activation of methanogenesis studied in *Methanosarcina acetivorans* under cadmium stress found an alternative process that increases ATP yield, which can be used as a biofuel (Lira-Silva *et al.*, 2012). Advancing proteomic analysis has identified the essential proteins to understand the mechanisms that defend microbes against Cd stress. For example, some bacteria resist Cd have been thoroughly studied, and their related genes have been identified. Zhai *et al.* (2017) demonstrated that *L. plantarum* CCFM8610 had prophage P2b 18, CadA, mntA, and lp −3327 proteins, as investigated by the proteomic analysis, and these proteins were associated with the genes: *cadA* and *cadC*. Some proteins have been identified as regulating active Cd translocation between cytoplasm and periplasm of the bacterial cells. These proteins mediate the transporter systems and regulate the Cd efflux, such as *OxyR*, and *OhrR* regulons in *Xanthomonas campestris* (Banjerdkij *et al*., 2005), and *czrA* regulon in *Caulobacter crescentus* (Valencia *et al*., 2013). Also, other types of proteins have been identified as regulating the active Cd uptake amongst the members of ZIP transporter, which are mainly involved in the Cd translocation across the cellular membranes. In *E. coli* GG48, two genes (*zntA* and *zitB*) were recognised to encode for ZIP transporter

(Grass *et al.*, 2002). Some studies indicate the ability of ZIP transporters to carry and uptake Cd, for example, the transporters ZntA, and RcnA contribute to the Cd uptake of *E. coli* ECA580 (Taudte and Grass, 2010). It has been demonstrated that the *zntA* gene of *E. coli* K-12, encodes the Cd transporter, P-type ATPase ZntA, which belongs to the MerR transcriptional regulator family (Binet and Poole, 2000). Many genes such as *cadA*, *cadB cadC*, *cadD* and *cadX*, and many operons such as *cadA* and *cadC* mediate the efflux system (Busenlehner *et al*., 2002). The *cadA* operon has been reported in many Cd resistant bacteria such as: *S. aureus* (Nucifora *et al*., 1989), *Bacillus subtilis* (Tsai *et al*., 1992), *Listeria monocytogenes* (Lebrun *et al*., 1994), *Helicobacter pylori* (Herrmann *et al*., 1999), *Stenotrophomonas maltophilia* (Alonso *et a*l., 2000) and *Pseudomonas putida* (Lee *et al*., 2001). The cadmium operon consists of two genes, the *cadA* gene, which acts as a P-type ATPase transporter, and the *cadC* gene, which acts as a control gene for the *cadA* gene. Figure 5 shows the *cadA* operon and regulation of the expression of Cd resistance in the *S. aureus* pl258 (Nucifora *et al*., 1989). When *S. aureus* pl258 is exposed to low concentrations of Cd, the Cd occupancy decreases it's binding to the regulatory binding protein of the *Rcad* promoter region, which inhibits the translation of mRNA. While, when *S. aureus* pl258 is exposed to a high concentration of Cd, the high occupation of Cd increases the binding of Cd to the *Rcad* promoter region, allowing the translation of mRNA and the expression of *cadA* gene, which confers the resistance to Cd.

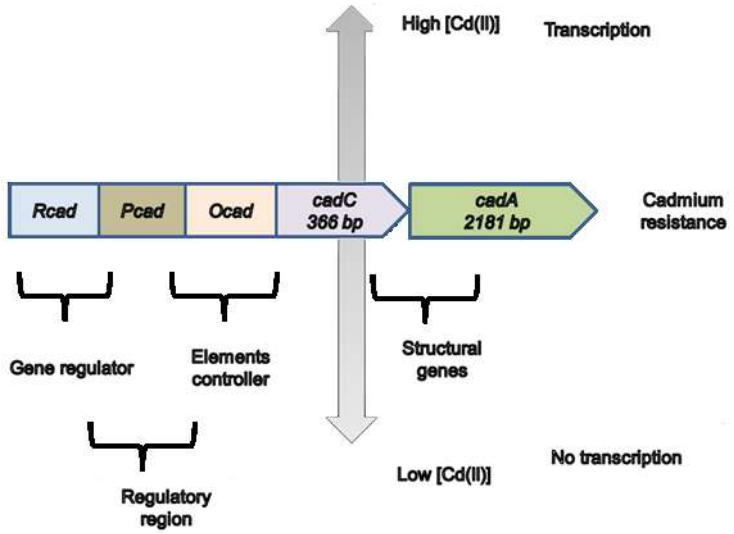

Figure 5. Molecular regulating of cadmium detoxification systems as an example of *cadA* operon structure in *Staphylococcus aureus* pl258 (Nucifora *et al*., 1989). This model was assumed and redrawn according to the regulation model of the expression of cadmium resistance in *Streptococcus thermophilus* 4134 (Schirawski *et al.*, 2002). The regulatory genes and levels of Cd can relieve mRNA-transcription and control the gene expression of *cadA*. The non-existence of binding protein with Cd at low Cd concentrations causes the *Rcad* promoter region to lose the ability of mRNA transcription. Stimulation of the binding of Cd to the *Rcad* promoter region at high Cd concentration causes the *Rcad* promoter region to gain the ability of the mRNA transcription and increases the gene expression of *cadA*.

The genes, which are responsible for Cd resistance in bacteria, can be located on either plasmids or chromosomes. It is reported that the plasmids can encode a reduced susceptibility to any pollutant, which was firstly involved in the toxic metals (Bruins *et al*., 2001). However, it has been suggested that the efflux system, which avoids any internal accumulation of Cd, is due to the plasmid-dependent cadmium resistance. The plasmid- dependent cadmium resistance, the operons *cadA*, and *cadB* have been described in *S. aureus* (Kuroda *et al*., 2001). In addition, the plasmid-dependent cadmium resistance of the transporter zinc-cobalt, *czcNICBADRS* has been demonstrated in plasmid pMOL30 of *R. metallidurans* CH3 (Nies, 1995). *czcNICBADRS* is an inducible non-ATPase cation efflux Cd, Zn, and Co system. However, the essential Cd resistance systems are usually chromosome-based and

are more complex than plasmid-based resistance systems (Khan *et al*., 2015). Chromosomal mediation of the bacterial resistance to Cd could occur in the gene, gaining the genetic elements overexpression of the cadmium detoxification systems (Bruins *et al*., 2001). The chromosome of *P. putida* KT2440 includes the genes: *cadA1* and *cadA2* for P-type ATPase and the two CBA transporters are CzcCBA1 and CzcCBA2 (Cánovas *et al*., 2003). The possibility of the gene expression of the transporters: *cadA1* (P-type ATPase) and *czcCBA1* (CBA) is very low, while the expression of the gene *cadA2* (P-type ATPase) is very high (Leedjärv *et al*., 2008).

1-4 Mechanisms of bacterial bioremediation for cadmium

The two resistance mechanisms that are capable of achieving cadmium bioremediation are biosorption and bioaccumulation. These mechanisms are physiochemical and/or catabolic processes. Physiochemical processes are non-biological, not dependent on metabolism, passive, and include biosorption. Catabolic processes are biological, active, and defined as the metabolic breakdown of molecules into smaller units, thus strictly dependent on cell metabolism and include bioaccumulation (Kim *et al*., 2016). However, both metabolic and non-metabolic processes can be responsible for the precipitation of Cd. The bacterial cell wall consists of peptidoglycan, teichoic acids, phospholipids, and lipopolysaccharides, which are the first useful elements for adsorbing Cd due to having anionic functional groups. Therefore, bacterial bioremediation can be divided into three main steps (Bruins *et al*., 2000):

1) Biosorption is a physicochemical process, in which Cd is passively adsorbed on to the surface of the bacterial cells. The bacteria cell wall consists of peptidoglycan ($C_9H_{17}NO_7$) that has sufficient anionic functional groups that enable binding with Cd. Therefore, biosorption occurs on the surface of either living or non-living

bacterial cells, as the functional groups are available in both forms of the bacterial cells. As discussed in section 1-3-2-1, the availability and types of these functional groups control the process, which is also dependent on the species and concentration of Cd, which is determined by the pH and ion strength of the solution.

2) Bacterial cells act as the precipitation surfaces for cadmium, in a process independent of metabolism, resulting in cadmium accumulation. As discussed in section 1-3-2-2, the adherence of Cd on the functional groups of the cell walls through different biosorption mechanisms is followed by the formation of Cd compounds with reagents produced by the cell that has low solubility and hence are prone to precipitation on the cell surface. The potential advantages of the precipitation of Cd as CdS compound over other compounds is the low solubility product compared to hydroxide, carbonate, and phosphate precipitation (see 1-3-2-2), leading to a fast precipitation rate and the re-use of sulfide. Several bacterial strains such as *Cupriavidus taiwanensis* KKU2500-3 and *P. aeruginosa* KKU2500-8 (Siripornadulsil and Siripornadulsil, 2013) can precipitate cadmium sulfide and generate sulphide under strict anaerobic or aerobic conditions. These strains can precipitate Cd as CdS due to having a cysteine desulfhydrase that has D-cysteine, which contains hydrogen sulfide (H_2S) (Sakimoto *et al*., 2016). This dissolved sulfide can then be complexed with Cd to form insoluble CdS precipitates. The precipitation of CdS is typically associated with the bacterial cell wall and occurs predominantly in the periplasmic space. Marusak *et al*. (2016) provided evidence for this process in engineered *E. coli*, from which they harvested, and purified nanoparticles (NP), and NP formed CdS.

3) Following the surface interactions (adsorption and precipitation), Cd-bioaccumulation as an intracellular interaction of cadmium ions with the cell

components may occur (see section 1-3-2-3). As Cd bioaccumulation is more efficient in live cells (Velásquez and Dussan, 2009), using live bacterial cells in bioaccumulation is desirable, and this requires adjustments of nutrients and other environmental conditions during bioremediation.

1-4-1 Phytoremediation of cadmium

Cd-bioaccumulation is well-applied in the remediation of Cd by rhizobia, diazotrophic bacteria to improve the accumulation of cadmium by plants in phytoremediation (Ike *et al*., 2007). Phytoremediation has also been used for the treatment of soil contamination with metals. The use of phytoremediation for cadmium and other compounds were first reported in the 1970s (Henry, 2000). Some plants have developed different mechanisms of selective phytoremediation of cadmium from soils. Most Cd phytoremediation in the root and shoot systems occurs via the process called phytoextraction, or through rhizofiltration, the adsorption and precipitation of cadmium in the plant`s roots. Another mechanism of phytoremediation is phytostabilisation, which is the process of reducing the migration of contaminants by limiting their mobility (Kuppusamy *et al*., 2016).

1-4-2 Bioremediation of cadmium involving extracellular polymeric substance (EPS)

Bioremediation of Cd may be facilitated by cadmium uptake through the production of EPS. EPS can be used in bioremediation as mixed culture EPS, single-cell EPS, live, dead, or immobilised EPS. EPS contains polysaccharides, proteins, and lipids, which have functional groups such as sulfhydryl, amino, carboxylic, and phosphate groups that enable binding to metals. The accumulation of the metal ions onto the cell wall by EPS is used widely in the bioremediation of Cd and other metals, as listed in Table 7.

The removal capacities for metals vary, depending on the reduction potential, atomic weight and the ionic size of the metal.

Table 7. The removal capacities of some of the bacterial species derived EPS used previously for the bioremediation of some metals.

Bacterial species derived EPS	Removal capacity (nmol /g EPS)	Reference
Gloeocapsa gelatinosa	396 Pb	Raungsomboon *et al*., 2006
Calothrix marchican	314 Pb	Ruangsomboon *et al*., 2007
Lactobacillus plantarump	1333 Pb	Feng *et al*., 2012
Wangia profunda SM-A87	535 Cd	Zhou *et al*., 2009
Paenibacillus jamilaen	1449 Pb	Morillo *et al*., 2006
	187 Cd	
Azotobacter chroococcumn	161 Pb	Rasulov *et al*., 2013
	190 Hg	
Chryseomonas luteola	7.5 Cu	Ozdemir *et al*., 2005a
	20 Ni	
Chryseomonas luteola	570 Cd	Ozdemir *et al*., 2005b
Ochrobactrum anthropic	1117 Cr	Ozdemir *et al*., 2003
	412 Cu	
	263 Cd	

Table 7 shows the variation in the removal capacities for certain metals that are related to the properties of the bacterium, such as active functional groups of EPS. Gupta and Diwan (2017) reviewed the advantages and disadvantages of using EPS in metal bioremediation: EPS is a cost-effective material and can be recycled for the adsorption and the recovery of metal ions. However, EPS shows low abilities for biosorption and requires maintaining the viability of live cells during the biosorption process. In addition

to the contribution of EPS of bacterial cells in the detoxification system of Cd, its role in the bioremediation of Cd has been well-studied (Zhou *et al*., 2009).

1-5 Bioremediation techniques for groundwater

Bioremediation techniques are classified as *ex situ* and *in situ*.

1-5-1 *In situ* bioremediation techniques

In situ bioremediation techniques involve the treatment of contaminates in their original location. The foundation of *in situ* bioremediation techniques contains the injection of oxygen or nutrients into contaminated sites via different methods, with the main aim of stimulating microbial activity to enhance the bioremediation process. Anaerobic *in situ* bioremediation techniques are more cost-effective than using aerobic *in situ* bioremediation techniques, which require oxygen supplying equipment (Evans and Furlong, 2003).

One of the possible *in situ* bioremediation techniques for cadmium is bioaugmentation. Bioaugmentation is a process, which involves the addition of materials such as manure, oleophilic fertilise force aeration and nutrient supplementation to enhance bioremediation by indigenous microbes, which either could be a pure consortium or genetically engineered bacterial strains (Liu *et al*., 2010). For example, *Micrococcus* sp. MU1 and *Klebsiella* sp. BAM1 were used in the bioaugmentation of cadmium from groundwater by adding 30 mg/kg of EDTA into 0.8 mM of Cd (Prapagdee *et al*., 2013). The main advantages of *in situ* bioremediation are the minimal operating equipment, which needs fewer site workers, resulting in a cost-effective process. Also, the completion of the bioremediation occurs in the same place, resulting in a reduction of risk to the ecosystem. However, the disadvantages of *in situ* bioremediation are the difficulties in optimising the environmental conditions

for bioremediation of the contaminants, resulting in low process efficiency (Sharma, 2019).

1-5-2 *Ex situ* bioremediation techniques and designs of bioremediation reactor

The common bioremediation technique is *ex situ*, which involves the pumping of groundwater to the surface, to be remediated by microbes with an installed system called a reactor. The reactor supports the bacteria during the desired process by controlling the environmental conditions (Mueller *et al*., 1993). The use of reactors for the treatment of wastewater has been practised in the 1990s, and the basic design was later adapted for groundwater treatment purposes (Fitch *et al*., 1998). However, the reactors used for the groundwater treatment for drinking purposes deals with low concentrations in µg/L, compared to wastewater, which deals with concentrations in mg/L.

There are two types of bioremediation reactor configurations, depending on the forms of bacteria, which include suspended and fixed film reactors. Suspended growth reactors, such as membrane reactors, involve the suspension of microorganisms in contaminated water. Fixed film reactors consist of fluidised, fixed-bead, and trickle-bead reactors, whereby the microorganisms are fixed to a support material.

The basic process of a membrane reactor includes an activated sludge. The membrane reactors consist of a combination of conventional bioremediation processes, such as bacterial cells and activated sludge with membrane filtration, which provides an advanced level of Cd removal in suspension. An example of the membrane reactor being practised for Cd treatment was designed by Huang *et al.* (2017) using *Pseudoalteromonas* sp. SCSE709-6. An air diffuser is introduced from the bottom of the reactor to supply oxygen and to lessen membrane catching.

On the other hand, many immobilised bacterial species have had cadmium removal applied through batch experiments or fixed film reactors.

The batch experiment is static and applied to investigate the optimal removal efficiency at different conditions, determining the best factors for removal, the equilibrium capacity, and the mechanism. However, dynamic column experiments practically use the removal process. The first fluidised reactor was used in the 1700s for the treatment of wastewater (Sutton and Mishra, 1994). The basic principle of the fluidised reactor is the fluidisation of the immobilised beads via high recycling rates of water, which are to be treated. The fluidised-bead reactor mainly involves the biomass produce on the granular support material. Fixed bead reactors are used for the absorption operations by randomly oriented packing material that has the purpose of bioremediation.

Langwaldt and Puhakka (2000) reviewed the benefits of the fixed-film reactors that were designed for groundwater treatments. Among them was the up-flow fixed film reactor, which was operated in anaerobic conditions and more beneficial, based on the adjustments of the residence time. Up-flow reactors are widely used for the clean-up of contaminated water that is applied at a bench, pilot, and full-scale process. Fixed bead reactors are filled with beads, in which the liquid reactants flow down or up. The fixed bead reactors are an assembly of randomly arranged beads that are bathed by the reactant fluid, which flows in a random manner around the beads. This reactor was applied successfully in different contexts in the 1950s in water treatment, industrial and laboratory applications (Kolev, 2006). Today, the immobilised column reactor is widely used in chemical industry processes such as hydro desulphurisation and hydrogenation, in wastewater effluent treatment, and enzymatic reactions. Fixed bead reactors are simple in construction and maintenance; however, flexible operations and a high mass transfer due to the ratio of liquids to solids is small (Coker, 2001).

Therefore several researchers have tested laboratory and pilot-scales using column-bead reactors for water treatments. Immobilised column reactors have been tested for Cd removal from contaminated water using pure and mixed bacterial cells. On a laboratory scale, a fixed bead reactor was used for cadmium treatment (Veneu *et al*., 2017). The application of this reactor has been shown to obtain reasonable removal rates (99 %), and Edwards *et al*., 1994 state that the removal could be obtainable at the short time of hydraulic residence time (12 minutes). Over the time of operation, the reactor, the efficiency decreased due to a desorption process. Zheng *et al*. (2019) found that Cd removal was obtained after 60 min from operating the reactor.

The trickle-bead reactor is another type of fixed-film reactor. The structure model of the trickle-bead reactor is similar to the fixed bead reactor, but the trickle-bead reactor has multiple columns. Although the suspended growth reactor usually establishes higher bioremediation activity than immobilised reactors, the immobilised reactors are cost-effective, easy to maintain, and ideal for water treatments due to the low requirements of the column area of the immobilised cells and the lack of air diffuser.

1-6 The present work

Aims of the project

This study aims to find methods for the bioremediation of cadmium from water. This alternative will be based on natural microbes with resistance to Cd that are isolated in order to augment their resistance then, to further enhance their application in the bioremediation of Cd. Recent developments in the bioremediation process have increased the need for greater development on three key issues:

1) Microbial resistance capability based on microbial relationships and cadmium concentration;

2) Lack of procedural knowledge needed to provide strategic guidance for environmental biotechnology, and

3) Lack of improvement in the bioremediation process.

Considering the above issues, this research will attempt to develop environmental biotechnology and the bioremediation process and investigate on a small laboratory scale the removal of cadmium from water.

This study hypothesises that the strain of developed Cd-resistant bacterium may improve cadmium removal. The initial concentration of cadmium in water is expected to affect the process, in addition to various environmental factors, including pH, ions, and humic acid present.

The objectives of this study are:

1. Isolation and identification of Cd-resistant bacterium from the soil of Hay Tor quarry, Dartmoor, England.
2. Improvement of the Cd-resistant ability of the isolated bacterium using UV light mutagenesis.
3. Assessment of the improved strain capacity in the development of Cd removal from artificial groundwater (AGW), using small laboratory bench-scale column reactors with different initial concentrations of Cd (4.4, 8.8, 13.4 and 17.4 μM).
4. Study of the effects of various environmental factors on the bioremediation of Cd from AGW in the reactor, including different pH values, and in the presence of existing ions and humic acid.
5. In general, cadmium precipitation and speciation will be tested in AGW, using the geochemical speciation software Visual MINTEQ.
6. Investigation of the bioremediation of Cd from natural river water (NRW, Walkham River), including the addition of Cd to the river sample.
7. Hazard classification and risk assessment of the developed bioremediation products in this study.

Chapter 2. General Methodology

2-1 Preparation of culture media

The wild type and mutant strains were cultured in a minimal growth medium: E-basal salts (EBS). Boden *et al*. (2008) developed an EBS, according to Kelly and Syrett (1964) and Tuovinen and Kelly (1973). The EBS was prepared and autoclaved separately with two-part solutions and mixed before use. The part A solution consisted of 4.0 g potassium dihydrogen phosphate and 4.0 g dipotassium phosphate dissolved in 250 mL ddH_2O. The part B solution consisted of 0.4 g ammonium chloride, 0.8 g magnesium chloride heptahydrate, and 10.0 mL of Kelly`sT solution dissolved in 750 mL dd$H_2O$. Kelly`sT solution was prepared, as described by Tuovinen and Kelly (1973). This solution was made by dissolving 11 g of sodium hydroxide in 500 mL ddH_2O, followed by 0.5 g $(NH_4)_6 Mo_7O_{24}$, 7.34 g $CaCl_2$ $2H_2O$, 0.2 g $CuSO_4$ $5H_2O$, 50 g EDTA-Na_2, 5 g $FeSO_4$ $7H_2O$, 2.5 g $MnCl_2$ $4H_2O$, and 11 g $ZnSO_4$. HCl (1M) was used to adjust the pH of Kelly`sT solution to 6.0 using a pH meter. A darkened glass bottle was used to store Kelly`sT solution at constant room temperature. When part A and part B mixed, D-fructose was added to give a concentration of 10 mM in the final volume of EBS using a volumetric flask (1000 mL). However, the concentration of the carbon source that was to be added to the EBS varied, depending on the designed experiment.

2-1-1 Batch culture cultivation and storage

A pure colony grown on EBS agar was picked up using a flame-sterilised wire loop, stained with Gram stain, and observed under a light microscope at X1000 magnification with oil immersion. From the same colony, an inoculum was prepared in 30 mL of EBS broth and transferred into 45 mL of EBS broth in a sterile Erlenmeyer flask (250 mL) and incubated at 37 °C for 24 h in an orbital incubator operating at 100 rpm (Gallenkamp, Loughborough, UK). Gram staining was used to check for culture

purity, and the culture was then harvested by centrifugation at 4 °C using an Avanti J-26XP centrifuge (Beckman Coulter) for 15 mins at 16000 rpm. The harvested cells were then washed by suspension in an ice-cold PSB buffer (pH 7.4) and centrifuged twice to remove any extracellular exonucleases. The cells were finally suspended in the PSB buffer and stored at − 80 °C until they were needed for experiments. For long-term storage, the growth cultures were maintained in sterilised glycerol (10% (*v*/*v*) in vials (1.5 mL). The vials were vortexed to ensure that the glycerol and bacterial cultures had mixed well. These vials were frozen in nitrogen liquid and kept in a freezer at − 80 °C.

2-1-2 Growth kinetics

The experiments were carried out in batch culture with 50 mL of EBS in a sterile Erlenmeyer flask (250 mL) in triplicate. One mL of bacterial inoculum was transferred into the broth medium and incubated at 37 °C for experiment times in an orbital incubator operating at 100 rpm.

The growth of cells in the EBS was determined in terms of dry biomass. From the batch cultures, samples were collected at regular times, and the dry biomass was determined. The growth of bacterial strains was determined by measuring the optical density (*OD*) at 440 nm using a UV visible spectrophotometer against a cell-free EBS medium as a blank. The *OD* should be within the range of 0.2 to 0.9. It was assumed that 0.1 of *OD* was equivalent to 23 mg/L of dry cell biomass of strains. After determining the dry biomass of the growth culture at regular times, the logarithmic dry biomass against the times was plotted to obtain the bacterial growth curve as a semi-logarithmic graph. The curve was fitted with the nonlinear regression of the biomass mean data using the SigmaPlot (version 13).

The growth curve was used to measure the specific growth rate by plotting one point of the exponential phase of the amount of biomass of bacterial growth (axis *y*) and its double point against time (axis *x*). Monod`s equation (1949) was used to calculate the growth rate.

2-2 Operation of small laboratory bench-scale reactors

2-2-1 Optimisation of the reactor

The reactor system consisted of three columns (10 mL), which had a 1.60 cm inner diameter and was 8.63 cm long (high-grade polypropylene); it was run by the up-flow pump-fed system, using a peristaltic pump (model MCP 3 channel, Pharmacia Fine Chemical Company) to pump Cd-AGW from one bioprocess bag. The eluants to be collected from each column separately. AGW was used as a source of Cd removal with a similar real groundwater composition to the study of removal under controlled composition. AGW was used as a source of Cd removal that has the same groundwater composition to that studied in the removal under a controlled composition. AGW was prepared in ddH_2O, according to Knobel *et al*. (1992), which contained potassium nitrate (40.3 μM), magnesium sulphate heptahydrate (448 μM), calcium chloride (175 μM), sodium nitrate (44 μM), sodium hydrogen carbonate (1100 μM), and potassium hydrogen carbonate (62.3 μM). The weight method was used to measure the total volume of the column reactor by fitting the adapter caps firmly on the top of the three columns and pumping the AGW into the columns. The column head (adapter) was removed, and the AGW was transferred into a beaker. The mass of AGW was determined by measuring the mass of holding AGW based on density (ρ) of AGW, which was determined using a pycnometer (50.329 mL at 22 °C). The pump flow rates were calibrated using the column reactor (Figure 6).

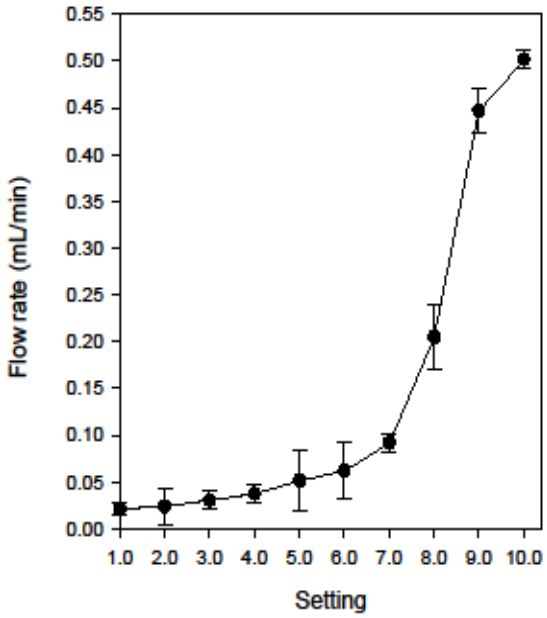

Figure 6. The flow rate curve at different settings of the peristaltic pump pumped through the column reactor filled with Ca-alginate beads. The error bar represents the standard error of the mean (*n* = 1, one reactor with three columns).

The hydrodynamic residence time (HRT) of the reactor system was calculated based on the volume occupied by the beads. Two methods were used to determine the volume of the selected beads. The first method was determined by measuring the mass of each column by filling them with AGW and beads. The difference between the volumes of the total liquid of an empty column and the volume of the filled column is the volume of the beads. The precise method of measuring the volume of the beads was determined by measuring the total areas of all beads that were placed in the column after initially measuring the diameter and the volume of each bead. After the volumes of the beads were determined, AGW liquid holdup was determined from the differences between the total volume of AGW and the volume of the number of beads that fitted into the columns. Then, the HRT was determined by dividing the value of the liquid held with the value of the flow rate.

2-2-2 Characterisation of embedding bacterial cells in Ca-alginate beads

Cells of *B. agri* C15 and *B. agri* C15 Cd^R were immobilised using an entrapment method with Ca-alginate gel (Li *et al*., 2018). Sodium alginate powder (3 g) was dissolved in 100 mL of sterilised ddH_2O by stirring for one h at 60 °C and was added to 100 mL of mixed cell suspensions-AGW, without $CaCl_2$. The cell suspension was obtained by growing strains in EBS/pyruvate (20 mM), with a nominal concentration of Cd (13 mM Cd for *B. agri* C15 and 18 mM for *B. agri* C15 Cd^R) and incubated shaking at 100 rpm, 37 °C. From the late exponential phase, the cells were cooled in ice for an hour, centrifuged, washed with, and suspended in AGW without $CaCl_2$. The obtained sodium alginate cells were mixed using a sterilised glass rod for 10 mins, loaded into a syringe (size 1mL) without the needle and dropped into $CaCl_2$ solution (100 mL, 2% *w/v*). The dropped mixture turned into beads within a few seconds. After an hour, the formed beads were hard, removed using a sieve, and washed to remove any $CaCl_2$ with sterilised ddH_2O. Finally, the beads were dried, transferred into the tube (50 mL, Falcon), stored at 4 °C and used within 48 h. Boiled-cells (killed-control cells) were used as adsorbents for Cd. To embed killed-control cells in calcium alginate matrix, estimates of the optimal killing times of both strains, which caused 100% of killing the cells, were obtained. The killed-control cells were obtained through the incubation of suspension cells at 100 °C in a water bath for 15, 30, 45, 60, and 90 mins, and a mercury-thermometer in a glass was used to measure the temperature of the cell suspensions. The cells from each incubation were spread on Reasoner's 2A (R2A) agar, incubated at 37 °C for 16 h, along with controlled cells, which were incubated at constant room temperature (22 °C). The CFU per plate was counted, and the percentage of CFU against the times of killed-curve was plotted. After the determination of the time that caused 100% of killing cells, the cell suspension, which

boiled at 100 °C for the optimal boiled time, was mixed with AGW, without $CaCl_2$ and with alginate solution (100 mL) in a 250 mL beaker. To obtain Ca-alginate beads without bacterial cells, AGW without $CaCl_2$ was used instead of bacterial cell suspension, and the preparation of the alginate beads in $CaCl_2$ was performed as explained above.

The mean volume and the mass of the beads were determined, and the diameter of all types of beads was measured using a micrometer. The bead diameters were recorded and presented in diameter distribution curves (Figure 7 (a, b, c, d, e)). The diameter values that have 50% in the distribution curve were chosen as the best bead diameters to be filled in the column reactor. The mean of the selected diameters was determined within the standard deviation (SD) of 200 beads. The diameters ranged from 0.5 mm to 5.0 mm, and a mean diameter of 2.9 mm (SD = 0.8266 mm) was obtained. Most beads (23%) showed a mean diameter ranging from 3.2 – 3.4 mm, and 50% of beads between 2.5 mm and 3.5 mm. The masses of the selected beads (50% of diameter values in the distribution curve) to be used in the column reactor were measured to normalise the recorded concentrations of cadmium. A sensitive analytical balance (Pioneer, Ohaus Company) was used to measure bead masses, and sterile forceps were used to hold and measure each bead. In addition, the different bead masses were recorded and presented in histogram charts, combined with the distribution curves. The distribution of bead diameters (Figure 7 (f, g, h, I, j)) showed a mean mass of 53 mg (SD = 64 mg) with a smaller mass distribution compared to diameter distribution. The bead mass ranged from 35 to 65 mg, and 30% of beads showed an average mass of 55 mg, with 50% of beads between 48 mg and 55 mg. After the beads were selected, they were stored in Falcon tubes, kept at 4 °C, and used in the column reactor within 48 h.

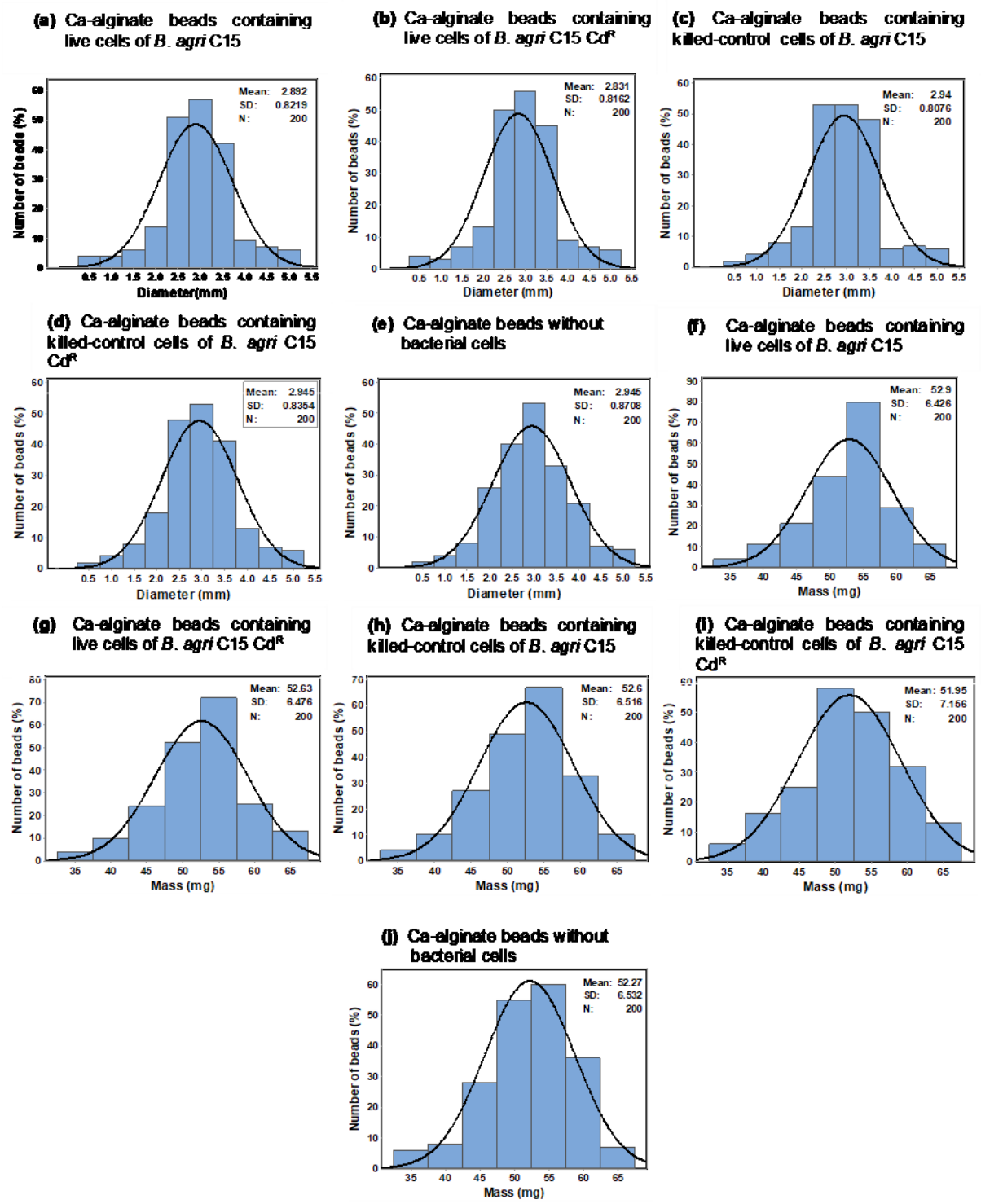

Figure 7. Characterisation of typical Ca-alginate beads containing live and killed-control cells of *B. agri* C15 and *B. agri* C15 Cd^R, and Ca-alginate without bacterial cells. The mean of the measured diameters and masses of the beads were determined within the standard deviation (SD) of the total number of 200 beads. **a, b, c, d** and **e** histograms of bead diameters measured by a micrometer and a mean of diameter was 2.9333 mm (SD = 0.8266 mm). The respective histograms of bead masses measured by a sensitive analytical balance and a mean mass was 53 mg (SD = 0.64 mg) as displayed in **f, g, h, i** and **j**.

After optimising the reactor system, as shown in Table 8, reactor experiments were identified and conducted as described in Chapters four and five.

Table 8. The conditions of the experimental setup and operating of the study reactor.

Parameter	Value
AGW density	1.0
Diameter of bead	Range:3.2 –3.4 mm
Mass of bead	Range:40 – 50 mg
The volume of liquid holdup	Mean:4.5 ± 0.6 mL
The total volume of bead	Mean:3.7 ± 0.25 mL
Flow rate	Mean:40 ± 0.32 µL/min
Hydraulic residence time	Mean:112.5 ± 0.9 min

2-3 Scanning electron microscopy

Bacterial cell colonies and Ca-alginate beads were examined using scanning electron microscopy (SEM, JEM-6610LV). Two fixation techniques were used in fixation samples before the observation: the standard technique (control, DEC (*N*-(3-dimethyl aminopropyl)-*N*′-ethyl carbodiimide) and the ABL technique (Alcian blue with L-lysine). Both methods briefly included cutting, fixing with osmium tetroxide, and serial dehydration. Samples, in triplicate, were fixed in 1% osmium tetroxide in a cacodylate buffer (0.1 M) for 60 mins. The blocks were transferred into a new 24 – well plate and fixed either in 3% *w/v* of EDC or in 16% paraformaldehyde, in 0.75% *w/v* of Alcian blue, in L-lysine hydrochloride (0.5 M), and 25% glutaraldehyde, for 60 mins, followed by subsequently washing it twice in cacodylate buffer for 30 mins. The samples were then post-fixed in 1% osmium tetroxide in a cacodylate buffer (0.1 M) for 2 h, followed by subsequently washing twice in filtered ddH_2O for 30 mins. The dehydration of the samples was carried out by subsequent washing in a series of ethanol (10%, 20%,

40%, 60%, 75%, 90%, and 100%) for two h and dehydration at 100% was repeated three times. A critical point drier (EMTECH K850) was used to dry the samples, and gold was used to coat the dried samples.

2-4 Transmission electron microscopy

Bacterial cell suspensions were examined using transmission electron microscopy (TEM) (JEM-1400). The cell suspensions, which were harvested and suspended in 1mL Dulbecco buffer and fixed in 2.5% glutaraldehyde (1 mL), in cacodylate buffer (0.2 M, pH 7.2, prepared in ddH_2O and filtered using a filter paper size 0.2 µm), were washed in 1mL of Kellenberger buffer. The Kellenberger buffer was prepared as follows: 5 mL of Veronal-acetate solution (2.94 g of sodium barbital (Veronal), 1.94 g of sodium acetate, 3.40 g of sodium chloride in 100 mL ddH_2O), 13 mL of ddH_2O, 7.0 mL of 0.1M hydrochloric acid, and 0.25 mL of calcium chloride solution (1M). The pellets were added to 0.2 – 0.5 mL of the Noble agar (0.2 g of Noble agar prepared in 10 mL Kellenberger buffer solution and heated to 95 °C in a water bath for 30 mins); it was then poured out onto a microscope slide and left for 30 mins. After solidification, the agar, with cell pellets, was trimmed into blocks with a sterilised blade, three blocks in total for each strain and treatment. The agar blocks were then post-fixed in 1% osmium tetroxide in a cacodylate buffer (0.1 M) for 16 h, followed by subsequent washing twice in Kellenberger buffer for 30 mins. The agar blocks were resin-embedded sequentially with 1) 30% resin and 70% ethanol, 2) 50% resin and 50% ethanol, 3) 70% resin, and 30% ethanol, and 4) 100% resin for 24 h, followed by sectioning, and mounting.

2-5 *Aqua regia* digestion

The determination of the elements in the soils and the Ca-alginate beads were analysed after *aqua regia* digestion. The *aqua regia* was prepared by mixing 1 volume of nitric acid (>68%) with three volumes of hydrochloric acid (<37%); the development of the golden solution was obtained after a few mins. To each sample in a Falcone tube (50 mL), 10 mL of the *aqua regia* was added and left for 24 h; the volume was then completed to 25 mL with 0.2% of nitric acid.

2-6 Statistical analyses

All experiments were carried out in triplicate (unless stated otherwise), and the resulting data were expressed as the mean ($n = 3$). SigmaPlot (version 13) was used to graphically express the data as mean, and the error bars represent the standard error of the mean ($n = 3$). IBM SPSS statistics 22 software was used to analyse the results using analysis of variance (ANOVA), followed by a Student's *t*-test or Tukey *post hoc* if a significant difference was found at the 95% confidence level ($p < 0.05$). Tests for significant differences were carried out between the isolates under different bacterial growth conditions, and the differences were indicated by distinct letters. Similarly, the differences in percentages of Cd species distribution in AGW (10 µM Cd), as predicted using Visual MINTEQ under the effect of different factors, were carried out. SigmaPlot (version 13) was used to fit bacterial growth curves with nonlinear regression (global curve fitting, four parameters), and to fit the curve of the amounts of total Cd measured in eluants of AGW with nonlinear regressions (exponential decay) and then with tangent lines. *B. agri C15* growth data and maximum amount of biomass formed by *B. agri* C15 and *B. agri C15* Cd^R were analysed using Student's *t*-test with the presence/absence of Cd. The differences in removal rates and cumulative amounts of Cd by each bead were tested using a Tukey

post hoc test and the differences in the amounts of Ca, Na, and Mg in the beads before and after the Cd uptake process was tested using a Student's *t*-test. The total and bioavailable concentrations of Al, Ca, Cd, Co, Cu, Fe, K, Mg, Na and Zn for *B. agri* C15 and *B. agri* C15 Cd^R, and the bioaccessible fractions for both strains in each adsorption matrix were compared between gastric and gastrointestinal phases using ANOVA, followed by Tukey *post hoc* test.

Chapter 3. The isolation and identification of cadmium-resistant *Brevibacillus agri* C15 and the use of ultraviolet-light mutagenesis to generate a mutant with elevated cadmium resistance, *B. agri* C15 Cd^R

Abstract

Cadmium (Cd) is toxic to living organisms; however, bacteria are adaptable to severe conditions, including Cd contamination. Bacteria can develop in the natural environment, as they generate resistant strains that can be used to remove Cd, but getting such adaptive strains usually takes a long time. In this study, strain isolation was performed from the soil, and UV light mutagenesis was used to accelerate the strain-resistant ability to generate Cd^R mutant with high resistance to Cd. Eight Cd-resistant bacteria were isolated from the soil. Based on the resistance and specific growth rate, one isolate from these was chosen. The 16S rRNA (*rrs*) gene sequence was used to ascertain that this isolate belongs to the genus of *Brevibacillus* and is closely related to *B. agri* DSM 6348^T (AB112716). The isolate was, thus, termed *B.agri* C15. Its minimum inhibitory concentration (MIC) to Cd was 16 ± 0.7 mM. The specific growth yields and the Cd-dependent fall in specific growth yield of *B.agri* C15 were determined under different concentrations of Cd. The UV light mutagenesis process resulted in the generation of the mutant *B. agri* C15 Cd^R (MIC: 21± 0.4 mM Cd). Morphological and biochemical tests showed that there were no major differences between *B. agri* C15 Cd^R and *B. agri* C15. Scanning electron microscopy (SEM) and transmission electron microscopy (TEM) showed no morphological effects of Cd on either of the strains. This study provides a basis for developing microbial Cd resistance and facilitating the application of Cd remediation.

3-1 Introduction

The contamination of groundwater with metals has become a global challenge in relation to human health (Shepherd *et al.,* 2006). Cd contamination in groundwater, exceeding the US EPA limit of 3 μg/L, has become a major concern, especially in relation to increasing groundwater withdrawals for human use and agricultural irrigation. This contamination may be subject to regulatory requirements for treatment, and more effective methods for removing Cd are required. Techniques, such as precipitation, adsorption, ion exchange, and bioremediation are used to remove Cd from groundwater (Hashim *et al*., 2011). Bioremediation is the process of transfer, forming contaminants to less harmful substances and, depending on the type of pollutant, and different approaches can be employed. One approach is the development of bacterial resistance to the pollutant with the aim of enhancing remediation efficiency. At this moment, engineering strategies are being investigated to increase further the Cd resistance of microbes, such as cloning the gene for metallothioneins (Ike *et al*., 2007), over-expressing metal-binding proteins, such as poly-histidine (Sousa *et al*., 1996) or poly-cysteines (Wu *et al*., 2006). Chemical mutagenesis approaches have been widely applied to develop bacterial detoxification systems for Cd, such as *Lactobacillus plantarum* ATCC 8014 (Hao *et al*., 1999) and *Enterobacter cloacae* TU (Xu *et al*., 2017). An alternative approach to increase bacterial resistant ability is the use of ultraviolet (UV) light mutagenesis. The advantages of using the UV light are its simplicity, safety, and cost-effectiveness; there is also no need to establish a genetic system for the target organism, which can be useful when using it to create a mutant from a newly isolated strain. Ultraviolet (UVC) causes direct DNA damage due to the induction of the formation of DNA lesions

(photoproducts), most notably pyrimidine dimers, which block DNA replication, and RNA transcription (Deng *et al*., 2015). Cd-resistant bacteria are often used as one of the remediation technologies for Cd. The main aims of this study were to isolate Cd-resistant bacteria from soil and to generate a mutant with elevated resistance to Cd using UV-light mutagenesis.

3-2 Methodology

3-2-1 Soil sampling from the contaminated site and isolation of bacteria to resistant cadmium

In this study, for the isolation of Cd-resistant bacteria, Hay Tor quarry, Dartmoor, England was chosen as a source for the isolation of the strains, as this soil has been contaminated with cadmium copper, tin, silver, and lead due to historic mining activities (Howard *et al*., 2015). The global positioning system (GPS) coordinates of Hay Tor are 50-577054" N latitude and 3.75549" W longitude. One kg of clayey soil was collected in a sterilised plastic box, transferred to the laboratory, and stored in a refrigerator at 4 ºC until required; within 24 h.

For elemental analysis, a sub-sample of the soil was dried at 50 ºC – 60 ºC for 72 h, then disaggregated and ground using a mortar and sieved by 180-micrometer particle sizes. Cadmium was extracted from the soil via *aqua regia* digestion (as described in Chapter 2), and the concentrations in the extract were determined using inductively coupled plasma mass spectrometry (ICP-MS). The ICP-MS analysis was conducted according to work carried out by McBride and Spiers (2001). Briefly, 1.0 g of sieved soil (n = 3 samples) was processed following *aqua regia* digestion using a Tecator digestion at 60 ºC for two h. After digestion, the solution was cooled, filtered (Whatman 541) into a clean volumetric flask, and the volume was completed with 2% HNO_3. The

limit of detection for the ICP-MS analysis (LOD) for Cd (0.02 μM) was established from the five standard deviations (SDs) of measuring the lowest standard (*n* = 10). No CRM containing appropriately high Cd concentrations was available and hence, an in-house reference material, contaminated soil SS-2, was used to indicate recovery.

The percentage recovery of ICP-MS via the use of contaminated soil- SS-2 was Cd (50%), which was calculated from the recorded (4.0 ± 0.3 μmolal Cd) and certified (8.0 ± 0.06 μmolal Cd) values of the reference material. However, the procedural blank (*n* = 3 samples) was of a similar magnitude (3.0 ± 0.03 μmolal Cd) as this reference material, explaining the poor recovery obtained.

For the enrichment of bacteria, 0.5 g of the soil sample was transferred into 250 mL of Erlenmeyer flask containing 50 mL of EBS supplemented with D-fructose (10 mM) as a carbon source. The flask was incubated at 37 °C for five days, and the turbidity was monitored regularly. After incubation, 5 mL of enriched bacterial culture was transferred to 45 mL of EBS/D-fructose. The serial subculture was repeated for four-time cycles until an enriched bacterial growth was obtained, at which point isolation was attempted.

The isolation was preliminarily done in terms of maximum tolerable concentration (MTC) to Cd (Schmidt and Schlegel, 1994). Five mL of the bacterial culture was inoculated into 45 mL of EBS/D-fructose in Erlenmeyer-flasks (250 mL) in triplicate, amended with Cd and incubated at 37 °C for 48 h. The nominal concentration of Cd (supplied as $Cd(NO_3)_2 \cdot 4H_2O$) started at 1 μM and increased by 2 μM at each transference of the screening process. A control without Cd was used to determine whether there was growth at each step. The concentration below that at which no growth occurred was accepted as the MTC. After the determination of MTC values,

three cultures were grown with Cd at their MTC values, which is 10 mM for two of the cultures and 15 mM for the third. To obtain single colonies from each bacterial culture (the MTCs of 10 mM and 15 mM), 100 μL of the culture was spread onto EBS/ D-fructose agar plates (in triplicate) supplemented with Cd. The nominal concentrations of Cd (mM) were below and above MTC values of the bacterial culture. The plates were incubated at 37 °C until the colonies were visible. After growing the colonies, each one was purified and considered as a Cd-resistant isolate.

3-2-2 Optimising growth conditions and the selection of isolates

Different bacterial growth conditions, including temperature, carbon, and nitrogen sources, were studied in 50 mL of EBS in Erlenmeyer-flasks (250 mL) in triplicate, and the amount of biomass was determined. The optimum temperature for the isolate was first studied by growing of the culture in EBS/D-fructose and incubation at different temperatures of 4 °C, 18 °C, 25 °C, 30 °C, 37 °C, 42 °C, 44 °C, 50 °C, and 60 °C for four days. The most suitable carbon source for the growth of isolates was studied using glucose and fructose (10 mM concentration), acetate, pyruvate, and sucrose (20 mM concentration), separately. The experiments were carried out at an optimised temperature of 37 °C for seven days and incubated at a shaking speed of 100 rpm. Finally, the suitable nitrogen source for the growth was studied by the addition of ammonia, urea, thiocyanate, cyanate, nitrate, or glycine (3 mM concentration), in addition to the dinitrogen in the air. The experiments were performed at 37 °C, and the carbon sources were either fructose for some isolates or pyruvate for other isolates. Based on their Cd MTC value, four out of eight Cd-resistant isolates with the highest MTC ability (C15-1, C15-2, C15-3 and C15-4), were chosen for further study.

3-2-3 Estimation of the specific growth rate and selection of one isolate

The specific growth rate was determined for isolates C15-1, C15-2, C15-3, and C15-4 under their respective optimised conditions. One mL of the growing culture of each isolate was inoculated into 50 mL of EBS/ pyruvate (20 mM), or D-fructose (10 mM) for isolate C15-4. During the incubation at 37 °C, samples were collected at regular time intervals, and the amount of biomass was determined. Based on the specific growth rates of four isolates, the isolate with the highest growth (re-coded as 'C15'), was chosen to achieve the objectives of this study.

3-2-4 Characterisation of isolate C15

3-2-4-1 Morphological and biochemical tests

The morphology of isolate C15 was observed after being stained with Gram stain and observed under a light microscope (Olympus) at X1000 magnification with oil immersion, according to the work of Vos (2011). Biochemical tests, including IMVIC (indole, methyl red, Voges-Proskauer, and citrate) were performed in triplicate, with control.

3-2-4-2 Genomic DNA extraction and 16S rRNA sequence analysis

The genomic DNA (gDNA) of isolate C15 was extracted according to the JGI (Doe joint genome institute) method of William *et al*. (2012). The biomass was collected after the inoculation of 50 mL from the growth of the culture into EBS/pyruvate (500 mL), in triplicate, and incubated at 37 °C in an orbital incubator operating at 100 rpm. After reaching the late exponential phase, the growth culture was cooled on ice for 60 min, centrifuged, and washed using EBS without pyruvate. The pellets were suspended in Tris EDTA buffer (TE) buffer, which was prepared according to Sambrook and Russell

(2001) as follows: 2 mL of Tris-HCl (10 mM, and pH 7.4) and 0.4 mL of Na_2-EDTA (0.5 M, pH 8.0). The optical density (OD_{600}) of the suspension cells was measured to be 1.0. The suspension cells were transferred into the Falcon tube (50 mL) for freezing using liquid nitrogen and kept in a freezer at – 20 °C. For extracting gDNA, suspension cells (24.6 mL) were dispensed into a 50 mL (Falcon tube) and 667 µL of lysozyme solution (10%*w*/*v*) was added to break down cell membranes; it was mixed gently and incubated at 37 °C for 30 mins in a water bath. Then, 1.33 mL of sodium dodecyl sulphate (SDS, 10%*w*/*v*) was added, and mixed well to digest the gDNA followed by adding 267 µL of proteinase K solution (20 mg/mL) to degrade any impurity proteins in the extracted gDNA; it was mixed well and incubated at 56°C for 3 h in a water bath. Then, a heated solution of sodium chloride (3.33 mL, 5 M), and 3.33 mL of CTAB/NaCl solution at 65 °C was added, respectively; it was mixed well and incubated at 65 °C for 10 mins in a water bath to precipitate the DNA. The CTAB/NaCl solution was prepared according to Sambrook and Russell (2001) as follows: 4.1 g of sodium chloride was dissolved in 80 mL of ddH_2O and heated to 65 °C in a water bath; 10.0 g of cetyl trimethyl ammonium bromide or hexadecyl trimethyl ammonium bromide (CTAB) was added slowly with occasional stirring. This solution was left for 4 to 5 h at 65 °C in a water bath and, after the incubation, the volume was completed to 100 mL with ddH_2O in a volumetric flask. After getting the precipitated DNA, 16.7 mL of each 24:1 chloroform: isoamyl alcohol, 25:24:1 phenol: chloroform: isoamyl alcohol, and 24:1 chloroform: isoamyl alcohol was added one after the other after mixing and centrifuging for 10 mins; the upper aqueous phase was transferred immediately to a Falcon tube (50 mL). After these steps, 0.6X volume of the cold isopropanol was added to the aqueous phase and incubated at – 20 °C overnight.

After 24 h, the final aqueous phase was centrifuged for 15 mins at 4 °C; the pellet was washed with cold 70% ethanol to precipitate the gDNA, centrifuged again, and then the pellets were left to dry at room temperature. The pellets were suspended in 0.18 mL of nuclease-free water. 10 µL of this suspension was removed to a sterile Eppendorf (1.5 mL, labelled as untreated), and the treated aqueous (170 µL) was transferred into another Eppendorf tube. gDNA (170 µL) was treated with 10 µL of RNase, mixed, centrifuged to pull the liquid back down in the tube, and incubated at 37 °C in a water bath for an hour. To qualify the isolated gDNA, 5 µL of treated and untreated, aqueous were run on an agarose gel. If the gel electrophoresis showed much RNA on the gel for the treated sample versus the untreated control, the previous step was repeated by adding 10 µL of RNase I, and the agarose gel electrophoresis was repeated until pure bands of gDNA were obtained. The final volume of gDNA (160 µL) was heated to 70 °C in a water bath for 15 mins, cooled in ice, and precipitated with 16 µL of sodium acetate solution (3 M) and 0.4 mL of ethanol (molecular biology grade).

The mixture was centrifuged for 2 mins to pull the liquid back down in the tube and incubated at – 20 °C overnight. To precipitate the gDNA, the final aqueous phase was decanted, and the pellet was washed with cold 70% ethanol, centrifuged at 4 °C for 5 mins at 4000 rpm. The ethanol was removed with a Gilson pipette, and the pellets were air-dried in the hood for 3 h. Finally, the total gDNA solution was obtained by resuspending the pellet in 0.1 mL of Tris-HCl (pH 8.0) and storing it in a freezer at – 20 °C.

3-2-4-2 Quality and quantity of gDNA

3-2-4-2-1 Agarose gel electrophoresis

Agarose gel electrophoresis was performed according to the method used by Sambrook and Russell (2001). The gels (1% *w*/*v*) were poured on a glass plate (110 mm^2), and the comb was placed; the gel was allowed to set, and the comb was removed. The glass plate was soaked in 1 TAE buffer. gDNA samples were mixed with loading buffer at a ratio of 2:1. Five µL of each sample, along with 5 µL of DNA ladder (1 kb) were loaded into the gel wells, and its lid covered the plate. The electrophoresis was run at 60 V for 60 mins. The gel was illuminated with a UV transilluminator and then photographed using the gel-imaging system. The acceptable gDNA samples should have given a higher molecular weight with no visible shearing of gDNA on the gel.

3-2-4-2-2 gDNA quantification using Nanodrop spectrophotometry

The quantity of pure gDNA was determined using a NanodropTM 1000 spectrophotometer (Thermo Scientific Ltd., DE, USA) at 260 nm based on the measurement ratios of A260/A230 and A260/A280. A260/A230 ratio indicates residual phenol and protein contaminations, whereas the A260/A280 ratio indicates isopropanol or phenol contaminations. The Nanodrop was first blanked using Tris-HCl (pH 8.0), according to the solution used to elute the gDNA. The reading was taken by using 2 µL of extracted gDNA. The acceptable gDNA samples should give a reading of Nanodrop for the ratio of A_{260}: A_{280} between 1.8 and 2, and for the ratio A_{230}: A_{260} between 0.3 and 0.9. The concentration of the extracted gDNA was measured in ng/mL.

3-2-4-2-3 gDNA quantification using the Qubit 2.0 Fluorometer

The accurate method for the quantity of pure gDNA was determined using the dsDNA BR Assay Kit (catalogue number Q32850, Q32853, Life Technologies) and the Qubit 2.0 Fluorometer (Life Technologies). The Qubit 2.0 fluorimeter was turned on for three h, before starting the measurements, to stable its signal. Two µL of the gDNA sample was diluted with 199 µL of Qubit dsDNA BR buffer and with 1 µL of Qubit dsDNA BR reagent (200X concentrate in DMSO) in an Eppendorf tube. A calibration curve, zero ng/µL DNA (Qubit® dsDNA BR standard #1) and 100 ng/µL DNA (Qubit dsDNA BR standard #2) were diluted with 190 µL of Qubit dsDNA BR buffer and with 1 µL of Qubit dsDNA BR reagent (200 concentrates in DMSO) in an Eppendorf tube. All samples were incubated for 2 mins, and the concentrations of gDNA were measured using the fluorimeter by sequentially putting in 2 µL from each sample and recording the gDNA concentrations. The acceptable gDNA samples for sequencing required a concentration of 10 – 30 ng gDNA /µLTris-HCl.

3-2-4-3 16S rRNA sequence

The gDNA was subjected to 16S rRNA (*rrs*) gene sequence. MUSCLE (Multiple Sequence Comparison by Log-Expectation) was used to make the multiple sequence alignment to be tested for the best fit of models, based on the Bayesian Information Coefficient (BIC) (Edgar, 2004). The Phylogenetic analysis was done using MEGA software (version7.0.26); the trees were reconstructed accordingly (with a percentage of 5,000 bootstrap replications) with a discrete gamma distribution to model rate differences across the sites (5 categories and gamma parameter 0.1466) allowance for some (40.39 %) evolutionarily invariant sites (Nei and Kumar, 2000).

3-2-5 Assessment of the inhibition effects of cadmium on *B. agri* C15

The identified isolate, *B. agri* C15, was tested for its inhibited specific growth yield under various Cd concentrations. The Cd stress was carried out according to the method described by Chudobova *et al.* (2015). The experiments were carried out in Erlenmeyer-flasks (250 mL) in triplicate by inoculating the cell suspensions (1 mL) into 50 ml of EBS/pyruvate. Cadmium nitrate tetrahydrate ($Cd(NO_3)_2 \cdot 4H_2O$) salt solution was added to make the Cd stress with nominal concentrations of Cd from 2.5, 5, 10, and 15 mM. The control was used without Cd. Samples were collected at intervals, and the dry biomass was determined as described in Chapter Two. At the same time, 1 mL of three independent cultures was centrifuged using a tabletop centrifuge at 4,000 for 10 mins at 4 °C. The supernatants were transferred into Eppendorf tubes and stored at – 20 °C until they could be analysed for the determination of unconsumed pyruvate concentrations. The concentration of pyruvate was measured using a pyruvate kit assay (Kit number MAK071, Sigma-Aldrich) with a calibration curve. According to the kit instruction, a master reaction mix was added to each sample in cuvettes (n = 3 cuvettes), and the cuvettes were covered by aluminium foil during the incubation at room temperature (22 °C) for 30 mins. To measure the unconsumed pyruvate after the reaction, the absorbance was scaled at 570 using a spectrophotometer (Jenway 7315 UV/Visible Spectrophotometer) and the concentrations of pyruvate in the samples were calculated according to the kit instruction. The concentrations of pyruvate utilised by the bacterial cells, and the respective values of the specific growth yields (Y_S) formed were determined. Y_S was obtained from the biomass produced, and the carbon source was consumed as follows:

$$Y_S = \frac{\Delta_{biomass}}{\Delta_{pyruvate}}$$

3-2-6 Mutagenesis of *B. agri* C15 and screening of mutant Cd^R

The *B. agri* C15 was mutagenised using a UV light, according to Yuan *et al*. (2013) with some modifications. To obtain large quantities of *B. agri* C15, which were exposed to Cd and needed for the mutagenesis assay, the specific growth rate was first determined in 500 mL. Three thoroughly mixed 50 mL batch cultures from the late exponential phase were inoculated into 500 mL of EBS/pyruvate in Erlenmeyer flasks (2000 mL), in triplicate and with a nominal concentration of 10 mM Cd. This concentration of Cd was chosen as the possible concentration for achieving high biomass of the cells under Cd stress. The cultures were grown at 37 °C in a rotary shaking incubator at 100 rpm, and the amount of biomass was estimated as described in Chapter Two. The effect of Cd (10 mM) on the growth of *B. agri* C15 was evaluated for the comparison of the specific growth rate values. These experiments were carried out with control in 50 mL and 500 mL of EBS without Cd. After determining the specific growth rate of *B. agri* C15 in 500 mL of batch cultures supplemented with 10 mM Cd, 50 mL culture of *B. agri* C15 was grown in a new fresh 500 mL of EBS /pyruvate in an Erlenmeyer flask (2000 mL) in triplicate, with a nominal concentration of 10 mM Cd, and incubated shaking at 100 rpm, 37 °C. The amount of biomass was determined, and from the late exponential phase, the cells were cooled in ice for an hour, centrifuged, and washed with and suspended in 0.5 EBS (two folds of diluted EBS with sterilised ddH_2O, without pyruvate).

The cell suspension was snap-frozen in liquid nitrogen. The counting of colony-forming units (CFUs) was used to estimate the survival of frozen cells using the serially diluting bacterial suspensions up to $1X10^6$ CFU/mL. Each dilution was then spread on the

nutrient agar plates in triplicate and incubated at 37 °C for 16 h. A CFU was determined from three sequential dilutions, and the mean was taken from all three.

During the actual experiment, UV exposure was optimised by determining a survival time of *B. agri* C15 under UV exposure, a 90% drop of CFU required to increase the chance of mutant isolation (Azin and Noroozi, 2001). Five mL of cell suspensions of 500 – 1000 CFU/mL was transferred into empty plates in triplicate and exposed to a UV light lamp of 340 nm, with a distance of 50 cm from the plate to the light. The plates were irradiated for the set times (0, 5, 10, 15, 20, 25, 30, 35, 40, 45, 50, and 60 mins) using a digital timer. For each UV-exposure time point, three plates were randomly removed. For determination, the number of dead CFUs, which were killed by incubation rather than by the UV light, 500 – 1000 CFU/mL was transferred into empty plates in triplicate, covered with aluminium foil, and incubated on the bench at constant room temperature (22 °C). At the same time, three plates were collected as before. The removed plates were recovered on ice in the dark for 10 mins, then, 100 µL of the cell from each suspension was spread directly on nutrient agar, in triplicate. All nutrient agar plates were incubated at 37 °C for 16 h, and CFU was determined, plotted as survivors *vs* exposure times. The lethal time for 50% mortality (LT_{50}) was estimated from the survival curve and the time, which kills 90% of the total CFU, was determined as 20 mins. Therefore, for mutation experiments, 5 mL of cell suspension having 500 – 1000 CFU/mL were irradiated for 20 mins, in triplicate. The exposed cells were recovered, then screened for mutants with elevated resistance to Cd. 100 µL of exposed, recovered cells of *B. agri* C15 were inoculated into 50 mL of EBS/ pyruvate in Erlenmeyer flasks (250 mL), in triplicate and with different nominal concentrations of Cd. The concentrations were below MTC of *B. agri* C15 (7 mM), equal (15 mM), and

above (18, 20, 22, and 24 mM). The control of EBS broth without Cd was used to determine whether there was growth at each concentration of the screening process.

The batch flasks were incubated at 37 °C for 72 h. The isolation of mutants was done in terms of MTC to Cd (Schmidt and Schlegel, 1994). 100 µL from each batch culture was transferred and spread onto EBS agar/ pyruvate and with the same nominal concentrations of Cd that used to the exposed batch cultures. After growing, the colonies of the mutants were purified and the mutant amongst several mutants, which had the highest MTC to Cd, was selected and coded as the mutant Cd^R. The selected mutant was further screened for its MTC to Cd. The nominal concentrations of Cd in the broth were MTC and 0.1 MTC of the selected mutant (increases of 2 µM). MTC value obtained was tested up to three separate occasions, followed by the confirmation on EBS agar.

3-2-7 Minimum inhibitory concentration (MIC) of cadmium for wild type *B. agri* C15 and mutant *B. agri* C15 Cd^R

The minimum inhibitory concentrations (MICs) for $Cd(NO_3)_2 \cdot 4H_2O$ were determined, according to Glendinning *et al*. (2005). Control strain, *Cupriavidus metallidurans* DSM 2839^T), purchased from the Leibniz Institute DSMZ–German Collection of Microorganisms and Cell Cultures (DSMZ) was used. *C.metallidurans* DSM 2839^T is a Cd-tolerant, Gram-negative aerobic bacterium; it was grown in 10 mL of H3BS basal medium, which contains three solutions that were mixed after being autoclaved and cooled. Solution I consisted of 2.3 g KH_2PO_4 and 2.9 g Na_2HPO_4-$2H_2O$ in 50 mL ddH_2O; solution II consisted of 1 g NH_4Cl, 0.5 $MgSO_4.7H_2O$, 0.01 g $CaCl_2.2H_2O$, 0.005 $MnCl_2$.4H2O, 0.005 g $NaVO_3.H_2O$ and 5 mL SL-6 solution in 915 mL ddH2O; and solution III consisted of 0.05 g $(NH_4)_5[Fe(C_6H_4O_7)_2]$ in 20 mL ddH_2O. The SL-6 solution

consisted of g/L: 0.1 g $ZnSO_4.7H_2O$, 0.03 g $MnCl_2.H_2O$, 0.3 g H_3BO_3, 0.2 g $CoCl_2.6H_2O$, 0.02 $NiCl_2.6H_2O$, 0.018 g $CuCl_2.2H_2O$, 0.03 g Na_2 $MoO_4.4H_2O$. One mL of vitamin sol^n (100 mg cyanocobalamin (B_{12}), 80 mg *p*-aminobenzoic acid (B_{10}), 10 mg biotin (B_7), 200 mg nicotinic acid (B_3), 100 mg calcium pantothenate (B_5), 300 mg pyridoxine hydrochloride (B_6), 200 mg thiamine hydrochloride (B_1), 50 mg lipoic acid, 50 mg riboflavin (B_2) and 20 mg folic acid (B_9) per L (Boden and Hutt, 2018)), and 10 mL of $NaHCO_3$ (0.5 g in 10 mL) were added to H3BS/pyruvate (20 mM). *C.metallidurans* DSM 2839^T was incubated at 30 °C for four days and then streaked on nutrient R2A and H3BS agar plates to ensure its purity. Pure colonies were selected, stained with Gram stain, and observed under a light microscope (Olympus) at X1000 magnification with oil immersion, according to Vos (2011). From the same colony, an inoculum was prepared in 5 mL of H3BS/pyruvate and transferred into 45 mL of H3BS/pyruvate in a sterile Erlenmeyer flask (250 mL) and incubated at 30 °C for 24 h in an orbital incubator operating at 100 rpm (Gallenkamp, Loughborough, UK). Gram staining was used to check for culture purity, and the culture was then harvested by centrifugation at 4 °C using Avanti J-26XP centrifuge (Beckman Coulter) for 15 min at 16000 rpm. The harvested cells were then washed and suspended in ice-cold sterile phosphate-buffered saline (PBS) and centrifuged twice. Cells were finally suspended in the buffer and stored at − 80 °C until they were needed for the experiments. For long-term storage, the growth cultures were maintained in sterilised glycerol (10% (*v*/*v*) in vials (1.5 mL) and the vials were frozen in nitrogen liquid and kept in a freezer at − 80 °C. The MIC for the *C.metallidurans* DSM 2839^T was determined by growing on H3BS/pyruvate agar in triplicate, with different nominal concentrations of Cd: 0.5, 1.5, 2.5, 3.5, 4.5, 5.5 and 6.5 mM (as its MIC reported 2.5 mM, Mergeay *et al*., 1985), and

incubated at 30 °C for four days. The MIC for *B. agri* C15 was determined by growing on EBS agar/pyruvate in triplicate with different nominal concentrations of Cd: 10, 11, 12, 13, 14, 15, 16 and 17 mM, and incubated at 37 °C for four days. The MIC for *B. agri* C15 Cd^R was determined by growing on EBS agar/pyruvate in triplicate with different nominal concentrations of Cd: 15, 16, 17, 18, 19, 20, 21, and 22 mM, and incubated at 37 °C for four days. After the incubation time, the colonies were observed, and the lowest Cd concentration that prevented the growth was considered as the MIC value.

3-2-8 Characteristics of *B. agri* C15 and *B. agri* C15 Cd^R

Several experiments were performed to evaluate whether the mutant had lost some of its physical characterisations identified in *B. agri* C15 due to UV mutagenesis.

3-2-8-1 Identification analyses and optimising growth conditions

The morphological test, including Gram stain and biochemical tests (IMVIC) was performed, in triplicate, with control. Optimal temperature, carbon, and nitrogen sources were also studied for the mutant *B. agri* C15 Cd^R, according to the previous protocol described for the wild type. Different pH (4.0, 4.6, 5.8, 6.4, 7.7, 8.8, and 9.0) in EBS/pyruvate were adjusted to obtain the optimum environmental conditions of these strains. The pH (4.0 and 4.6) was adjusted using acetic acid and sodium acetate. K_2HPO_4 and KH_2PO_4 were also used to acquire pH between 5.0 and 8.5, while pH 8.6 and 9.0, HCl, Trise-base were used. According to the ratio of each solution, 2 mL was added in a Falcon tube (50 mL) containing 20 mL of EBS/pyruvate. The bacterial culture was inoculated in triplicate and incubated at the optimal temperature (37 °C) for 72 h. Turbid growth was observed, and the results were recorded.

3-2-8-2 Measurement of core kinetic parameters

The growth curve, specific growth rate, and pyruvate utilised with its respective values of specific growth yields were studied for *B. agri* C15 and *B. agri* C15 Cd^R. The experiments were carried out by inoculating 1 mL of overnight culture into 50 mL of EBS/pyruvate in Erlenmeyer-flasks (250 mL), in triplicate, incubated at 37 °C and shaken at 100 rpm. 1 mL of growth culture was collected at interval times, and the dry biomass was measured; the culture was then centrifuged, and the supernatants were kept in Eppendorf tubes and stored at − 20 °C until being analysed for pyruvate concentration using a pyruvate kit assay as described under section 3-2-5.

3-2-9 Inhibition effects of cadmium on the specific growth rate and maximum amount of biomass formed

The effect of Cd on specific growth rate and the maximum amount of biomass formed *B. agri* C15 and *B. agri* C15 Cd^R were investigated under different concentrations of Cd according to the method used by Helbig *et al*. (2008). One mL of the culture was inoculated into 50 mL of EBS/pyruvate in Erlenmeyer-flasks (250 mL), in triplicate, and with different nominal concentrations of Cd: 2.5, 5, 7.5, 9, 10, 11, 12.5, 15, 16, 17.5, and 20 (mM), while the control was without Cd. Then, flasks were incubated at 37 °C for 72 h shaken at 100 rpm. The samples were collected at intervals, the amount of biomass formed was determined, and the growth curve was plotted, followed by the determination of the specific growth rate and the maximum amount of biomass formed.

3-2-10 Inhibition effects of cadmium on bacterial cell-surface morphology and structure

To determine any physiological changes of the bacterial cells when growing with Cd, SEM analyses were used. Two independent experiments and fixation processes were

conducted for each strain. The strains were grown on EBS/pyruvate agar, in triplicate, and with a nominal concentration of 13 mM Cd for *B. agri* C15 and 18 mM Cd for *B. agri* C15 Cd^R. In addition, to determine whether there were any differences in cell-surface morphology and structure between both strains, as mentioned above, growing was done without Cd. The plates were incubated overnight at 37 °C. After growing the colonies, agars with single colonies were selected and trimmed into blocks with a sterilised blade with a total of six blocks for each strain and treatment. The blocks with the bacterial cell colonies and agar blocks with uninoculated cell colonies were processed for the fixation (as described in Chapter Two) before the SEM observations. Furthermore, TEM analyses were performed to visualise the effects of Cd on the cell structures of both strains, grown with a nominal concentration of 13 mM Cd for *B. agri* C15 and 18 mM Cd for *B. agri* C15 Cd^R, according to the method used by Bozzola (2007). Cells were grown in 50 mL of EBS/ pyruvate in an Erlenmeyer flask (250 mL) in triplicate. In addition, to observe the cell structures of both strains without Cd effects, as mentioned above, the strains were grown in triplicate without Cd. These flasks were incubated at 37 °C. From the late exponential phase, the cells were harvested, and the pellets were washed twice in a sterile PBS and suspended in 1 mL of Dulbecco buffer to process the fixation (as described in Chapter Two) before the TEM observations.

3-2-11 Biofilm production assay

Congo red agar was used for the evaluation of biofilm formation of *B. agri* C15 and *B. agri* C15 Cd^R (Freeman *et al*., 1989). The Congo red agar was prepared as follows: brain-heart infusion broth powder (15 g), glucose (20 g), sucrose (50 g), Congo red dye (0.8), NaCl (15 g), and agar (20 g) were dissolved in a bottle containing 1000 mL of ddH_2O and autoclaved, before powering into Petri dishes. The strains were then

streaked on the Congo red agar plates, in triplicate, and incubated at 37 °C for 48 h. According to the colour produced by the colonies after the incubation period, biofilm formation colonies showed a black colour. In contrast, the non-biofilm formation colonies showed a red to brown colour.

3-2-12 Test for the detection of endospores

The Schaeffer–Fulton method was used for the detection of endospores in *B. agri* C15 and *B. agri* C15 Cd^R, with *Bacillus subtilis* as a control. A malachite green solution (0.5%, *w*/*v*) was added to smears of each strain on slides (*n* = 3 slides) and warmed using a Bunsen flame for 5 mins while avoiding drying out the solution. The slides were then washed with tap water, dried, and stained with safranin O for 30 s, then washed again with water and dried. The slides were observed under a light microscope at X1000 magnification with oil immersion. The endospore-forming cells appeared bright green, and the vegetative cells seemed to be brownish-red.

3-2-13 Test for the detection of poly-*β*-hydroxybutyrate granules

The granules of poly-*β*-hydroxybutyrate of *B. agri* C15 and *B. agri* C15 Cd^R, with *B. subtilis* as a control for the formation of poly-*β*-hydroxybutyrate, were ascertained using Sudan black B solution (Sudan stain 0.3% in 70% ethanol). The solution was added to smears of each strain on slides (*n* = 3 slides) and left for 15 mins; the slide was then dried and cleaned with xylene. After drying, the slides were stained with safranin O for 10 s, washed with tap water, and dried. The slides were then observed under a light microscope at X1000 magnification with oil immersion. Poly-*β*-hydroxybutyrate granules appeared as black droplets, and the cytoplasm of the cells seemed to be pink.

3-2-14 Test for the detection of polyphosphate (volutin) granules

The granules of polyphosphate in *B. agri* C15 and *B. agri* C15 Cd^R, with *P. aeruginosa* as a control, were discovered using toluidine blue stain. Smears of each strain on slides (*n* = 3 slides) were stained with toluidine blue stain for 30 s, then washed with tap water and dried so they could be examined under a light microscope at X1000 magnification with oil immersion. The polyphosphate granules appeared as red spheres, and the cytoplasm of the cells seemed to be blue. *P. aeruginosa* was grown on EBS plates prepared with the NH_4Cl, reduced to 0.05 g/L (1 mM), and using succinate (40 mM) as the carbon source to force it for production of volutin granules.

3-2-15 Statistical analysis

Statistical analysis for these data was performed. All values were expressed as the mean and standard error of the mean (SEM). The statistical significance of the differences between the accuracies of CRM and elements were examined using the Student's *t*-test. The analysis of variance (ANOVA) was used to find the differences between the data in IBM SPSS Statistics 22 software, followed by the Tukey *post hoc* test. The bacterial growth curves were fitted with nonlinear regression (global curve fitting, four parameters) of the mean data utilising the SigmaPlot (version 13). The specific growth rates on the bacterial growth curves were subjected to the Student's *t*-test.

3-3 Results

3-3-1 Isolation of bacteria resistant to cadmium

The wild type isolation was carried out from the soil of Hay Tor quarry. For the soil, a concentration of 490 ± 50 µmolal Cd was determined after *aqua regia* acid extraction and analysis by ICP-MS. Although the reference material used for quality control of the

showed poor recovery (50%), this concentration is two orders of magnitude higher than Cd in the reference material. Therefore, the Cd concentration in the soil clan is seen as a reasonable, probably low estimate. Compared to soil contamination assessment criteria in the UK (EA, 2015; CLEA: e.g., for residential lifetime exposure: 98 µmolal Cd or allotment soil: 9.38 µmolal Cd, both at pH 7) and the US EPA (2011) guidelines for soil (recommendation: Cd < 44 µmolal), this soil is considered as contaminated with Cd concentrations greater than one order of magnitude higher than the guidelines levels.

Based on the MTC values of bacterial cultures, eight Cd-resistant bacteria were isolated from three different Cd-tolerant bacterial cultures. These isolates were named depending on their MTC abilities as C10-1, C10-2, C10-3, C10-4, C15-1, C15-2, C15-3, and C15-4 (Table 9). The isolates C15-1, C15-2, C15-3, and C15-4 showed the highest MTC (15 mM Cd), followed by the isolates C10-1, C10-2, C10-3, C10-4 (10 mM Cd).

Table 9. MTC values of Cd-resistant bacterial isolates. The isolate names were coded depending on MTC values; 10 means the isolate resist to 10 Cd mM, 15 means the isolate resist to 15 Cd mM, and 1, 2, 3, and 4 mean the number of the isolate from each resistant culture.

Isolate	MTC (mM Cd)
C10-1	10
C10-2	10
C10-3	10
C10-4	10
C15-1	15
C15-2	15
C15-3	15
C15-4	15

3-3-2 Optimising growth conditions and selection of isolates

The growth conditions were optimised. Figure 8 shows the amounts of the biomass of eight Cd-resistant isolates at different temperatures (4 °C, 18 °C, 25 °C, 30 °C, 37 °C, 42 °C, 44 °C, 50 °C, and 60 °C). The optimum temperature for the growth of these isolates was 37 °C, which showed the significant highest dry biomass (Figure 8, $^{a}p<0.05$). At 37 °C, the lowest growth was demonstrated by the isolates C10-1 and C10-2, compared to isolates C10-3 and C10-4. Similarly, the isolates C15-1, C15-2, C15-3, and C15-4 showed the highest dry biomass at 37 °C, and there was no difference observed between them (Figure 8,$^{a}p<0.05$). Eight isolates showed no growth at temperatures, 4 °C, 18 °C, 50 °C, and 60 °C compared to other temperatures. With the temperature increase to 25 °C and 30 °C, all the isolates showed a significant increase in biomass amounts compared to lower temperatures. However, the increase in the temperatures to 42 °C and 44 °C significantly decreased the biomass amounts.

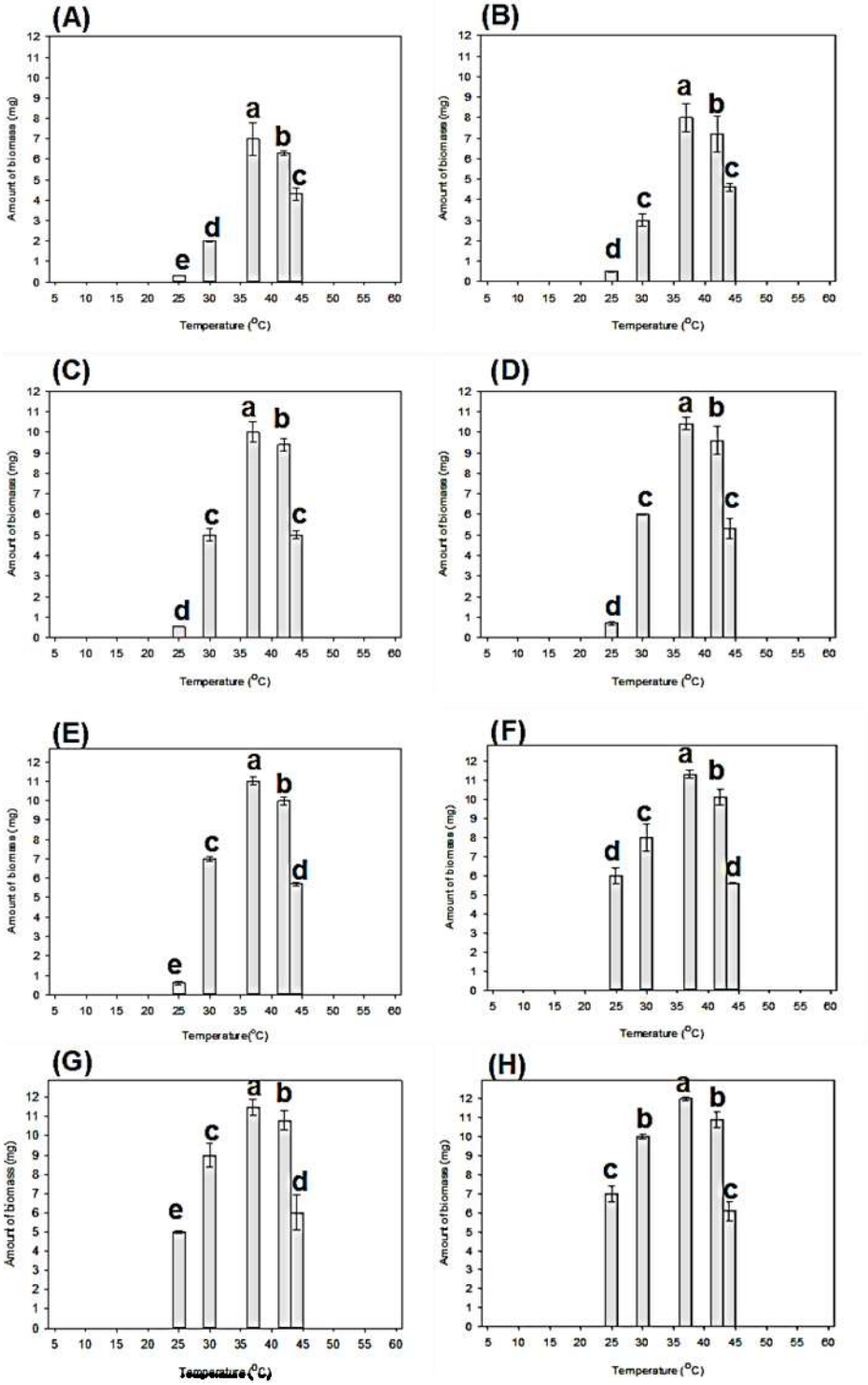

Figure 8. Determination of suitable temperature for the growth of eight Cd-resistant isolates. **(A)** Isolate C10-1, **(B)** isolate C10-2, **(C)** isolate C10-3, **(D)** isolate C10-4, **(E)** isolate C15-1, **(F)** isolate C15-2, **(G)** isolate C15-3, and **(H)** isolate C10-4. These isolates were grown in EBS/D-fructose, incubated for 48 h at 37 °C and shaken at 100 rpm. The error bars represent the standard errors of the mean (*n* = 3, batch experiments). A different letter indicates a significant difference between temperature within isolates.

The determination of a suitable carbon source was identified by measuring the growth of each isolate in batch cultures, supplemented with glucose or fructose (10 mM), acetate, sucrose, or pyruvate (20 mM). The suitable carbon source for the growth of eight isolates showed that the isolates C10-1, C10-2, C10-3, C10-4, and C15-4 had the highest biomass when growing with 10 mM of fructose (Figure 9, A, B, C, D and H, $^{a}p<0.05$) compared to other isolates, C15-1(Figure 9, E $^{c}p<0.05$), C15-2 (Figure 9, F $^{b}p<0.05$) and C15-3 (Figure 9, G $^{c}p<0.05$). At the same time, the isolates C15-1 (Figure 9, E), C15-2 (Figure 9, F) and C15-3 (Figure 9, G) showed the highest biomass ($^{a}p<0.05$) in growing within 20 mM pyruvate compared to their growth within other carbon sources.

The suitable nitrogen sources for growing the eight isolates were optimised under different nitrogen sources at an optimised temperature (37 °C) and carbon sources, either with fructose (10 mM) for isolates C10-1, C10-2, C10-3, C10-4, and C15-4 or pyruvate (20 mM) for isolates C15-1, C15-2, and C15-3. All isolates showed the highest growth when grown with ammonia (Figure 10, $^{a}p<0.05$), which was initially used in the composition of EBS medium, compared to other nitrogen sources. Based on the MTC abilities of the eight Cd-resistant isolates, four isolates (C15-1, C15-2, C15-3, and C15-4), which had the highest MTC abilities, were chosen for further study.

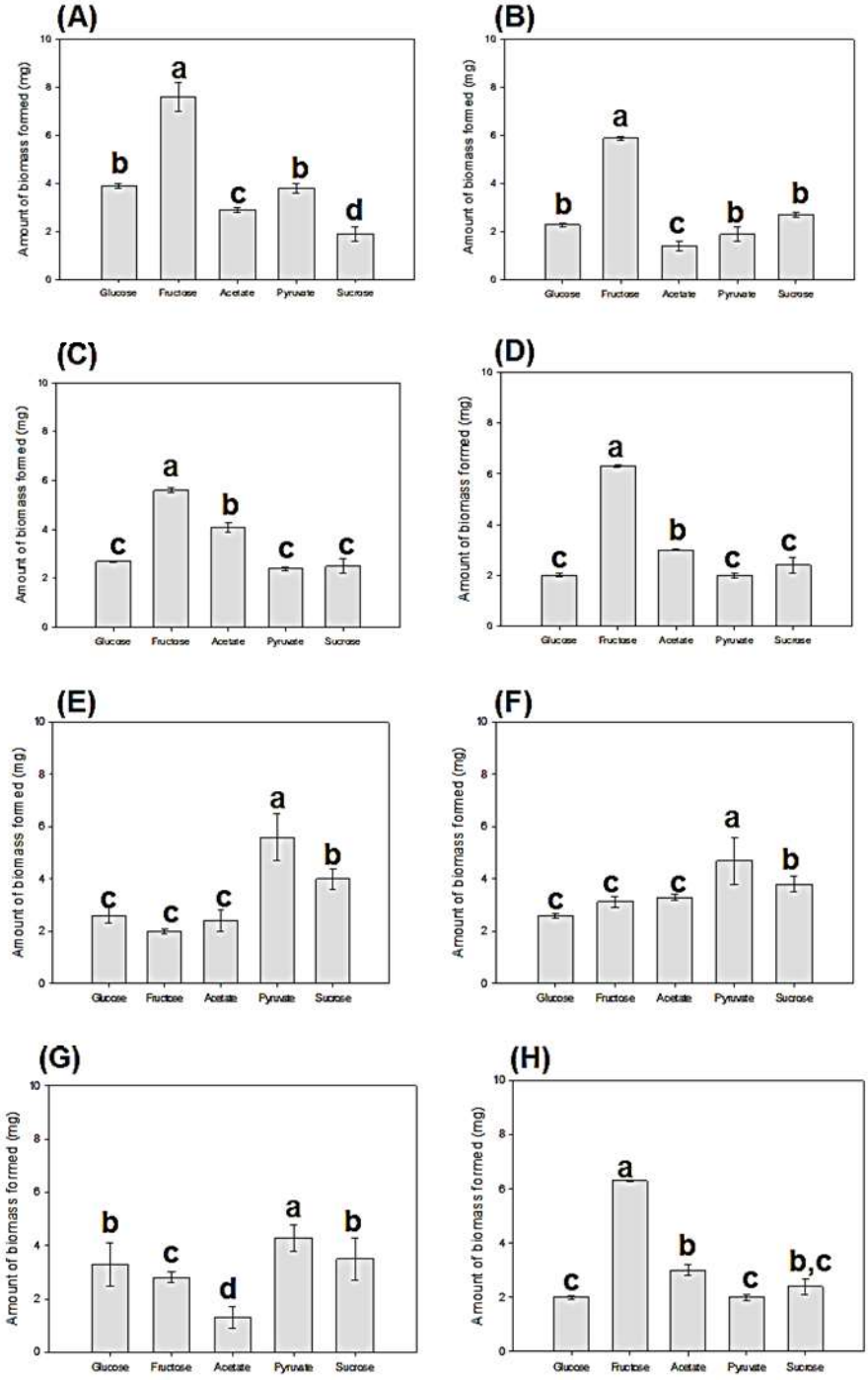

Figure 9. Determination of suitable carbon sources for the growth of eight Cd-resistant isolates. **(A)** Isolate C10-1, **(B)** isolate C10-2, **(C)** isolate C10-3, **(D)** isolate C10-4, **(E)** isolate C15-1, **(F)** isolate C15-2, **(G)** isolate C15-3, and **(H)** isolate C10-4. The isolates were grown in EBS supplemented with different carbon sources, incubated for seven days at 37 °C and shaken at 100 rpm. The error bars represent the standard errors of the mean (*n* = 3, batch experiments). A different letter indicates a significant difference between carbon sources within isolates.

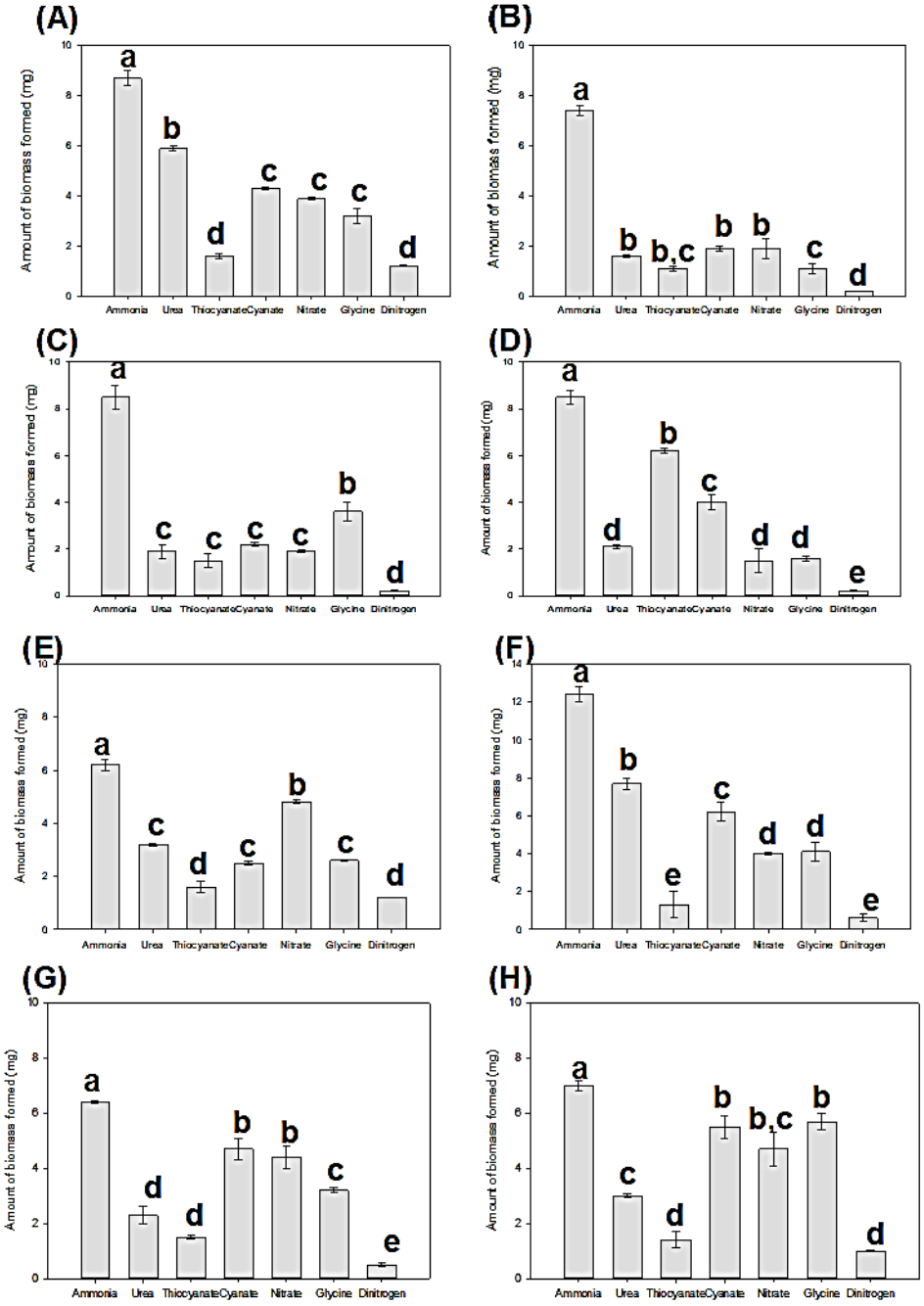

Figure 10. Determination of nitrogen sources for the growth of eight Cd-resistant isolates. **(A)** Isolate C10-1, **(B)** isolate C10-2, **(C)** isolate C10-3, **(D)** isolate C10-4; **(E)** isolate C15-1, **(F)** isolate C15-2, **(G)** isolate C15-3, and **(H)** isolate C10-4. The isolates were grown in EBS supplemented with fructose (10 mM) for isolates C10-1, C10-2, C10-3, C10-4, and C15-4 or with pyruvate (20 mM) for isolates C15-1, C15-2, and C15-3, incubated for seven days at 37 °C and shaken at 100 rpm. The error bars represent the standard errors of the mean (n = 3, batch experiments). A different letter indicates a significant difference between nitrogen sources within isolates.

3-3-3 Estimation of the specific growth rate and selection of one isolate

The selection of the potential isolate was based on its specific growth rate in addition to its MTC ability. The dry biomass of isolates C15-1, C15-2, C15-3, and C15-4 were determined, and their growth curves were plotted to identify a specific growth rate (Figure 11). The values of the specific growth rate ranged from 0.09 to 0.12 h^{-1}. Among the four isolates, C15-1 and C15-2 significantly showed (Figure 11A, B, $^{c}p<0.05$) the lowest specific growth rate (0.09 ± 0.004 h^{-1} and 0.09 ± 0.005 h^{-1}, respectively). The isolate C15-3 showed the highest specific growth rate (0.12 ± 0.007 h^{-1}) (Figure 11C, $^{a}p<0.05$), followed by the isolate C15-4 (0.11 ± 0.02 h^{-1}) (Figure 11D, $^{b}p<0.05$). Therefore, the isolate C15-3 was re-coded as 'C15' and chosen for further experiments.

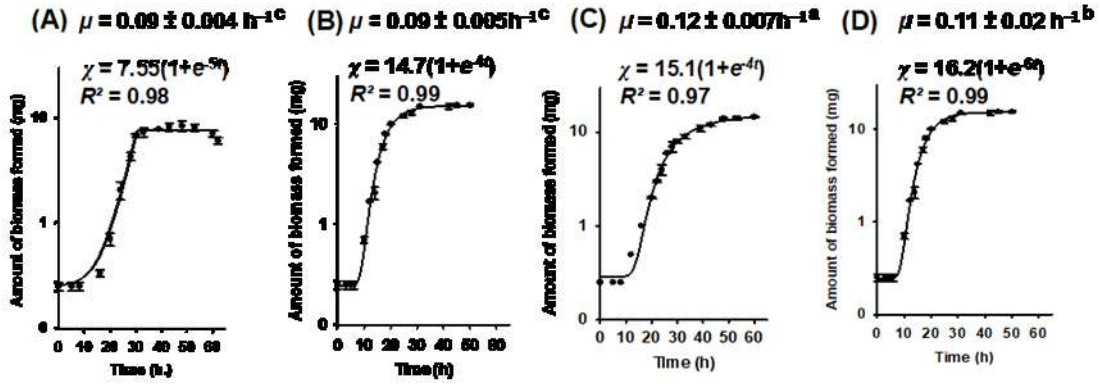

Figure 11. Growth curves of four Cd-resistant isolates. **(A)** Isolate C15-1, **(B)** Isolate C15-2, **(C)** Isolate C15-3, and **(D)** Isolate C15-4. The isolates were grown in EBS supplemented with D-fructose (10 mM) for isolate C15-4 or with pyruvate (20 mM) for isolates C15-1, C15-2, and C15-3, incubated at 37 °C and shaken at 100 rpm for 72 h. The error bars represent the standard errors of the mean (n = 3, batch experiments). The specific growth rate (μ) is shown.

3-3-4 Morphological, biochemical and 16S rRNA sequence analysis

Morphological observation of isolate C15 showed Gram-stain-positive bacilli (Figure 12A). The biochemical characterisation (IMVIC test) of the isolate C15 was performed. The isolate was negative and did not produce indole from tryptophan; the acid formed from glucose but produced acetone from the glucose and did not use the citrate as a carbon source. The 16S rRNA (*rrs*) gene sequence of the isolate C15 identified that the isolate belongs to the genus of *Brevibacillus*, closely related to *B. agri* DSM 6348^{T} (AB112716) with 100% identification. The isolate C15 was named *B.agri* C15 (Figure 12E).

3-3-5 Assessment of the inhibition effects of cadmium on *B. agri* C15

The inhibition effects of Cd on *B. agri* C15 under 2.5, 5, 10, and 15 mM Cd were studied. An increase in the Cd concentration led to an increase in the amounts of unconsumed pyruvate. The exposure to 2.5 mM Cd decreased the utilised pyruvate (mM) from 14.1 (Figure 13A) to 12.3 (Figure 13B). The amounts of unconsumed pyruvate were inhibited with the nominal concentrations of 5 mM Cd (Figure 13C) and 10 mM Cd (Figure 13D). In contrast, the amounts of unconsumed pyruvate under 15 mM Cd was reduced to 9.76 mM (Figure 13E). Nevertheless, the amounts of the biomass under the inhibited effect of Cd were recorded as small differences, and the specific growth rates under these toxic concentrations were significantly inhibited at the nominal concentration of 15 mM Cd (Figure 13E, $^{a}p<0.05$). These results indicated that the toxic effect of Cd controlled the consumed amounts of pyruvate.

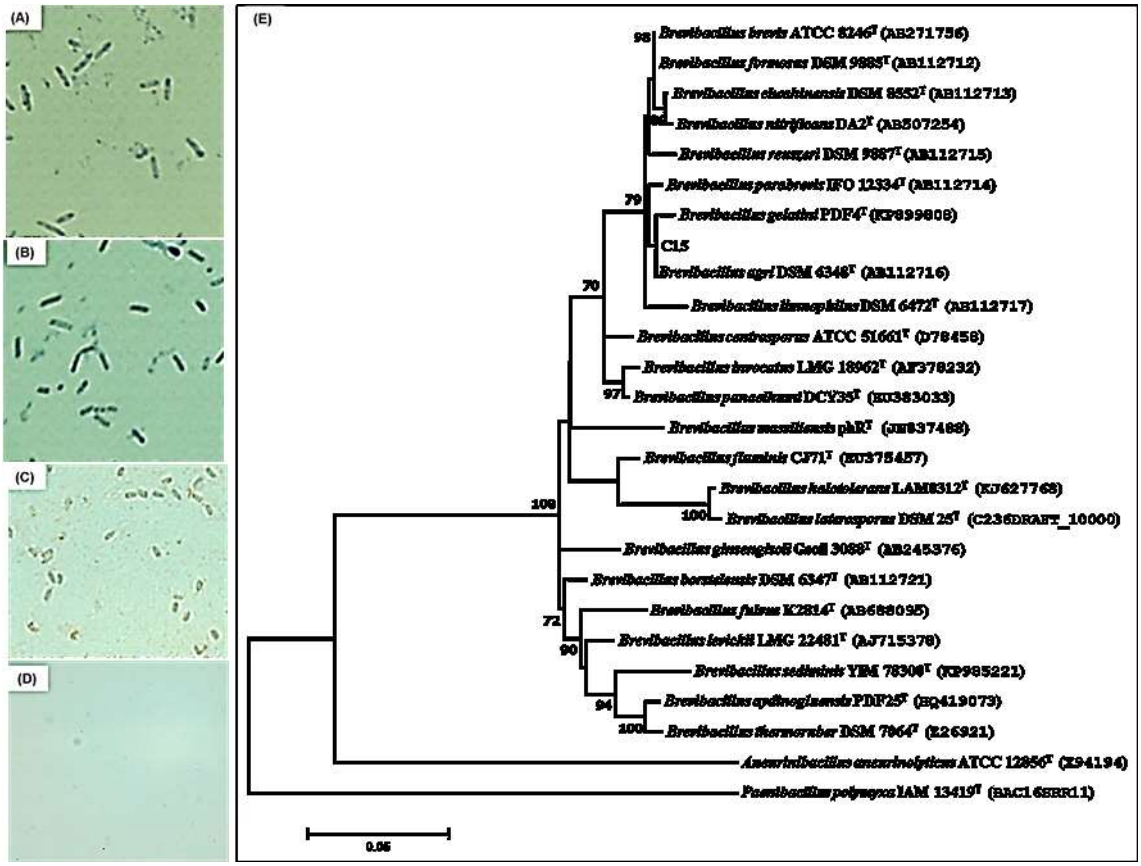

Figure 12. *Brevibacillus agri* C15. **(A)** Light microscopy observation Gram-stain-positive. The stains were analysed simultaneously in triplicates of three separately grown on nutrient agar plates. Control strains **(B)** *Bacillus subtilis*, showing Gram-stain-positive, **(C)** *Cupriavidus metallidurans* DSM 2839^{T}, showing Gram-stain-negative and **(D)** uninoculated slide. **(E)** Phylogenetic analysis. The maximum likelihood tree produced based on the 16S rRNA (*rrs*) gene showing the positions of isolate C15 *versus Brevibacillus* species with validly published names. The tree shown is the optimal tree with the lowest log-likelihood (-4773.56), with numbers at nodes indicating the percentage of 5,000 bootstrap replications in which the topology was preserved (values <70 % omitted for clarity). All of the positions at which there was less than 95 % coverage were omitted from the final analysis, in which 1,342 nucleotides were used. The branch lengths are to scale, and they indicate the number of substitutions per site, and the bar represents 0.05 substitutions per site. The outgroup is the same gene from *Paenibacillus polymyxa* IAM 13419^{T}, type genus of the *Paenibacillaceae*, in which all members of the in-group are circumscribed. The accession numbers are given in parentheses and refer to the GenBank or Integrated Microbial Genomes (IMG) databases (the latter contain an underscore "_").

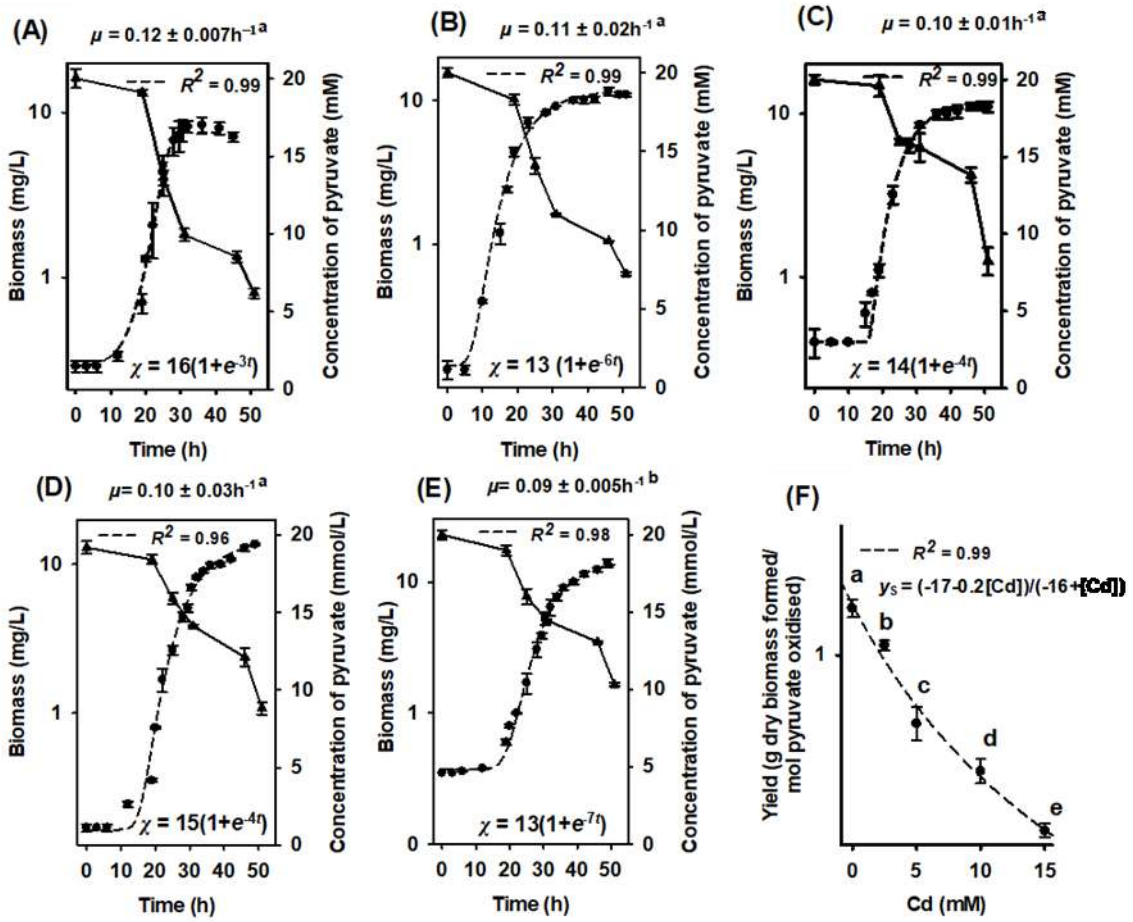

Figure 13. The effects of Cd on the concentration of biomass (●) and pyruvate utilisation (▼) of *B. agri* C15. The strain was grown in EBS/ pyruvate, **(A)** control and with nominal concentrations of Cd **(B)** 2.5 mM, **(C)** 5 mM, **(D)** 10 mM, and **(E)** 15 mM. The specific growth rate (μ) is shown. Inhibition effects of Cd on **(F)** their respective values of the Y_S formed. The error bars represent the standard errors of the mean of three independent cultures at each Cd concentration. b, c, d, and e are significantly different compared to the value of control without Cd.

The results showed that the specific growth yields were intensely inhibited under the Cd concentrations (Figure 13F); the highest yield was obtained in grown without Cd; this showed statistical differences (Figure 13F, $^{a}p \leq 0.05$) compared to growth under other Cd exposures (2.5 mM, $^{b}p \leq 0.05$), (5 mM, $^{c}p \leq 0.05$), (10 mM, $^{d}p \leq 0.05$), and (15 mM, $^{e}p \leq 0.05$).

3-3-6 UV-mutagenesis of *B. agri* C15 and screening of mutant Cd^R

It was essential to keep the cells of *B. agri* C15 in EBS/ pyruvate completely frozen at -20°C for three weeks until the UV-mutagenesis was complete. Frozen cell beads have been known to be stable against freezing damage. It is not expected that the variable number of frozen cells will be affected for three months at − 20 ° C (Rindala *et al.*, 2019). To obtain large quantities of the cells, the specific growth rate of *B. agri* C15, grown in a 500 mL of batch culture, was determined with a nominal concentration of 10 mM Cd. This experiment was carried out along with growth in a 50 mL batch culture with 10 mM Cd for the comparison in the specific growth rate between both volumes of cultures. The growth of *B. agri* C15 in 50 mL and 500 mL without Cd was studied. The specific growth rate of *B. agri* C15 grown under the effect of Cd in 500 mL was significantly low (μ= 0.11 ± 0.07 h^{-1}, Figure 14D, ^{b}p<0.05) compared to growth in 500 mL without Cd, which showed a higher specific growth rate (0.19 ± 0.1 h^{-1}, Figure 14C, ^{a}p<0.05). Similarly, specific growth rates were decreased from 0.12 ± 0.01h^{-1} (Figure 14A, ^{b}p<0.05) when grown in 50 mL of batch culture without Cd to 0.11 ± 0.03 h^{-1} (Figure 14D, ^{b}p<0.05) when grown in 50 mL of batch culture under the effect of Cd. However, there were no significant differences observed between specific growth rates when grown under Cd effects in 50 or 500 mL (Figure 14B, D, ^{b}p<0.05).

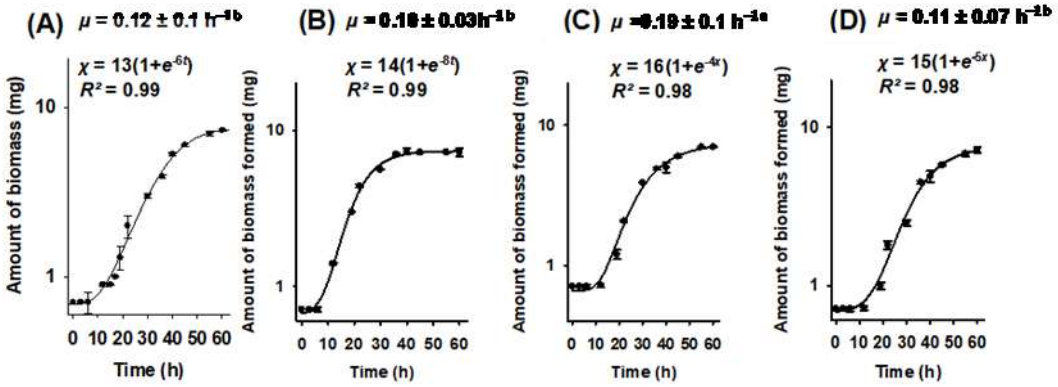

Figure 14. The growth scale of *B. agri* C15 under the effects of Cd. *B. agri* C15 was inoculated into EBS/pyruvate, incubated at 37 °C and shaken at 100 rpm. The growth was studied in different batch volumes **(A)** 50 mL (control) and **(B)** 50 mL with a nominal concentration of 10 mM Cd, **(C)** 500 mL (control), and **(D)** 500 mL with a nominal concentration of 10 mM Cd. The specific growth rate (μ) is shown. The error bars indicate the standard error of the mean of three batch cultures.

After the determination of the specific growth rate during growth at 500 mL of EBS under Cd effects, the growth of *B. agri* C15 in EBS broth (500 mL) was performed; the cells were harvested and suspended in 0.5 EBS without pyruvate to make the cell suspension form as beads to keep the cells of frozen at – 20°C until the UV-mutagenesis was complete. After forming the frozen cells as beads, CFU/mL of *B. agri* C15 in these beads was estimated at 1 X10^6 CFU/mL.

The length of UV light exposure that would kill 90% of cells (as CFU) to increase the chance of mutant isolation was determined at a fixed distance. Controls for CFU death just by incubation at room temperature were performed; 90% of *B. agri* C15 cells were killed after 20 mins of UV exposure (Figure 15). Thus, this was chosen as the length of exposure to induce the mutagenesis. The 50% mortality (LT_{50}), which was the time for 50% of *B. agri* C15 CFU to die, was 5.92 mins.

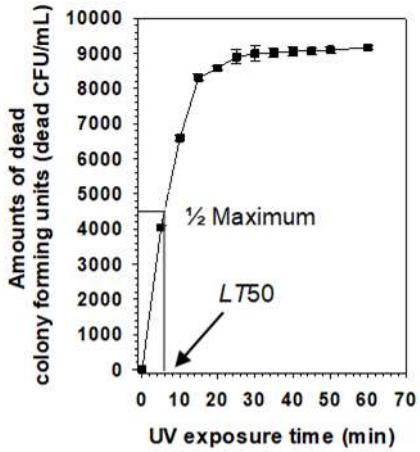

Figure 15. The lethal time curve for *B. agri* C15 after UV light exposure. 5 mL of 500–1000 CFU/mL in empty plates in triplicate were exposed to UV light (340 nm, brand Pisces, watt 13) at a 50 cm distance. The control plates were incubated on the bench at a constant room temperature of 22 °C (data not shown, used to get the final amounts of CFU death). The error bars represent the standard error of the three plates. The lethal time for 50% mortality (LT_{50}) after UV light exposure was estimated to be at 5.92 mins.

UV-mutagenesis of *B. agri* C15 was done for 20 mins, followed by the growth of exposed cells in batch cultures, with nominal concentrations of Cd: 7, 15, 18, 20, 22, and 24 mM Cd. The selection of putative mutants on EBS/pyruvate agar supplemented with the same concentrations of Cd was performed. The mutant selection was based on the growth of exposed cells at a given concentration of Cd in the plates. This showed no growth on plates with > 20 mM Cd, with few colonies at 15, 18, and 20 mM Cd. Among these, the most resistant colony to Cd was selected and considered a Cd-resistant mutant strain due to its ability to grow at 20 mM Cd and was termed as '*B. agri* C15 Cd^R'. The MTC of this mutant was 20.00 mM Cd, giving a higher MTC value than the wild type (15 mM).

3-3-7 Minimum inhibitory concentration (MIC) of cadmium for wild type *B. agri* C15 and mutant *B. agri* C15 Cd^R

The MICs of Cd were determined for *B. agri* C15 and *B. agri* C15 Cd^R with nominal concentrations of Cd at 10 – 17 mM and 15 – 22 mM, respectively. The presence of colonies on EBS agar plates containing 16 mM Cd for *B. agri* C15 and 21 mM Cd for *B. agri* C15 Cd^R was observed. Nevertheless, at 17 mM Cd (*B. agri* C15) and 22 mM Cd (*B. agri* C15 Cd^R), no colonies were observed; thus, growth had been inhibited. The results achieved from the MIC assay (Table 10) showed that the Cd resistance of *B. agri* C15 and *B. agri* C15 Cd^R was much higher than the resistance of the control strain (*Cupriavidus metallidurans* DSM 2839T), which reports MIC as 4.5 mM Cd. Based on these observations, MICs were confirmed as 4.5, 16, and 21 mM Cd of the control (*C.metallidurans* DSM 2839^T), the wild type (*B. agri* C15), and the mutant (*B. agri* C15 Cd^R), respectively.

Table 10. MIC values of $Cd(NO_3)_2 \cdot 4H_2O$ (mM) for *B. agri* C15 and *B. agri* C15 Cd^R along with the control strain, *C. metallidurans* DSM 2839T. Data are shown from three plates (*n* =3, plates) at each Cd concentration. [a]Significant differences between MICs.

Strain	Relevant charsteristic	MIC (mM)
* *C.metallidurans* DSM 2839^T	Control	4.5 ± 0.2
** *B. agri* C15	Wild type	16 ± 0.7
** *B. agri* C15 Cd^R	Mutant (derivate of *B. agri* C15)	21 ± 0.4[a]

*Grown on H3BS/pyruvate agar at temperature 30 °C.
** Grown on EBS/pyruvate agar at temperature 37 °C.

3-3-8 Characteristics of *B. agri* C15 and *B. agri* C15 Cd^R

Several experiments were carried out to compare the different characteristics between *B. agri* C15 and *B. agri* C15 Cd^R.

3-3-8-1 Identification analyses and optimising growth conditions

Optimal growth conditions were studied to investigate whether *B. agri* C15 Cd^R had major phenotypic changes other than *B. agri* C15. Gram-stained smears of the *B. agri* C15 and the *B. agri* C15 Cd^R showed no key morphological changes. Both remained Gram-stain-positive (Figure 16A, B).

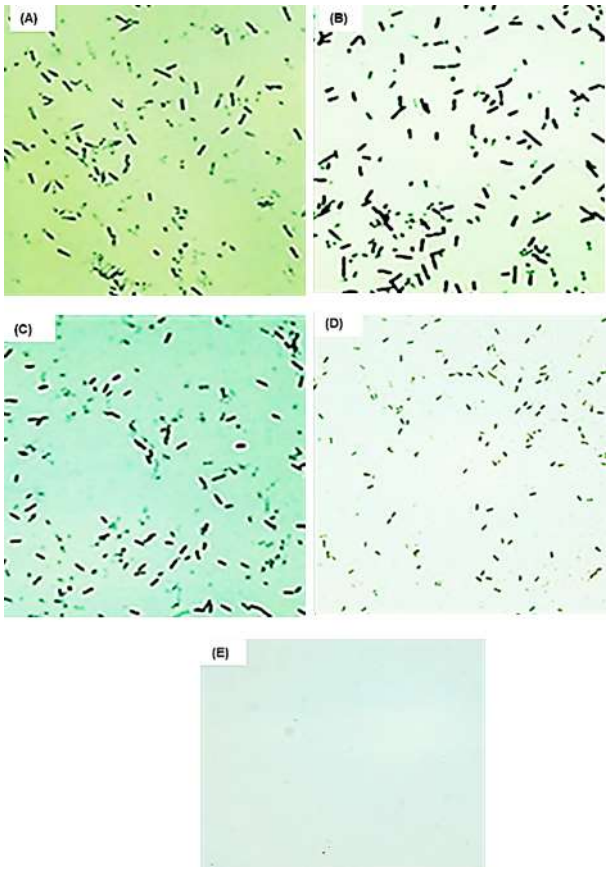

Figure 16. Morphological characterisation using Gram stain of **(A)** *B. agri* C15, **(B)** *B. agri* C15 Cd^R, **(C)** *Bacillus subtilis* (Gram-stain-positive control), **(D)** *C. metallidurans* DSM 2839^T (Gram-stain-negative control) and **(E)** uninoculated slide. Stains were performed symultaneously in triplicate on three separately grown nutrient agar plates. Gram-stain-positive: purple to the blue colour; Gram-stain-negative: orange to brown colour, Bismarck brown.

Basic chemotaxonomic characters (IMVIC test) showed the same results for *B. agri* C15 $Cd^{R,}$ as reported for *B. agri* C15 earlier in this chapter. This data and the morphological data gave a preliminary indication of no major phenotypic changes and that *B. agri* C15 Cd^R was a *bona fide* mutant, not a contaminate. Amounts of biomass

formed by both strains under various conditions are compared in Table 11. The statistical analysis of the biomass values showed the significant biomass obtained at 37 °C, using pyruvate and ammonia as carbon and nitrogen sources, respectively. These biomasses were not significantly different between the two strains ($^{*}p$<0.05). The growth at a different range of pH showed that both strains could grow within a range of 4.00 to 7.70, with no significant differences between them.

Table 11. The growth conditions of the wild type *B. agri* C15 and the mutant *B. agri* C15 Cd^R. ± represents the standard errors of the mean (*n* = 3, batch experiments). The biomass values for the growth conditions of each strain were subjected to a *t*-test to analyse the difference within each growth condition, and * show a significant difference in growth values resulting from different temperature, carbon source or nitrogen source, respectively within the strain. ** No biomass was obtained.

Growth conditions	**Growth conditions values of :**	
	***B. agri* C15**	***B. agri* C15 Cd^R**
Temperature	(amount of biomass formed (mg)	
4 °C	**	**
18 °C	**	**
25 °C	0.3 ± 0.8	2.1 ± 0.6
30 °C	6.6 ± 0.1	6.5 ± 0.3
30 °C	9.9 ± 0.1*	11 ± 0.5*
42 °C	6.1 ± 0.08	8.8 ± 0.2
44 °C	6.0 ± 0.7	3.9 ± 0.6
50 °C	**	**
60 °C	**	**
Carbon source	(amount of biomass formed (mg)	
Glucose (10 mM)	3.3 ± 0.8	3.9 ± 0.1
Fructose (10 mM)	2.8 ± 0.2	6.6 ± 0.6
Acetate (20 mM)	1.3 ± 0.4	2.9 ± 0.1
Pyruvate (20 mM)	4.3 ± 0.5*	9.8 ± 0.1*
Sucrose (20 mM)	3.5 ± 0.08	1.9 ± 0.01
Nitrogen	(amount of biomass formed (mg)	
Ammonium	6.4 ± 0.1*	8.7 ± 0.3*
Urea	2.3 ± 0.2	5.9 ± 0.1
Thiocyanate	1.5 ± 0.2	1.6 ± 0.6
Cyanate	4.7 ± 0.3	4.3 ± 0.6
Nitrate	4.4 ± 0.8	3.9 ± 0.2
Glycine	3.2 ± 0.2	3.2 ± 0.6
Dinitrogen	0.5 ± 0.02	1.2 ± 0.06
pH	4.00 – 7.70	4.00 – 7.70

3-3-8-2 Measurement of core kinetic parameters

Specific growth rates for *B. agri* C15 and *B. agri* C15 Cd^R are 0.12 ± 0.07 h^{-1} and 0.11 ± 0.02h^{-1}, respectively, with no statistically significant differences (Figure 17A, B, respectively). Mutant *B. agri* C15 Cd^R formed a specific growth yield higher than the wild type *B. agri* C15 (Figure 17C).

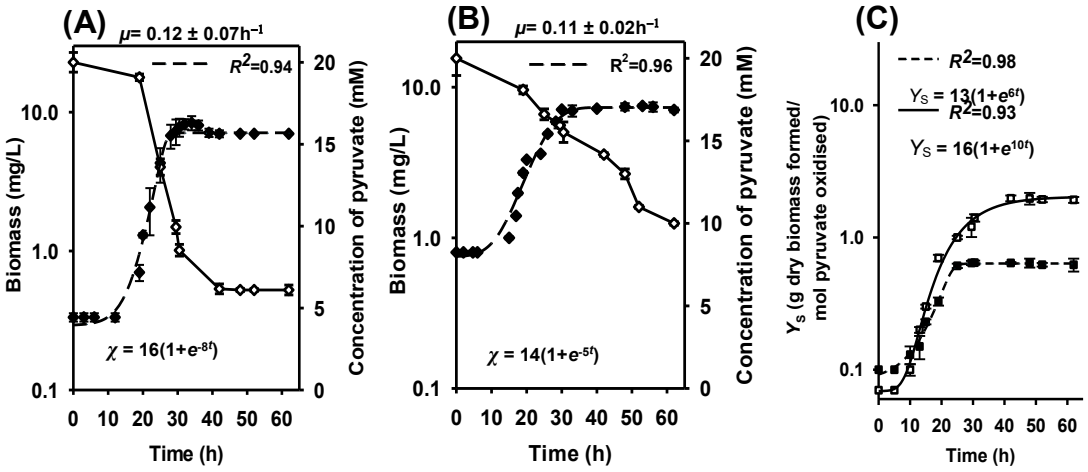

Figure 17. The amount of dry biomass formed **(♦)** and pyruvate utilisation **(◊)** of **(A)** *B. agri* C15 and **(B)** *B. agri* C15 Cd^R, and their respective **(C)** Y_S of **(■)** *B. agri* C15 and **(□)** *B. agri* C15 Cd^R. The specific growth rate (μ) is shown. The error bars indicate the standard error of the mean of three batch cultures.

3-3-8-3 Inhibition effects of cadmium on the specific growth rate and maximum amount of biomass formed

The effects of Cd on the specific growth rate and maximum amounts of biomass formed *B. agri* C15 and *B. agri* C15 Cd^R were compared. Both strains showed a Cd-dependent fall in a specific growth rate, and the significant rate was for *B. agri* C15 (Figure 18A). The maximum amount of biomass under different concentrations of Cd showed that the lethal doses for *B. agri* C15 and *B. agri* C15 Cd^R were 15.80 and 20.00 mM Cd, respectively (Figure 18B).

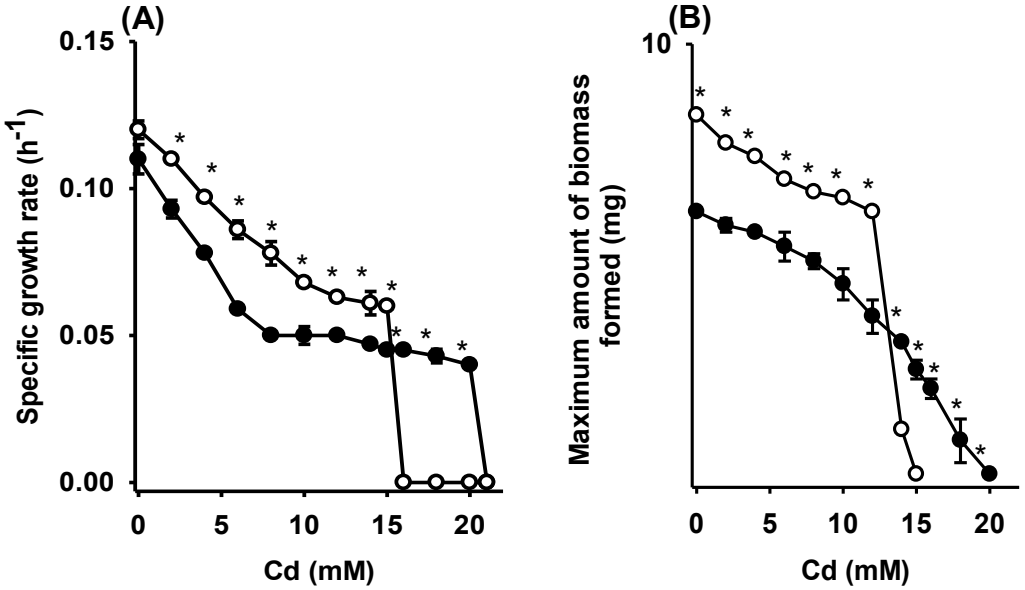

Figure 18. The inhibition effects of Cd on **(A)** specific growth rate and **(B)** maximum amounts of biomass formed of **(○)** *B. agri* C15 and **(●)** *B. agri* C15 Cd^R. The error bars indicate the standard error of the mean of three batch cultures at each Cd concentration. *Significant difference between strains at each Cd concentration.

3-3-8-4 Inhibition effects of cadmium on bacterial cell-surface morphology and structure

The effects of Cd on the cell-surface structure and morphology were investigated. SEM was used to ascertain any cell-surface or morphological differences between *B. agri* C15 and *B. agri* Cd^R grown with and without Cd. As the cell

surface and glycocalyx do not fix well when using a traditional SEM sample preparation method (Fischer *et al*., 2012), two alternative methods specifically designed to preserve these structures were compared. One used DEC (*N*-(3-dimethyl aminopropyl)- *N'*-ethyl carbodiimide) to cross-link glycocalyx sugar and proteins to avoid loss and was termed 'DEC' fixation; the other used the polysaccharide- binding stain (used in light microscopy), Alcian blue with L-lysine to support these structures (Geisler *et al*., 2019). This was termed 'ABL' fixation. It should be noted that DEC fixation was originally erroneously published as *N*, *N* -dicyclohexyl carbodiimide (DCCD) fixation in Fischer *et al*. (2012). Still, there was an error on behalf of the author (Elizabeth R. Fischer, *pess.comm*. to R. Boden).

The SEM micrographs are presented in Figure 19. Generally, the SEM observations showed that all the cell strains were bacilli, were uncontaminated with different cells, and were organised as net and ordered cells. There were no major variations in the cell morphology between *B. agri* C15 (Figure 19 A[B1, B2]) and *B. agri* Cd^R (Figure 19B [B1, B2]) grown either with or without Cd. That said, the cell-surface morphology changed considerably in the presence of Cd. Figures 19A (B2, D2) and 19B (B2, D2) show that the surfaces of the Cd-exposed cells were coated with glycocalyx or a similar structure, but this was absent from the cells. In general, the glycocalyx was better preserved when an ABL fixation was used (Figure 19 A [B1]) than when DEC fixation was used (Figure 19 A[D1]).

B. agri C15 grown with Cd showed a more massive glycocalyx structure when fixed with DEC (Figure 19 A[B2]), and a more 'filamentous' glycocalyx structure appeared when fixed with ABL, which may be a fixation artefact (Figure 19 A[D2]).

This also appeared on *B. agri* Cd^R grown with Cd (Figure 19 B [B2]); however, without Cd and with DEC (Figure 19 B[B1]), glycocalyx structures were observed (Figure 19 B[D1]). The dense lipopolysaccharides were observed on the cells of *B. agri* Cd^R grown with Cd and fixed with DEC (Figure 19 B[B2]). The heavy, dense lipopolysaccharides were also observed when the *B. agri* C15 Cd^R was fixed with the ABL fixation (Figure 19 B[D2]).

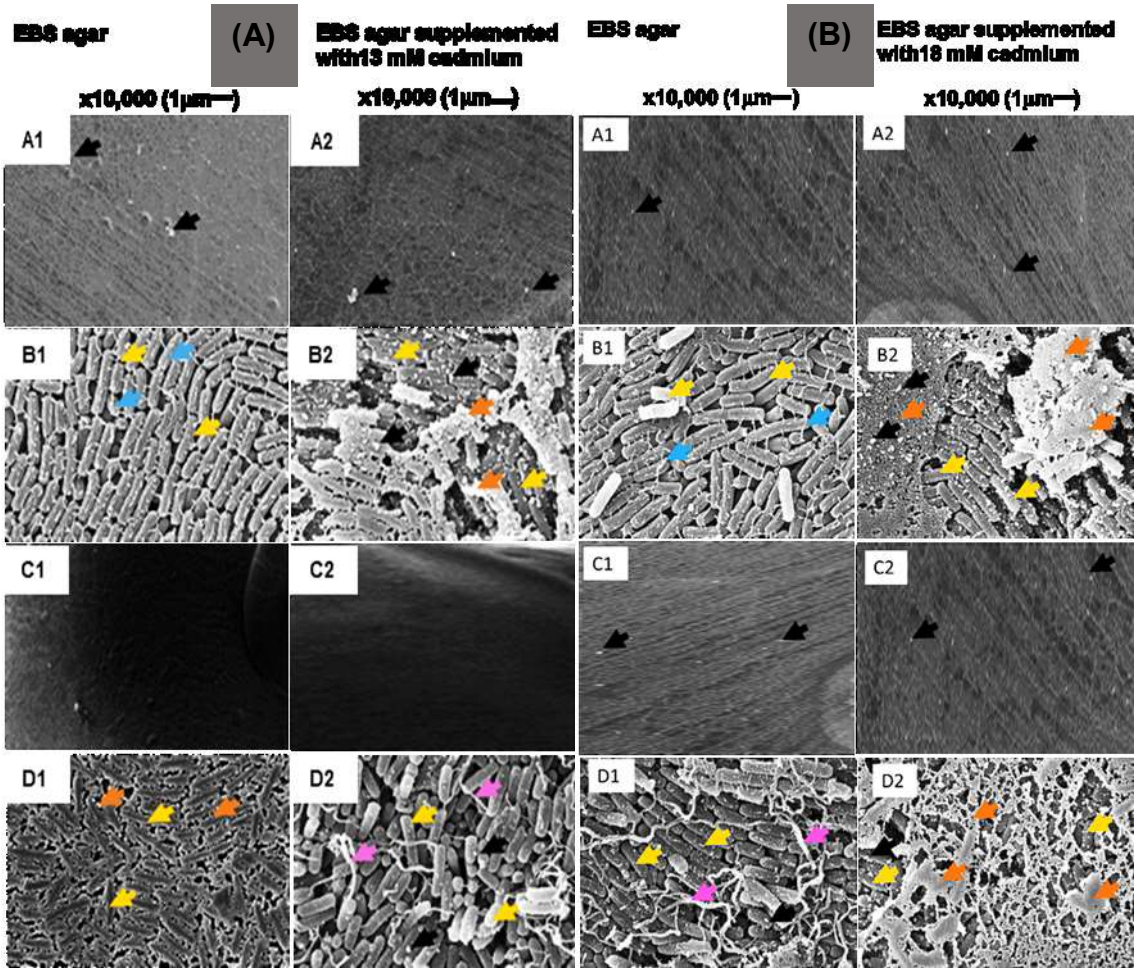

Figure 19. SEM micrographs of **(A)** *B. agri* C15 and **(B)** *B. agri* C15 Cd^R. Three biological replicates of the cell colonies were obtained and fixed with DEC or ABL. Two independent experiments of each strain are shown in which the growth on EBS is on the left panels and with Cd on the right panels. Uninoculated agars, **A (A1**and **A2)** and **B (A1** and **A2),** fixed with DEC or **A (C1** and **C2) and B (C1** and **C2),** fixed with ABL**,** showing no bacterial cells with few impurities (black arrows). *B. agri* C15 produced glycocalyx (blue arrows) **(A[B1])**, which was phenotypically similar to that produced by *B. agri* C15 Cd^R **(B[B1])** in the same media, fixed with DEC. In contrast, more glycocalyx was observed in *B. agri* C15 **(A[D1])**, fixed with ABL (blue arrows), but showed filamentous glycocalyx **(A[D2])** (purple arrows), fixed with the same fixation and produced lipopolysaccharides (brown arrows), fixed with DEC **(A[B1])** in grown with Cd. *B. agri* C15 Cd^R produced densely **(B[B2])**, very dense **(B[D2])**, lipopolysaccharides in grown with Cd, fixed with DEC or ABL, and filamentous glycocalyx (purple arrows) **(B[D1])**, fixed with ABL. **Arrows:** black, impurities; yellow, cells; blue, glycocalyx; brown, lipopolysaccharides; and purple, filamentous glycocalyx

To investigate the formation of exopolysaccharides and biofilms, production was assayed on a Congo red agar. The staining of these exopolysaccharides could be used to observe these biofilms, specifically, with the amyloidophilic Congo red dye. This stain changes the colour of the polysaccharides and amyloid fibres to a brown colour during the biofilm's development. No biofilm production was observed for either *B. agri* C15 or *B. agri* C15 Cd^R grown with or without Cd. The ultrastructures of *B. agri* C15 and *B. agri* C15 Cd^R were observed using TEM. TEM micrographs (Figure 20 A[A], B[A]) showed that both strains were bacilli and similar in shape and size. Some 'blebs' on the cell walls were observed in both strains in addition to electrondense granules. The observation of endospores under Cd exposure was obtained. No differences in the cell structures were observed for either of the strains when grown with Cd (Figure 20 A[B], B[B]).

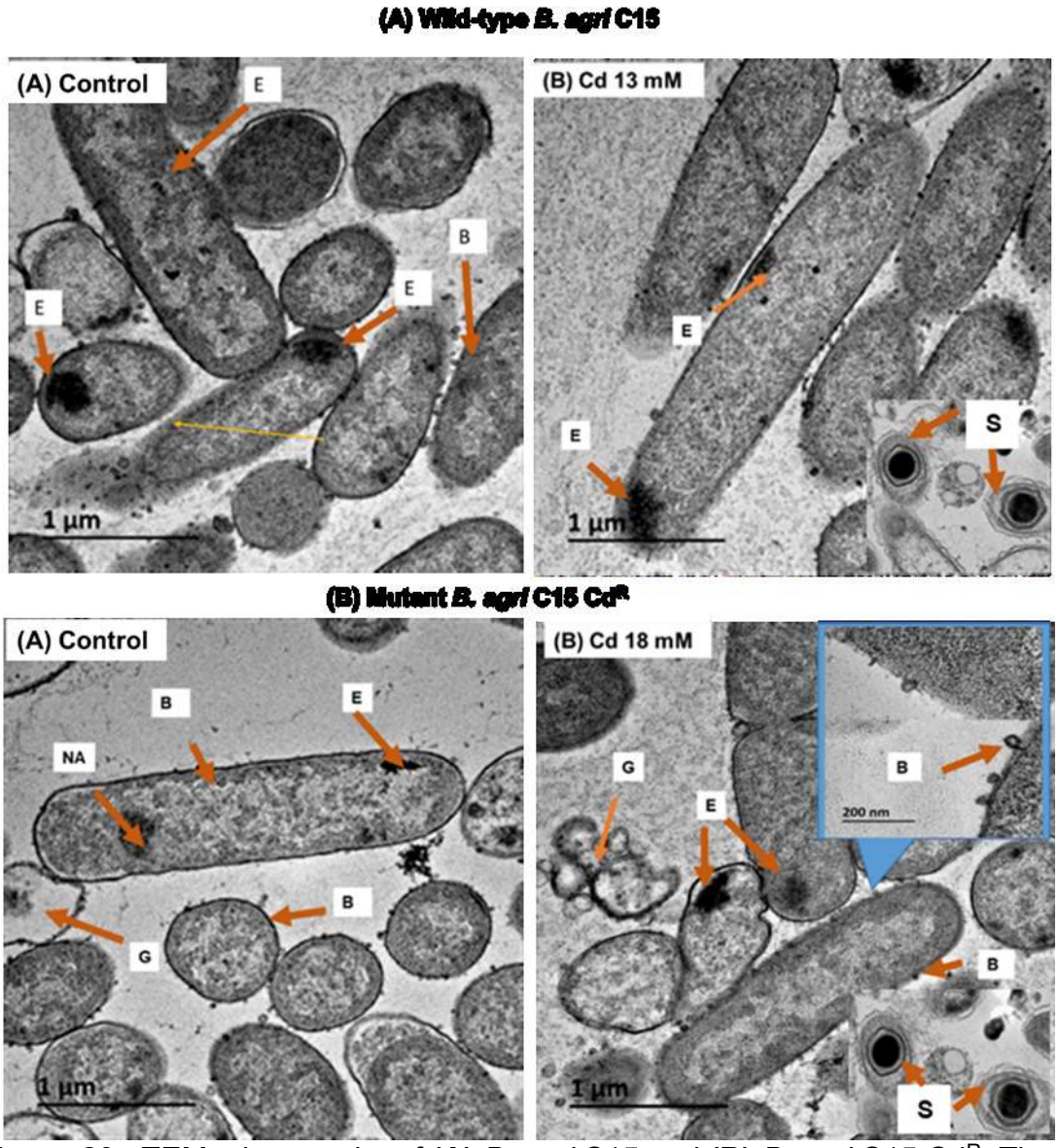

Figure 20. TEM micrographs of **(A)** *B. agri* C15 and **(B)** *B. agri* C15 Cd^R. Three experimental replicates of the cell suspensions were obtained. Two independent experiments for each strain are shown in which the growth in EBS is in the left panel and with Cd in the right panel. **A(A) and B(A)** show cells of *B. agri* C15 and *B. agri* C15 Cd^R, respectively, have electrodense and 'blebs' (insect picture '**B**'), which are phenotypically similar **(A[B]** and **B[A])** when grown with Cd in addition to observing endospore (insect picture '**S**'). Abbreviations shown on the cells are **B**: 'blebs'; **E**: electrodense granules; **G**: 'ghost'; and **S**: endospore.

3-3-8-5 Detections of endospore-forming and poly-*β*-hydroxybutyrate and polyphosphate (volutin) granules

Endospore formation by *B. agri* C15 and *B. agri* C15 Cd^R is shown in Figure 21 (B, C). *B. agri* C15 and *B. agri* C15 Cd^R formed terminal endospores. The strains also produced poly-*β*-hydroxybutyrate granules (Figure 22, B, C), but no polyphosphate granules were observed (Figure 23, B, C).

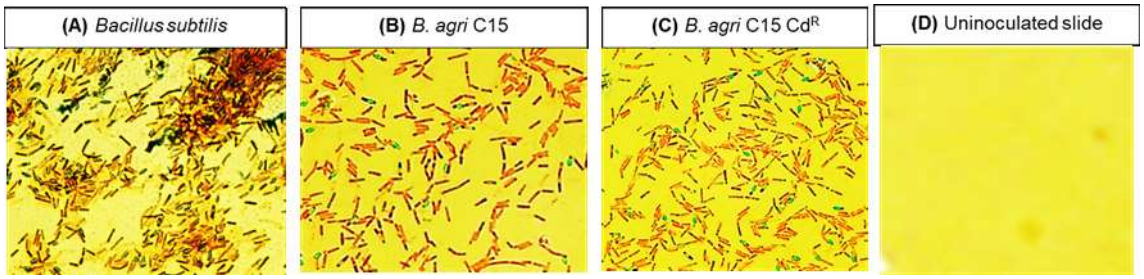

Figure 21. Light microscopic observations of endospores of **(A)** control strain, *B. subtilis*, **(B)** *B. agri* C15, **(C)** *B. agri* C15 Cd^R and **(D)** uninoculated slide.

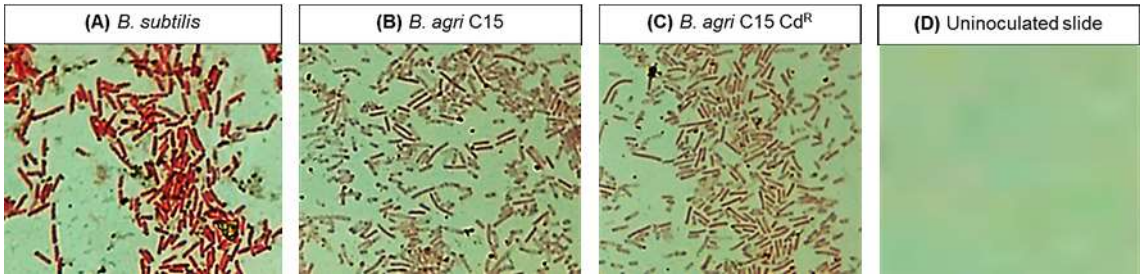

Figure 22. Light microscopic observations of poly-*β*-hydroxybutyrate granules of **(A)** control strain, *B. subtilis*, **(B)** *B. agri* C15, **(C)** *B. agri* C15 Cd^R and **(D)** uninoculated slide.

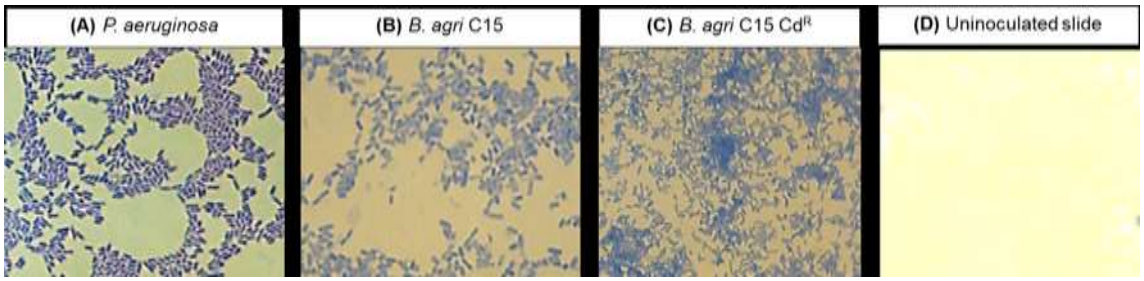

Figure 23. Light microscopic observations of polyphosphate granules of **(A)** control strain, *P. aeruginosa* and absence of polyphosphate granules in **(B)** *B. agri* C15 and **(C)** *B. agri* C15 Cd^R. **(D)** Uninoculated slide.

3-4 Discussion

In this study, soil from Hay Tor quarry was chosen for the isolation of Cd-resistant bacteria, due to its history of mining, where metal ores have been observed in the soil. This soil is known to be contaminated with Cd (this study) and with other metals (Howard *et al*., 2015; Raikova *et al*., 2019). Therefore, it was assumed that it could be possible to isolate Cd-resistant bacteria from it. The isolation of Cd-resistant bacteria was screened sequentially by increasing the Cd concentration in the cultures, and the isolates were obtained from the highest concentrations that permitted culture survival. Increases in Cd concentrations affect the properties of bacterial cells such as protein activity and DNA stability, leading to evolutionary adaptations in phenotype (adaptation) and acclimatisation (changes in gene expression) (Podrabsky and Somero, 2004).

Eight Cd-resistant isolates showed Cd-tolerant abilities, and their growth was optimised under different conditions. The best incubation temperature was established at 37 °C. It is common to assume that different bacteria will prefer different carbon sources for the enrichment and that structurally similar carbon sources, which are metabolised by relevant biochemical pathways, are selected by the same microbial strains. About 55% of the carbon taken by the bacteria serve as substrates of the metabolic network after being broken down to supply pools of amino acids and other components of a cell (Lehninger *et al*., 2008). The isolated bacteria in this study were enriched in EBS medium on five different carbon sources. The biomass of the isolates generated from enrichment cultures containing different carbon sources showed that pyruvate or fructose were the preferred sources of different strains. Fructose was added as the carbon source

in the first steps of the enrichment culture of the soil sample; therefore, some isolates choose this source. Other strains preferred pyruvate as a carbon source. This could be as a result of using more than one carbon source for the enriched isolates and the changes in the composition of the growth medium over time will be reflected by changes in the behaviour of the isolates (Wawrik *et al*., 2005). Costa *et al*. (2002) found bacteria chose fructose as the sole carbon source and did not use glucose at all. Ammonia, which was used in the original EBS medium, was preferred among the nitrogen sources added. The specific growth rate of the selected four isolates (C15-1, C15-2, C15-3 and C15-4) from the eight isolates showed that isolate C15-3 grew faster than other isolates, so it was chosen for further experiments and re-coded as 'C15'. Isolate C15 was tolerant to 15 mM of Cd (supplied as $Cd(NO_3)_2 \cdot 4H_2O$); it was considered as a potential isolate to be mutagenised to generate resistance to high concentrations of Cd. Isolate C15 was identified as *Brevibacillus agri* C15 that used pyruvate as a carbon source, showed a new characteristic compared to other *Brevibacillus* species, which was reported by Vos *et al*. (2011). It has been published in a recent study that many species of *Brevibacillus* have been isolated from diverse habitats and geographical locations (Gomri *et al*., 2018). *Brevibacillus* sp. has been previously demonstrated to have the ability to grow in the presence of Cd (85 mg/kg or ~760 µmolal) (Ruiz-Lozano and Azcón, 2011).

The bacteria's mechanisms to resist Cd have been described and involve an efflux pump, adsorption, precipitation, and intracellular accumulation processes (Bruins *et al*., 2000). The bioaccumulation process consists of the accumulation and localisation of Cd in specific organelles; Cd-resistant bacteria can resist Cd

through other mechanisms as well. The proposed Cd resistance of *B. agri* C15 may be due to a mechanism mentioned above. The isolate *B. agri* C15, which had a natural resistance in Cd-contaminated soil, may harbour one or several ATP, RND, or CDF transporter responsible for the efflux system (Leedjärv *et al*., 2008). Nongkhlaw *et al.* (2012) detected a PIB-type ATPase gene in a uranium-resistant bacterium isolated from uranium-contaminated soil. Similar efflux systems were reported with Cd resistance in *Acidithiobacillus ferrooxidans* (Ramos-Zúñiga *et al.*, 2019). Another mechanism of effective resistance is the precipitation or the adsorption of Cd on the cell surface. The extracellular polymeric substance (EPS) produced by *B. agri* C15 could allow the binding of Cd to anionic carboxyl groups (COO^-) on the EPS.

When exposed to Cd, the growth of *B. agri* C15 was adversely affected. The efflux of Cd outside the cells was likely responsible for the higher concentrations of Cd in the growth medium that changed the efflux process, increasing the intracellular uptake of Cd. Consequently, Cd may cause damage to the cells through the accumulation of reactive oxygen species (ROS) (Stohs and Bagchi, 1995). Ramos-Zúñiga *et al.* (2019) found that the cell numbers of *Acidithiobacillus ferrooxidans* were reduced when exposed to $CdSO_4$. It has also been reported that the growth of *Pseudomonas fluorescens* H2 was affected by Cd exposure (McEldowney, 2000). These results agreed with other studies reporting that Cd damages bacteria and leads to growth inhibition (Peptides, 2009; Chudobova *et al.*, 2015). The inhibition effect of Cd on the specific growth yield of *B. agri* C15 could also be due to the presence of other cations in the EBS growth medium. McEldowney (2000) found that Cd toxicity in cells decreased with the presence

of Zn in the medium, a result of the inhibition of Cd uptake due to competing effects. In the present study, the EBS growth medium was used, and the possible competing effects were EDTA and Zn, both with lower concentrations compared to the Cd concentrations used in the exposure test. The high concentration of Cd suggests that the Cd were the cause of inhibited bacterial growth.

In this study, a distinct approach was carried out to achieve increased resistance in the *B. agri* C15. Isolate *B. agri* C15, which has an intrinsic ability to resist Cd (MTC: 15 mM), was used to increase its natural resistance to Cd. Wu *et al.* (2019) found that growing a bacterium with Cd induces a mutant with elevated resistance to Cd. Using this process, several mutants were successfully generated from the wild type *B. agri* C15 by UV light mutagenesis; one of these mutants *B. agri* C15 Cd^R was able to grow in the highest Cd concentration (20 mM) and was chosen. The generation of Cd-resistant mutants in the growth medium can be affected by the concentration of Cd, the steps to isolate the mutants and the increase of the Cd concentrations in the medium during each step. Exposing cells, cultivating in the medium (with a high Cd concentration), and spreading exposed cells on agar plates containing Cd may have increased the resistance of the *B. agri* C15 by an MTC value of 0.25 fold. However, if the process was used repeatedly with increasing Cd concentrations in the low fold (Qin *et al.*, 2019), it could generate a mutant with higher MTC value (eightfold). Mutant *B. agri* C15 Cd^R had improved resistance to Cd, tolerant to 20 mM, and showed no key morphological or biochemical characteristics compared to wild type *B. agri* C15. Mutant *B. agri* C15 Cd^R had higher biomass than the wild type and exhibited slower growth when grown with Cd than wild type *B. agri* C15. The

inhibition of the bacteria's growth led to a diminished specific growth yield; these results are similar to the results of the study performed by Horitsu and Kato (1980) on the Cd- mutant *P. aeruginosa* G-1.

After three days of Cd exposure, it was found that wild type *B. agri* C15 was less likely to respond to Cd compared to mutant *B. agri* C15 Cd^R. Also, the inhibition appeared Cd-dependent, and both strains showed similar responses in specific growth rate and biomass under different Cd concentrations. Still, mutant *B. agri* C15 Cd^R had less specific growth rates and biomass with addition Cd concentrations (15-20 mM). Few studies have investigated Cd effects on mutants. The mutants of *Escherichia coli* were found to be less responsive to a concentration of 6 mM Cd (Qin *et al.*, 2019). Helbig *et al*. (2008) found that the mutants of *E. coli* had slower growth rates when exposed to a tolerant Cd concentration of 0.7 mM. These results, together with this study, suggest that Cd concentrations influence mutant growth.

The MICs of wild type *B. agri* C15 and mutant *B. agri* C15 Cd^R were estimated as 16 ± 0.7 mM and 21 ± 0.4 mM, respectively. *C. metallidurans* DSM 2839^T was chosen for quality control as it is known to resist Cd. Mergeay *et al.* (1985) reported that the MIC of $CdCl_2$ for *C. metallidurans* DSM 2839T was 2.5 mM, achieved on Tris-gluconate- agar plates. The current study showed that the MIC of $Cd(NO_3)_2 \cdot 4H_2O$ for *C. metallidurans* DSM 2839T was 4.5 ± 0.2 mM on H3BS/pyruvate. The composition of the Tris-gluconate- agar is sodium gluconate, which is utilised as a chelating agent because of its ability to bond with Cd ions and form coordinate bonds. Consequently, the availability of the added Cd into Tris-gluconate agar could be lower than its actual nominal concentration.

However, in this study, H3BS basal medium was used and solidified with granulated agar to determine the MIC of Cd for *C. metallidurans* DSM 2839^T as H3BS medium is a preferred medium for its growth.

The H3BS basal medium does not have any chelating agents. Therefore, this study found that *C. metallidurans* DSM 2839^T resists Cd up to 4.5 ± 0.2 mM. Recently, Alviz Gazitua *et al.* (2019) found that the MIC of Cd for *C. metallidurans* DSM 2839^T was 4.0 mM, determined by the growth of this strain on phosphate Tris-buffered mineral salts (LPTMS) solidified with agar. It is essential to choose the proper agar when doing an assessment related to toxicity and metal availability. The quality of agar relies on two components: agarose (70%) and agaropectin (30 %). Agarose is a polysaccharide containing many carboxyl groups that can establish van der Waals interactions with metal ions. By this, agarose reduces the bioavailability of Cd ions in an agar medium. However, the agarose does not provide the metal bonding of agaropectin. Agaropectin is a galactan, which has polysaccharides in its structure that provide carboxyl groups. In addition to its main feature is the presence of ester sulfates, D-glucuronic acid, and pyruvic acid. These compounds create strong bonds with metal ions; in this way, it causes the heterogeneous distribution of metal ions, which exposes cells to a lower concentration of metal ions and has a high MIC value.

The MICs of wild type *B. agri* C15 and mutant *B. agri* C15 Cd^R were higher than their MTCs, which were determined in EBS broth. The mathematical model of bacterial growth on an agar plate (Pirt, 1967) is based on the fact that nutrients form over time, causing a heterogeneous distribution of ions versus the

homogenous distribution seen in liquid media. The effect of these distributions has been observed for almost a hundred years (Fawcett, 1925). However, during the determination of the MIC in agar, some of the colony cells were exposed to Cd, as it is known that a colony structure has different cell phases. These phases are cell division, followed by the post exponential growth and stationary phases of the cells (Hobley *et al.*, 2015). Therefore, cells at the top are usually not exposed to as many toxic effects as cells in division or post exponential phases. The MICs of wild type *B. agri* C15 and mutant *B. agri* C15 Cd^R revealed that the mutant type was the most Cd-tolerant. This variance may be due to the modification accumulation of Cd on cell surfaces. The mechanisms for enhanced tolerance to toxic effects of Cd in the UV-mutant have been described as the result of the introduction of –SH (sulfhydryl) compounds that combine with Cd and reduce its bioavailability (Cooley *et al.*, 1986; García *et al.*, 2002). Nevertheless, the resistance variance in mutant cells is likely due to the activation of an efflux system, which causes the reduction of Cd uptake into the cells and increases its Cd tolerance, and this could be the possible mechanism. This study is not aware of other reports of an efflux system, which leads to an increase in tolerance ability.

To investigate the role of the extracellular polysaccharides, slime, or glycocalyx materials in response to Cd resistance during the fixation techniques, the gas-phase O_5O_4 was used to stabilise the lipids of the cells before cross-linking with DEC or ABL fixation. Overall, both fixation techniques provided equivalent morphological information, but the ABL method showed more glycocalyx preservation of cell structures compared with the DEC method; the Cd-exposed

cells were coated with a visible glycocalyx structure. The effectiveness of the ABL fixation of bacterial polysaccharides was observed more recently (Geisler *et al*., 2019) than DEC fixation (Fischer *et al*., 2012). The SEM micrographs showed that the strain cells were slime-layer producers due to the production of extracellular polysaccharides. Still, the biofilm formation assay showed that neither cell strain produced biofilm with or without Cd on Congo red agar. Congo red stain can bind with the proteins and polysaccharides of the cells, and its colour can be changed from blue to red between pH 3.0 and 5.2. Freeman *et al*. (1989) used the Congo red agar method for the detection of biofilm production; however, it is not a rich medium to support healthy growth. Kaiser *et al*. (2013) modified the Congo red agar method to detect biofilm production by adding different concentrations of NaCl and glucose. Recently, Lima *et al*. (2017) found that the Congo red agar method is an ineffective method for the detection of biofilm production compared to the biofilm quantification assay method. In the literature, none of *Brevibacillus* spp. were recorded as biofilm production (Shida *et al.*, 1996) due to nonhydrophobic nature of its cell surface (Hadad *et al*., 2005). However, Narisawa *et al*. (2008) reported that *B. borstelensis* S1, as a biofilm producer, was grown within continuous-culture flow cells based on the pre-established biofilm of a pyocyanin producer. Also, Wu *et al*. (2014b) found that *Brevibacterium* sp. was a biofilm producer, which used a quantification method including grown cells, washing, staining with crystal violet, and resolubilising cells into a dimethyl sulfoxide with a prior measurement *OD* at 570 to present biofilm biomass. So, the formation of the glycocalyx, which was observed in SEM images, could be a slime layer as these strains were non-biofilm

producers. The slime layer is a mixture of EPS glycoproteins and glycolipids. Despite the fact that the Congo red agar could not support the growth of cells for biofilm production, EBS agar had rich materials that showed support medium of *B. agri* to form biofilm layers observed under SEM.

It is clear from SEM micrographs that *B. agri* C15 and *B. agri* C15 Cd^R produced slime layers, and some of these layers could be washed off through the fixation method. In this study, the cell colonies were fixed in 2.5% of glutaraldehyde; this solution has been reported as an EPS removal solution, and is suitable for washing and observing a clear image of the cells. Chao and Zhang (2011) performed a comparative study of the standard fixation solutions to evaluate the best solution to use for a clear image of bacterial cell morphology and ultrastructures. In their research, for the quantitative and qualitative assessments, 2.5% glutaraldehyde and ethanol/acetic acid (3:1) solutions were used to remove the EPS from bacterial cells. The glutaraldehyde failed to preserve the EPS compound effectively due to the insufficient stability of highly replaceable and variable polysaccharide moieties during the dehydration process of EPS matrices, which can be distorted (Ratnayake *et al*., 2012). Therefore, it is common to use cross-linking agents to stabilise bacterial EPS compounds. A cross-linking agent makes a net inside the biofilm structure, thereby calming the EPS. This step, along with the subsequent post-fixation, is designed to prevent the breakdown of the cell's biological structures (Hong *et al.*, 2007). The effects of Cd on the cell morphologies of both strains after 48 h of exposure were observed via the formation of the EPS. The EPS was produced as a way for cells to protect against the toxic effects of Cd. The EPS consists of carbohydrates or proteins

that provide sufficient hydroxyl groups for Cd to bind to, preventing Cd from entering the cells and increasing their resistance.

TEM micrographs of *B. agri* C15 and *B. agri* C15 Cd^R were grown without Cd showed that *B. agri* C15 has a three-layer wall structure, unlike *B. agri* C15 Cd^R which has one layer. However, this does not mean that each strain belongs to a different species. It has been revealed that *Geobacillus* spp. (closely related to *Brevibacillus* spp.) have been observed as a Gram-stain-positive bacteria: a thin peptidoglycan layer surrounds their cytoplasmic membranes along with a covered surface layer with a zone of low contrast between these layers (Nazina *et al.*, 2001). In a recent study, it was noticed by Marche *et al.* (2017) that the TEM image of *B. laterosporus* showed the cells had two different properties, each seen in the same TEM section of the bacterial cells. This phenomenon of changing the cell wall characterisations from Gram-stain-negative to Gram-stain-positive is common in *Brevibacillus* spp. since they are defined as positive, negative, or variable depending on the stage of their growth cycles (Vos *et al.*, 2011). For example, TEM images of *B. reuszeri* showed a comparable three-layer wall structure, although this species is defined as a Gram-stain-positive bacterium (Zhao *et al.*, 2018). However, Thomas (2006) observed *B. choshinensis* ARBG1 as a Gram-stain-negative bacterium, despite it being described earlier as a Gram-stain-positive bacterium. He concluded that some Gram-stain-negative bacterial species such as *B. invocatus*, *B. limnophilus,* and *B. levickii* had been identified initially as Gram-variable bacteria. The cell wall structure of *B. agri* C15 and *B. agri* C15 Cd^R did not fix adequately as Takebe *et al*. (2012) observed the canonical wall structure of the

Gram-stain-positive bacteria, *B. nitrificans* under TEM after treating with 1% phosphotungstic acid.

The TEM observations showed that some 'blebs' surrounded the cell walls. This observation was similar to the detection of *Lactococcus lactis* subsp*. Lactis,* grown with Cd (Sheng *et al*., 2016); however, some *B*. *laterosporus* phages were also similar to the observed 'blebs' in topology and size in this study (Berg *et al*., 2016). Electrondense granules and endospores were observed in *B. agri* C15 and *B. agri* C15 Cd^R; therefore, it was essential to ascertain the nature of these granules. The staining of the cells with hot malachite green solution revealed endospores that were topologically similar to the endospores observed in *B. laterosporus* (Marche *et al*., 2017). Poly-*β*-hydroxybutyrate was observed in both strains, while polyphosphate granules were not observed. Therefore, the electrondense granules observed under TEM were likely poly-*β*-hydroxybutyrate formed under Cd stress. Leonel *et al*. (2019) found that the production of poly-*β*-hydroxybutyrate, as reserves of carbon and energy, increased in *Rhizobium tropici* LBMP-C01 under copper and chromium exposure. It is known that polyphosphate granules are a starvation response in bacteria, and they are vital for survival and resistance to toxic stresses. Copper tolerance in *E. coli* was mediated by polyphosphate metabolism due to *pitA* gene expression (Grillo-Puertas *et al*., 2014). In this study, neither strains (*B. agri* C15 and *B. agri* C15 Cd^R) produced polyphosphate granules; this may be due to the absence of genes responsible for polyphosphate metabolism.

3-5- Conclusion

The *B. agri* C15 Cd^R mutant was generated from isolated *B. agri* C15 by UV light mutagenesis, and this mutant showed enhanced resistance to Cd and had a MIC value of 21 ± 0.4 mM to Cd, which was higher than the MIC of the wild type (16 ± 0.7 mM). Thus, it is concluded that this mutant could be suitable for the development of a Cd-bioremediation process; therefore, further studies are needed to investigate this possibility.

Chapter 4. Cadmium removal with mutant *Brevibacillus agri* C15 Cd^R entrapped in calcium alginate gel: a new process

Abstract

With large-scale mining and industrial use of cadmium (Cd), contamination with this metal increased steadily. Concerns due to its toxicity and potential damage to the environment and human health have led to the introduction of legislation that regulates acceptable environmental concentrations in different contexts. Therefore, many treatment methods for water and soils have been developed to limit the concentration of Cd in the environment and comply with regulations. In this chapter, a small laboratory bench-scale column reactor was constructed, optimised, and used to evaluate the removal of Cd from artificial groundwater (AGW) with mutant *Brevibacillus agri* C15 Cd^R and its wild type *B. agri* C15 entrapped in calcium alginate beads at different Cd concentrations. The morphological properties of the beads were studied by scanning electron microscopy (SEM), and energy-dispersive X-ray (EDX) spectroscopy and the location of Cd adsorbed in the beads was detected using a dithizone histochemical method. The experimental results showed that the mutant had significantly higher removal rates than its wild type *B. agri* C15 (9 and 5 nmol per day per gram of biomass, respectively) due to the presence of the Cd-dithizone complexes on the bead containing the mutant, compared with the less presence of these complexes on the beads containing the wild type. In conclusion, a new process was developed that achieved a higher Cd removal rate from AGW by the mutant *B. agri* C15 Cd^R. In addition, an alternative detection method of Cd (Cd-dithizone complexes) was introduced that showed that Cd was distributed throughout the Cd-loaded beads.

4-1 Introduction

Cd is considered as a serious environmental issue because of its toxicity, non-biodegradability and bioaccumulation (Shahryari *et al.*, 2019). The contamination of groundwater with Cd has become a global challenge, and more effective methods for removing Cd are required. Several treatment technologies, such as precipitation, adsorption, ion exchange, and bioremediation, are used for this purpose (Hashim *et al.*, 2011). Among these technologies, the bioremediation– the use of bacteria to remove Cd from water – is known as one of the processes applied for removing Cd from solutions and water, and this can be achieved in both batch and reactor experiments. Microbial mass, on its own, is not a mechanically stable material to be used for an effective process within a reactor. Therefore, to protect the bacterial cells against washing out, caused by the circulating fluids in the reactor or associated turbulence and shear force, the immobilisation of bacterial cells is required (Hochstrat *et al.*, 2015). In recent times, bioremediation processes have employed immobilisation methods to achieve highly efficient pollutant removal, a reduction in the risk of cell mutations, an increase in the resistance of biocatalysts to toxic compounds, and an increase in the survival rate of the biocatalyst during the treatment (Dzionek *et al.*, 2016). Although the immobilisation of the cells is an additional processing step, it is a cost-effective preparation method for high-stability laboratory operations. In recent times, bioremediation processes have employed immobilisation methods to achieve highly efficient pollutant removal, a reduction in the risk of cell mutations, an increase in the resistance of biocatalysts to toxic compounds, and an increase in the survival rate of the biocatalyst during the treatment (Dzionek

et al., 2016). Five techniques are used to immobilise cells, based on the supporting material and the bond types involved (Figure 24):

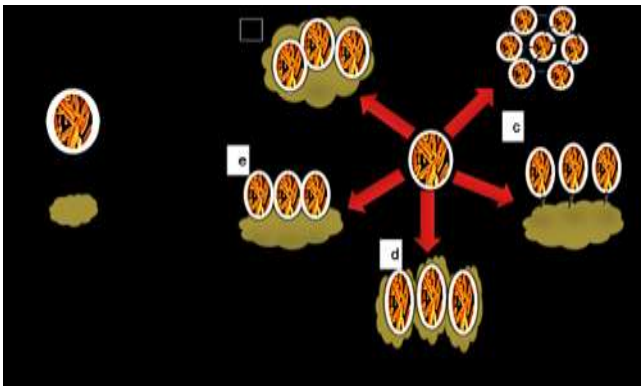

Figure 24. Schematic diagram of the five methods of cell immobilisation: **(a)** Encapsulation, **(b)** Cross-linking, **(c)** Entrapment, **(d)** Adsorption, and **(e)** Covalent bond (Brena *et al.*, 2013).

(a) The encapsulation method blocks cells inside the hollow microspheres of the polymeric matrices, protecting against the external environment. This method is cheap and straightforward when immobilising a large number of cells. It involves the mixing of cells with calcium chloride solution, followed by dropping it into the alginate solution to form beads. This method is applied in individual therapy in medicine and biotechnology. Still, it is rarely used in bioremediation, as high porosity of microspheres may pose a problem when the goal is to keep the bacterial cells away from their environment (de Vos *et al.*, 2009).

(b) The cross-linking method of cell immobilisation is used in the absence of support materials. Covalent bonds are formed by direct links of various groups of cells and polyfunctional reagents, such as glutaraldehyde. Therefore, this method involves carrier-free immobilisation, during which the bacterial cell acts as the support material, unlike other methods (Brena *et al.*, 2013). This immobilisation

leads to a modified cell structure, which is less active by losing catalytic properties (Mateo *et al*., 2004).

(c) The entrapment method is the most straightforward and widely used technique for cell immobilisation and is well known in bioremediation. This method is very similar to the encapsulation method. The entrapment method involves entrapping cells physically inside porous materials using covalent or non-covalent bonds. This is achieved, for example, by mixing alginate with cells and then dropping it into a calcium chloride solution, which forms Ca-alginate beads. The entrapment method usually minimises cell leaching from porous materials into the aqueous and improves the stabilisation of cells, as cells do not chemically interact with the carried materials; therefore, the denaturation of the cells is usually avoided (Shen *et al*., 2011).

(d) The process of adsorption is to bind the cells using different forces (e.g., ionic, van der Waals, Carrasco *et al*., 2014) on the surface of the supporting material by immersing the support in the cell solution and incubating it to allow time for physical absorption. Different support carriers have been used when carrying out the adsorption method, including coconut fibres, microcrystalline cellulose, kaolin, chitosan, activated carbon, and other materials. The adsorption method is a simple process, solid enough to prevent particles from leaking into the environment; however, this method is less effective when using it as a biocatalyst because it allows for cell denaturing (Brena *et al.*, 2013).

(e) The covalent binding method is the interaction between the chemical groups of cells (hydroxyl, amino) with chemical groups or rings on the support material (amino, hydroxyl, carboxyl, thiol, methylation, guanylyl, imidazole, and phenol).

Different associations have occurred through this interaction, such as diazotisation links between the amino groups of the support material and the tyrosil or histidyl group of cell binding, peptide. Several gel matrixes have been used when carrying out the covalent binding method, including carbohydrates (cellulose and agarose), synthetic agents (polyacrylamide), amino group (amino-benzyl cellulose), protein (collagen and gelatine), cyanogen bromide, and inorganic materials (porous and silica). This method has been used in cell immobilisation as it is simple and causes no leaching problems. However, the chemical interaction between the support materials and the cells leads to the loss of the functional conformation of cells. It affects their activity when experimenting with a specific treatment (Brena *et al*., 2013). The selection of the carrier material (support) is crucial because it affects the overall process and performance of bacterial cells. The carrier material must be non-toxic to microorganisms, non-biodegradable, have strong mechanical stability, be low-cost, have high biomass retention, and have good permeability. These properties reduce the negative impact of the carrier material on the structure and properties of the cells; thus, the immobilised cells keep high catalytic activities (Mattiasson, 2018). Different matrix materials have been used in the entrapment of cells, such as polyacrylamide gels, cellulose triacetate, agar, gelatine, carrageenan, or alginate. These carrier materials provide functional groups in their structure, mainly hydroxyl and amine groups, which allow for direct interaction between the immobilised cells and metal cations, thus, facilitating the vital uptake of metals (Brena *et al.*, 2013). These materials are renewable and easy to obtain; in many cases, they are by-products of various algae, making them low-cost, reducing the

expenses associated with the immobilisation process. Sodium alginate is one of the most common matrices for the entrapment of cells for the accumulation of toxic materials by microbial cells. The alginate is less toxic than other polymers; it is an anionic polysaccharide that provides attractive properties for gel formation, concentration, and stabilisation (Draget and Taylor, 2011). Sodium alginate, with an acid dissociation constant (p*K*a) of 1.5 – 3.5, has been used to treat metal and other substances from water and wastewater as reviewed by Wang *et al*. (2019). Therefore, the main purpose of this chapter was to investigate the Cd removal by Ca-alginate beads containing bacterial cells that are resistant to Cd and sodium alginate as a bacterial support matrix. The qlive cells of mutant *B. agri* C15 Cd^R were subjected to the process of Cd removal along with its wild type *B. agri* C15 in addition to their boiled-cells (called killed-control). Since the Ca-alginate beads, without bacterial cells, were identified as a good Cd- adsorbent (El-Naggar *et al.*, 2018), their ability to remove Cd in this reactor was investigated first, functioning also as an experimental control that evaluates the contribution of Cd removal by the Ca-alginate beads versus by the bacterial cells. The investigation was carried out with the objectives: setting up and operation of the column reactor for the removal of Cd for 28 days, followed by the evaluation of the Cd removal rates at higher concentrations of Cd (8.8, 13.4, and 17.3 μM) for several days. The morphology of the Ca-alginate beads containing bacterial cells before and after the removal was observed with SEM, while the distribution of Cd in the beads was observed under a light microscope, using a dithizone histochemical method.

4-2 Methodology

4-2-1 Removal of cadmium from AGW in a small laboratory bench-scale column reactor

The reactor system was constructed and optimised, as described in Chapter Two. In Cd removal experiments, AGW (pH 7.00) with a nominal concentration of 4.4 μM Cd, chosen from the mean levels of Cd-contaminated freshwater reported in the literature, was pumped into five column-packing materials (n = 1), one reactor with three columns):

(1) Ca-alginate beads containing live cells of *B. agri* C15,

(2) Ca-alginate beads containing live cells of *B. agri* C15 Cd^R,

(3) Ca-alginate beads containing killed-control cells of *B. agri* C15,

(4) Ca-alginate beads containing killed-control cells of *B. agri* C15 Cd^R, and

(5) Control Ca-alginate beads without bacterial cells.

Reactor systems were in operation for 28 days, and samples were collected daily from eluants to measure the total concentration of Cd.

The embedding of live or killed cells in the Ca-alginate matrix was carried out, as described in Chapter Two. The Ca-alginate beads containing killed-control cells of *B. agri* C15 and *B. agri* C15 Cd^R were obtained after incubating the strain cells at 100 °C in a water bath for 15, 30, 45, 60, and 90 mins. These incubations at different temperatures were carried out to estimate the optimal kill times of both strains, which caused 100% cell death. The results showed that 30 mins of boiling were enough time to kill 100% of the cells (Figure 25). Therefore, this time was chosen as the boiling period for both strains at 100 °C to obtain inactive cells (killed-control).

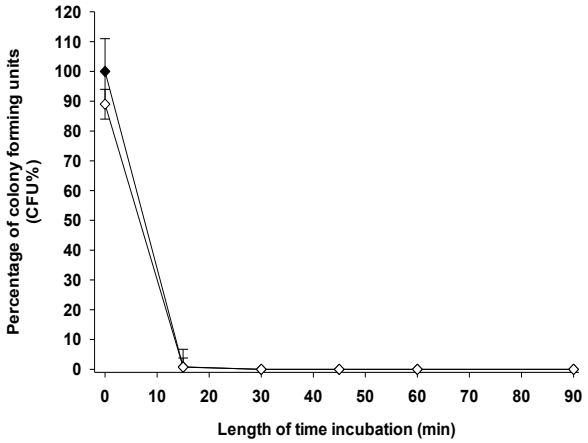

Figure 25. The lethal time curves of (♦) *B. agri* C15 and (◊) *B. agri* C15 Cd^R. 100 mL of a diluted sample of a mixed bacterial cell-AGW was boiled in a water bath at 100°C for 15, 30, 45, 60, and 90 mins. Control of a mixed bacterial cell-AGW was incubated at constant room temperature (22 °C) for 90 mins. The boiled and controlled cell-AGW were spread on R2A agar and incubated at 37 °C for 16 h. The total viable count (CFU/mL) was counted to determine the percentages of CFU. The percentages were the mean, and error bars indicate the standard error of the mean of three independent experiments (*n* = 3).

Under the same optimised process, the effects of different Cd concentrations (8.8, 13.4, and 17.4 μM Cd) in AGW on Cd removal were investigated by all types of Ca-alginate beads for 10 days, including the collection of samples from eluants every day. Following collection, samples were acidified immediately with 1% nitric acid, and indium (in final concentration, 0.43 μM) was added to be used as an internal standard for ICP-MS. The total concentrations of Cd in samples were determined as described in 'Elemental Analyses'. These concentrations were normalised per dry biomass (mg) according to He and Chen (2014) by firstly determining the amount of the dry biomass (mg) of cells in the suspension per mass of beads formed by the suspension of cells (mg dry biomass/mg bead) (except Ca-alginate beads without bacterial cells [per beads]). Then, the concentration of Cd was normalised, per mass of beads in a column, to determine the amount per the volume of water holdup. The tangent lines were applied to the

curves to give approximate rates of Cd removals during the initial time of operating the reactor.

4-2-2 SEM bead analyses

The beads, loaded with Cd-AGW, were drained and washed with ice-cold physiological normal saline. After draining water from the column, the column was closed from the top using dental wax, and from the bottom using a blue Tack and kept at − 20 °C for the fixation process before SEM observations. Single beads (six for each type and treatment) were selected and cut in half with a sterilised blade. The beads were then subjected to DEC fixation (*N*-(3-dimethyl aminopropyl)-*N*′-ethyl carbodiimide), as described in Chapter Two.

4-2-3 Distribution of cadmium in the beads using a dithizone histochemical method

It is well known that dithizone is used for Zn histochemistry and chelates Mg, Fe, Co, Pb, Hg, and Cd (Kiernan, 2008); therefore, dithizone was used for the localisation of Cd within the beads.

To prepare beads for histochemistry, exposure of the beads to Cd was carried out as part of a batch of adsorption tests. For this, Ca-alginate beads containing live cells of *B. agri* C15 and *B. agri* C15 Cd^R and control Ca-alginate beads not containing bacterial cells were subjected to this assay. The Ca-alginate beads were prepared using the entrapment method in Ca-alginate gel, as described in Chapter Two.

Cd uptake into Ca-alginate beads was obtained from AGW with a nominal concentration of pyruvate (20 mM) and 10 mM Cd. The adsorption experiments

were carried out in flasks (250 mL Erlenmeyer flask), incubated at 22 °C for 48 h, which were stirred regularly using a glass rod. After two days of the adsorption, the beads were collected from each batch using a sieve, rinsed quickly with physiological normal saline, and transferred into a Falcon tube for the histochemical procedure.

The histochemical method for Cd localisation in the beads involved the dehydration of the beads using a tissue processor (Leica, TP 1020), which usually takes 12 to 24 h. The beads were held in mesh biopsy cassettes to be placed on the tissue processer in graded percentages of ethanol: 50%, 70%, 90%, and 100%. The beads were embedded in paraffin using an embedder (Leica EG 1150H). A microtome sectioner (Leica RM 2235) was used to cut the embedded beads to a thickness of 20 μm. After the sectioning, the paraffin sections were transferred onto slides, without being flattened on water, and the sections were fixed onto the slides using a hot plate before clearing in xylene over three changes for 10 mins.

The staining of Zn and Cd in the beads was carried out, according to Kiernan (2008), using mixed dithizone solutions. For the staining of Zn, the reagent consisted of 24 mL of solution A (100 mg dithizone and 100 mL anhydrous acetone), 5.8 mL of solution B (55 g sodium thiosulphate, 5.9 g sodium acetate, potassium cyanide 1.0 g and 100 ddH_2O), 2 mL of solution C (2 mL of acetic acid (1.0 M), 0.2 mL of solution D (sodium potassium tartrate solution, 2%*w*/*v*), and 18 mL ddH_2O. CCl_4 was used to extract traces of Zn, which occurred in solution B, by using a separatory funnel. The dithizone reagent used for the staining of Cd consisted of 24 mL of solution A and 14 mL ddH_2O. During the staining procedure,

the mixed dithizone solution was applied to the slide for 10 mins, followed by rinsing in two changes of chloroform for 30 s. The slides were then washed in water and left to dry. Before staining for Cd, Zn was removed by applying 1% acetic acid to the beads. Observations of Zn or Cd in the beads were carried out under a light microscope (Leica).

4-2-4 Elements analyses

The uptake of Cd from AGW by the beads was analysed by determining the concentrations of Cd remaining in the eluants after operating the reactors using inductively coupled plasma mass spectrophotometry (ICP-MS, Thermo Scientific, X Series 2). The instrument's limit of detection (LOD) of Cd was established from the five times the standard deviation (SD) of measuring the lowest standard (n = 10) at 0.02 μM. Certified Reference Material (CRM, drinking water, EnviroMAT, Cat 140-025-031) was analysed to verify the recovery of the Cd analysis; the percentage recovery of ICP-MS via the use of CRM was 100 ± 0.03, which was calculated from the recorded (2.34 ± 0.03 μM Cd) and certified (1.7 ± 0.01 μM Cd) values of the reference material.

4-2-5 Statistical analysis

A two-way ANOVA, followed by a Tukey *post hoc* test (IBM SPSS statistics 22 software) was used to determine whether the removal rates of absorbents or the different Cd concentrations in the AGW, returned results that were significantly different from each other. SigmaPlot (version 13) was used to graphically express the data as the mean concentrations, and the error bars represented the standard error of the mean (n = 3). The curves were fitted with nonlinear regressions

(exponential decay). The tangent lines were applied to the curves to give approximate rates of Cd removals during the initial time of operating the reactor.

4-3 Results

4-3-1 Removal of cadmium from AGW in a small laboratory bench-scale column reactor

During the operation of the reactors, the samples were collected every day to measure the total concentrations of Cd remaining in the eluants. HRT values were varied in the single experiment, mainly due to the slight differences in the bead masses, resulting from the changes in the volume of the liquid holdup and flow rate. The average HRT was measured, which depended on the flow rate and the liquid hold up of 112.5 $\pm$ 0.9 min. Therefore, the extent of Cd removal in the column reactor systems depends on the biomass (mg) within the number and mass of the filled beads in the reactor per column.

Figure 26A, using Ca-alginate beads without bacterial cells, showed that the amount of Cd remaining in the eluant from the column reactor involves three stages over 28 days. First, there was a rapid reduction in the amount of Cd in the eluent, indicating an increase in Cd removal during the first five days (9.4 nmol/g of wet beads). Second, the removal has reached a maximum within 8 to 9 days, resulting in low Cd amounts in the eluent (1.6 nmol/g of wet beads). Finally, the Cd removal decreased gradually from day 10 to day 28 and recorded a higher amount of Cd in the eluant (15 nmol/g wet of beads) at the end of the experiment. Surface complexation and electrostatic attractions played an important role in Cd removal from a solution containing non-growing bacterial cells. It is clear from Figure 26B and C that the Ca-alginate bead containing killed-control cells of either

B. agri C15 or *B. agri* C15 Cd^R had similar patterns in the removal amounts. In the Ca-alginate beads containing killed-control cells of *B. agri* C15, the removal amounts reached 10.3 nmol/g of dry biomass on the second day of operating the reactor (Figure 26B). Similarly, the equivalent amount was removed (10.6 nmol/g of dry biomass) by Ca-alginate beads containing killed-control cells of *B. agri* C15 Cd^R on the second days of reactor operation (Figure 26C).

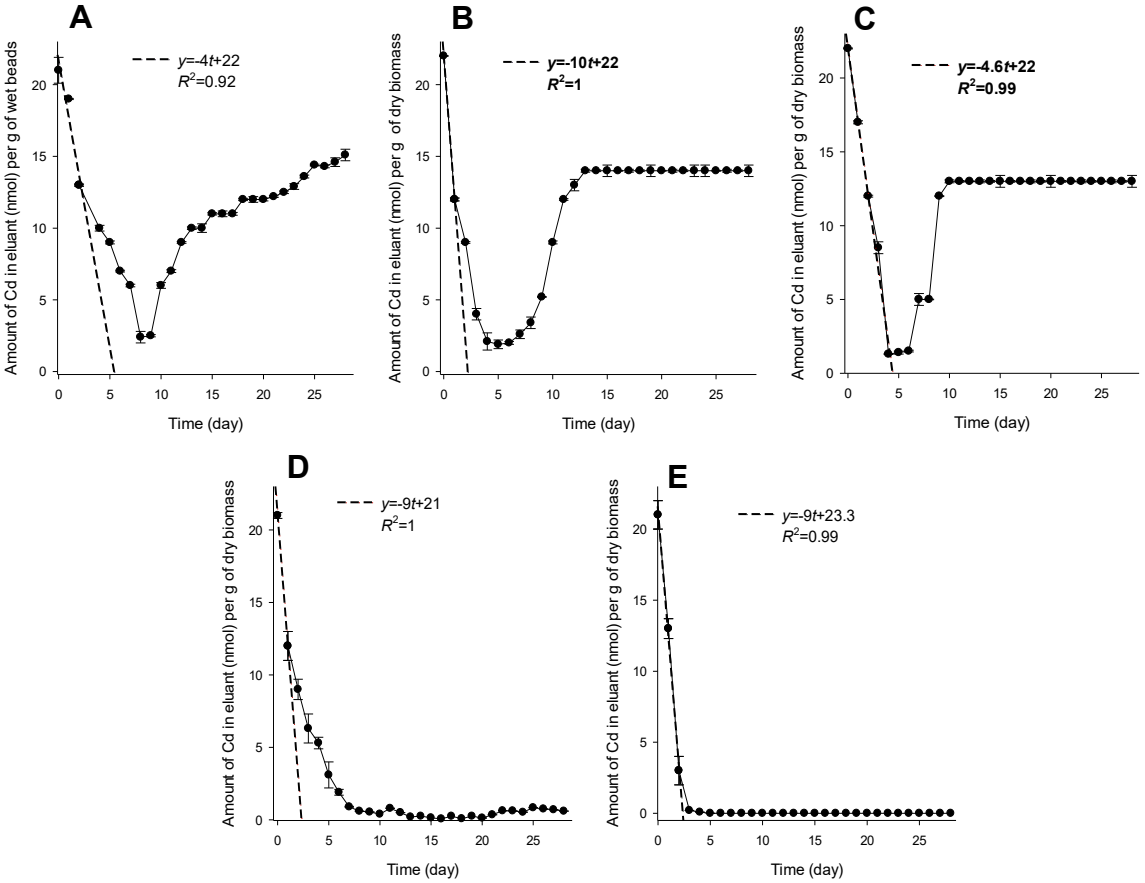

Figure 26. The amounts of total Cd measured in eluants of AGW with a nominal concentration of 4.4 µM Cd at pH 7.00 in the column reactor, filled with **(A)** Control Ca-alginate beads without bacterial cells, Ca-alginate beads containing killed-control cells of **(B)** *B. agri* C15 and **(C)** *B. agri* C15 Cd^R. Ca-alginate beads containing live cells of **(D)** *B. agri* C15 and **(E)** *B. agri* C15 Cd^R. The amounts were the mean, and error bars indicate the standard error of the mean SEM (*n* = 1, one reactor with three parallel columns of each). The amounts were obtained from normalising the total measured concentrations of Cd in the eluent, with the mass of the filled beads in each column reactor and finally normalised per biomass of the respective beads (except Ca-alginate beads without bacterial cells [per beads]) in the volume of AGW hold up (4.5 ± 0.6 mL). The tangent lines were applied to the curves to give approximate rates of Cd removals during the initial time of operating the reactor.

The highest Cd removal amount was obtained within 5 to 8 days (20 nmol/g of dry biomass), leaving similar amounts of Cd recorded in the eluants. Between days 8 and 10 of the reactor operation, both killed-control cells of *B. agri* C15 or *B. agri* C15 Cd^R showed a reduction in their abilities to remove Cd from AGW and reached a plateau of high amounts Cd (13 – 14 nmol per g of dry biomass) in the eluants and these

amounts were similar to the amounts recorded by the Ca-alginate beads without bacterial cells.

The removal amount of Ca-alginate beads containing live cells of *B. agri* C15 was 12.8 nmol/g dry of biomass after one day of operating the reactor, and this was analogous to the amount removed by the killed-control cells (Figure 26D, B, respectively). However, the live cells of *B. agri* C15 showed increasing amounts of Cd removal over the next few days, out-performing both Ca-alginate beads without bacterial cells and the killed-control cells in their abilities to remove Cd. The initial Cd removal rate for live cells of *B. agri* C15 Cd^R (Figure 26E), was similar to that of live cells of *B. agri* C15. However, the Cd amounts recorded in the eluants on the second day (3.6 nmol/g of dry biomass) was substantially lower, compared to the live cells of *B. agri* C15 (8.7 nmol/g of dry biomass). The Ca-alginate beads containing live cells of *B. agri* C15 showed lower and a somewhat unstable removal amount over 28 days. Thus, Ca-alginate beads containing live cells of *B. agri* C15 exhibited a much slower Cd removal, 21 nmol/g of dry biomass within 16 days, compared to the Ca-alginate beads containing live cells of *B. agri* C15 Cd^R that achieved the same amount of removal (21 nmol/g of dry biomass) within just four days of operating the reactor.

4-3-2 Evaluation of the cadmium removal from AGW with higher concentrations of cadmium

The Cd removal from AGW at pH 7.00 was further evaluated with concentrations of 8.8, 13.4, and 17.4 μM Cd in the column reactors, operated under the same conditions as the control concentration (4.4 μM), except for a shorter operating time (10 days). As before, the study was undertaken with five sets of Ca-alginate beads: without bacterial cells, containing killed-control cells of *B. agri* C15 or *B. agri* C15 Cd^R, and live cells of *B. agri* C15 or *B. agri* C15 Cd^R.

The results in columns not containing bacterial cells (Figure 27) show a slight increase in the initial Cd removal rates (tangent slopes; - 4.8 to -6.0) of the experiments. This indicates that during the early days, the removal rates of Cd from AGW were slightly more at higher initial Cd concentrations. Around days 8 – 10, the amount of Cd in the eluent plateaued at approximately the maximum removal of 14, 15, 22, and 27 nmol Cd per g of beads for the starting concentrations of 4.4, 8.8, 13.4, and 17.4 µM Cd, respectively. This shows that, although the proportion of Cd removed from AGW is higher (66%) at lowest initial Cd concentrations than it is at highest ones (28%), the capacity for Cd removal by Ca-alginate beads without cells has not been exhausted by day 10, even at 17.4 M Cd in AGW. The increase in the amount of Cd in the eluent observed at AGW with 4.4 mM Cd in the previous section (the final stage in Figure 26A) was not reached in this experiment, as it concluded on day 10. However, there is an indication of a slight upturn in Figure 27 (C, D) on day 10.

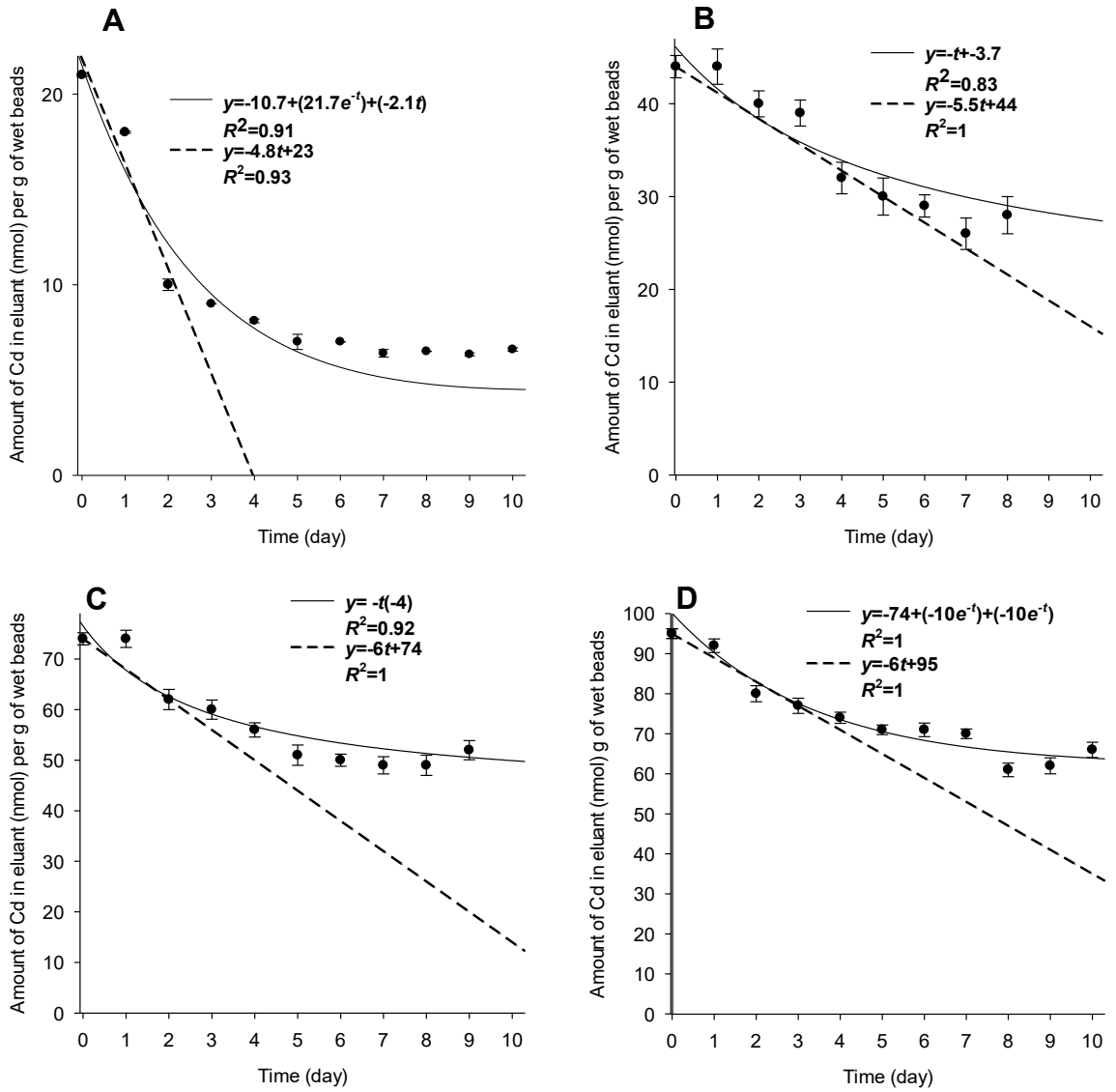

Figure 27. The evaluation of Cd removal by the Ca-alginate beads without bacterial cells from AGW at pH 7.00 with nominal concentrations of Cd: **(A)** 4.4 µM (control), **(B)** 8.8 µM, **(C)** 13.4 µM, and **(D)** 17.4 µM. The amounts were the mean, and the error bars indicate a standard error of the mean SEM (n = 1, one reactor with three parallel columns). The amounts of Cd were obtained, and tangent lines were applied, as described in Figure 26.

In contrast to Ca-alginate beads without cells, reactors containing Ca-alginate beads with killed-control cells showed a higher initial removal rate at the lowest AGW Cd concentrations (slope = - 7), compared to higher Cd concentrations (slope = - 3.5 to - 5.3) (Figures 28, 29). The minimum amount of Cd in the eluant was lower (1.5 to 3 nmol per g of dry biomass) at AGW 4.4 μM Cd with killed-controlled than without killed-controlled cells (Figure 27A). The overall reduction in the amount of Cd in the eluant by the end of the experiment was higher or similar for reactors containing killed-control cells than no cells (22, 15, 30, and ~30 nmol per g biomass for AGW concentrations of 4.4, 8.8, 13.4, and 17. 4 μM Cd, respectively).

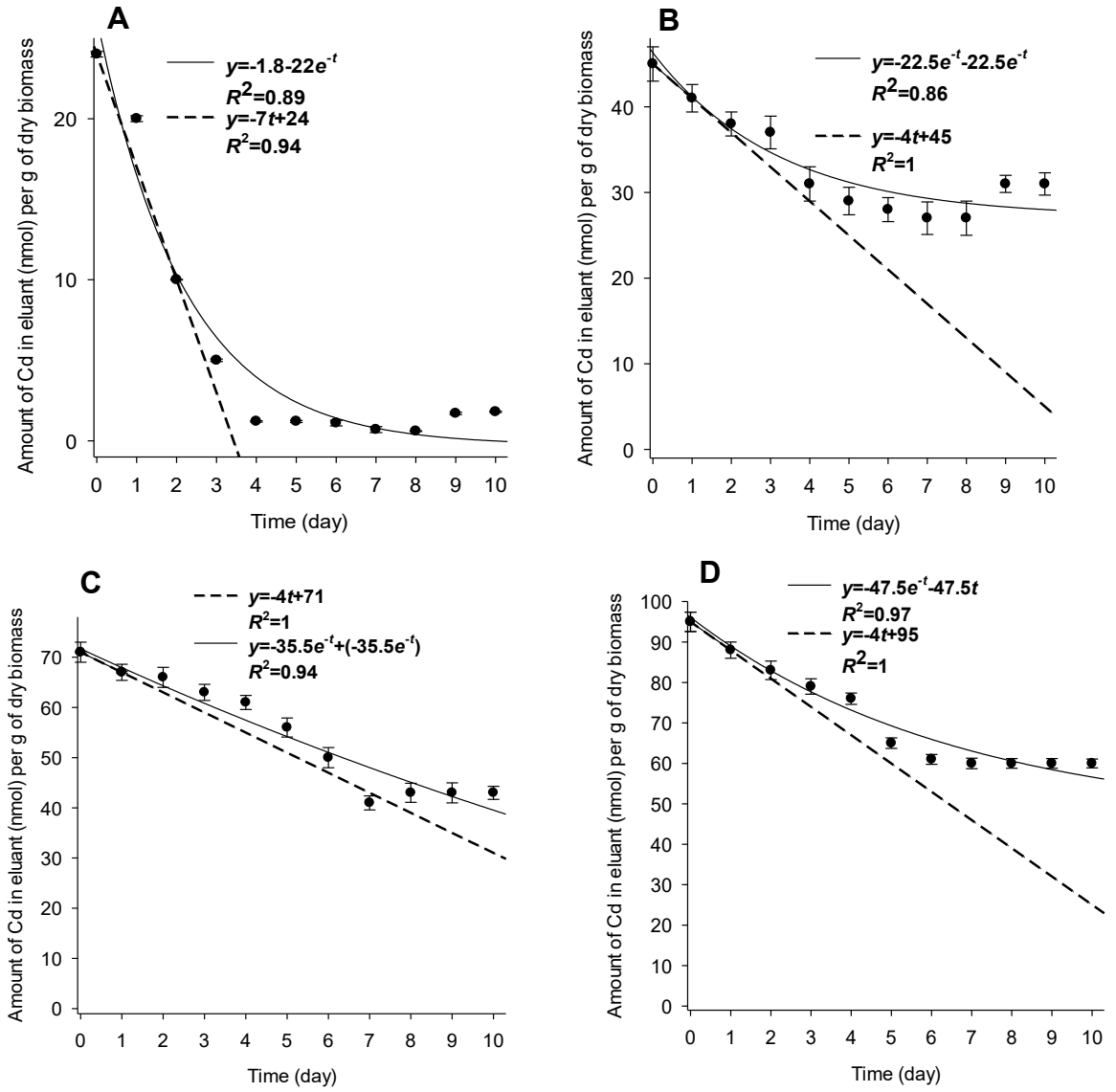

Figure 28. The evaluation of Cd removal by the Ca-alginate beads containing killed-control cells of *B. agri* C15 from AGW at pH 7.00 with nominal concentrations of Cd: **(A)** 4.4 µM (control), **(B)** 8.8 µM, **(C)** 13.4 µM and **(D)** 17.4 µM. The amounts were the mean, and error bars indicate standard error of the mean S.E.M (n = 1, one reactor with three parallel columns). The amounts of Cd were obtained, and tangent lines were applied, as described in Figure 26.

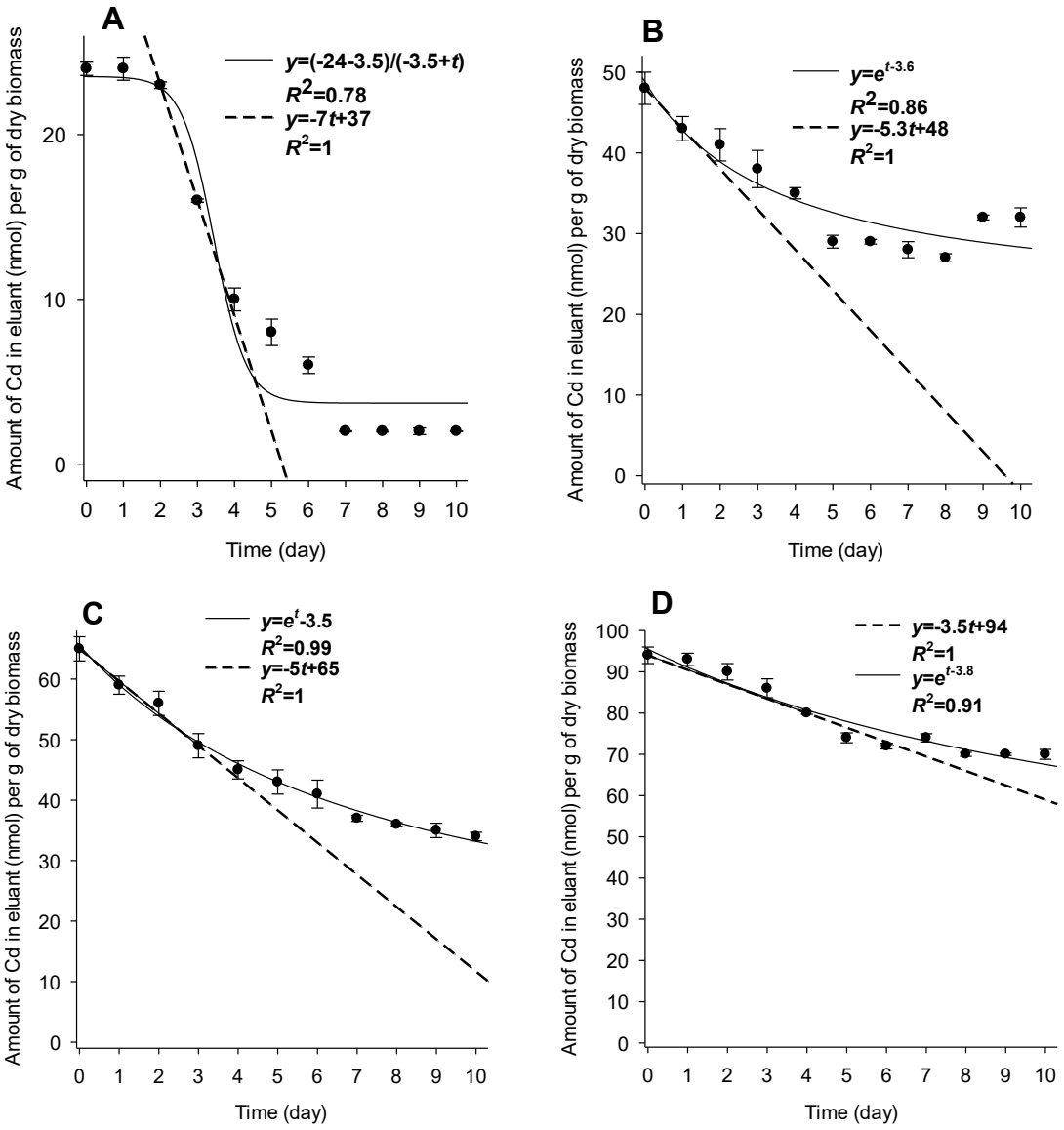

Figure 29. The evaluation of Cd removal by the Ca-alginate beads containing killed-control cells of *B. agri* C15 Cd^R from AGW at pH 7.00 with nominal concentrations of Cd: **(A)** 4.4 µM (control), **(B)** 8.8 µM, **(C)** 13.4 µM and **(D)** 17.4 µM. The amounts were the mean, and error bars indicate standard error of the mean S.E.M (*n* = 1, one reactor with three parallel columns). The amounts of Cd were obtained, and tangent lines were applied, as described in Figure 26.

Cd removal from AGW took place at slightly lower initial rates in reactors containing live cells of *B. agri* C15 (slope = - 2 to - 5; Figure 30), compared with killed-control cells (slope = - 3.5 to - 7; Figures 28, 29) and the amount of Cd in eluant remained relatively high at high AGW Cd concentrations (Figure 30 C, D) throughout the experiment.

In contrast, initial removal rates (slope = - 8 to - 9.3; Figure 31) of reactors containing live cells of *B. agri* C15 Cd^R was substantially higher than in any other reactor in this experiment and displayed a weak trend towards increased initial removal rates with increasing Cd concentrations in AGW. In addition, the employment of *B. agri* C15 Cd^R in the reactor resulted in the lowest amounts of Cd in the eluant. The absence of a plateau in the amount of Cd in the eluant at higher Cd AGW concentrations (Figure 31 C, D) indicates a further capacity for Cd removal in the reactors at the end of the experiment. Overall, approximately 22, 42, 70, and 85 nmol Cd per g of dry biomass were removed from AGW with initial concentrations of 4.4, 8.8, 13.4, and 17.4 µM Cd, respectively.

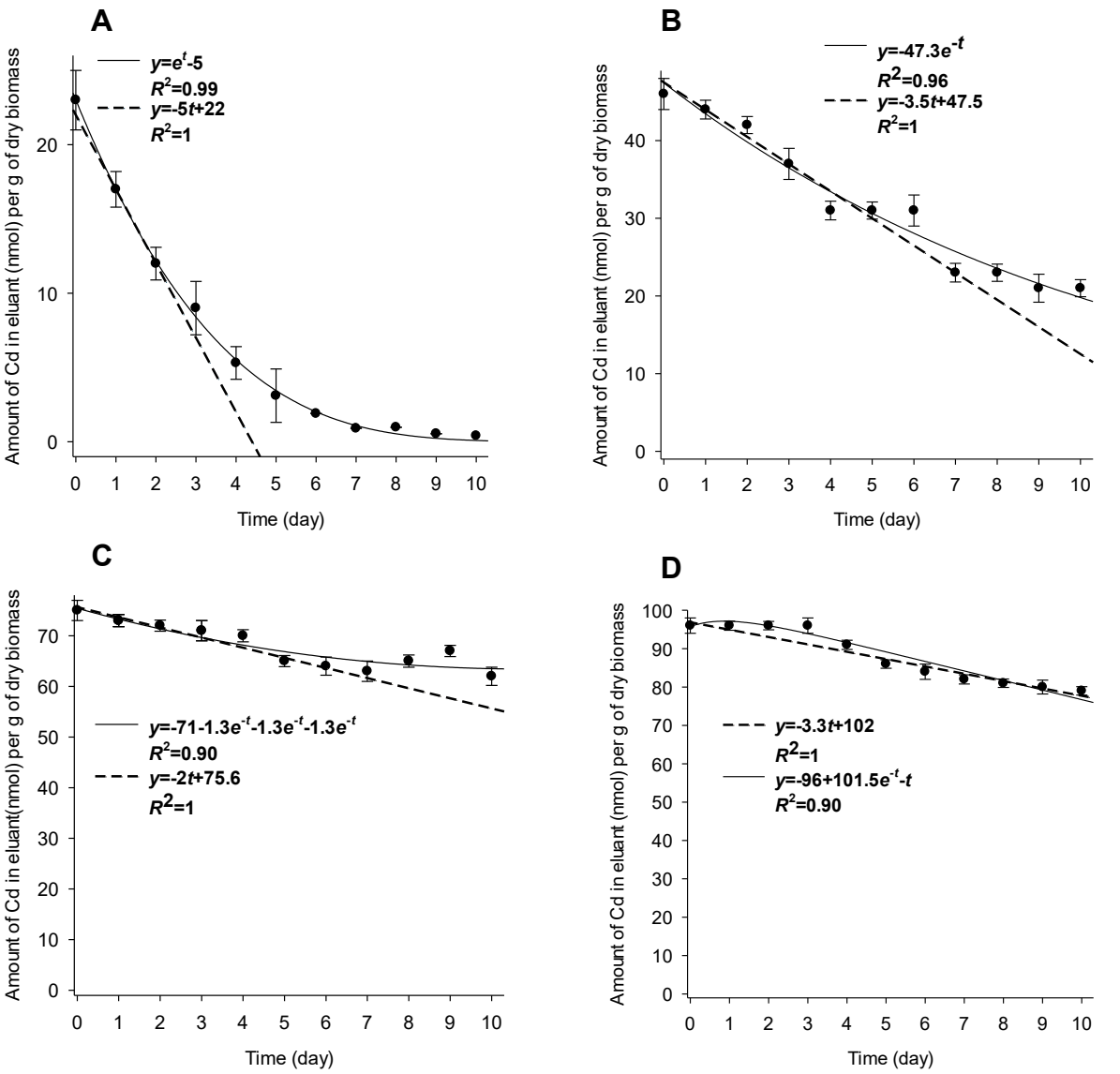

Figure 30. The evaluation of Cd removal by the Ca-alginate beads containing live cells of *B. agri* C15 from AGW at pH 7.00 with nominal concentrations of Cd: **(A)** 4.4 µM (control), **(B)** 8.8 µM, **(C)** 13.4 µM, and **(D)** 17.4 µM. The amounts were the mean, and the error bars indicate a standard error of the mean SEM (n = 1, one reactor with three parallel columns). The amounts of Cd were obtained, and tangent lines were applied, as described in Figure 26.

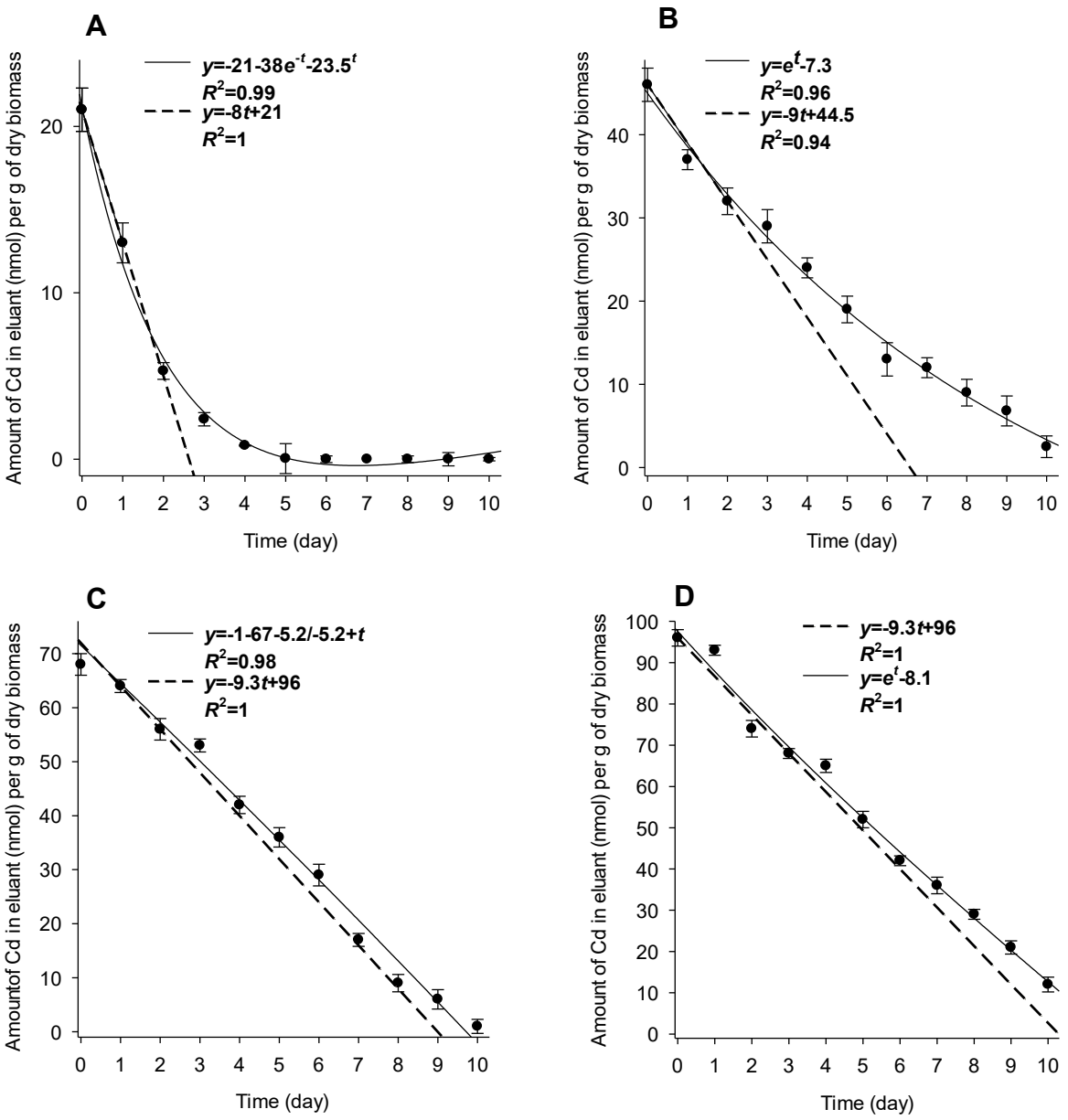

Figure 31. The evaluation of Cd removal by the Ca-alginate beads containing live cells of *B. agri* C15 Cd^R from AGW at pH 7.00 with nominal concentrations of Cd: **(A)** 4.4 µM (control), **(B)** 8.8 µM, **(C)** 13.4 µM, and **(D)** 17.4 µM. The amounts were the mean, and the error bars indicate a standard error of the mean SEM (n = 1, one reactor with three parallel columns). The amounts of Cd were obtained, and tangent lines were applied, as described in Figure 26.

4-3-3 Determination of maximum initial rates of cadmium removals

The effect of initial Cd concentrations on the Cd removal was obtained by applying the tangent lines to the curves (Figures 27, 28, 29, 30, 31) to give approximate rates of Cd removals during the initial time of operating the reactor.

Figure 32 shows that the rates of Cd removal decreased in the Ca-alginate beads containing live cells of *B. agri* C15 with increasing Cd-AGW concentrations from 4.4 to 13.4 μM. The Ca-alginate beads, containing live cells of *B. agri* C15 Cd^R displayed significantly higher Cd removal rates (9 nmol per day per gram of biomass) than its *B. agri* C15 (5 nmol per day per gram of biomass) or than other beads ($^a p<0.05$) at different initial Cd-AGW concentrations, with no differences observed between the concentrations of the mutant.

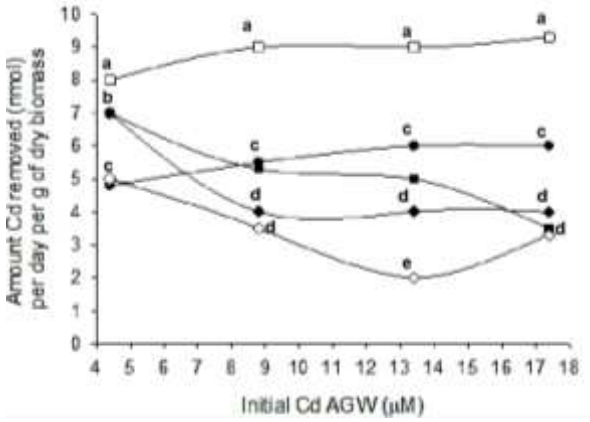

Figure 32. The respective maximum initial rates of Cd removal by the Ca-alginate beads (•) without bacterial cells, containing live cells of (◊) *B. agri* C15 and (□) *B. agri* C15 Cd^R, killed-control cells of (♦) *B. agri* C15 and (■) *B. agri* C15 Cd^R that were used as adsorbents in the reactor system operated with nominal concentrations of Cd: 4.4, 8.8, 13.4, and 17.4 μM in AGW (pH 7.00). The rates were subjected to a two-way ANOVA, Tukey *post hoc* test, and a different letter indicates a significant difference between groups at each Cd concentration.

4-3-4 Observation of SEM and SEM-EDX of Cd-loaded beads after Cd removal

The Cd-loaded beads from the reactors were used for Cd removal from AGW (17.4 μM Cd), as shown in Figure 30E of *B. agri* C15 and Figure 31E of *B. agri* C15 Cd^R, were examined with SEM analyses. These analyses were also carried out with control beads (beads filled within the column reactor, containing AGW without Cd) for each bacteria strain for comparison between the control and Cd-loaded beads.

Furthermore, the control beads (Ca-alginate beads without bacterial cells from the experiment shown in Figure 27E) were examined, as well as the control beads (filled within the column reactor, containing AGW without Cd). The images showed that all types of beads had ample pores and showed a heterogeneous structure (Figures 33, 34). The Cd-loaded beads, containing live cells of *B. agri* C15 (Figure 33 b1, b3), which seemed to be a cavity or Ca-alginate beads containing live cells of *B. agri* C15 Cd^R (Figure 34 b3) appeared to have wrinkles, compared to the structure of the control beads (Ca-alginate beads without bacterial cells (Figure 33 a1, a3). The heterogeneous composition of the Ca-loaded beads, as shown in Figure 33 a3 and Figure 34 a3, indicated that their surfaces were covered with more impurities. The higher magnification of these impurities showed the filamentous structures in the Ca-alginate beads without bacterial cells (Figure 35 A1) or containing live bacterial cells (Figure 35 B1). The EDX spectra of the beads acquired from SEM images assessed the difference of the elements before and after the removal of Cd. EDX spectra for all the beads showed the distribution of different element peaks of Ca, Na, C, P, Au, U, Fe, and Os in addition to Cd peak, which was rarely detected in Cd-loaded beads (Figure 33 b4).

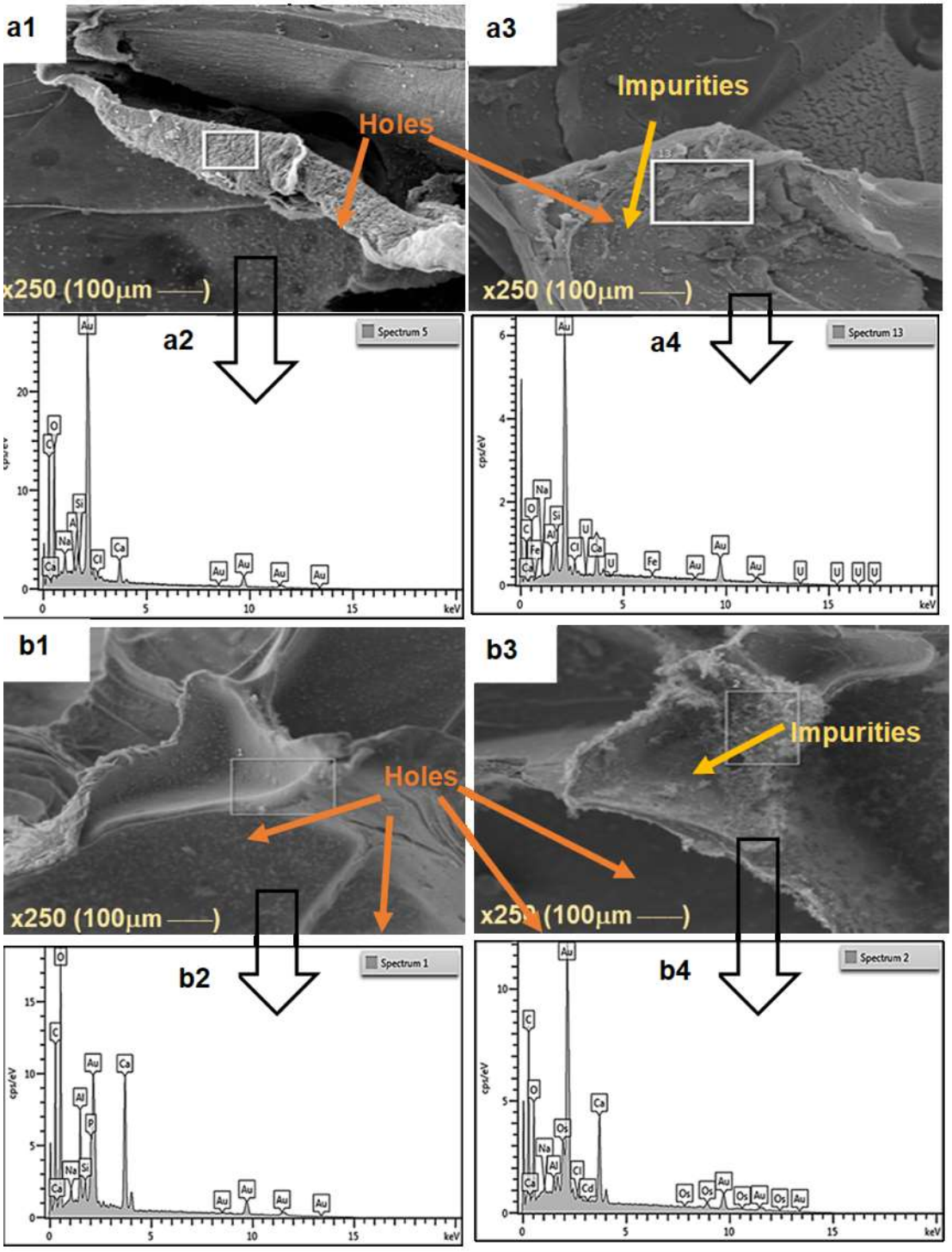

Figure 33. The SEM micrographs and EDX spectra of the beads obtained after Cd removal from **(a)** AGW or **(b)** AGW with a concentration of 17.4 µM Cd. Three replicates of the beads, using DEC fixation, were employed for the pictures and representative images from three replicates are shown. SEM image of Ca-alginate beads without bacterial cells (a1 and a3), and respective EDX spectra (a2 and a4), SEM image of Ca-alginate beads containing live cells of *B. agri* C15 (b1 and b3), and respective EDX spectra (b2 and b4).

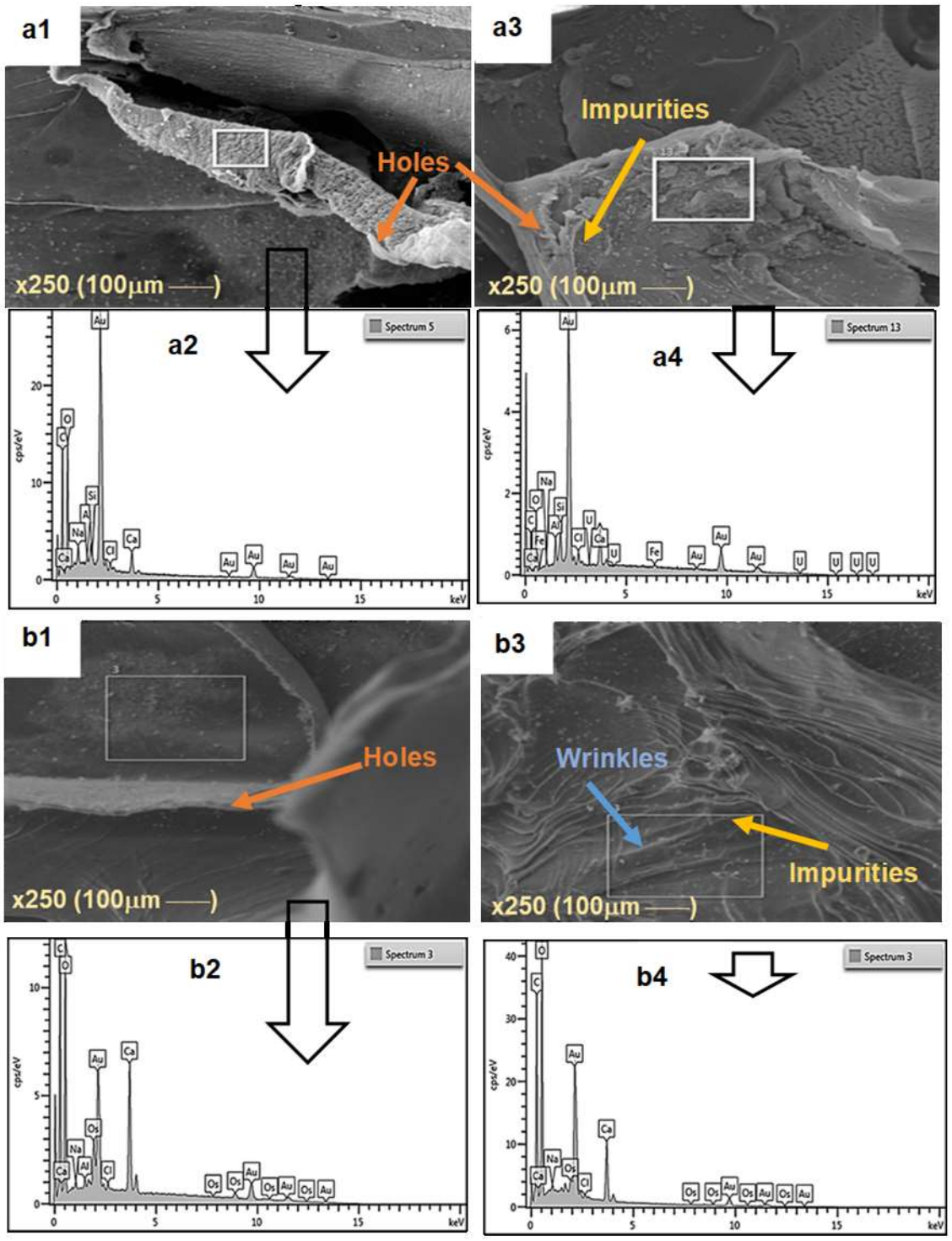

Figure 34. The SEM micrographs and EDX spectra of the beads obtained after Cd removal from **(a)** AGW or **(b)** AGW with a concentration of 17.4 µM Cd. Three replicates of the beads, using DEC fixation, were employed for the pictures, and representative images from three replicates are shown. SEM image of Ca-alginate beads without bacterial cells (a1 and a3), and respective EDX spectra (a2 and a4), SEM image of Ca-alginate beads containing live cells of *B. agri* C15 Cd^R (b1 and b3), and respective EDX spectra (b2 and b4).

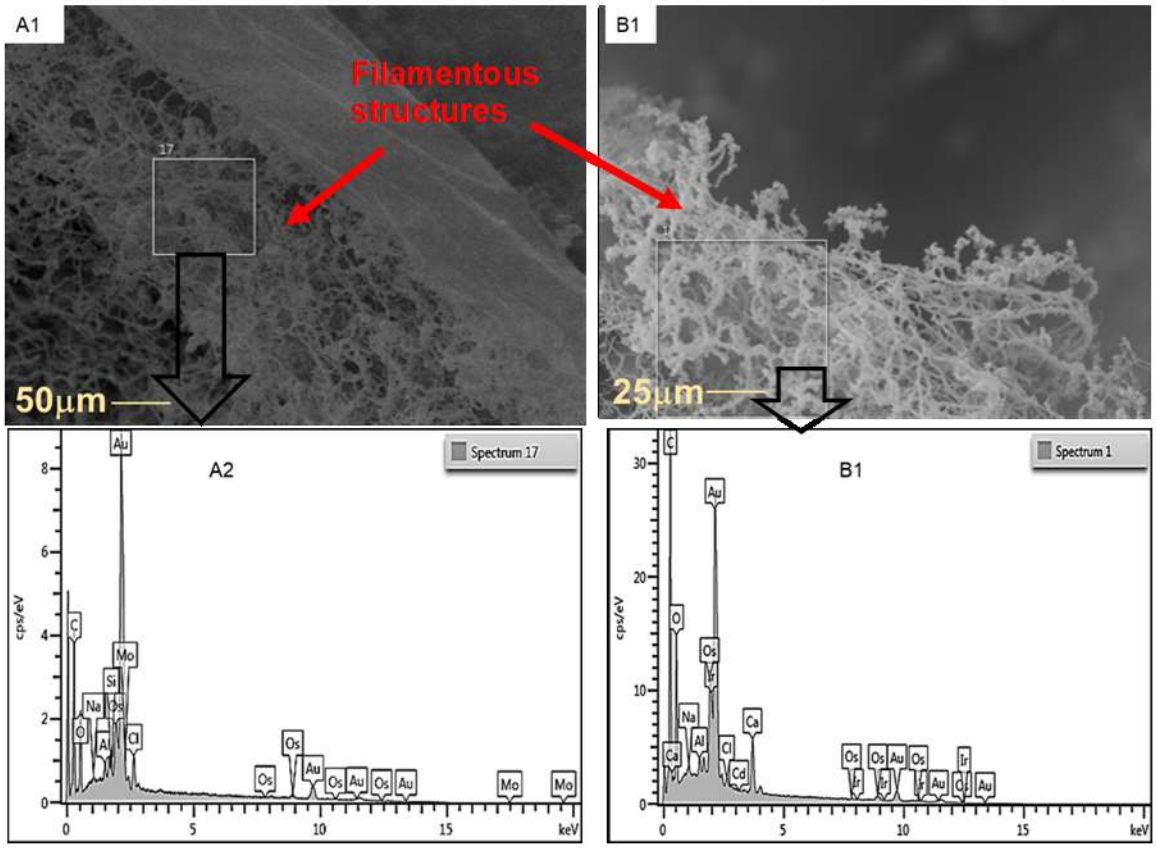

Figure 35. The SEM microphotographs and EDX spectra of Cd-loaded beads **(A1** and **A2,** respectively**)** Ca-alginate beads without bacterial cells and **(B1** and **B2,** respectively**)** Ca-alginate beads with bacterial cells.

4-3-5 Distribution of cadmium in the beads using a dithizone histochemical method

Sometimes it is impossible to detect the EDX spectra of Cd in the Cd-loaded beads under SEM-EDX analyses; therefore, alternative detection technique was investigated using a histochemical method. The beads were treated as a tissue, and the localisation of Cd was observed after the staining with a mixed dithizone solution. The detection of Zn was carried out for comparison. The unstained beads were observed to find the effects of staining on the beads. The main observations were differences in bead colour. Figure 36 A(A1), B(A1), C(A1) showed that the unstained beads seemed to have alginate (observed as dark brown), with differences between the beads with and without bacterial cells. As shown in Figure 36 A(B2), B(B2), C(B2), the beads loaded

with Cd and stained with Zn stain, appeared to have lost some alginate (transparent colour of the beads) without detecting Zn. In contrast, Cd-loaded beads, stained with Cd stain, showed a red colour (Cd-dithizone complexes), locating Cd. However, Ca-alginate beads that contained bacterial cells and were exposed to Cd showed a much darker colour.

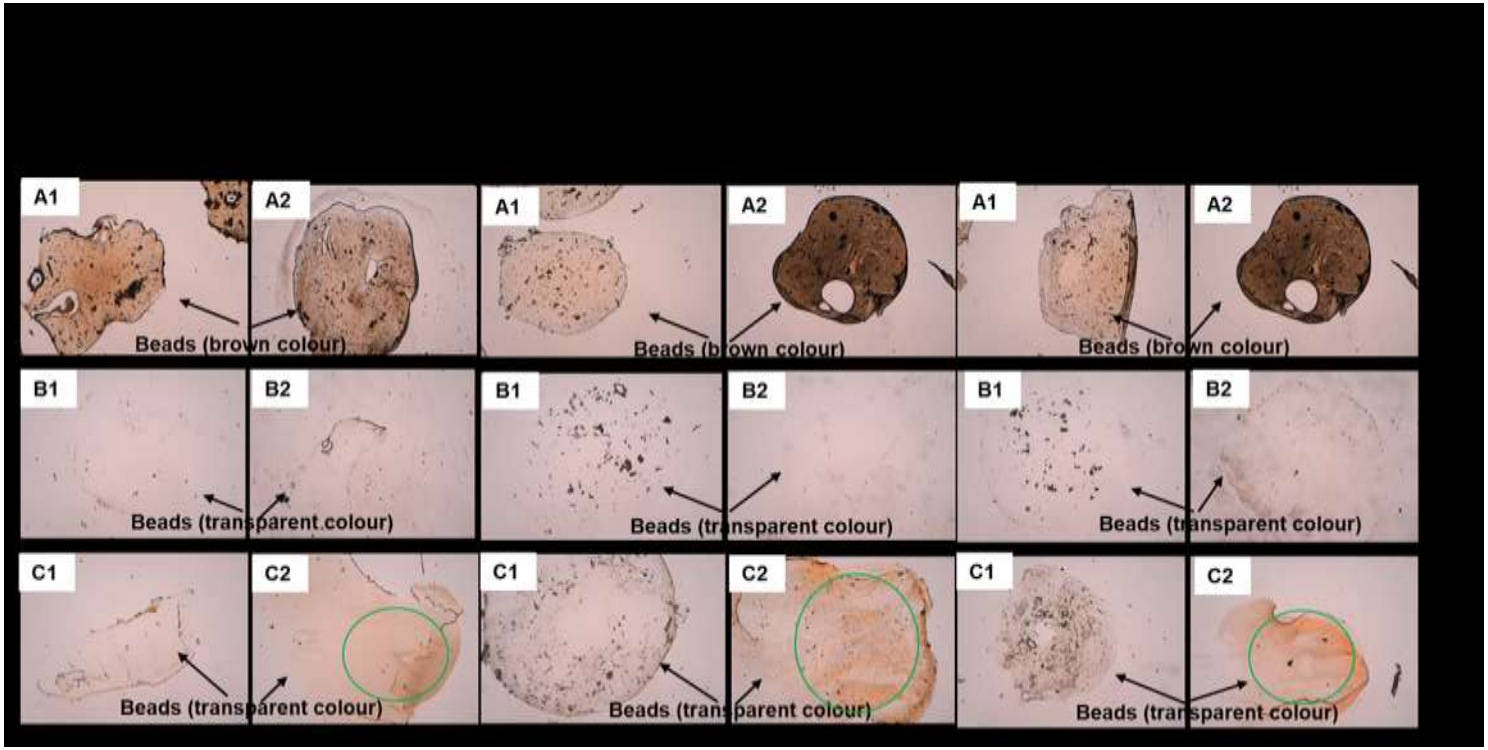

Figure 36. The light microscopy observations of **(A)** Ca-alginate beads without bacterial cells, and containing live cells of **(B)** *B. agri* C15 and **(C)** *B. agri* C15 Cd^R after the exposures to AGW (containing 20 mM pyruvate) or AGW with Cd (containing 20 mM of pyruvate) and incubation for 48 h. Three sections of the beads were employed for the pictures of staining Zn and Cd. Two independent experiments for each bead are shown in which the unexposed beads are in the left panels, and the exposed beads are in the right panels. **Row A** comprises unstained beads. **Row B** exhibits beads stained with Zn stain. **Row C** shows beads stained with Cd stain. **A(A1, A2)**, **B(A1, A2),** and **C(A1, A2)** unstained beads are showing different colour in response to Cd. **A(B1, B2)**, **B(B1, B2)** and **C(B1, B2)** showing no Zn presence. **A(C2), B(C2,)** and **C(C2)** showing Cd-dithizone complexes (green circles) compared to unexposed beads **A(C1)**, **B(C1),** and **C(C1)**.

4-4 Discussion

The ability to remove Cd from AGW by the mutant *B. agri* C15 Cd^R, compared to the wild type *B. agri* C15 entrapped in Ca-alginate gel, was investigated. Experiments were performed in an up-flow column reactor, using a slow flow rate (40 µL/min) in accordance with the optimisation experiment (Chapter Two, section 2-2), which aimed at using a stable flow rate and hydraulic residence time (1.5 h) and achieved the rapid removal of Cd from AGW during the operation of the reactor.

In this study, the reactor was operating for approximately a month, treating AGW with a concentration of 4.4 µM Cd at a pH 7.00. The results showed that Ca-alginate beads containing live cells of *B. agri* C15 or *B. agri* C15 Cd^R removed higher amounts of Cd than Ca-alginate beads without bacterial cells. Similar observations have been recorded in previous studies (El-Naggar *et al*., 2018; Valdez *et al*., 2018), who reported that the Ca-alginate beads containing bacterial cells are more able to remove Cd due to having more functional groups.

According to SEM images of the beads' morphological characterisations, Ca-alginate beads without bacterial cells had larger cavities than those of the Ca-alginate beads containing bacterial cells. This characteristic may provide effective adsorption by allowing Cd to move through the pores. However, this is only applicable in the initial time of the removal experiments, as described by Duan and Su (2014). The long-term performance (>10 to 28 days) of reactors containing no cells or killed-control cells reached a plateau that indicated the establishment of an equilibrium between the supply of Cd with AGW and its amount of removal. The primary mechanism of Cd removal by Ca-alginate beads alone is the ion exchange between Ca in the beads with Cd from AGW. Besides, the possible Cd binding sites of the functional groups in

Ca-alginate beads are carboxyl and hydroxyl groups. However, when Ca-alginate beads are combined with bacterial cells, additional, more diverse, functional groups are available on the cell wall structure of the bacteria.

It has been reported that the carboxyl, amino, and phosphate groups are the main functional Gram-stain-positive group (Jiang *et al*., 2004; Buszewski *et al*., 2015). Therefore, the role of surface interaction on Ca-alginate beads and Ca-alginate beads containing cells in the mechanisms of Cd removal can be proposed by drawing framework structures of Ca-alginate bead and bacterial cells, showing functional groups (Figure 37) that are analogous to the published literature (Zou *et al*., 2007; Shim *et al*., 2019). The possible Cd binding sites on the functional groups in Ca-alginate beads are carboxyl and hydroxyl groups (Figure 37A). The cell wall of Gram-stain-positive bacteria, such as *B. agri* C15, consists of peptidoglycan, which provides carboxyl, hydroxyl, and amide functional groups. The phosphate functional group is added by other constituents of teichoic acid and teichuronic acid. The primary functional groups of *B. agri* C15 are illustrated in Figure 37B. Stability constants between Cd and functional groups containing N, P, or S are at least one order of magnitude higher compared to stability constant or Cd complexes with -OH functional groups (PHREEQC, 2017; Saha *et al.*, 1996), and hence, binding between Cd and the functional groups in Ca-alginate beads containing cells was more than in the Ca-alginate beads without bacterial cells. In contrast, the mutant *B. agri* C15 Cd^R could provide absorbency with different characterisation. As we stated in the previous chapter (Three), the better ability to resist Cd by the mutant could be analogous with conclusions of other studies (Cooley *et al*., 1986; García *et al.*, 2002), due to the introduction of –SH (sulfhydryl) compounds. Therefore, the role of the surface interaction on Ca-alginate beads containing cells of the mutant *B. agri* C15 Cd^R can

be proposed (Figure 37C). This biosorbent, with additional–SH compounds or with other functional groups, produced a new biosorbent with more ability to adsorb Cd.

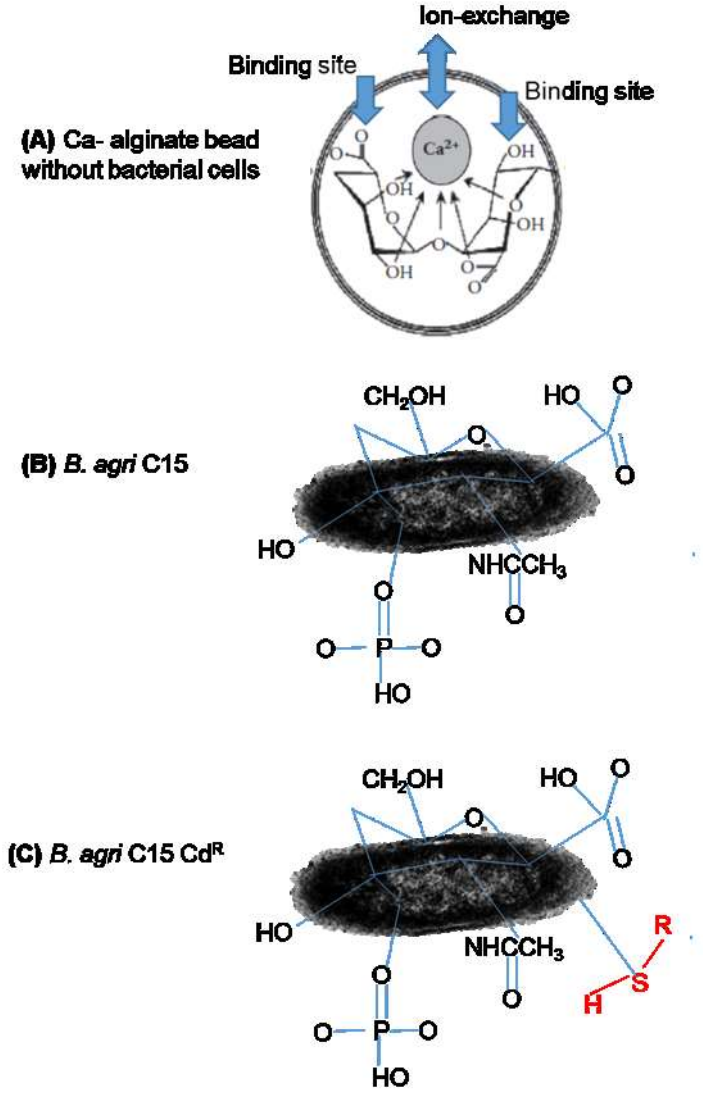

Figure 37. Framework structures of **(A)** Ca-alginate without bacterial cells, **(B)** cell of *B. agri* C15 and **(C)** cell of *B. agri* C15 Cd^R (TEM micrographs), showing different functional groups. The structures were adopted and redrawn, according to Zou *et al.* (2007) and Shim *et al.* (2019).

Most of the studies have been amid to develop the uptake process of Cd by finding a novel component of alginate beads (Mao *et al.*, 2013; Shim *et al.*, 2019). All these studies have been succeeded by introducing new absorbents with new functional groups to coordinate with Cd. In this study, two different biosorbents produced, one

Ca-alginate bead containing live cells of *B. agri* C15 and other Ca-alginate beads containing live cells of *B. agri* C15 Cd^R. Both biosorbents are new, but they are different in their absorption capacities due to the differences in their bead composition. The combination of the functional groups of the Ca-alginate beads and bacterial cell wall structure is the primary mechanism that contributed to the uptake of Cd by biosurface adsorption in killed-control cells as the bioaccumulation inside the cell is absent due to the inactivation of the cell. Interestingly, the uptake by killed-control cells gave a lower uptake amount than the live cells, as an intracellular accumulation of Cd is active in live cells (Silva *et al*., 2012). Recently, Mohapatra *et al*. (2019) reported the equivalent relationship in *Bacillus xiamenensis* PbRPSD202 as an electron dense particle was observed inside the live bacterial biomass.

The metal concentration is essential to factors of the removal experiments; therefore, the removal in the reactor was also evaluated with higher concentrations of Cd (8.8, 13.4, and 17.4 μM). High removal rates were achieved by mutant *B. agri* C15 Cd^R, providing a new development Cd process. No observed differences in their removal rates were evaluated based on the effect of the Cd concentrations, which were the same. It is reported previously that the UV mutant of *B. subtilis* 38 could uptake Cd higher than the wild type (Jiang *et al*., 2009).

The structure of the observed bead was similar to the construction of Ca-alginate beads reported by Zazzali *et al*. (2019). The heterogeneous composition of the beads provides effective adsorption (Zheng *et al*., 2019). The more varied structure of the bead surface after Cd loading showed surface impurities, which could demonstrate that Cd was deposited onto the surface of the beads by one of the previously above- discussed mechanisms, such as the electrostatic interaction with the functional groups (Peng *et al*., 2018).

SEM analyses were employed to the Cd-loaded beads to detect Cd and resulted in the detection of only a few peaks of some elements. The presence of Ca and Na peaks originate from the composition of the bead matrix, and C or P peaks from the AGW composition. U and Os are the main elements used in fixing the beads for SEM analysis, while Au peaks were from the gold used for coating the blocks. Other elemental peaks could be present due to contamination. SEM-EDX analyses suggest that the percentages of the elemental compositional detection (EDX data) resulting from Cd loading were impossible in the beads. This obstacle is comparable with previous studies, which excluded EDX data due to the nature of absorbents and the presence of Cd in low concentrations (Duan and Su, 2014; Sun *et al*., 2018; Siswoyo *et al*., 2019). Alternatively, the detection of the distribution of cadmium on the absorbents using EDX mapping (Boparai *et al*., 2013) or polished samples to produce a flat section (Vinci *et al*., 2020) can support the adsorption mechanism of Cd.

The dithizone histochemical method employed in this study to determine the distribution of Cd on the Cd-loaded beads showed that the stain revealed information on the beads' compositions as the colour changed from brown (related to alginate) to transparent (loss of alginate). Unstained beads showed a visible structure, and the brown colour mainly appeared in Cd-exposed beads. Furthermore, a denser, or more intense colour was observed in Ca-alginate beads containing bacterial cells. Zn was not detected when beads were stained with a Zn-specific mixed dithizone solution, which confirmed that the method could differentiate between Zn and Cd within the beads.

In contrast, the staining of Cd-loaded beads with Cd-specific mixed dithizone solution showed red pigments, and their distributions through the beads indicated removal mechanisms of Cd from AGW. The pigment distribution on the Ca-alginate beads

without bacterial cells (control beads) illustrated that Cd just deposited on the beads' surface, suggesting that removal relied on surface interactions, such as ion exchange. The pigment distribution on Ca-alginate beads containing live bacterial cells showed Cd present inside the beads, suggesting that active Cd uptake by bacterial cells (i.e., bioaccumulation) played a role in Cd removal from AGW. The presence of Cd on edge could explain the ion exchange process that occurred as well, while the presence of Cd inside the beads could support the bacterial cell activity, especially in these experiments; pyruvate was added as a source of carbon, which could support their activities.

4-5 Conclusion

The Ca-alginate beads containing live cells of the mutant *B. agri* C15 Cd^R could uptake Cd from AGW with the maximum rate. *B. agri* C15 could also be used for Cd removal, but its removal rate was low compared to the mutant. The uptake mechanism of this process is that the Cd was making contact with the Ca-alginate beads, firstly due to the ion exchange with Ca or the combination of carboxyl, hydroxyl, amide, phosphate, and sulfhydryl (for mutant) functional groups and the bioaccumulation with bacterial cells. Thus, it is concluded that the localisation of Cd in Cd-load beads, showed that the Cd localised through the beads, giving evidence that two mechanisms of the bioremediation occurred during the removal of Cd: bioaccumulation and biosorption by bacterial cells. Hence, the uptake may be affected by the existence of groundwater compounds. The effect remaining unclear requires further investigation. The investigation can be potentially studied by using a multi-reactor set up instead of a single reactor set up, as used in this study. These reactors can maximise the effects of the existence of groundwater compounds on uptake efficiency due to the differences in the operation parameter between the reactors.

Chapter 5. Cadmium removal with mutant *Brevibacillus agri* C15 Cd^R entrapped in calcium alginate gel: multi-constituent ionic exchange

Abstract

The ability of mutant *B. agri* C15 Cd^R to remove cadmium (Cd) from artificial groundwater (AGW) under varied pH and the interactions of Cd, calcium, phosphate, and humic acid competing for ion exchange sites on Ca-alginate beads containing cells of strains, were investigated in small laboratory bench-scale column reactors. Visual MINTEQ was used to compute Cd speciation in AGW in changing the pH and the presence and absence of the constituent. The results show that Cd^{2+} is the dominant form of pH 4.00, 7.00 and 7.50, $CdCl^+$ under the calcium effect, $CdHPO_4$ under the phosphate effect, and complex HA1-Cd under the humic acid effect. It was found that the highest removal rate and accumulative amount of Cd from AGW were achieved at pH 4.00. A significant impact was observed in the rate of Cd uptake due to the cation/anion or the humic acid effect. The preferential removal of Cd from natural river water (NRW, Walkham River) was also obtained. The hazard classification of this Cd-absorbent was classified as non-hazardous waste. Altogether, these results show that with mutant *B. agri* C15 Cd^R entrapped in calcium alginate gel, there was potential to remove Cd from the freshwater. Nonetheless, process efficiency can be stalled by the presence of cation/anion and humic acid that reduces availability and/or attraction for ion exchange.

5-1 Introduction

Alginate-immobilised cell beads are suitable packing materials for remediation in the column reactor system. Alginate is a biopolymer composed of homopolymeric blocks of *β*- D-mannuronate and *α*-L-guluronate. Both components have different functional groups, such as amides, amines, carboxyls, phosphates, and sulphates, which provide adequate metal-binding capacity combined with an acidic nature (pK_a) of 1.5 – 3.5 (Deze *et al.*, 2012). Alginate biosorbents are usually prepared as Ca-alginate-based ion-exchange resins. This Ca-alginate form (bead) adds the additional binding capacity of metal ions. It has been reported that the removal of metals using Ca-alginate beads is mainly achieved through the ion exchange between metal cations, especially Ca. The surface coordination of metal cations with hydroxyl groups of the Ca-alginate beads is another possible mechanism. Alternatively, the precipitation on the Ca-alginate beads occurs when the pH of the metal ions reached precipitation forms. These mechanisms suggest that there are different ways to remove metal ions from the solutions using Ca-alginate beads. When the bacterial cells are entrapped in the alginate matrix, and the uptake of Cd bioaccumulation contributes to this process.

As a cation exchange mechanism characterises the binding interaction, it is crucial to investigate whether the removal of Cd by the Ca-alginate beads occurs by the ion exchange with Ca in the Ca-alginate beads or whether it occurs by the Cd species. Moreover, the removal of Cd must be investigated under various groundwater geochemical conditions; therefore, the environment's pH is a critical parameter that affects the capacity for removal, as the pH may change the surface charges of Ca-alginate beads and the species of Cd.

The constitution of groundwater is complex, and selecting the inhibiting compounds is challenging. Recently, Yu *et al.* (2019) investigated the effect of geochemical conditions, such as pH, calcium, and organic matter on arsenic removal from groundwater. Organic matter (OM) is present in water from the natural production of organisms as a sequence and could leach into the groundwater. The molecular weight and composition of these compounds vary, but many studies have estimated the molecular weight of isolated OM. The effect of OM on the uptake process is likely due to the high competition for hydroxyl groups in the Ca-alginate beads, and the inhibition of the process results in the reduction in the removal of the contaminants.

In natural water, cations and anions exist in the salt and ore minerals, exhibiting as competition in the uptake process of Ca-alginate beads. Therefore, it is essential to study the removal of Cd using the beads with the utilisation of cation and anion in the AGW. The removal, under various groundwater geochemical conditions, enables the evaluation later in the natural source water. Thus, the Cd removal process with Ca-alginate beads in natural water can be studied.

This chapter addresses the interactions of Cd, cations/anions, and humic acid competing for ion exchange sites in Ca-alginate beads containing live cells of mutant *B. agri* C15 Cd^R in addition to the effect of pH (4.00 – 7.50) on the ion exchange's performance. This study was carried out along with the use of control beads and Ca-alginate beads without bacterial cells, without containing live cells of wild type *B. agri* C15, or the killed-control cells of both. The thermodynamic calculation (MINTEQ program) was used to predict Cd speciation in AGW theoretically. The natural water from the Walkham River was supplemented with Cd, and the removal process of Cd was investigated.

5-2 Methodology

5-2-1 Cadmium removal from AGW

The removal of Cd from the water was conducted in a multi-reactor set up (*n* = 3, each reactor constructed from one column). The beads were used in this reactor for the Cd removal from AGW with a nominal concentration of 10 µM Cd at pH 7.00. The reactors were constructed and operated, as described in Chapter Two. The starting concentration of Cd was chosen based on the expected concentrations of Cd in the eluted solution during the removal experiment, which is suitable for measuring using ICP-MS. The removal experiments were performed using Ca-alginate beads containing live cells of *B. agri* C15 or live cells of *B. agri* C15 Cd^R, control beads (Ca-alginate beads without bacterial cells) and Ca-alginate beads containing killed-control cells of *B. agri* C15 or killed-control cells of *B. agri* C15 Cd^R. The preparation of killed-control cells and the embedding of bacterial cells in the Ca-alginate matrix were performed, as described in Chapter Two. The reactors were operated based on the estimation that the 100 mL of AGW can be passed through it at a flow rate of 40 µL/min for five days. The samples were collected every two hours on the first day of operating the reactor, followed by collection twice-per day, acidified with nitric acid (1%) directly after collecting, and indium was used with a final concentration of 0.43 µM as an internal standard. It was essential to consider the release of Ca, Mg, and Na from the Ca-alginate into the AGW during the reactor's operation, without Cd as previously reported by Carro *et al.* (2015). Therefore, the beads were filled in the reactor to estimate the release concentrations of these elements into AGW without adding Cd.

When the operating of the reactor was completed, the AGW was drained, and the Cd-loaded beads were washed quickly using ice-cold physiological normal saline and

were then drained. The beads were digested with *aqua regia*, as described in Chapter Two, and the total concentrations of Cd, Ca, Mg, and Na were analysed. The total concentrations of Cd remaining in AGW and the total concentrations of Na, Mg, and Ca that were released from the beads into AGW were measured in the eluants and normalised per dry biomass (mg) according to He and Chen (2014) as described in Chapter Four. The tangent lines were applied to the curves to give approximate rates of Cd removals during the initial time of operating the reactor.

5-2-2 Effect of AGW pH on the cadmium removal

During the removal experiments, the pH of AGW was altered. pH plays a vital role in the state of the functional groups of Ca-alginate beads and the species of Cd in AGW. It was essential to investigate whether the higher concentration of H^+ ions at pH 4.00 of AGW competes with Cd in the ion exchange with Ca of Ca-alginate beads. However, with a pH of more than 7.00 of AGW, the higher concentration of OH^- ions in the beads may provide a strong attraction to Cd.

On the contrary, the pH affects the Cd-speciation as it is well-known that Cd^{2+} ions are present at pH < 6; however, with the increase of pH, fractions of Cd(OH) or $Cd(OH)_2$ dominated (Taty-Costodes *et al.*, 2003). The effect of pH on removal experiments at pH 4.00 and 7.50, under the same protocol as mentioned above, was conducted by adjusting the pH of AGW with HCl (0.1 M) or NaOH (0.1 M).

5-2-3 Effect of cation-anion concentrations in AGW on the cadmium removal

Calcium was added to assess the effect of the cation in AGW on the competition with Cd in ion exchange with calcium. Calcium was the central cation of the AGW; therefore, the ion exchange was studied by increasing its concentration. The

concentration of calcium in AGW was increased from 1.75 to 17.5 mM, applied as $CaCl_2$.

Similarly, the effects of the higher concentration of the anion on the ion exchange process were studied by adding phosphate (10 mM), which does not consist of AGW. Phosphate (10 mM) consisted of two components of 6.15 mL of K_2HPO_4 (1 M) and 3.85 mL of KH_2PO_4 (1 M) in a liter. The effects of cation/anion were studied under the same protocol mentioned above (Section 5-2-1), by adding the cation/anion onto AGW at pH 7.00.

5-2-4 Effect of organic matter in AGW on the cadmium removal

The investigation of the removal process under the presence of organic matter (OM) was studied. The OM effects on the ion exchange process in different situations. When OM presents, different kinds of interactions and complexations of OM with Cd could occur. Alternatively, OM competes with Cd for the ion exchange with Ca on the Ca-alginate beads.

Moreover, the most effective impact OM situation is that the OM adsorbs Cd (Ming *et al*., 2014). Therefore, the effect of OM on the uptake process, under the same protocol mentioned earlier (Section 5-2-1), was conducted by adding OM into the AGW. Humic acid constitutes the significant fractions of OM in natural water, which consists of 90% of the total dissolved organic carbon (DOC) (Croué, 2004). Thus, humic acid (Sigma-Aldrich) was added at the concentration of 10 mg/L to Cd-AGW. This concentration of humic acid was chosen as the average concentration is presented in natural water (Hudson *et al*., 2007).

5-2-5 Cadmium removal from NRW

The removal of Cd was carried out with the NRW, Walkham River (tributaries of Tamar River) at Magpie Bridge near Horrabridge, Plymouth, UK. The Walkham River was chosen on the basis that no major pollution was recorded (Handy *et al*., 2002). The water sample was sterilised using membrane filtration (0.22 μm, Fisherbrand) to avoid any interference. The water was analysed using ICP-MS for its chemical composition, as shown in Table 12.

Table 12. Chemical composition of the Walkham River. The parameters were expressed as the mean (*n* = 3 samples), and ± presents the standard error of the mean.

Environmental parameter	Value	Unit
pH	6.78 ± 0.03	*
Hardness	0.140 ± 0.01 0.002 ± 0.0003 0.446 ± 0.007 0.019 ± 0.004	mmol/L °dH $CaCO_3$ °Clark
DOC	0.037 ± 0.03	mg/L
Ca	83 ± 0.2	μM
Na	202 ± 6	μM
Mg	58 ± 0.6	μM
Al	2 ± 0.03	μM
K	4 ± 0.1	μM
Fe	2 ± 0.02	μM
Cu	31 ± 0.8	nM
Zn	8 ± 0.05	nM
Cd	0.1± 0.02	nM
Pb	0.4 ± 0.06	nM

* No unit established.

The pH was measured, and the hardness was calculated as an average hardness (mmol/L), hardness as $CaCO_3$ (ppm), hardness as degree Deutsche Härte (°dH, CaO), and hardness as mg-$CaCO_3$/L (°Clark). The hardness of the Walkham River was classified according to the US Geological Survey (USGS) as soft water in mg-CaCO3/L, mmol/L, °dH, and $CaCo_3$ ppm. To determine dissolved organic carbon (DOC), the dry ashing technique was used by placing a bottle (25 mL) in a muffle

furnace at a temperature of 450 °C overnight. The river sample was preserved in the cleaned bottle and stored at – 20 °C to determine DOC using a Total Organic Carbon analyser (TOC-V) (Shimadzu TOC5000A).

The actual experiment of Cd removal from NRW was performed by supplying the river water with a nominal concentration of 10 μM Cd. The Ca-alginate beads were prepared as described in Chapter Two using normal physiological saline instead of AGW without $CaCl_2$.

5-2-6 Cadmium precipitation and speciation in AGW versus pH; the increase of calcium concentration and the addition of phosphate and humic acid

It was essential to evaluate the effects of pH and constituents on the species distribution and concentration of Cd in AGW before starting the investigation process under different factors according to the method described by Boparai *et al*. (2013). To theoretically assess the experimental conditions of Cd-AGW, the inorganic chemical speciation at 22 °C was calculated using the geochemical speciation software Visual MINTEQ, version 3.1 (Gustafsson, 2011). The input file contained the components and concentrations of AGW, with a concentration of 10 μM Cd at pH 7.00; as specified in Table 13, oversaturated solids were allowed to precipitate, ionic strength was calculated, and activity corrections were performed after Davies. Redox calculations were not performed.

With the addition of humic acid (10 mg/L), the NICA-Donnan model in Visual MINTEQ was used. It was found that the parameters and constants for a ‘generic’ fulvic acid were assumed to be 82.5% of the input; dissolved organic carbon (DOC) consists of fulvic acid with a carbon content of 50% (the portion designated ‘active’ concerning metal complexation because humic acid is assumed not to be dissolved in solution), as described by Pearson *et al.* (2018). Fifty percent was in a DOC: DOC ratio of 1.65,

which is an average based on stream and lake sediments from the Swedish environmental monitoring network. However, default parameters were used for VMINTEQ for humic acid: 1.4. The total molar concentration of DOC was10 mg/L (gave 551% C in HA), which is equal to 459 μM. Therefore, the input parameter for humic acid is 459 μM (Table 13).

Table 13. The input file of software Visual MINTEQ contained the components and their concentrations in AGW with a concentration of 10 μM Cd at pH 7.00 under the increase of calcium concentration (17.5 mM) and the addition of a phosphate (10 mM) and humic acid (10 mg/L).

Component	Concentration (μM)			
	Cd-AGW	Increase of $CaCl_2$	Addition of phosphate	Addition of humic acid
Ca^{2+}	1750	17500	1750	1750
Cd^{2+}	10	10	10	10
Cl^-	1750	17500	1750	1750
CO_3^{2-}	1162	1162	1162	1162
K^+	103	103	103	103
Mg^{2+}	448	448	448	448
Na^+	1144	1144	1144	1144
NO_3^-	44	44	44	44
PO_4^{3-}	*	*	10000	*
SO_4^{2-}	448	448	448	448
Humic acid	*	*	*	459

* No component added.

5-2-7 Measurement of elements

The ion exchange process of Cd in AGW with the elements, Na, Mg and Ca of the beads were estimated by determining the total concentration of these four elements remaining in the eluants after operating the reactors using inductively coupled plasma mass spectrophotometry (ICP-MS, Thermo Scientific, X Series 2) or equivalent optical emission (ICP-OES, Thermo Scientific, iCAP 700 Series). Similarly, these elements were measured in the Ca-alginate beads, after *aqua regia* digestion, before and after the process. Instrument-limited detection (LOD) was established after five times of the standard deviation (SD) of measuring the lowest standard (n = 10). Table 14 presents the LODs and analytical techniques of each element. The quality control for the

consistency of the measurement was evaluated by the analysis of the procedural blank samples (without any beads or AGW, *n* = 3 blanks).

Table 14. The LOD (derived from 5 X SD of *n* = 10 analyses) and procedural blank (*n* = 3), and analytical techniques for each element.

Element	Analytical technique	LOD	Procedural blank	Unit
Ca	ICP-OES	0.01	<LOD	mM
Cd	ICP-MS	0.2	<LOD	μM
Mg	ICP-OES	0.8	<LOD	μM
Na	ICP-OES	0.04	<LOD	mM

Certified Reference Material (CRM, drinking water, EnviroMAT, Cat 140-025-031) was analysed to verify the recovery of the analysis. The measured and certified values for the four elements (Cd, Na, Mg, and Ca) showed good accordance between them (Table 15).

Table 15. The recovery percentage values of CRM, drinking water. The recovery percentage values were estimated from the mean of recorded and certified values of CRM. ± SEM, (*n* = 3 samples).

Element	Concentration (μM)		Recovery (%)
	Recorded	Certified	
Ca	12 ± 0.2	10 ± 0.6	100 ± 0.3
Cd	2.5 ± 0.04	1.7 ± 0.01	100 ± 0.01
Mg	2 ± 0.01	1.8 ± 0.02	100 ± 0.01
Na	14 ± 0.05	11 ± 0.05	100 ± 0.04

5-2-8 Statistical analysis

All the data of the experiments were the mean and standard error of the mean. Statistical analyses, Student's *t*-test, and one-way ANOVA were performed on the data in IBM SPSS Statistics 22 software to evaluate whether the amounts of Ca, Na, and

Mg in the beads were different before and after the Cd uptake process. The rates and cumulative amounts of Cd by each bead were statistically analysed to find a significant difference. ANOVA followed by Tukey *post hoc* was performed on the data of Cd species distribution of AGW with a concentration of 10 μM Cd, which predicted using Visual MINTEQ to find the differences under the effect of different factors on the percentages of Cd species. SigmaPlot (version 13) was used to illustrate the data. The curves were fitted with nonlinear regressions (exponential decay, exponential linear combination). Tangent lines were applied to the curves to give an approximate rate of Cd removal in the initial period after operating the reactor.

5-3 Results

5-3-1 Cadmium precipitation and speciation in AGW versus pH; the increase of calcium concentration and the addition of phosphate and humic acid

The inorganic Cd speciation at different pH values (fixed at pH 4.00, 7.00, 7.50, and 8.50, respectively) was calculated. At pH 8.50, calcium carbonate species (e.g., calcite) and Cd carbonate (otavite) were predicted to precipitate, and the proportion remaining in the AGW was 84.9% of Ca^{2+}, 4.8% of Cd^{2+}, and 76.5% of CO_3^{2-}. The otavite precipitation predicts that only 0.48 μM remained in AGW as Cd^{2+}. Consequently, the experiment was not run at pH 8.50.

At pH 7.50, the calculations revealed the precipitation of otavite (80% of the added Cd concentration), as shown in Table 16, leaving a dissolved concentration of 2 μM in AGW. At pH 7.00, the calculations indicated that the precipitation of otavite (57.7% of the added Cd concentration), leaving a dissolved concentration of 4.22 μM in AGW. The calculations revealed the potential loss of Cd from the solution, as the initial concentration in the AGW was 10 μM Cd. At pH 4.00, the calculated saturation index for all species was negative, and Cd was not predicted to precipitate.

Table 16. Effect of pH on the percentages of dissolved and precipitated components in AGW with a concentration of 10 µM Cd. The percentages of values were predicted using Visual MINTEQ.

Component	pH 4.00		pH 7.00		pH 7.50	
	Dissolved (%)	Precipitated (%)	Dissolved (%)	Precipitated (%)	Dissolved (%)	Precipitated (%)
Ca^{2+}	100	0.00	100	0.00	100	0.00
Cd^{2+}	100	0.00	42	57.7	19.5	80
Cl^{-}	100	0.00	100	0.00	100	0.00
CO_3^{2-}	100	0.00	99	0.40	99	0.40
K^{+}	100	0.00	100	0.00	100	0.00
Mg^{2+}	100	0.00	100	0.00	100	0.00
Na^{+}	100	0.00	100	0.00	100	0.00
NO_3^{-}	100	0.00	100	0.00	100	0.00
SO_4^{2-}	100	0.00	100	0.00	100	0.00

However, when $CaCl_2$ was increased from 1.75 mM to 17.5 mM (for the removal process under cation competition), the calculated saturation index for all species was negative, and no precipitation was predicted (Table 17). The dissolved Cd concentration at the beginning of the experiment can be assumed as 10 µM, and the initial measured concentration was approximately 10 µM. Also, the addition of a phosphate (10 mM) showed no potential precipitation of Cd in AGW (Table 17). The NICA-Donnan model indicated that there was no Cd precipitated (Table 17), leaving a dissolved concentration of 10 µM in the test AGW.

The measured and predicted dissolved Cd concentrations were the same, due to the low concentration of humic acid, which explains the lack of Cd complexation with the humic acid. Gondar *et al*. (2006) used 200 mg/L of humic acid, which is higher than concentration in this study, and they found that the log activities of binding of $Cd(OH)_2$ and $CdOH^{+}$ with humic acid were -9.5 and -8.4 mol/L, respectively. While, in this study, the log activities for the same species of Cd were low -11.5 and -8.5 mol/L, respectively.

Table 17. Effect of increased calcium (17.5 mM), additional phosphate (10 mM), and humic acid (10 mg/L) on the percentages of dissolved and precipitated components in AGW with a concentration of 10 µM Cd. The percentages were predicted using Visual MINTEQ.

Component	Calcium (17.5 mM)		Phosphate (10 mM)		Humic acid (10 mg/L)	
	Dissolved (%)	Precipitated (%)	Dissolved (%)	Precipitated (%)	Dissolved (%)	Precipitated (%)
Ca^{2+}	100	0.00	0.59	99.4	100	0.00
Cd^{2+}	100	0.00	100	0.00	100	0.00
Cl^{1-}	100	0.00	100	0.00	100	0.00
CO_3^{2-}	100	0.00	100	0.00	100	0.00
K^{1+}	100	0.00	100	0.00	100	0.00
Mg^{2+}	100	0.00	100	0.00	100	0.00
Na^{1+}	100	0.00	100	0.00	100	0.00
NO_3	100	0.00	100	0.00	100	0.00
PO_4^{3-}	*	*	94.7	5.21	*	*
SO_4^{2-}	100	0.00	100	0.00	100	0.00
FA1	*	*	*	*	100	0.00
FA2					100	0.00
HA1					100	0.00
HA2					100	0.00

* No component added.

The predicting of Cd speciation in AGW versus pH showed that Cd^{2+} was the dominant type in AGW with a concentration of 10 µM Cd at a different pH (Figure 38A, $^{a}p<0.05$), compared to other dissolved Cd species. Similarly, $CdCl^{+}$ recorded no differences at different pH values (Figure 38A). The appearance of $Cd(SO_4)_2^{2-}$ at pH 4.00 and 7.00, which disappeared at pH 7.50, showed no significant differences between pH 4.00 and 7.00. The occurrence of $CdHCO_3^{+}$ was the unique species predicted at pH 7.00 and 7.50 (Figure 38A, $^{c}p<0.05$). The effect of increased Ca concentration (17.5 mM) of Cd speciation in AGW at pH 7.00 showed Cd^{2+} was lower than the value recorded at a natural concentration of Ca (1.75 mM). However, Cd^{2+} was the dominant species and showed significant differences (Figure 38B, $^{a}p<0.05$) compared to other Cd species. However, $CaCl^{+}$ was predicted to be 41%, which was higher than the percentage recorded at the initial concentration of $CaCl_2$ (1.75 mM). Moreover, both species of $CdHCO_3^{+}$ and $Cd(SO_4)_2^{2-}$ were predicated at an increase of Ca as a natural

concentration of Ca (1.75 mM), without any differences between them (Figure 38B, $^{c}p<0.05$).

While the addition of a phosphate (10 mM) showed that the domain of Cd species was $CdHPO_4$ (89%), the presence of other Cd-species was rare. Fraction Cd^{2+} was the highest predicted percentages (9.2%) among $CdCl^{+}$, $Cd(SO_4)_2^{2-}$, $CdHCO_3^{+}$, and $CdCO_3^{+}$ (Figure 38C). Similarly, as Cd^{2+} was the dominant species in AGW at pH 7.00, with the addition of humic acid (10 mg/L) into the AGW, Cd^{2+} was the dominant species (84%), followed by $CdCl^{+}$ (10%, Figure 38D).

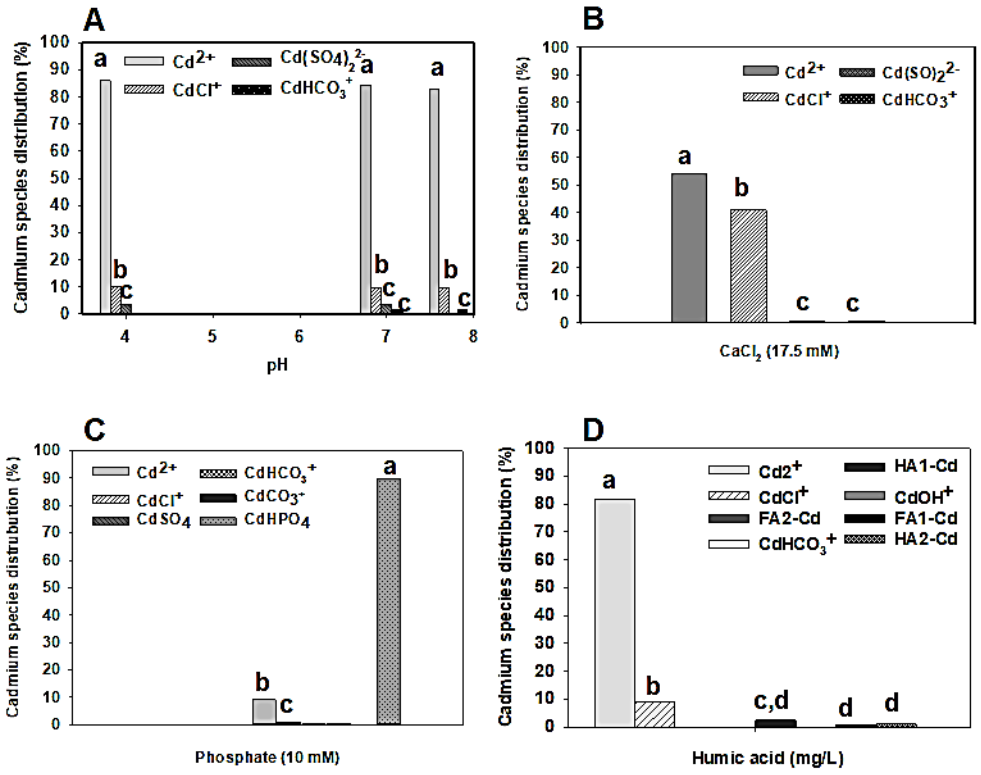

Figure 38. The effect of different factors on the percentages of Cd species distribution of AGW with a concentration of 10 µM Cd, predicted using Visual MINTEQ. **(A)** At pH 4.00, 7.00, and 7.50, **(B)** increase of calcium (17.5 mM), additions, **(C)** phosphate (10 mM), and **(D)** humic acid (10 mg/L) on Cd speciation in AGW. The Cd species were subjected to two-way ANOVA, Tukey *post hoc* test, and a different letter indicates a significant difference between Cd species under different factors.

With the use of two types of Cd-binding with fulvic and humic acids in the NICA-Donnan model, complex HA1-Cd occurred in addition to other complexes in rare percentages (FA1-Cd, FA2-Cd, and HA2-Cd) as well as the occurrence of fractions $CdHCO_3^+$ and $CdOH^+$.

5-3-2 Cadmium removal from AGW

The ion exchange process is considered to be the primary mechanism responsible for the metals ion removal using Ca-alginate beads. Therefore, the different Ca-alginate beads (without bacterial cells or containing live or killed-cells of both strains) were used for the Cd removal from AGW with a nominal concentration of 10 μM Cd, in the reactor, which was operated for four days. For the evaluation of the ion exchange process, the reactors were operated to determine the amounts of Ca, Na, and Mg that were released into the AGW, even without Cd. It is shown that the amounts of Ca and Na were released up to 30 and 56 μmol per g of dry biomass, respectively, without releasing Mg (Figure 39). Ca-alginate beads without bacterial cells released more Ca and Na compared to other types of beads. It is possible to consider these approximate released amounts in the next results of the Cd removal process.

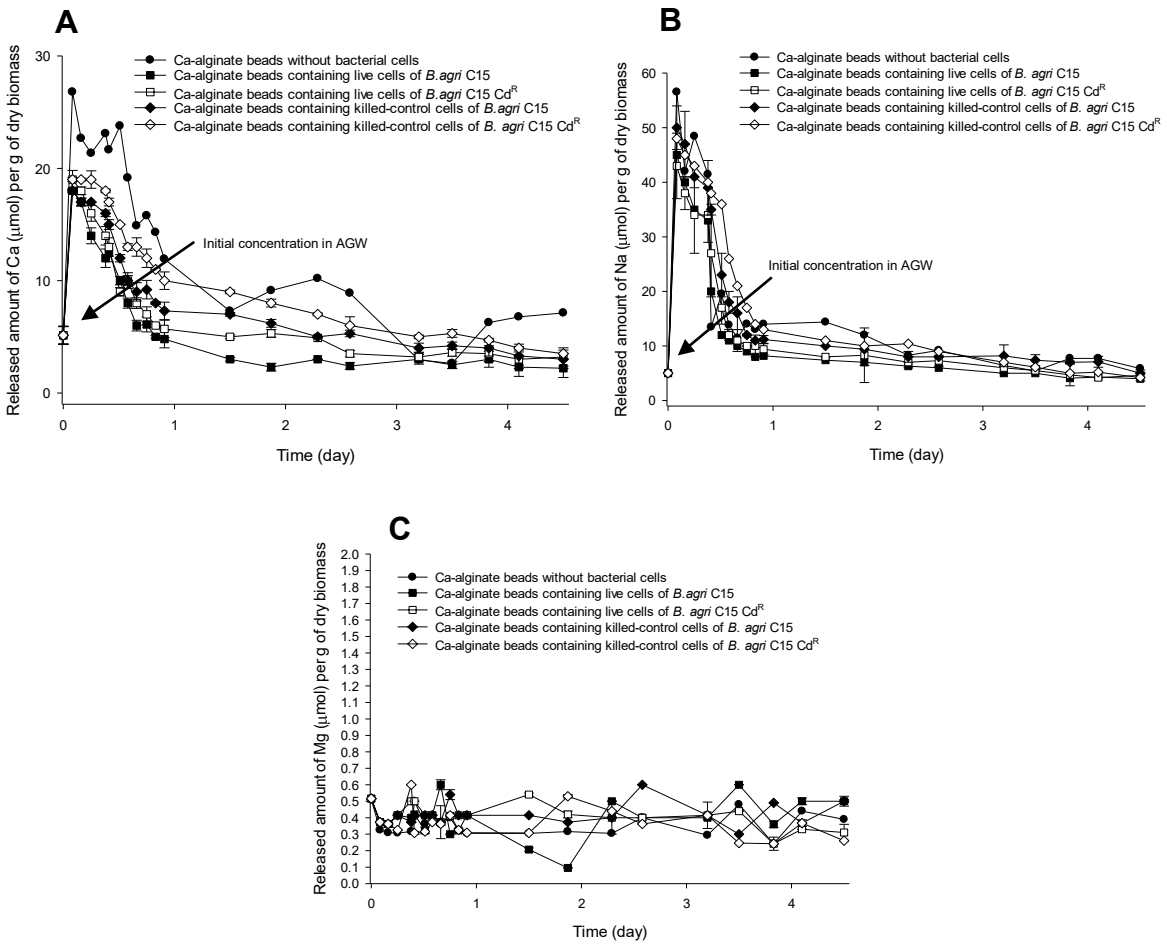

Figure 39. Release amounts of **(A)** Ca, **(B)** Na, and **(C)** Mg from the beads into AGW without adding Cd. The amounts were obtained from normalising the total measured concentrations of elements in the eluent with the mass of the filled beads in each column reactor and, finally, normalised per biomass of the respective beads (except Ca-alginate beads without bacterial cells [normalised per beads]). The error bars represent the standard error of the mean of three independent reactors (*n* = one column reactor). The scale between the Figures is different.

At first, the removal of Cd from AGW was carried out at a natural pH of the AGW (pH 7.00). This experiment was conducted to determine the amounts of Cd exchanged from AGW with Ca, Na, and Mg from the beads in addition to comparing these results with the results under a different pH (see below). All beads showed the ability to reduce the amount of Cd from AGW with the decreasing remaining total concentrations of Cd measured in the eluants over time. The tangent line fitted to the residual amounts of Cd in AGW at the beginning of the experiments, together with its linear equation, indicated that the maximum removal rate of ion exchange occurred during the first few hours of the operation. The process of Cd ion exchange was confirmed by the observation of the released amounts of Ca, Na, and Mg into the AGW from the beads (Figures 40, 41, 42, 43, 44).

Released amounts of these elements from these beads were also determined by measuring their amounts in the beads before and after operation using an ion exchange process. The results showed that the amounts of Na and Ca were higher in the beads before they were used in the process (Figures 41 E, 44E); however, the other beads (Figures 41E, 42E, 43E) had more elevated amounts of Ca after they were used in the process. The uptake amounts of Cd in the beads were estimated by measuring the total concentrations of accumulated Cd. The comparisons of cumulative amounts of Cd between the different types of beads showed that there were no significant differences between their capacities (Figure 45, $^{a}p<0.05$), except live *B. agri* C15, which had the lowest capacity (Figure 45, $^{b}p<0.05$).

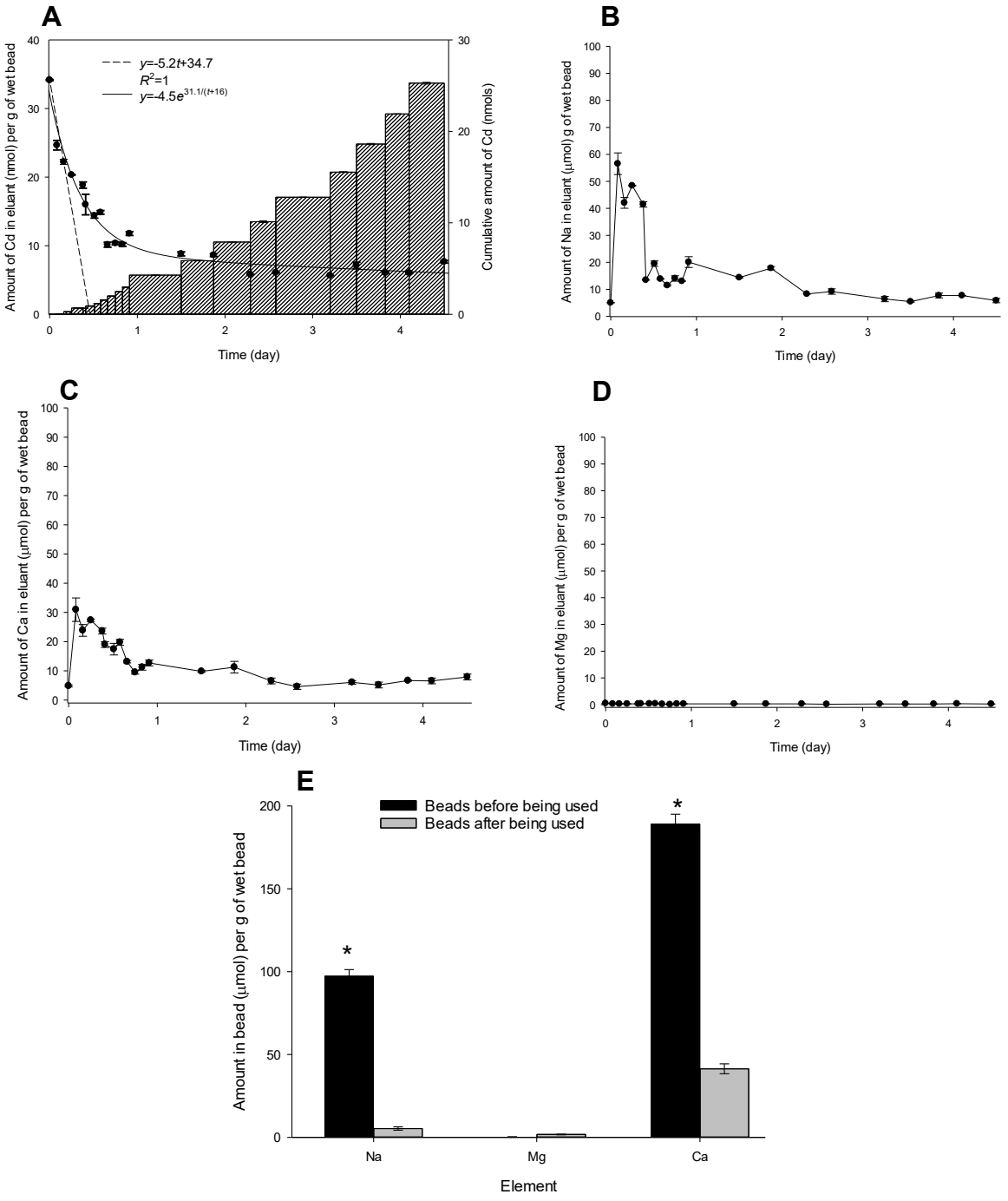

Figure 40. (A) Amounts of the remaining Cd in AGW and Cd accumulated by Ca-alginate beads without bacterial cells from 100 mL of AGW, with a nominal concentration of 10 µM Cd at pH 7.00. Amounts of **(B)** Na, **(C)** Ca, and **(D)** Mg released from the beads and measured in the AGW. **(E)** Respective amounts of Cd, Ca, Na, and Mg in the beads, measured after *aqua regia* digestion, before and after being used in the process. The error bars represent the standard error of the mean of three independent reactors. *Significant difference between beads before and after being used.

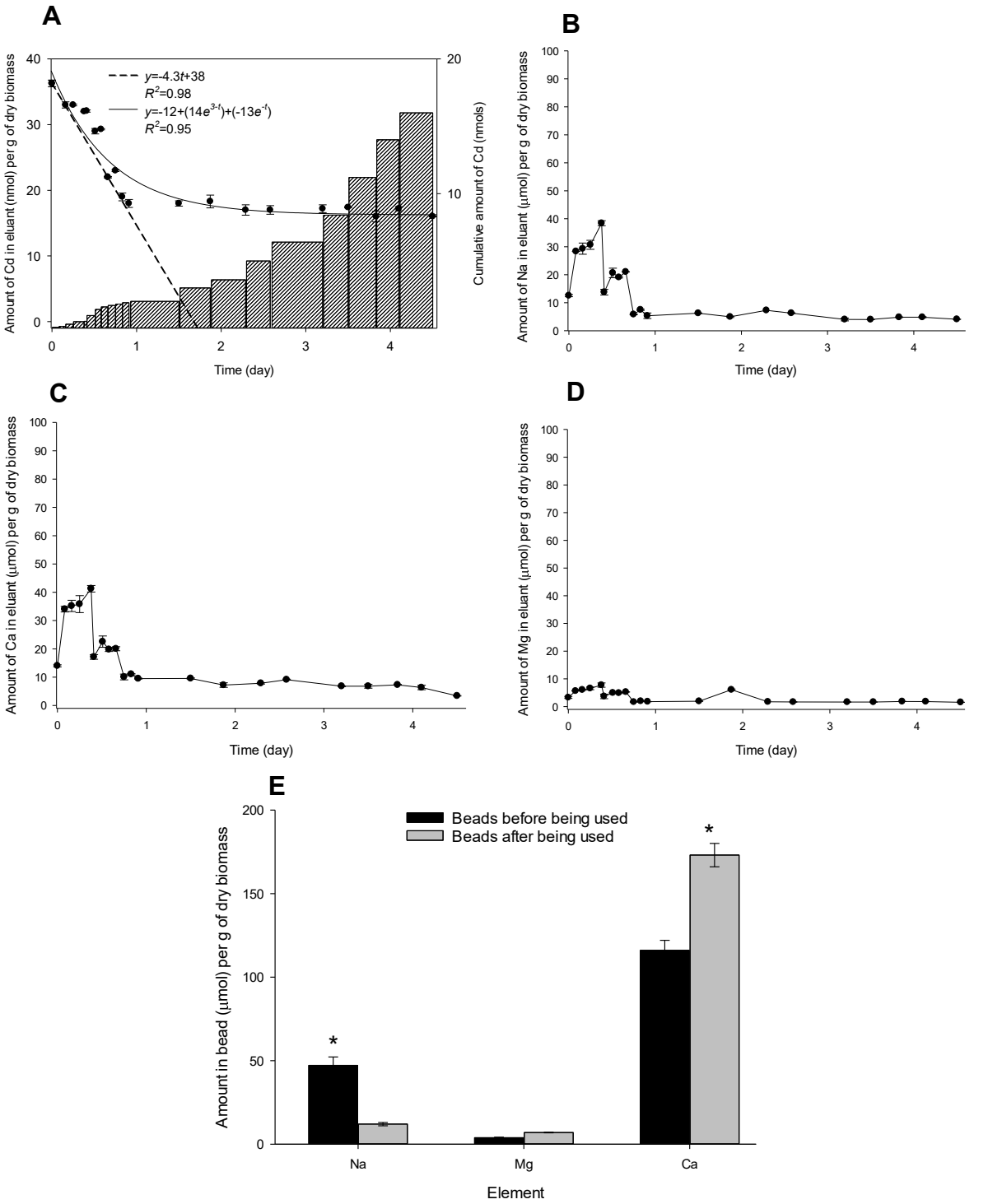

Figure 41. (A) Amounts of the remaining Cd in AGW and Cd accumulated by Ca-alginate beads containing live cells of *B. agri* C15 from 100 mL of AGW, with a nominal concentration of 10 µM Cd at pH 7.00. Amounts of **(B)** Na, **(C)** Ca, and **(D)** Mg released from the beads and measured in the AGW. **(E)** Respective amount of Ca, Na, and Mg in the beads, measured after *aqua regia* digestion, before and after being used in the process. The error bars represent the standard error of the mean of three independent reactors. *Significant difference between beads before and after being used.

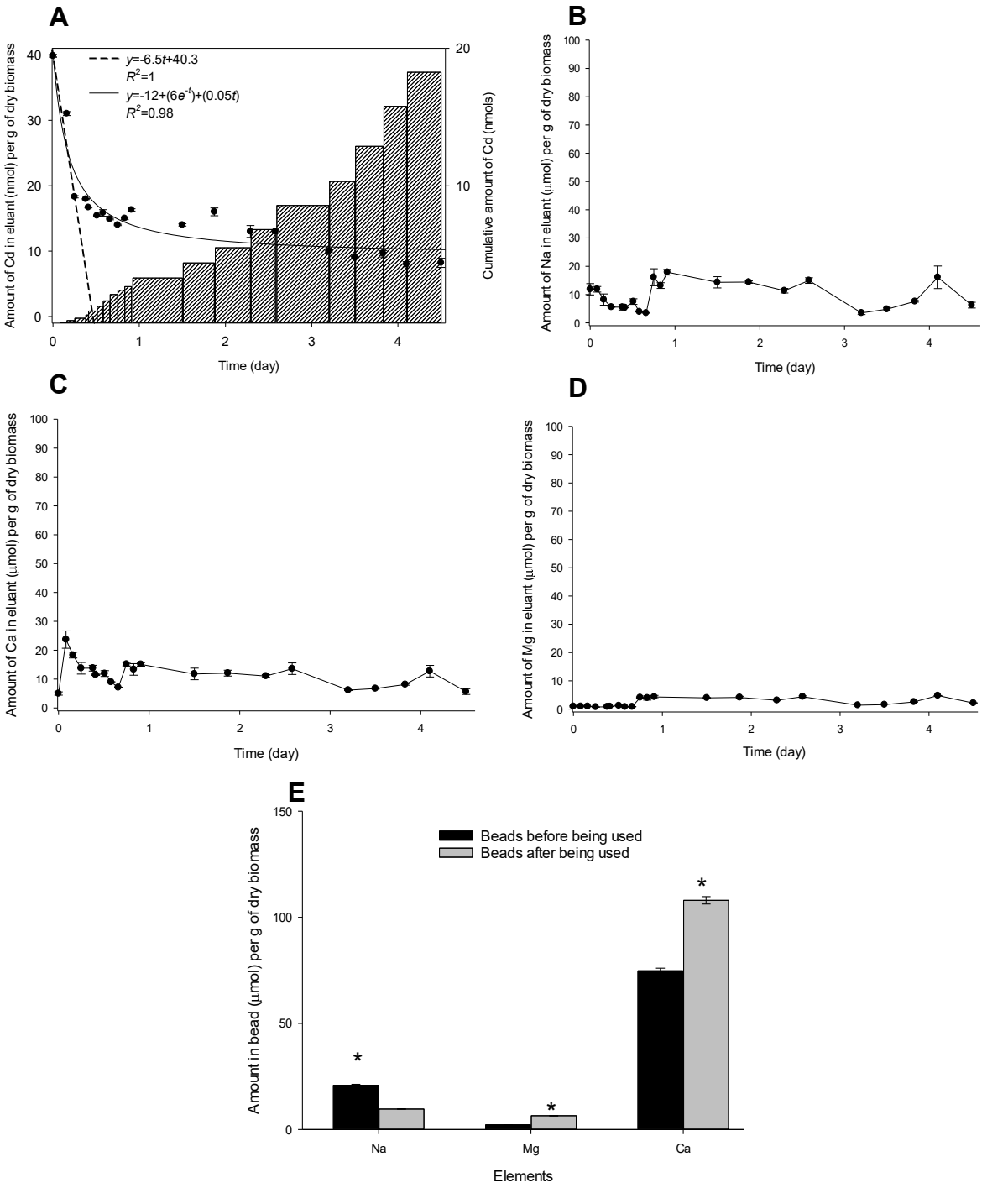

Figure 42. (A) Amounts of the remaining Cd in AGW and Cd accumulated by Ca-alginate beads containing live cells of *B. agri* C15 Cd^R from 100 mL of AGW, with a nominal concentration of 10 µM Cd at pH 7.00. Amounts of **(B)** Na, **(C)** Ca, and **(D)** Mg released from the beads and measured in the AGW. **(E)** Respective amounts of Ca, Na, and Mg in the beads, measured after *aqua regia* digestion, before and after being used in the process. The error bars represent the standard error of the mean of three independent reactors. *Significant difference between beads before and after being used.

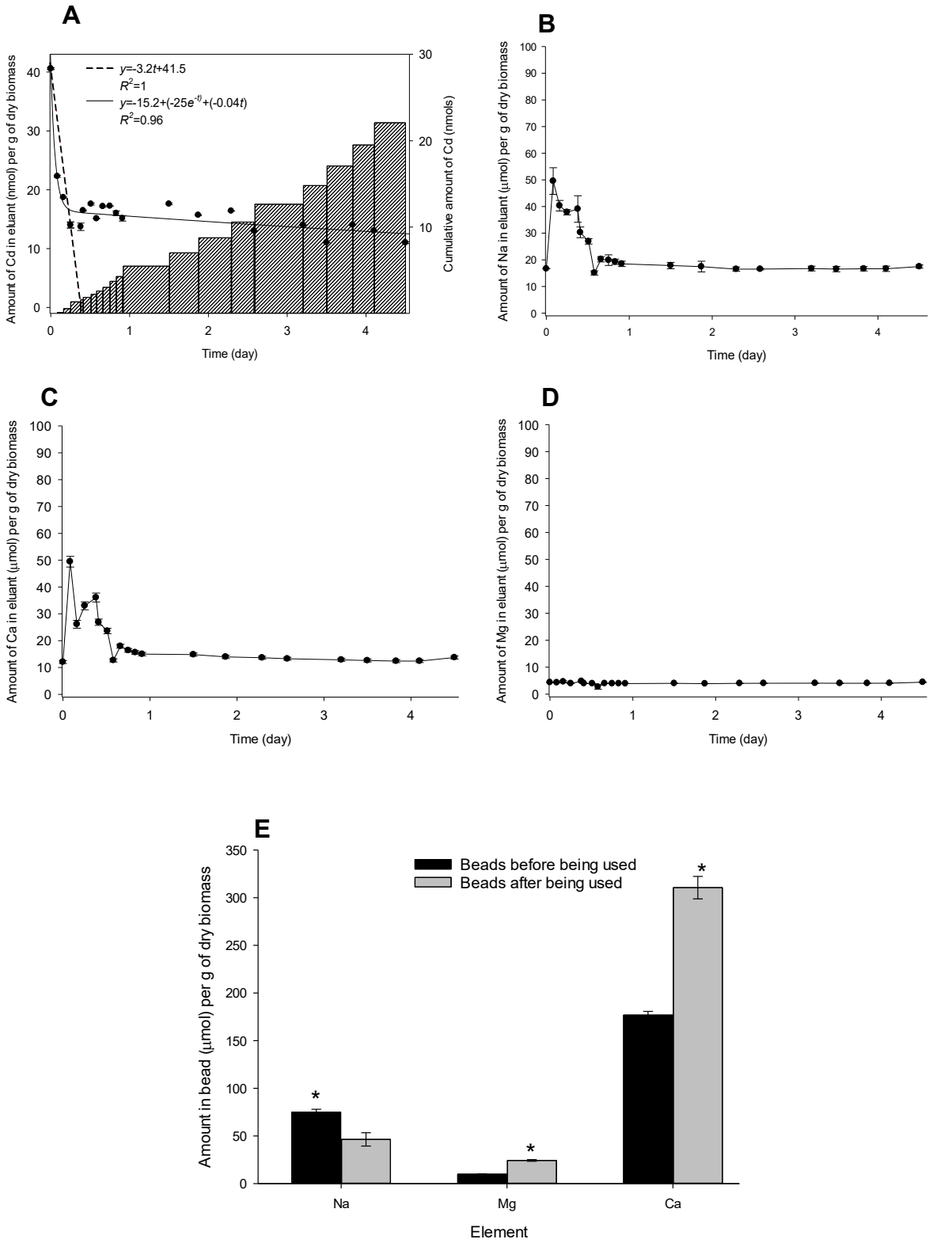

Figure 43. (A) Amounts of the remaining Cd in AGW and Cd accumulated by Ca-alginate beads containing killed-control cells of *B. agri* C15 from 100 mL of AGW, with a nominal concentration of 10 µM Cd at pH 7.00. Amounts of **(B)** Na, **(C)** Ca, and **(D)** Mg released from the beads and measured in the AGW. **(E)** Respective amounts of Cd, Ca, Na and Mg in the beads, measured after *aqua regia* digestion, before and after being used in the process. The error bars represent the standard error of the mean of three independent reactors. *Significant difference between beads before and after being used.

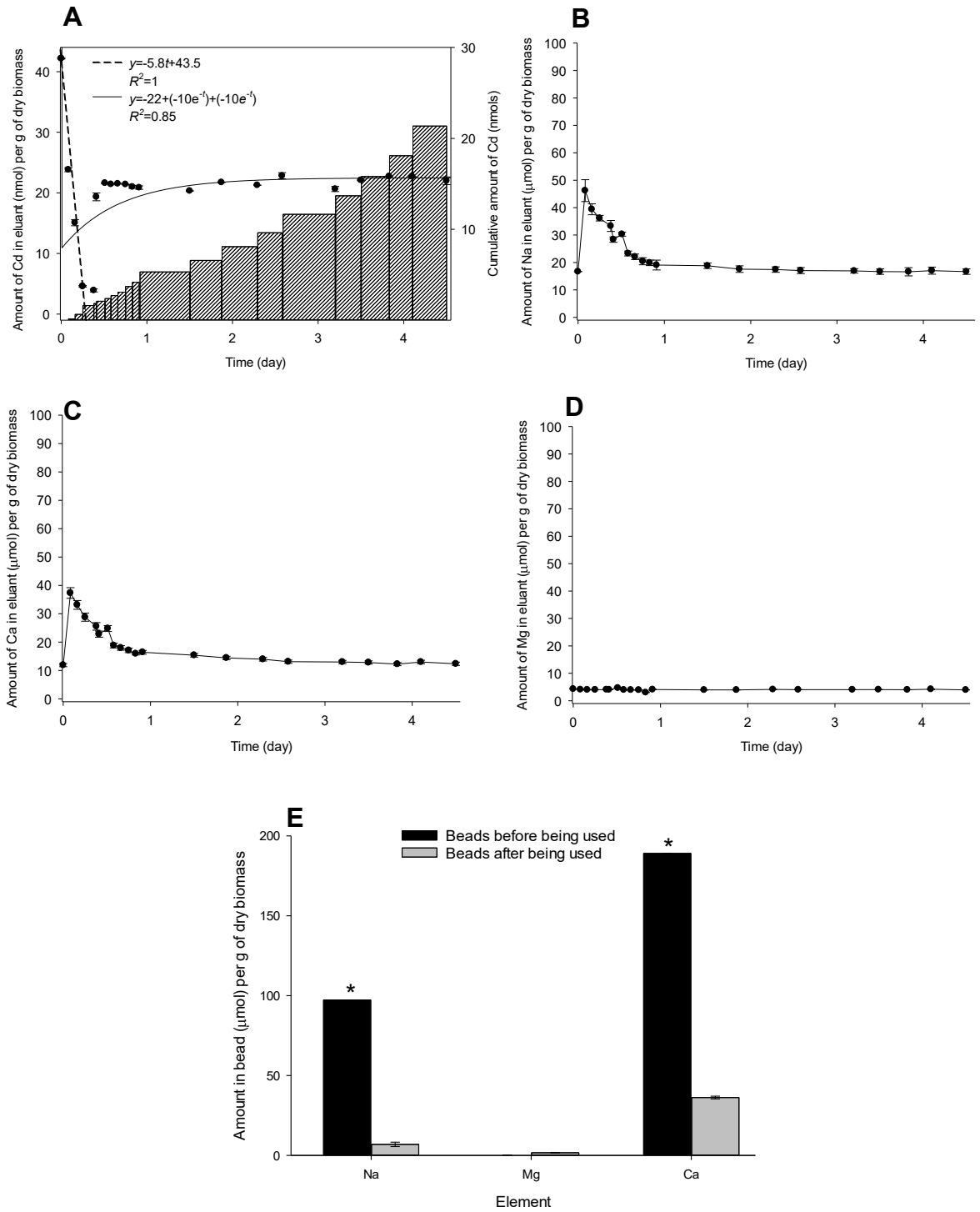

Figure 44. **(A)** Amounts of the remaining Cd in AGW and Cd accumulated by Ca-alginate beads containing killed-control of *B. agri* C15 Cd^R from 100 mL of AGW, with a nominal concentration of 10 µM Cd at pH 7.00. Amounts of **(B)** Na, **(C)** Ca, and **(D)** Mg released from the beads and measured in the AGW. **(E)** Respective amounts of Ca, Na, and Mg in the beads, measured after *aqua regia* digestion, before and after being used in the process. The error bars represent the standard error of the mean of three independent reactors. *Significant difference between beads before and after being used.

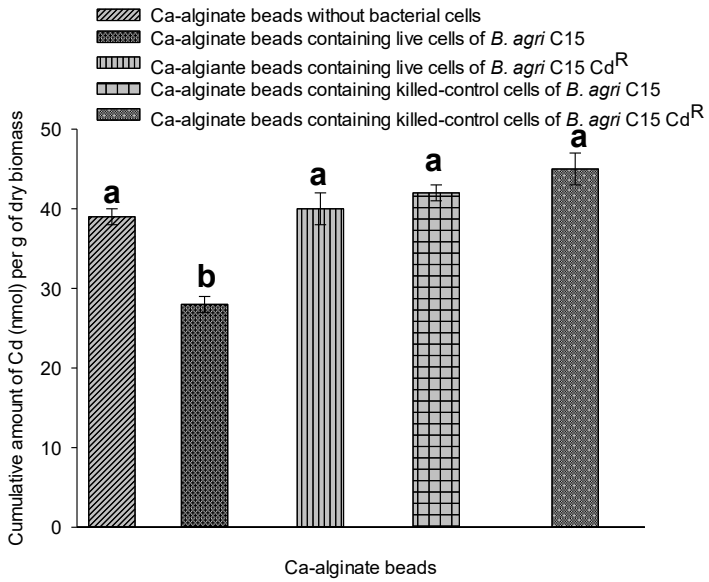

Figure 45. Respective cumulative amounts of Cd in Ca-alginate beads measured after *aqua regia* digestion. The error bars represent the standard error of the mean of three independent reactors. The amounts were subjected to two-way ANOVA, Tukey *post hoc* test, and a different letter indicates a significant difference in amounts between the groups.

5-3-3 Effects of AGW pH on the cadmium removal

The removal experiments were carried out at pH 4.00 and 7.50 to compare the initial Cd-exchanged from AGW with ions versus pH. As in the previous experiments, the amounts of Ca, Na, and Mg, which were released into the AGW and the remaining amounts of Cd in the AGW, were measured. It was predicted in this study that some of Cd would be precipitated at pH 7.50, but it can be seen that the experiments conducted at this pH had the initial amounts that somewhat similar to that under pH 4.00 and 7.00. The differences between the measured and predicted concentrations of Cd were similar to the study by Sandrin and Maier (2002). They used the Visual MINEQL model to predict Cd concentrations versus pH. All beads at pH 4.00 and 7.50 showed the ability to reduce the amounts of Cd from the AGW (Figures 46, 47, 48, 49, 50, 51, 52), as it was shown earlier at pH 7.00 of AGW, with the release of Ca and Na from the beads into eluent AGW

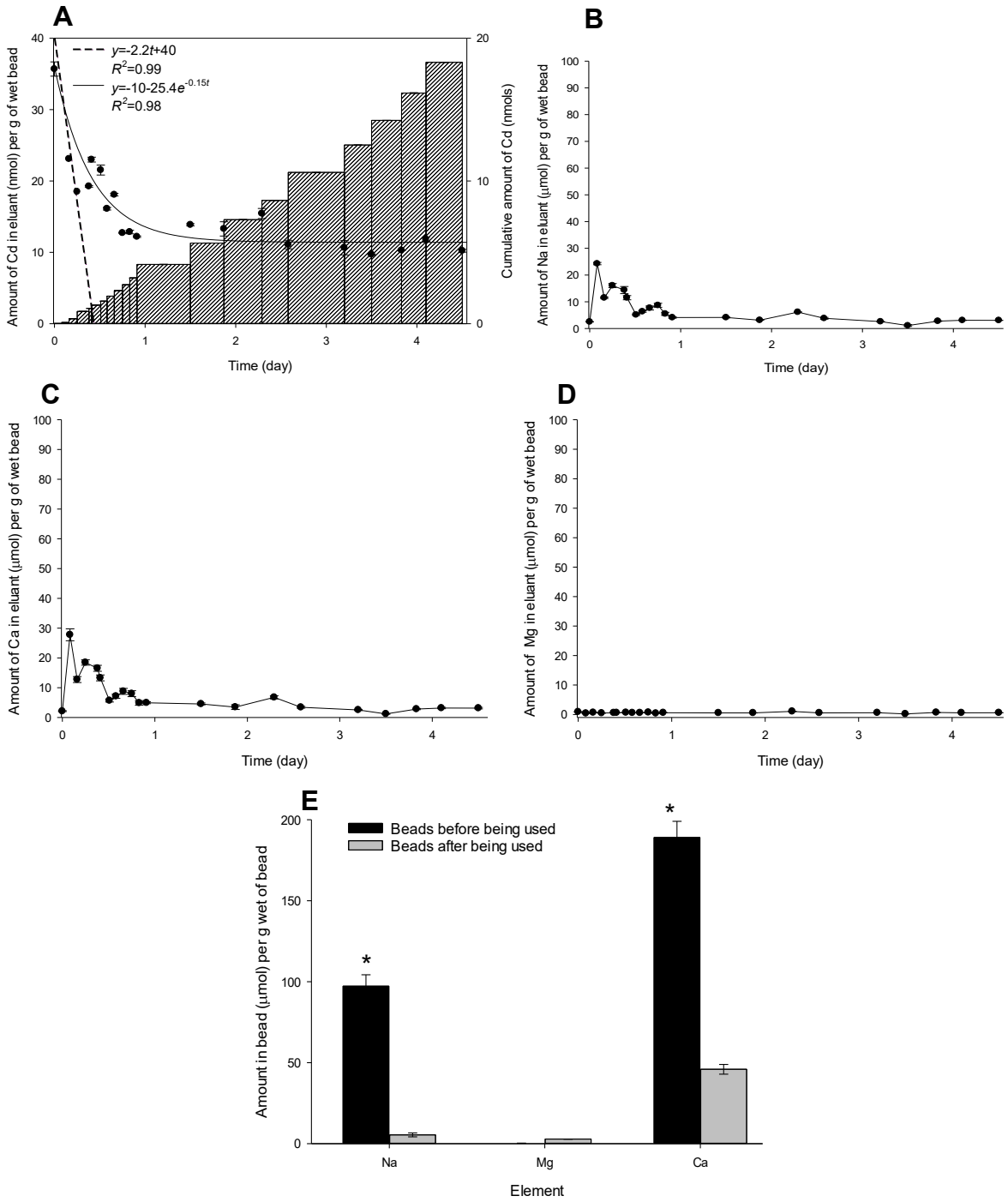

Figure 46. (A) Amounts of the remaining Cd in AGW and Cd accumulated by Ca-alginate beads without bacterial cells from 100 mL of AGW with a nominal concentration of 10 µM Cd at pH 4.00. Amounts of **(B)** Na, **(C)** Ca, and **(D)** Mg released from the beads and measured in the AGW. **(E)** Respective amounts of Ca, Na, and Mg in the beads, measured after *aqua regia* digestion, before and after being used in the process. The error bars represent the standard error of the mean of three independent reactors. *Significant difference between beads before and after being used.

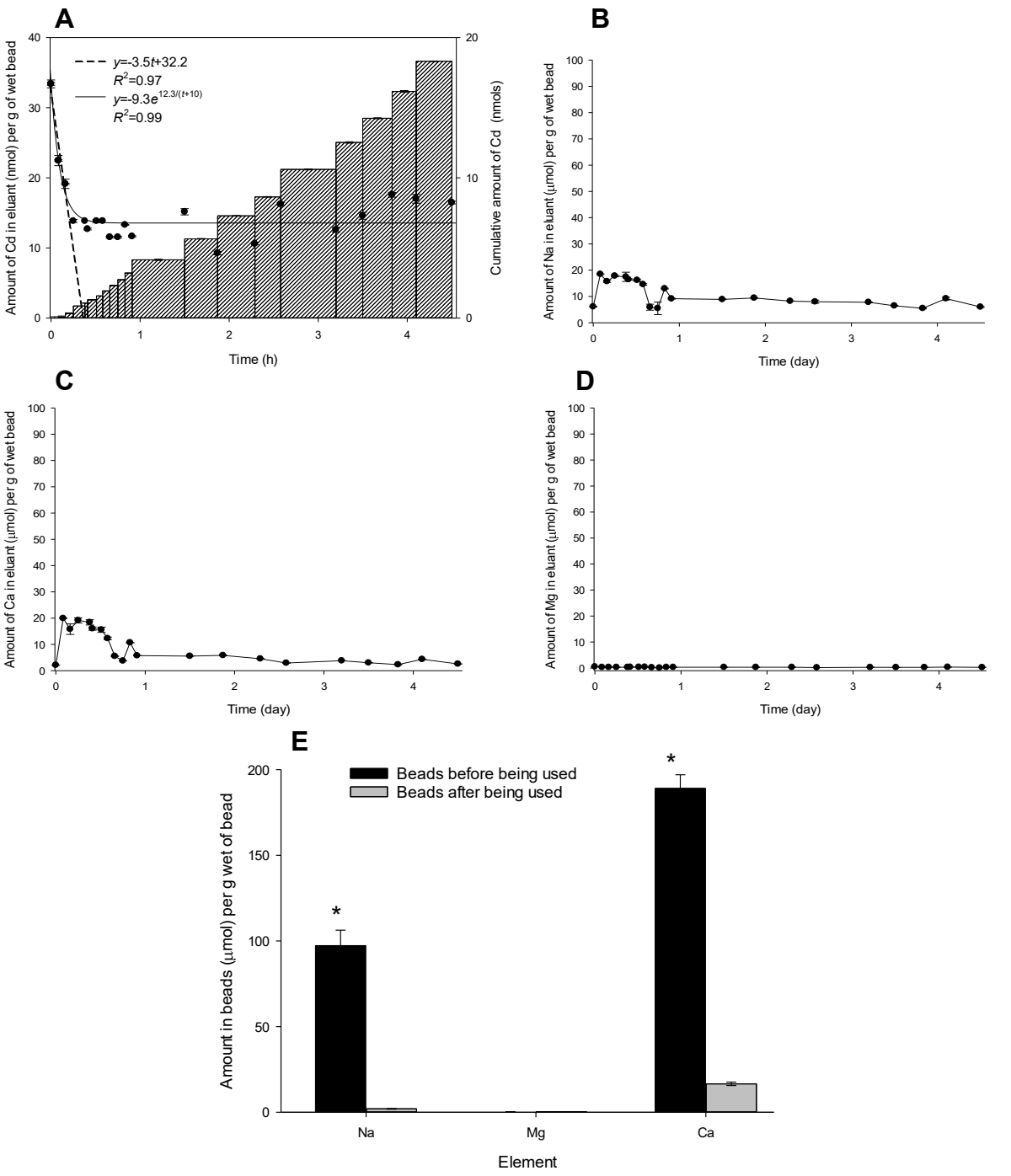

Figure 47. **(**A) Amounts of the remaining Cd in AGW and Cd accumulated by Ca-alginate beads without bacterial cells from 100 mL of AGW with a nominal concentration of 10 µM Cd at pH 7.50. Amounts of **(B)** Na, **(C)** Ca, and **(D)** Mg released from the beads and measured in the AGW. **(E)** Respective amounts of Ca, Na, and Mg in the beads, measured after *aqua regia* digestion, before and after being used in the process. The error bars represent the standard error of the mean of three independent reactors. *Significant difference between beads before and after being used.

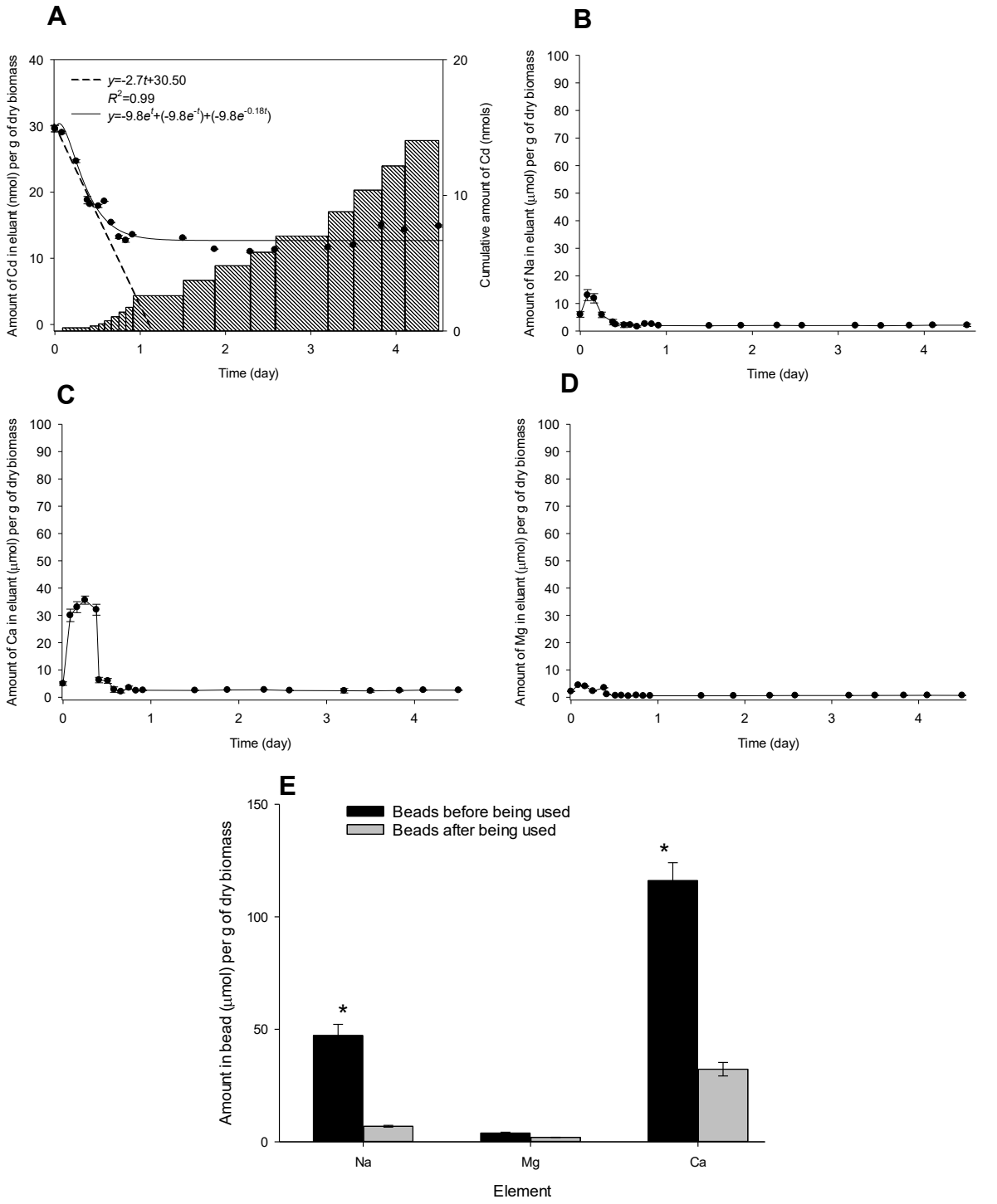

Figure 48. (A) Amounts of the remaining Cd in AGW and Cd accumulated by Ca-alginate beads containing live cells of *B. agri* C15 from 100 mL of AGW with a nominal concentration of 10 µM Cd at pH 4.00. Amounts of **(B)** Na, **(C)** Ca, and **(D)** Mg released from the beads and measured in the AGW. **(E)** Respective amounts of Ca, Na, and Mg in the beads, measured after *aqua regia* digestion, before and after being used in the process. The error bars represent the standard error of the mean of three independent reactors. *Significant difference between beads before and after being used.

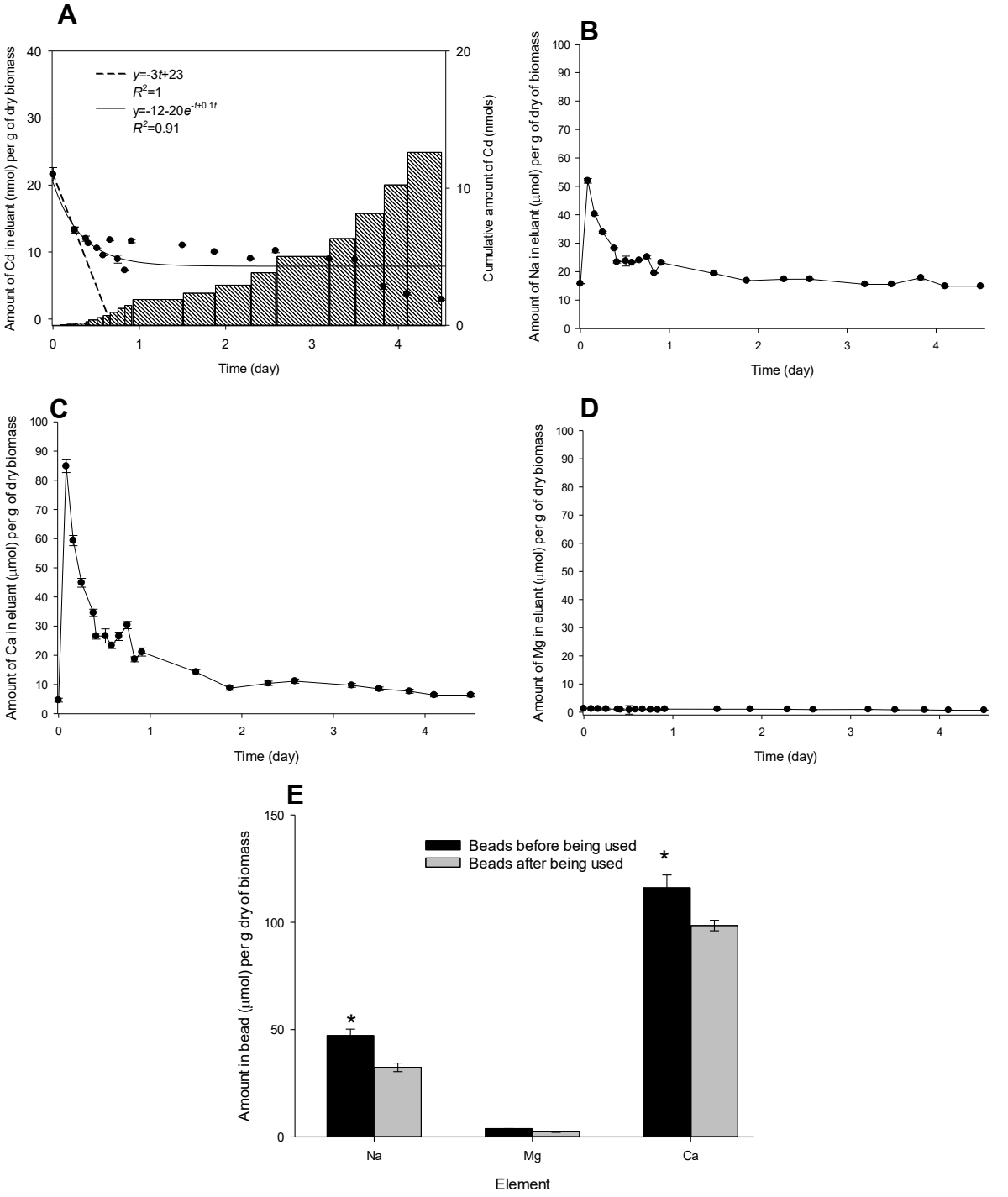

Figure 49. (A) Amounts of the remaining Cd in AGW and Cd accumulated by Ca-alginate beads containing live cells of *B. agri* C15 from 100 mL of AGW with a nominal concentration of 10 µM Cd at pH 7.50. Amounts of **(B)** Na, **(C)** Ca, and **(D)** Mg released from the beads and measured in the AGW. **(E)** Respective amounts of Ca, Na, and Mg in the beads, measured after *aqua regia* digestion, before and after being used in the process. The error bars represent the standard error of the mean of three independent reactors. *Significant difference between beads before and after being used.

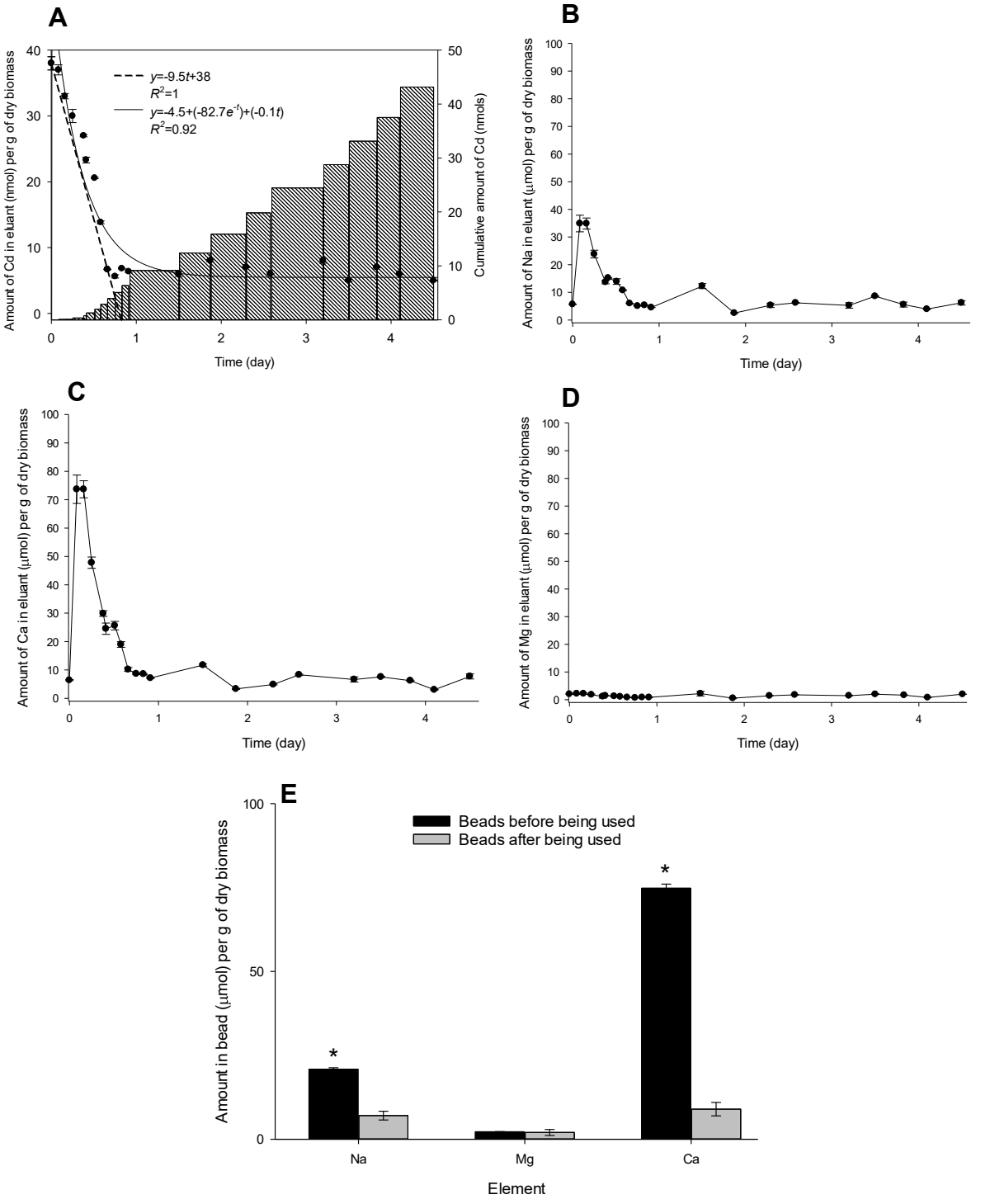

Figure 50. (A) Amounts of the remaining Cd in AGW and Cd accumulated by Ca-alginate beads containing live cells of *B. agri* C15 Cd^R from 100 mL of AGW with a nominal concentration of 10 µM Cd at pH 4.00. Amounts of **(B)** Na, **(C)** Ca, and **(D)** Mg released from the beads and measured in the AGW. **(E)** Respective amounts of Ca, Na, and Mg in the beads, measured after *aqua regia* digestion, before and after being used in the process. The error bars represent the standard error of the mean of three independent reactors.*Significant difference between beads before and after being used.

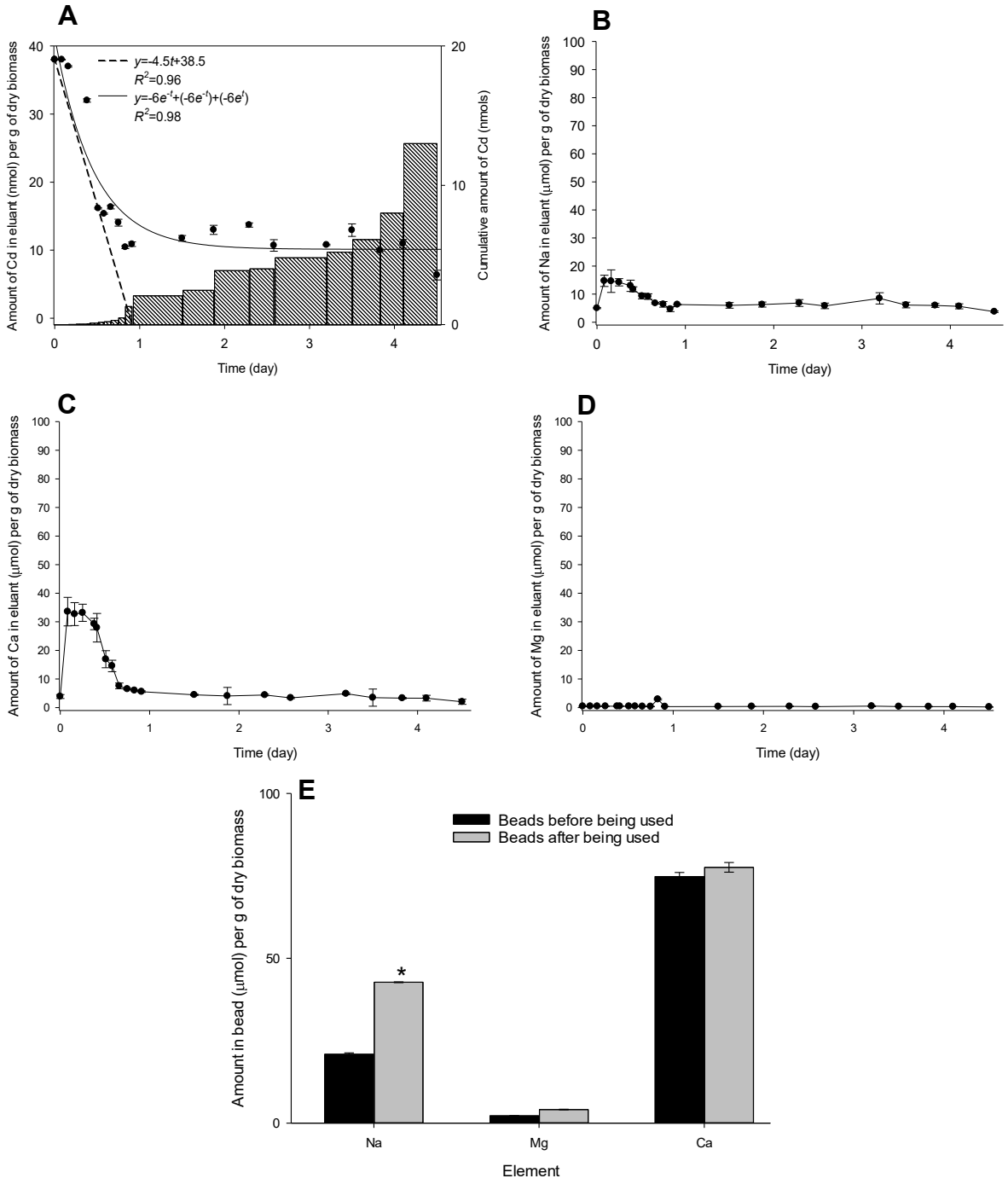

Figure 51. (A) Amounts of the remaining Cd in AGW and Cd accumulated by Ca-alginate beads containing live cells of *B. agri* C15 Cd^R from 100 mL of AGW with a concentration of 10 µM Cd at pH 7.50. Amounts of **(B)** Na, **(C)** Ca, and **(D)** Mg released from the beads and measured in the AGW. **(E)** Respective amounts of Ca, Na, and Mg in the beads, measured after *aqua regia* digestion, before and after being used in the process. The error bars represent the standard error of the mean of three independent reactors. *Significant difference between beads before and after being used.

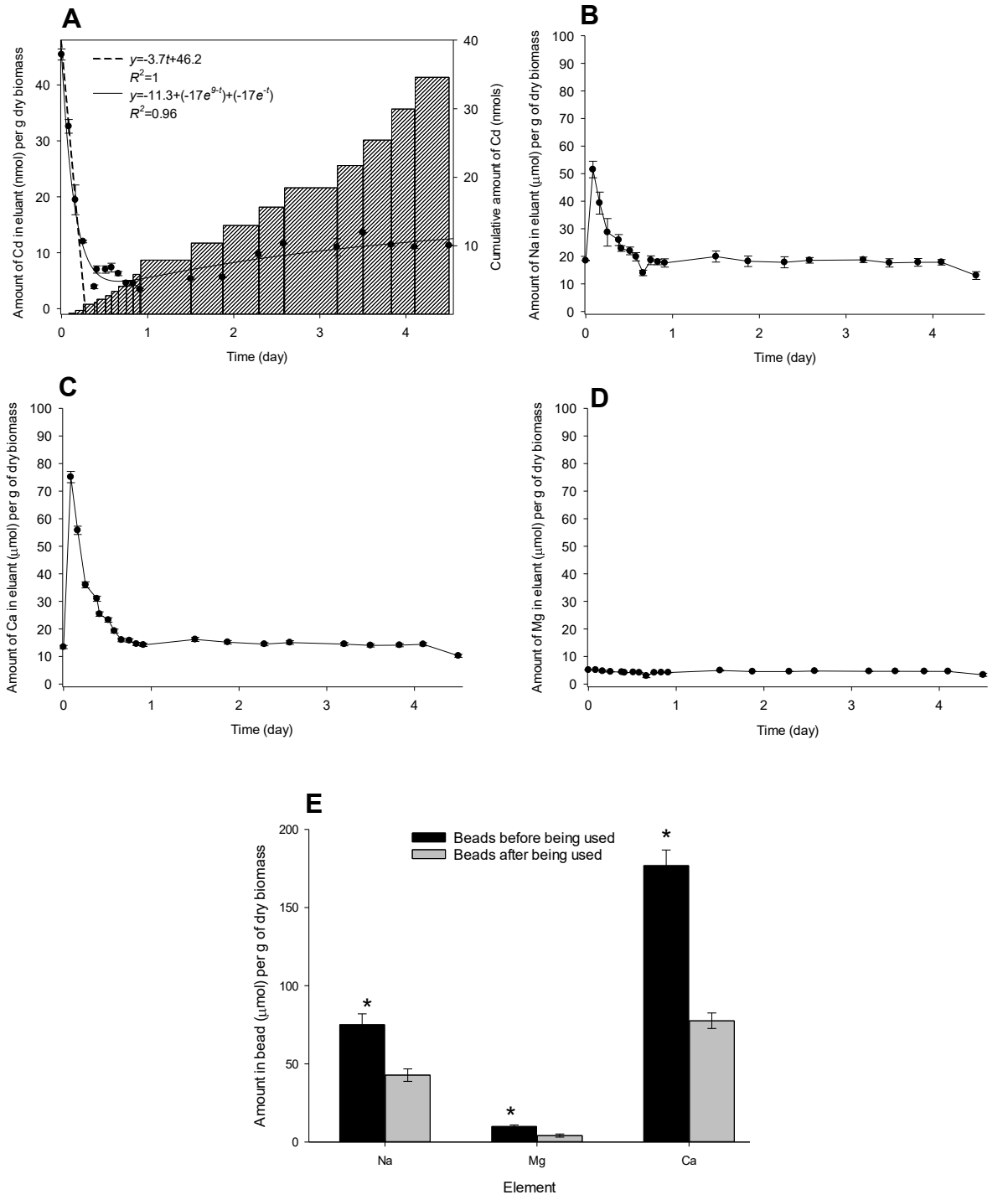

Figure 52. (A) Amounts of the remaining Cd in AGW and Cd accumulated by Ca-alginate beads containing killed-control cells of *B. agri* C15 from 100 mL of AGW with a nominal concentration of 10 µM Cd at pH 4.00. Amounts of **(B)** Na, **(C)** Ca, and **(D)** Mg released from the beads and measured in the AGW. **(E)** Respective amounts of Ca, Na, and Mg in the beads, measured after *aqua regia* digestion, before and after being used in the process. The error bars represent the standard error of the mean of three independent reactors. *Significant difference between beads before and after being used.

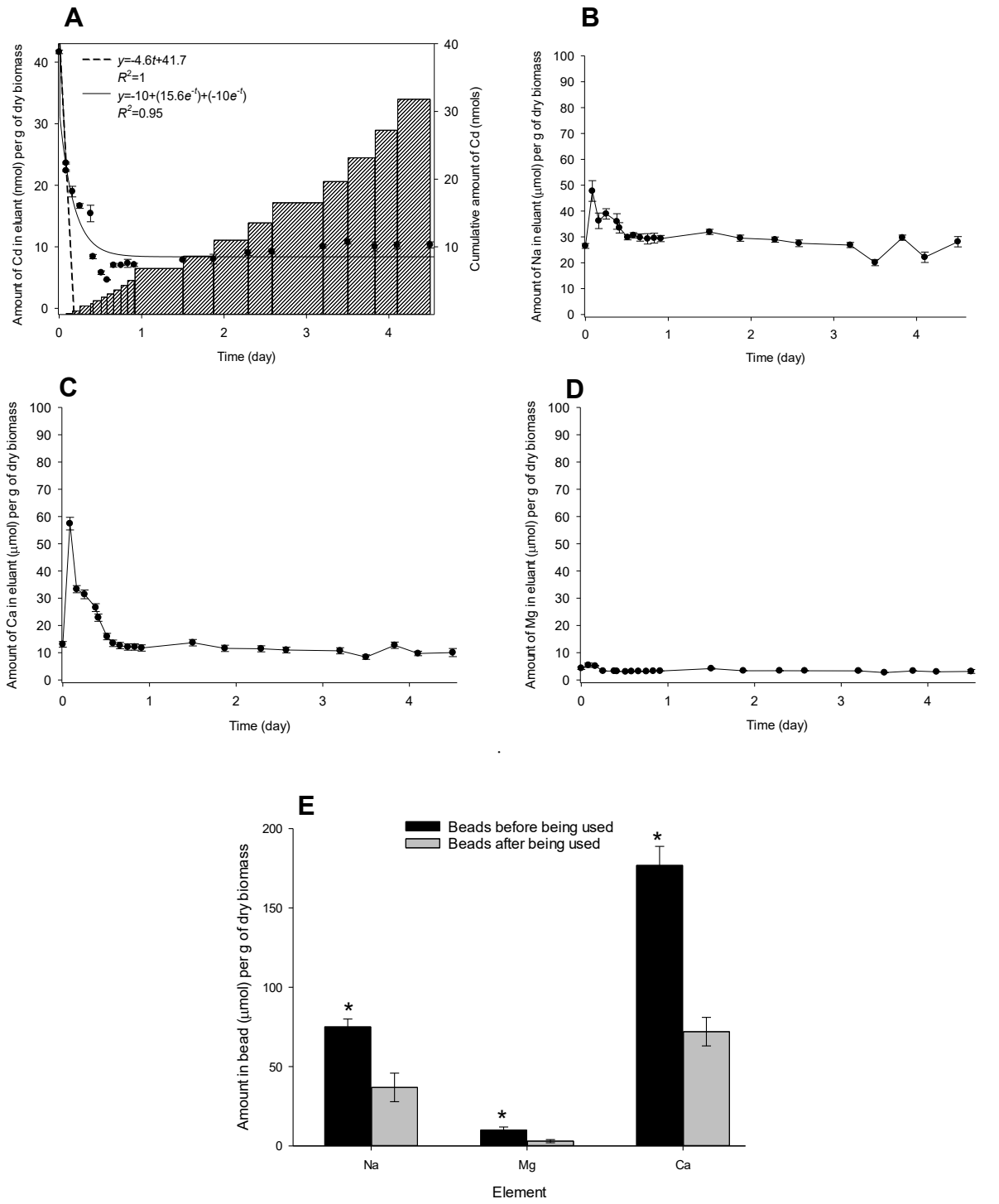

Figure 53. (A) Amounts of the remaining Cd in AGW and Cd accumulated by Ca-alginate beads containing killed-control cells of *B. agri* C15 from 100 mL of AGW with a nominal concentration of 10 µM Cd at pH 7.50. Amounts of **(B)** Na, **(C)** Ca, and **(D)** Mg released from the beads and measured in the AGW. **(E)** Respective amounts of Ca, Na, and Mg in the beads, measured after *aqua regia* digestion, before and after being used in the process. The error bars represent the standard error of the mean of three independent reactors. *Significant difference between beads before and after being used.

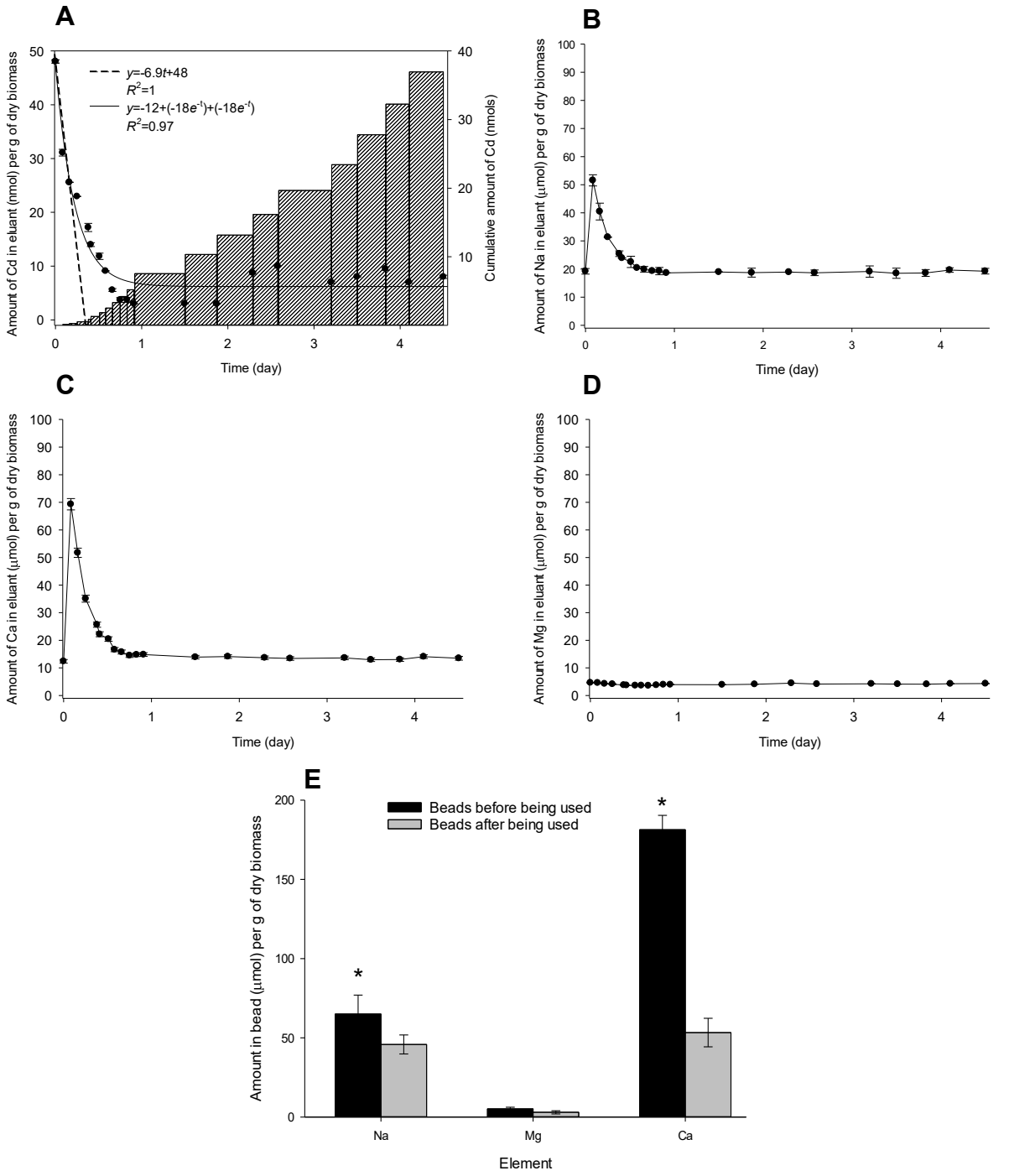

Figure 54. (A) Amounts of the remaining Cd in AGW and Cd accumulated by Ca-alginate beads containing killed-control cells of *B. agri* C15 Cd^R from 100 mL of AGW with a nominal concentration of 10 µM Cd at pH 4.00. Amounts of **(B)** Na, **(C)** Ca, and **(D)** Mg released from the beads and measured in the AGW. **(E)** Respective amounts of Ca, Na, and Mg in the beads, measured after *aqua regia* digestion, before and after being used in the process. The error bars represent the standard error of the mean of three independent reactors. *Significant difference between beads before and after being used.

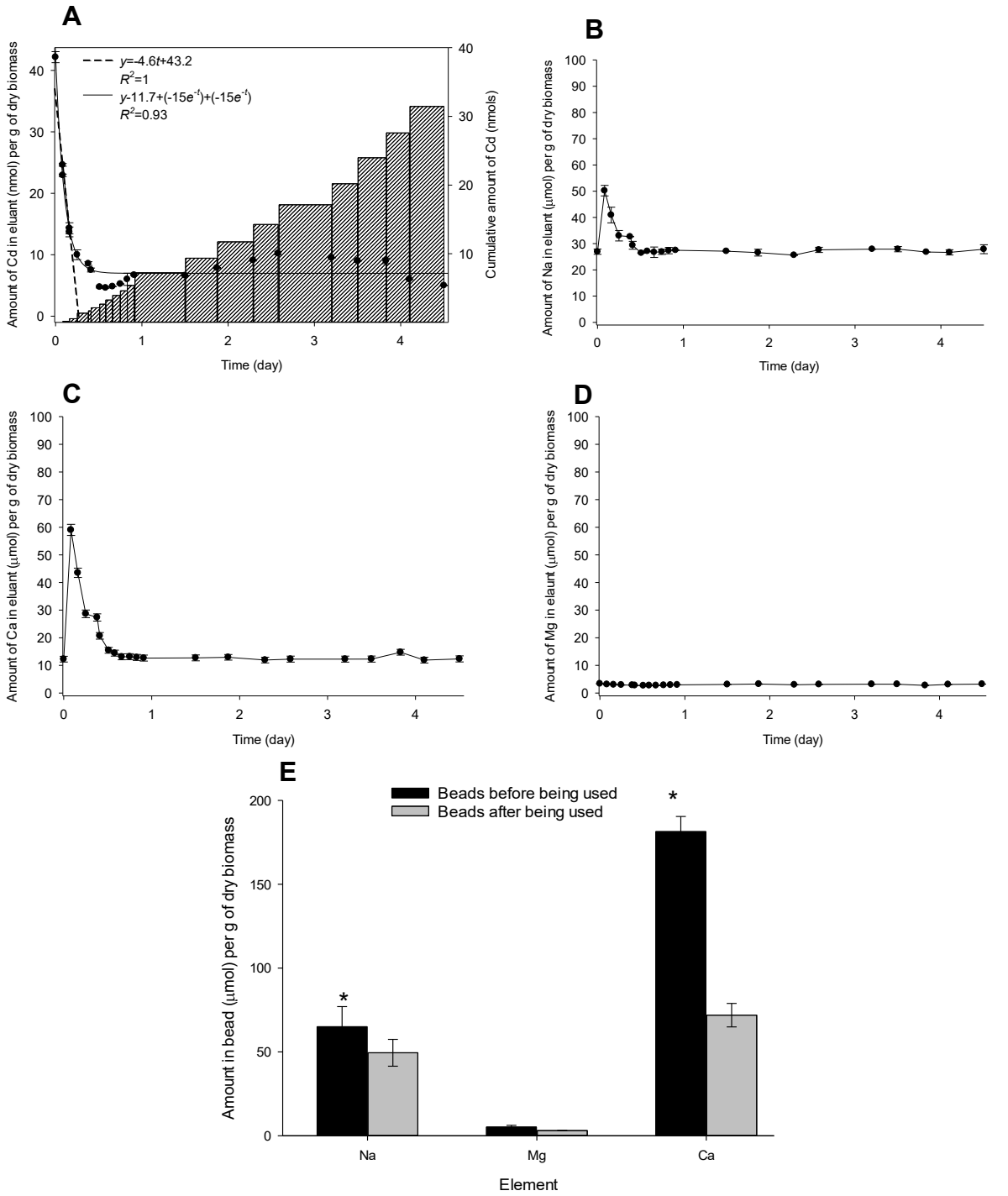

Figure 55. (A) Amounts of the remaining Cd in AGW and Cd accumulated by Ca-alginate beads containing killed-control cells of *B. agri* C15 Cd^R from 100 mL of AGW with a nominal concentration of 10 µM Cd at pH 7.50. Amounts of **(B)** Na, **(C)** Ca, and **(D)** Mg released from the beads and measured in the AGW. **(E)** Respective amounts of Ca, Na, and Mg in the beads, measured after *aqua regia* digestion, before and after being used in the process. The error bars represent the standard error of the mean of three independent reactors. *Significant difference between beads before and after being used.

The effect of pH on the Cd removal from AGW by the beads was evaluated by applying the tangent lines to the curves of Cd remaining in the eluents, whereby the slopes

of their linear equations gives approximate rates of Cd removal during the initial time of operating the reactors. Then, these removal rates are plotted versus pH (4.00, 7.00, and 7.50) for each of the five bead types (Figure 56).

Ca-alginate beads without bacterial cells or containing live cells of *B. agri* C15 had similar amounts of removal rates at different pHs. Their maximum removal rate was observed at pH 7.00 (**p<0.05, Figure 56 A, B, respectively), whereas the removal rates at pH 4.00 and 7.50 were not statistically significantly different from each other (**p<0.05). In contrast, Ca-alginate beads containing live or killed control cells of *B. agri* C15 Cd^R showed a decreasing trend (Figure 56 C, E, respectively), with significantly higher removal rates at pH 4.00 (*p<0.05) than pH 7.50 (***p<0.05). In comparison, the removal rate of Cd by Ca-alginate beads killed control cells of *B. agri* C15 (Figure 56 D) increased significantly at pH 7.50 (**p<0.05).

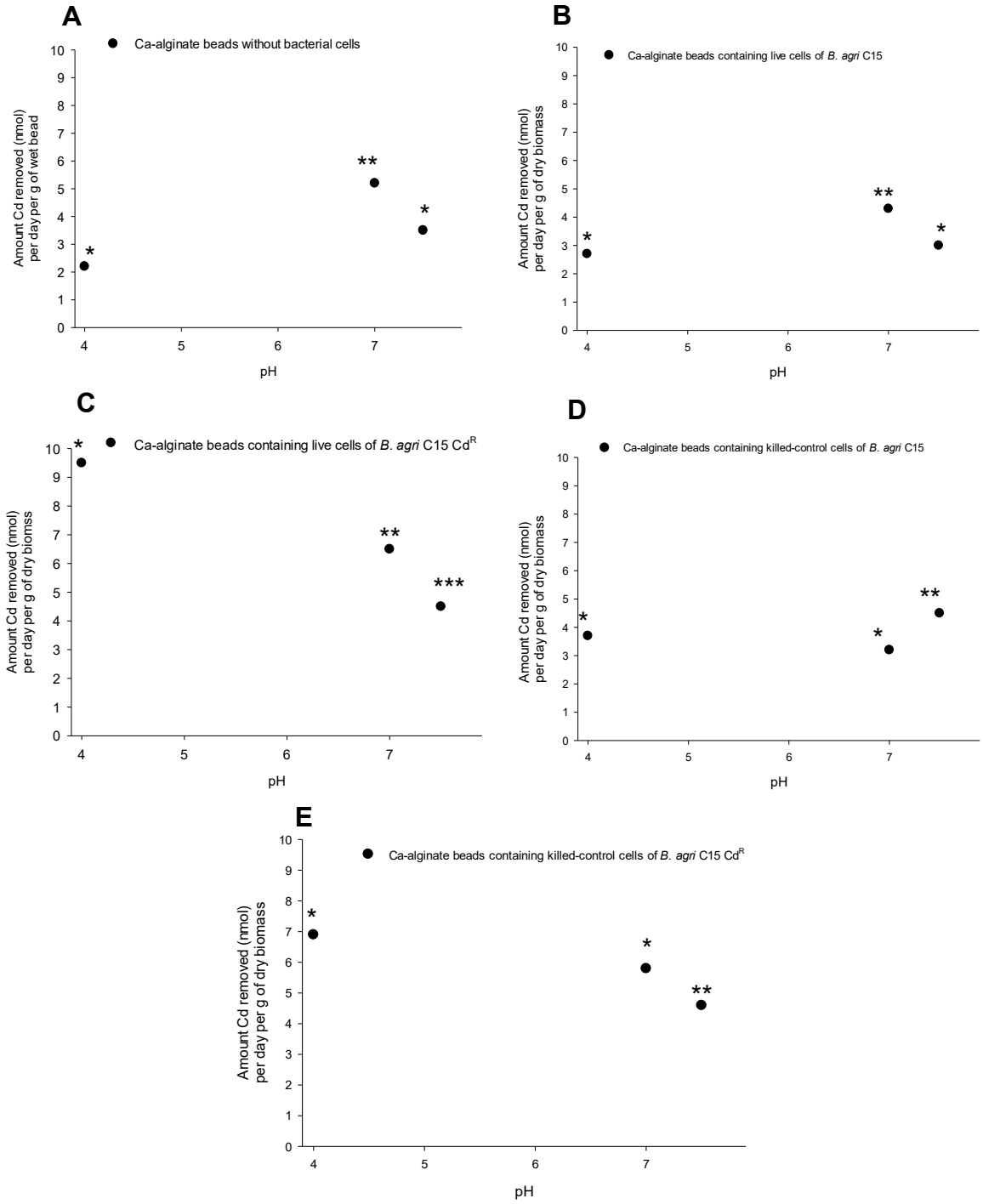

Figure 56. Respective maximum initial rates of Cd removed at different pH by **(A)** Ca-alginate beads without bacterial cells or containing live cells of **(B)** *B. agri* C15 and **(C)** *B. agri* C15 Cd^R, and killed-control cells of **(D)** *B. agri* C15 and **(E)** *B. agri* C15 Cd^R. The tangent lines were applied to the curves to give approximate rates of Cd removals during the initial time of operating the reactor. The rate of each group was obtained from one tangent line; therefore, error bars are not displayed. The rates were statistically analysed with ANOVA, and the points labelled by different numbers of *, **, *** are significantly different (p<0.05) from each other.

The effect of different pHs on the accumulative amounts of Cd in the beads was obtained by measuring the concentrations of Cd in the beads after *aqua regia* digestion. The accumulative amounts showed a different level of each type of bead under different pH levels (Figure 57). Ca-alginate beads without bacterial cells (Figure 57 A) or containing live cells of *B. agri* C15 (Figure 57 B) showed no significant difference in accumulative amounts of Cd at different pH values ($p<0.05$). The effect of pH on the accumulative amounts of Cd in Ca-alginate beads containing killed-control cells of *B. agri* C15 and *B. agri* C15 Cd^R showed similar cumulative amounts at pH 4.00 and pH 7.50. In contrast, significantly lower amounts were determined at pH 7.00 (**$p<0.05$, Figure 57 D, E, respectively). There was a clear trend towards lower accumulative amounts in beads with *B. agri* C15 Cd^R (Figure 57 C) with the increase in the pH. For this strain, the highest amount of Cd was recorded, compared to other beads or pH.

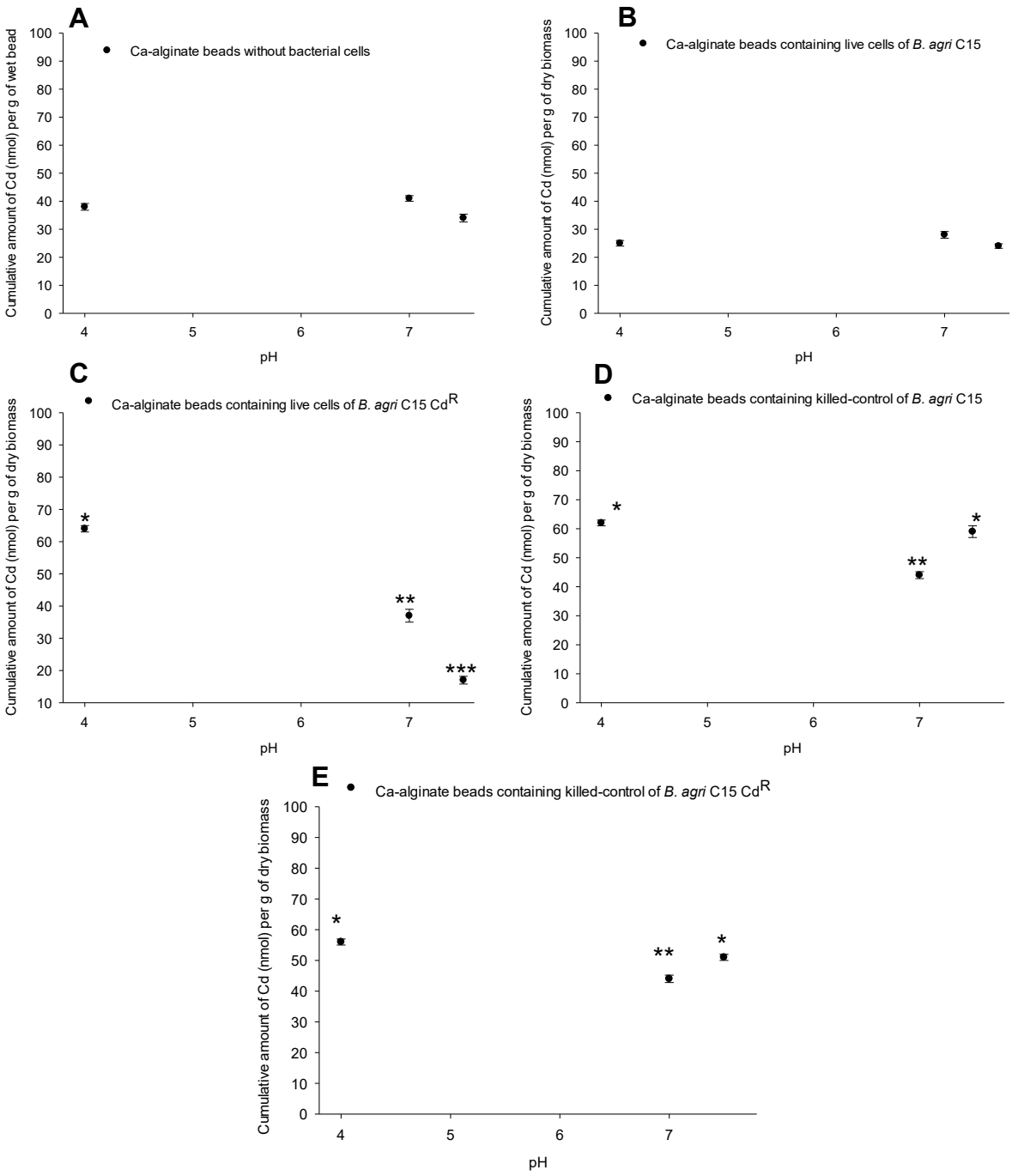

Figure 57. Cumulative amounts of Cd at different pH by **(A)** Ca-alginate beads without bacterial cells or containing live cells of **(B)** *B. agri* C15, and **(C)** *B. agri* C15 Cd^R, and killed-control cells of **(D)** *B. agri* C15 and **(E)** *B. agri* C15 Cd^R, measured after *aqua regia* digestion. The amounts are the mean, and the error bars represent the standard error of the mean between the reactors (n = 3). The amounts were statistically analysed with ANOVA, and the points labelled by different numbers of *, **, *** are significantly different (p<0.05) to each other.

5-3-4 Effects of cation-anion concentrations in AGW on the cadmium removal

At a neutral pH of AGW (7.00), it was essential to investigate the Cd exchange with Ca/Na from the beads under the effect of the co-existing cation/anion. The major cation is calcium, and the essential anion is phosphate. Therefore, the effect of increasing the concentration of $CaCl_2$, from 1.75 to 17.5 mM, in AGW on the Cd exchange was studied by determining the amounts of Ca, Na, and Mg that were released into the AGW and the remaining amounts of Cd in AGW. The released amounts of Na and Mg from the beads into the AGW were similar to the amounts obtained at different pH (as shown in the previous Figures). However, the released amounts of Ca were high (Figures 58, 59, 60, 61, 62) compared to the amounts released without increasing the Ca as the previous Figures have shown.

The removal of Cd at the higher Ca concentration (17.5 mM) was lower than at lower Ca concentration, indicating that $CdCl^+$ species (Figure 38B) may have a noticeable deleterious effect on the process. The removal rates of Cd from AGW were obtained (Figure 63) by applying the tangent lines to the amounts of Cd removal *vs.* the time. Ca-alginate beads containing killed-control cells of *B. agri* C15 Cd^R showed a significantly higher initial removal rate of Cd ($^a p<0.05$) compared to any other beads. Overall, however, the cumulative amounts of Cd in the beads, obtained by measuring the amounts of Cd in beads after *aqua regia* digestion, was significantly higher in Ca-alginate beads that contained live cells of *B. agri* C15 Cd^R (Figure 64, $^a p<0.05$), indicating that this strain has the highest capacity at both tested concentrations of Ca in the AGW.

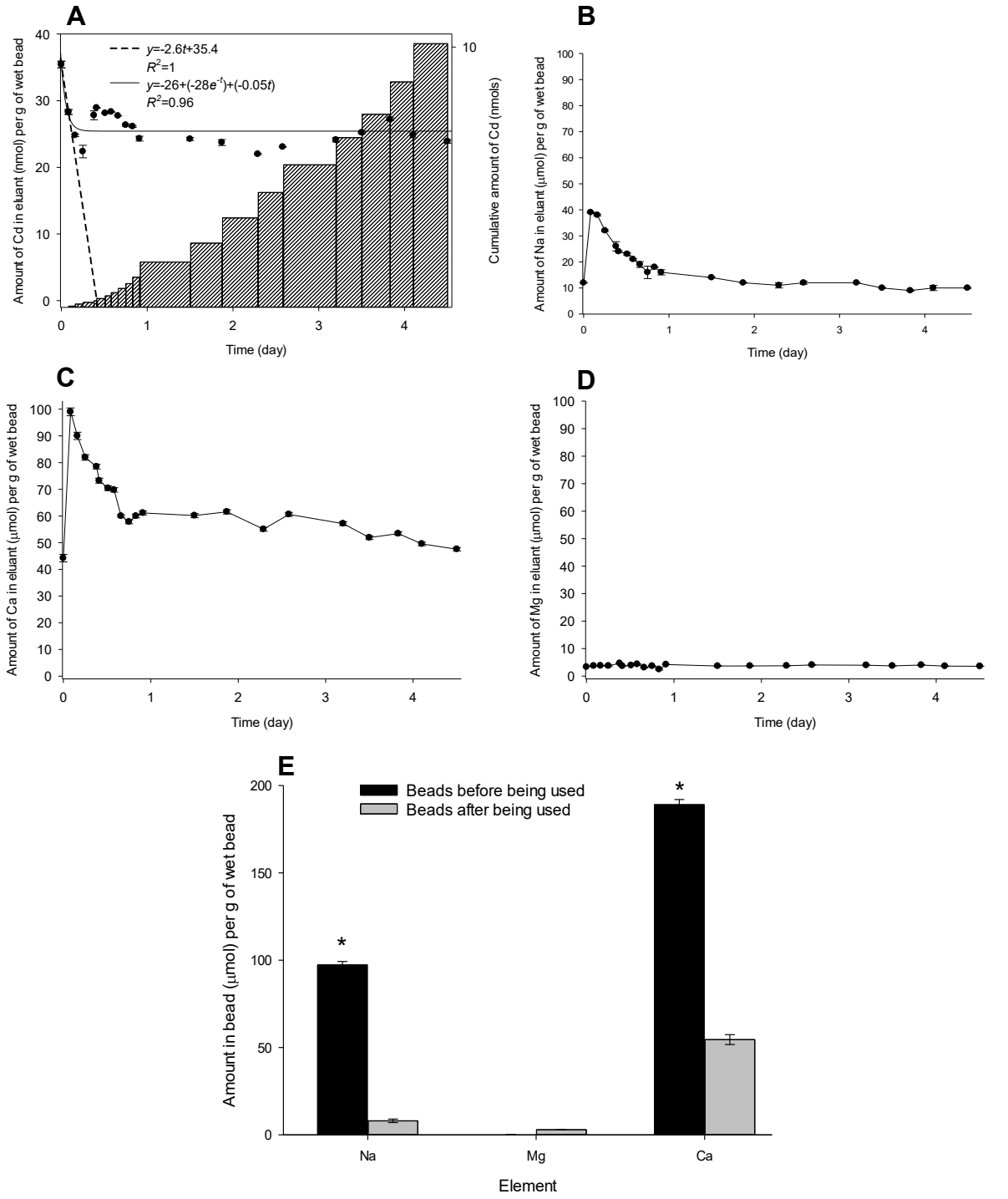

Figure 58. (A) Amount of the remaining Cd in the AGW and Cd accumulated by Ca-alginate beads without bacterial cells from 100 mL of AGW, with a nominal concentration of 10 µM Cd at pH 7.00 under the effect of 17.5 mM calcium. Amounts of **(B)** Na, **(C)** Ca, and **(D)** Mg released from the beads and measured in the AGW. **(E)** Respective amounts of Ca, Na, and Mg in the beads, measured after *aqua regia* digestion, before and after being used in the process. The error bars represent the standard error of the mean of three independent reactors. *Significant difference between beads before and after being used.

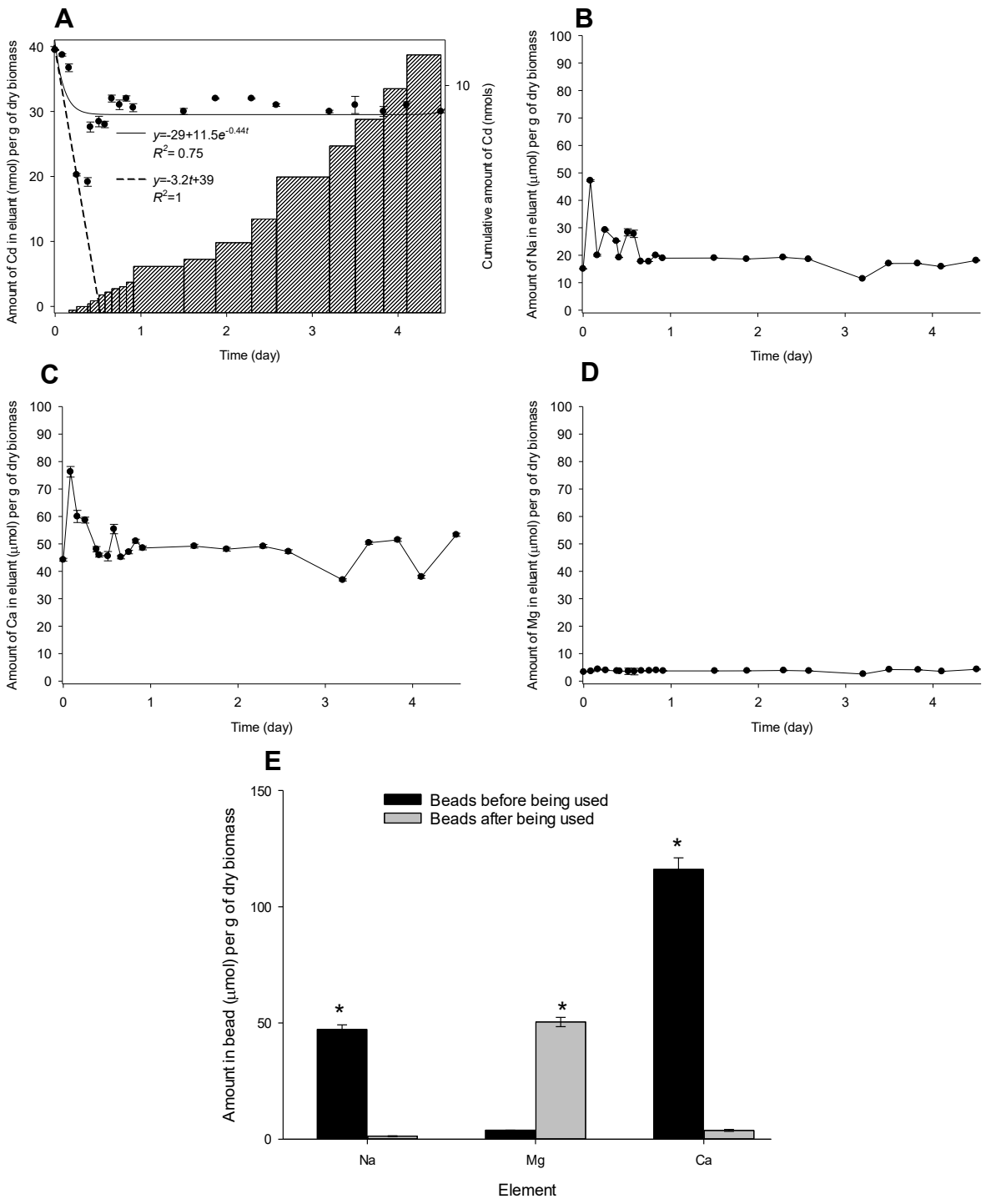

Figure 59. (A) Amounts of the remaining Cd in the AGW and Cd accumulated by Ca-alginate beads containing live cells of *B. agri* C15 from 100 mL of AGW, with a nominal concentration of 10 µM Cd at pH 7.00 under the effect of 17.5 mM calcium. Amounts of **(B)** Na, **(C)** Ca, and **(D)** Mg released from the beads and measured in the AGW. **(E)** Respective amounts of Ca, Na, and Mg in the beads, measured after *aqua regia* digestion, before and after being used in the process. The error bars represent the standard error of the mean of three independent reactors. *Significant difference between beads before and after being used.

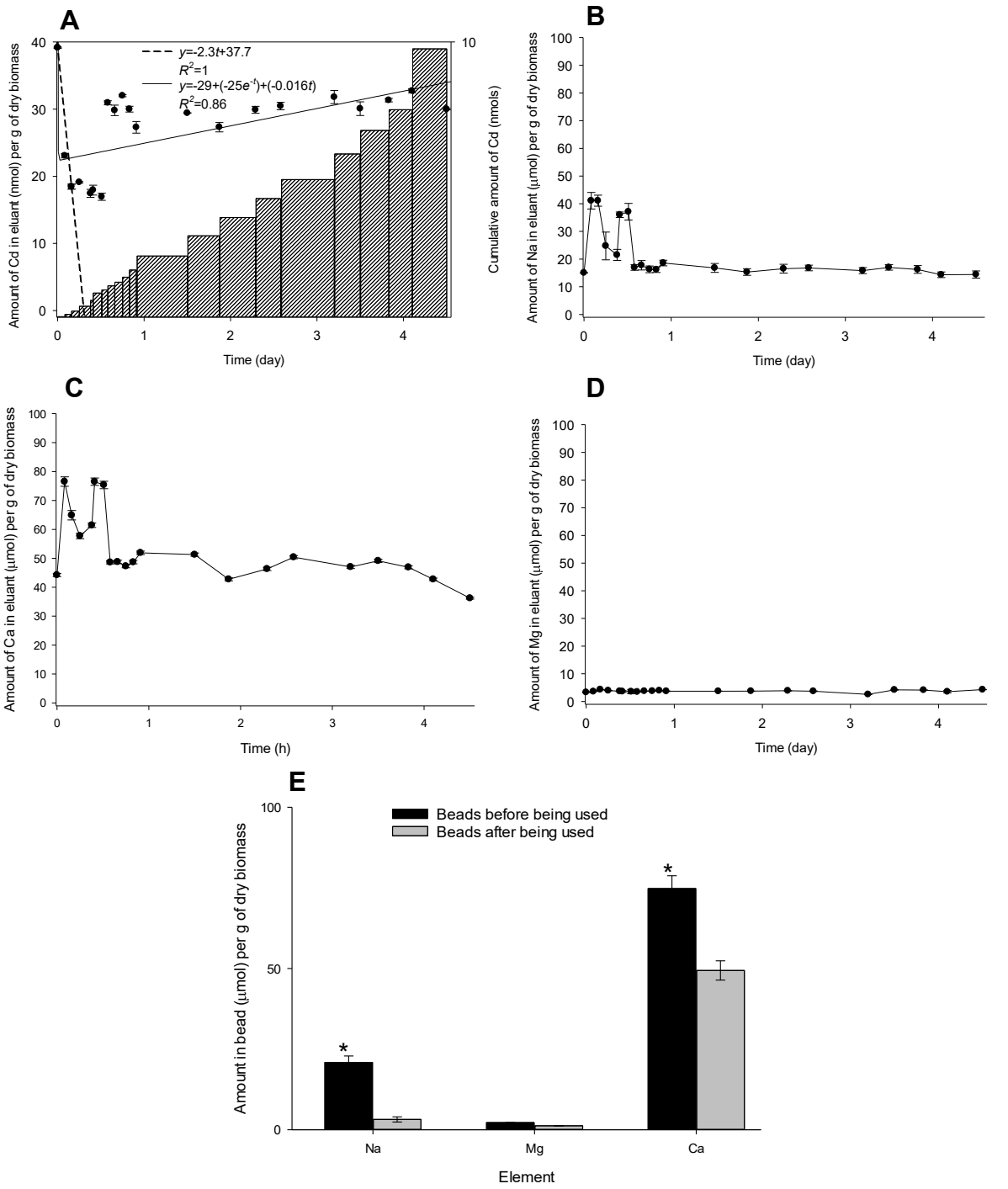

Figure 60. (A) Amounts of the remaining Cd in the AGW and Cd accumulated by Ca-alginate beads containing live cells of *B. agri* C15 Cd^R from 100 mL of AGW, with a nominal concentration of 10 µM Cd at pH 7.00, under the effect of 17.5 calcium. Amounts of **(B)** Na, **(C)** Ca, and **(D)** Mg released from the beads and measured in the AGW. **(E)** Respective amounts of Ca, Na, and Mg in the beads, measured after *aqua regia* digestion, before and after being used in the process. The error bars represent the standard error of the mean of three independent reactors.*Significant difference between beads before and after being used.

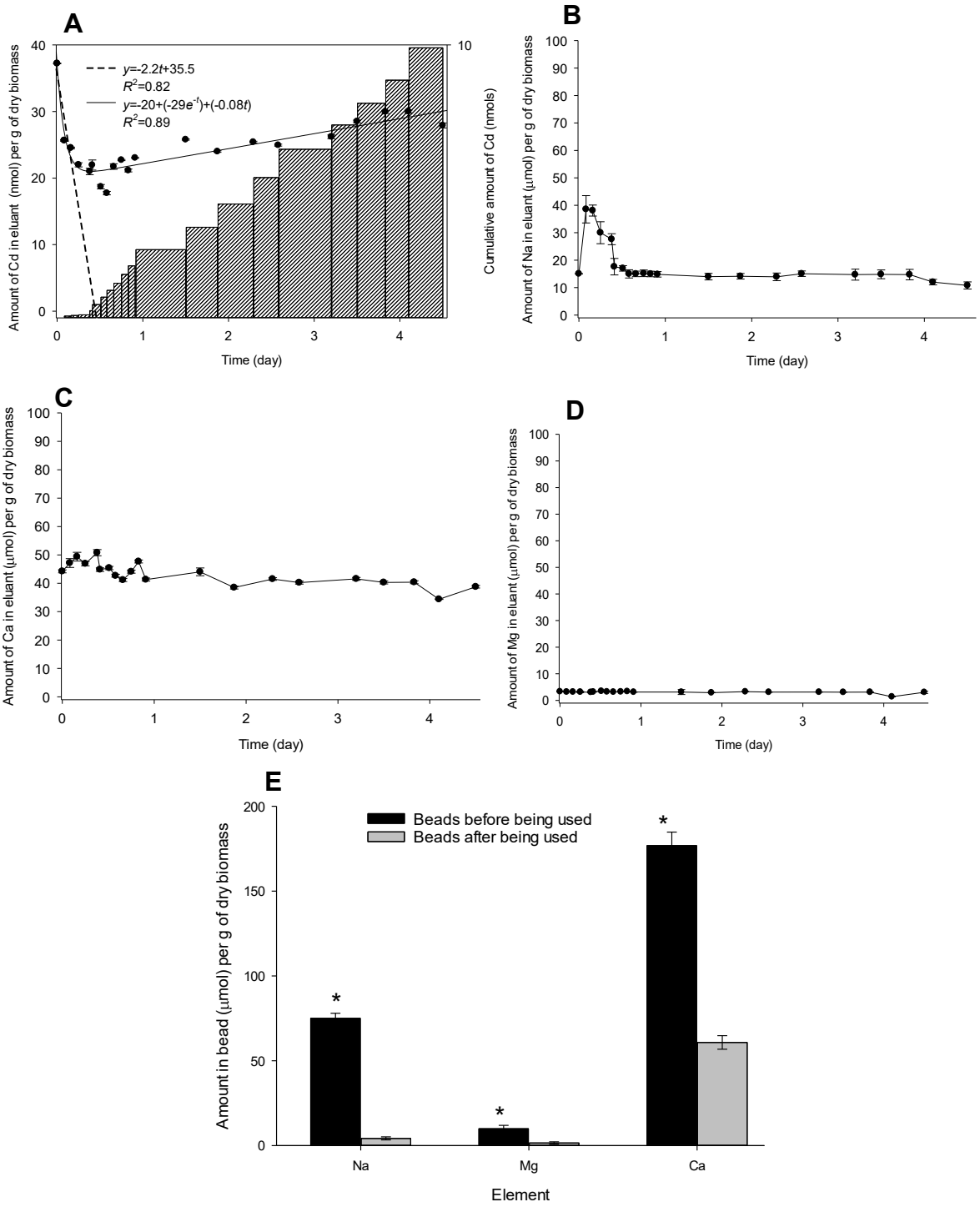

Figure 61. (A) Amounts of the remaining Cd in the AGW and Cd accumulated by Ca-alginate beads containing killed-control cells of *B. agri* C15 from 100 mL of AGW with a nominal concentration of 10 µM Cd at pH 7.00, under the effect of 17.5 calcium. Concentrations of **(B)** Na, **(C)** Ca, and **(D)** Mg released from the beads measured in the AGW. **(E)** Respective amounts of Ca, Na, and Mg in the beads, measured after *aqua regia* digestion, before and after being used in the process. The error bars represent the standard error of the mean of three independent reactors.*Significant difference between beads before and after being used.

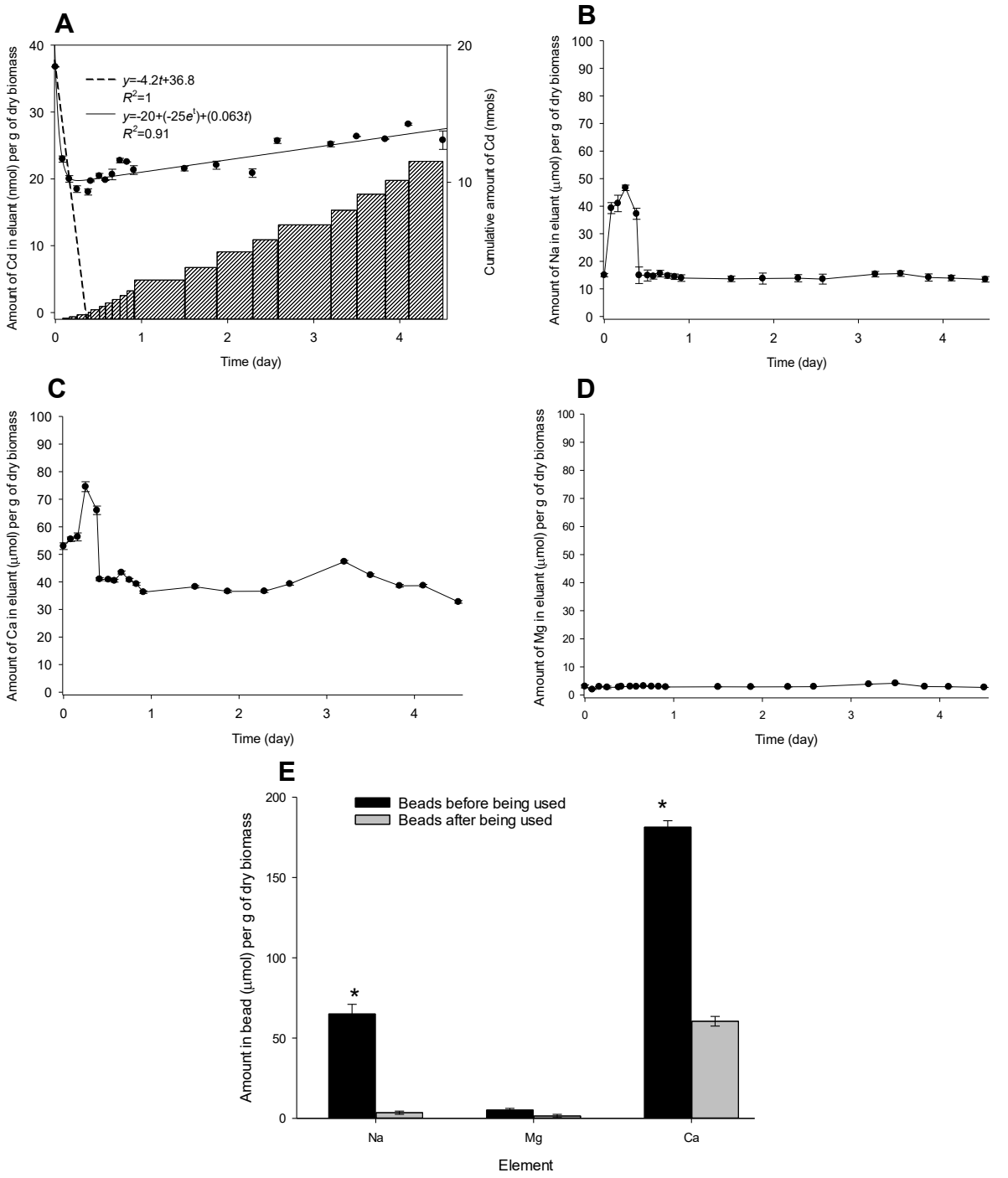

Figure 62. (A) Amounts of the remaining Cd in the AGW and Cd accumulated by Ca-alginate beads containing killed-control cells of *B. agri* C15 Cd^R from 100 mL of AGW with a nominal concentration of 10 µM Cd at pH 7.00, under the effect of 17.5 calcium. Concentrations of **(B)** Na, **(C)** Ca, and **(D)** Mg released from the beads measured in the AGW. **(E)** Respective amounts of Ca, Na, and Mg in the beads, measured after *aqua regia* digestion, before and after being used in the process. The error bars represent the standard error of the mean of three independent reactors. *Significant difference between beads before and after being used.

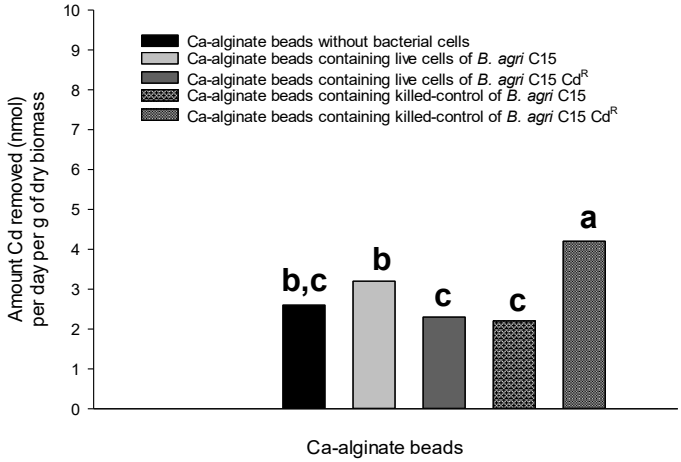

Figure 63. Respective maximum initial rates of Cd removed by the Ca-alginate beads under the effect of 17.5 calcium. The rate of each group was obtained from one tangent line; therefore, error bars are not displayed. The rates were subjected to two-way ANOVA, Tukey *post hoc* test, and a different letter indicates a significant difference in the rates between the groups.

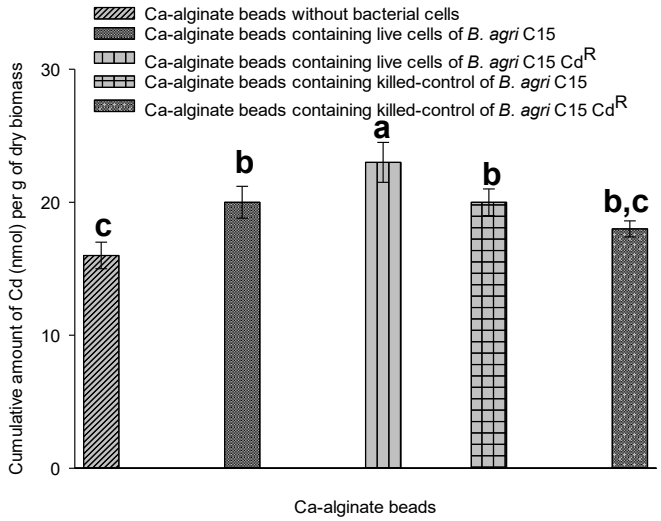

Figure 64. Cumulative amounts of Cd by the beads from AGW under the effect of 17.5 calcium, measured after *aqua regia* digestion. The amounts are the mean, and the error bars represent the standard error of the mean between the reactors (n = 3). The amounts were subjected to two-way ANOVA, Tukey *post hoc* test, and a different letter indicates a significant difference in the amounts between the groups.

To evaluate the effect of anion on the uptake process, the level of phosphate, remaining amounts of Cd in the eluent AGW, and the released amounts of Ca, Na, and Mg from the beads into the AGW was determined (Figures 65, 66, 67, 68 and 69). The removal of the Cd in the presence of phosphate was hindered, indicating that $CdHPO_4$ (Figure 38 C) has a noticeable deleterious effect on Cd removal.

Under the effect of phosphate, the removal rates of Cd (Figure 70) was highest with Ca-alginate beads containing without bacterial cells ($^{b}p<0.05$) or killed-control cells of *B. agri* C15 Cd^R ($^{a}p<0.05$). Overall, the cumulative amounts of Cd measured in the beads ranged from 3 to 20 nmol/g of dry biomass, and the highest accumulation was achieved by Ca-alginate beads without bacterial cells or containing the killed-control cells of *B. agri* C15 Cd^R (Figure 71, $^{a}p<0.05$).

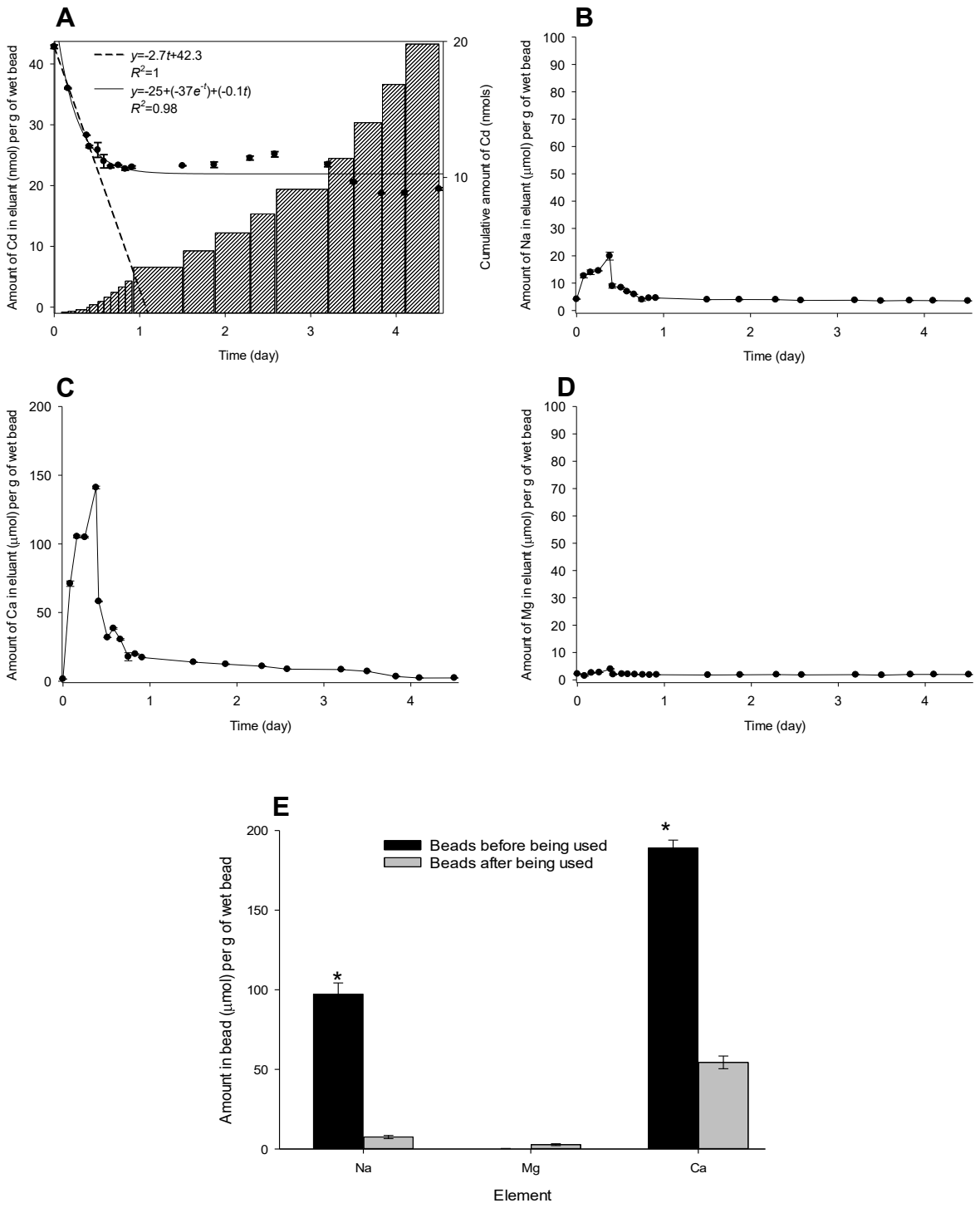

Figure 65. (A) Amounts of the remaining Cd in the AGW and Cd accumulated by Ca-alginate beads without bacterial cells from 100 mL of AGW, with a nominal concentration of 10 µM Cd at pH 7.00, under the effect of 10 mM phosphate. Amounts of **(B)** Na, **(C)** Ca, and **(D)** Mg released from the beads and measured in the AGW. **(E)** Respective amounts of Ca, Na, and Mg in the beads, measured after *aqua regia* digestion, before and after being used in the process. The error bars represent the standard error of the mean of three independent reactors.*Significant difference between beads before and after being used.

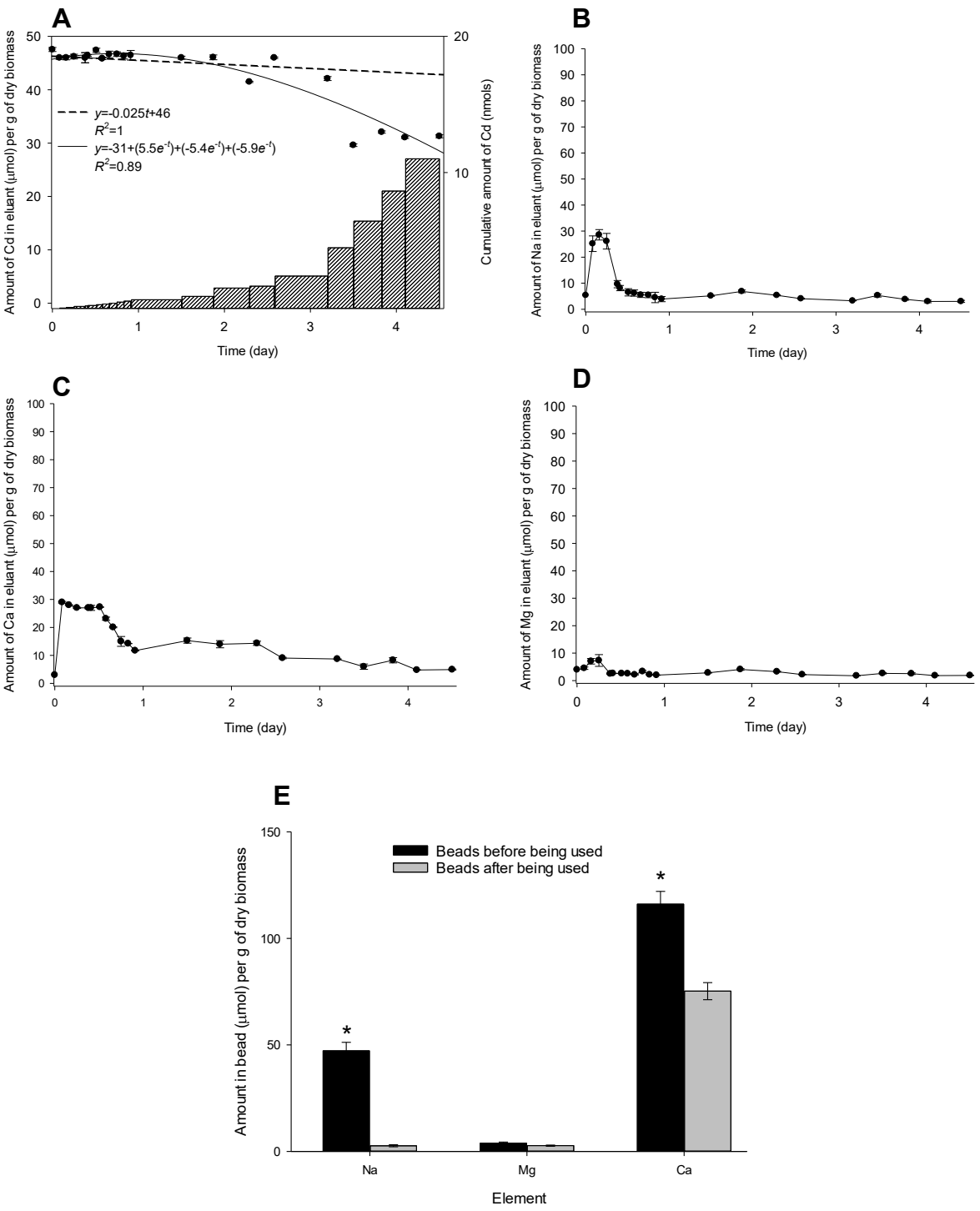

Figure 66. (A) Amounts of the remaining Cd in the AGW and Cd accumulated by Ca-alginate beads containing live cells of *B. agri* C15 from 100 mL of AGW, with a nominal concentration of 10 µM Cd at pH 7.00, under the effect of 10 mM phosphate. Amounts of **(B)** Na, **(C)** Ca, and **(D)** Mg released from the beads and measured in the AGW. **(E)** Respective amounts of Ca, Na, and Mg in the beads, measured after *aqua regia* digestion, before and after being used in the process. The error bars represent the standard error of the mean of three independent reactors.*Significant difference between beads before and after being used.

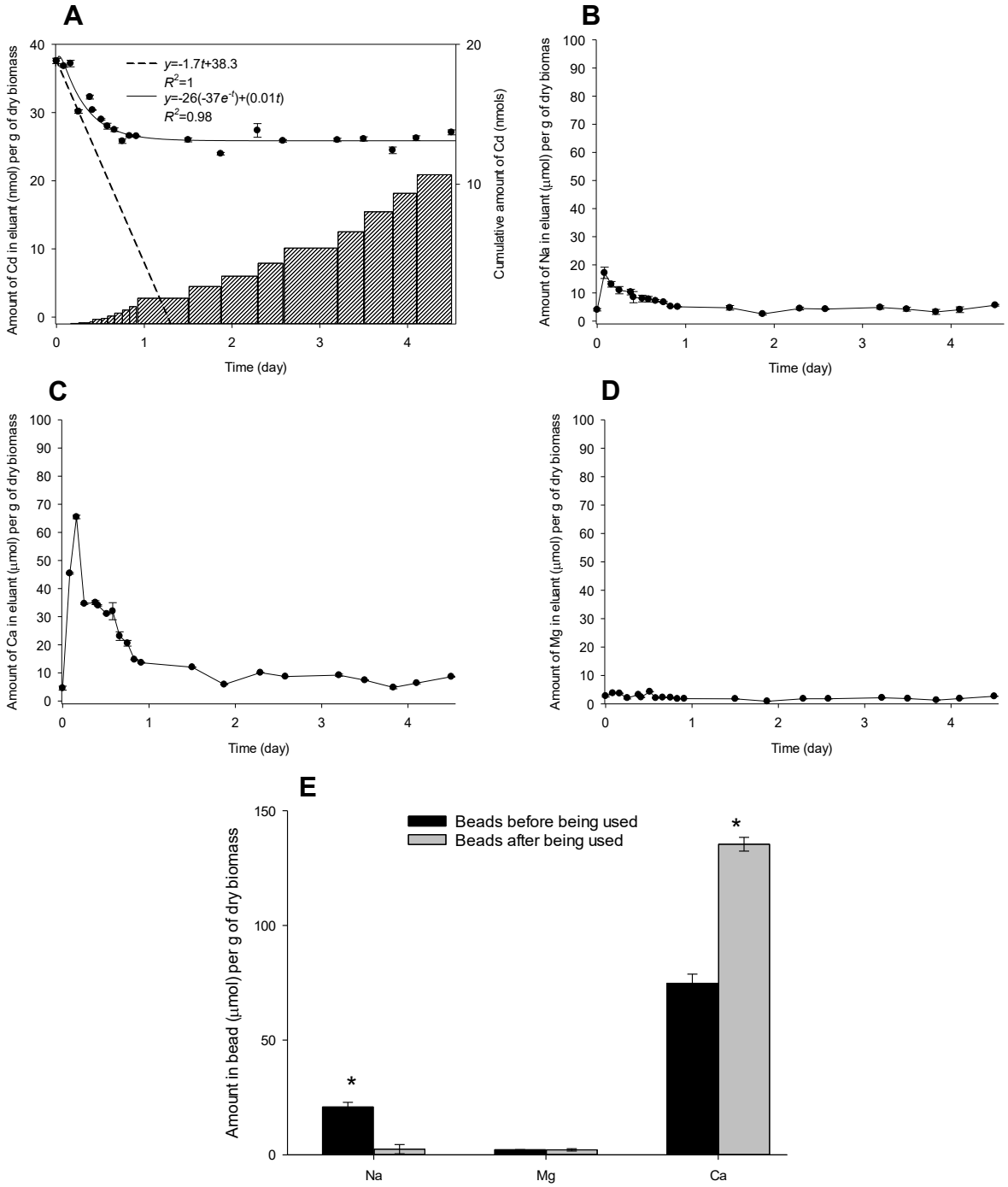

Figure 67. (A) Amounts of the remaining Cd in the AGW and Cd accumulated by Ca-alginate beads containing live cells of *B. agri* C15 Cd^R from 100 mL of AGW, with a nominal concentration of 10 µM Cd at pH 7.00, under the effect of 10 mM phosphate. Amounts of **(B)** Na, **(C)** Ca, and **(D)** Mg released from the beads and measured in the AGW. **(E)** Respective amounts of Ca, Na, and Mg in the beads, measured after *aqua regia* digestion, before and after being used in the process. The error bars represent the standard error of the mean of three independent reactors. *Significant difference between beads before and after being used.

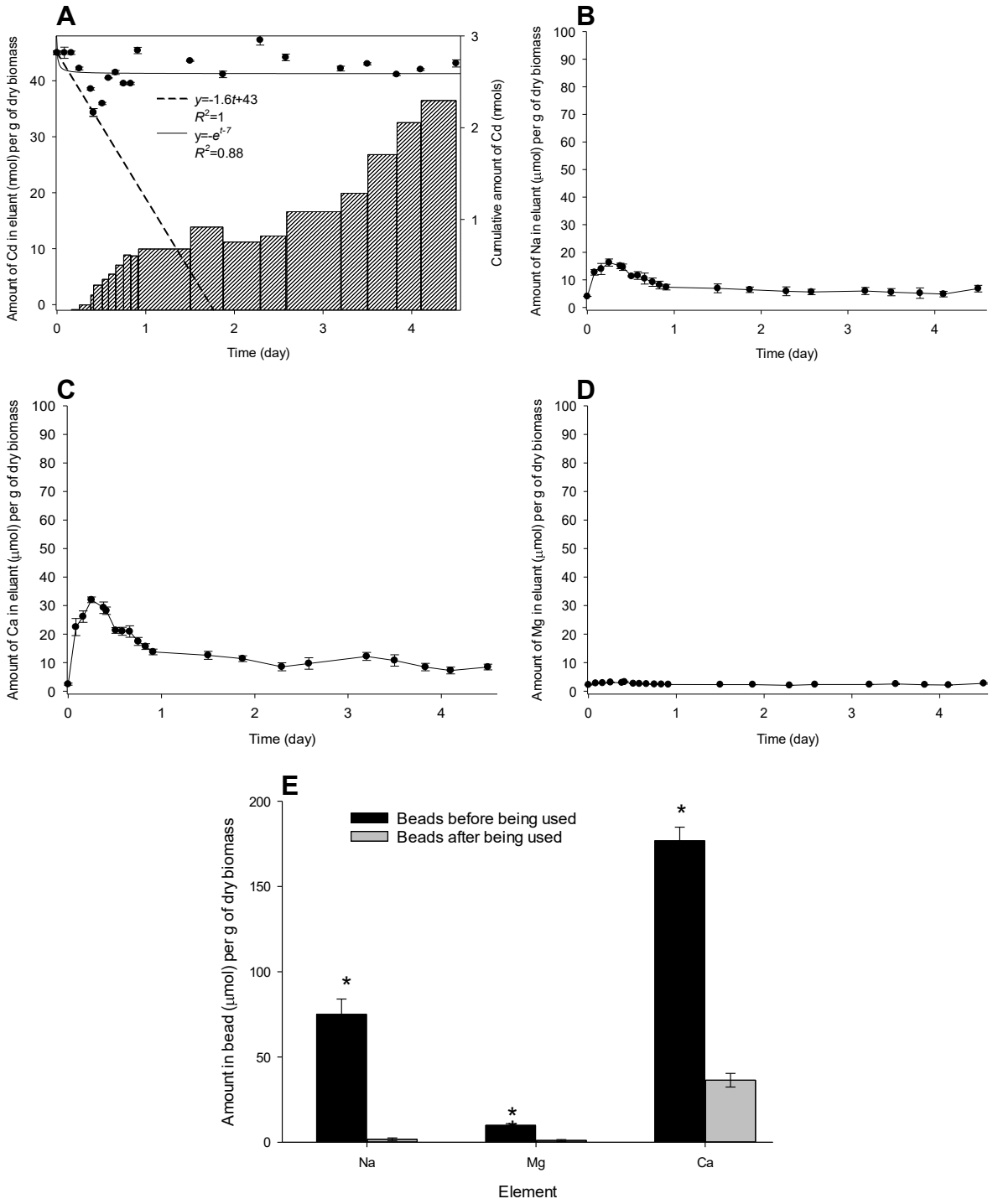

Figure 68. (A) Amounts of the remaining Cd in the AGW and Cd accumulated by Ca-alginate beads containing killed-control cells of *B. agri* C15 from 100 mL of AGW, with a nominal concentration of 10 µM Cd at pH 7.00, under the effect of 10 mM phosphate. Amounts of **(B)** Na, **(C)** Ca, and **(D)** Mg released from the beads and measured in the AGW. **(E)** Respective amounts of Ca, Na, and Mg in the beads, measured after *aqua regia* digestion, before and after being used in the process. The error bars represent the standard error of the mean of three independent reactors.*Significant difference between beads before and after being used.

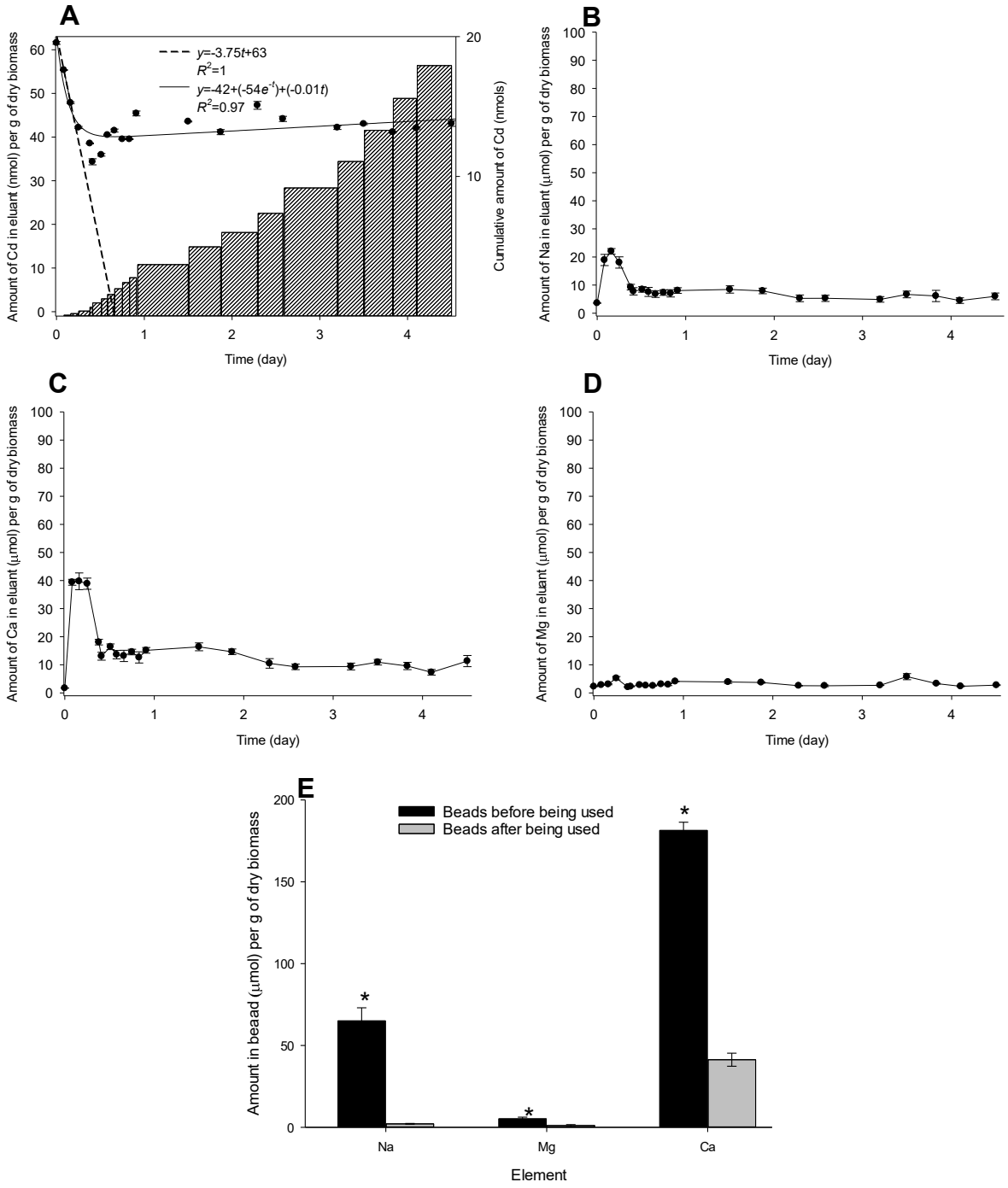

Figure 69. (A) Amounts of the remaining Cd in the AGW and Cd accumulated by Ca-alginate beads containing killed-control cells of *B. agri* C15 Cd^R from 100 mL of AGW, with a concentration of 10 µM of Cd at pH 7.00, under the effect of 10 mM phosphate. Amounts of **(B)** Na, **(C)** Ca, and **(D)** Mg released from the beads and measured in the AGW. **(E)** Respective amounts of Ca, Na, and Mg in the beads, measured after *aqua regia* digestion, before and after being used in the process. The error bars represent the standard error of the mean of three independent reactors.*Significant difference between beads before and after being used.

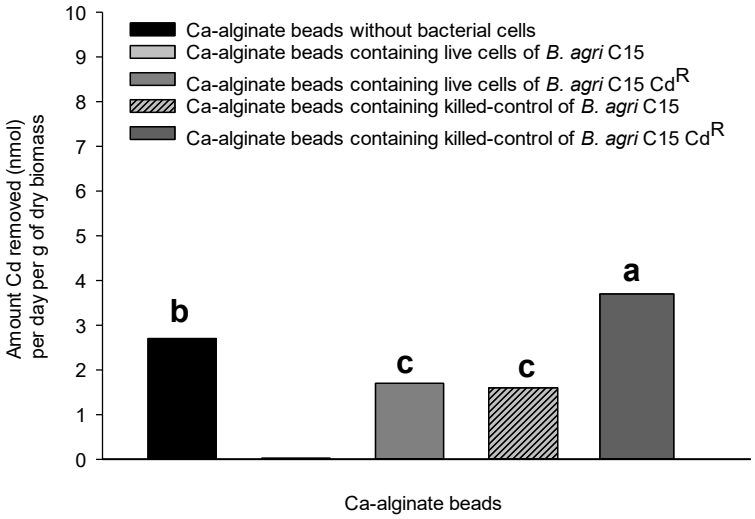

Figure 70. Respective maximum initial rates of Cd removed under the effect of 10 mM phosphate by the Ca-alginate beads. The rate of each group was obtained from one tangent line; therefore, error bars are not displayed. The rates were subjected to two-way ANOVA, Tukey *post hoc* test, and a different letter indicates a significant difference in the rates between the groups.

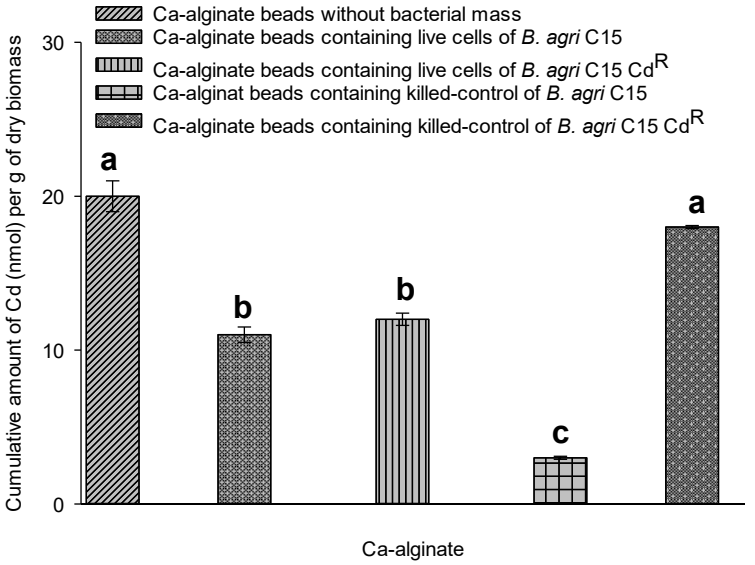

Figure 71. Cumulative amounts of Cd by the beads from AGW under the effect of 10 mM phosphate, measured after *aqua regia* digestion. The amounts are the mean, and the error bars represent the standard error of the mean between the reactors (n = 3). The amounts were subjected to two-way ANOVA, Tukey *post hoc* test, and a different letter indicates a significant difference in the amounts between the groups.

5-3-5 Effects of humic acid in AGW on the cadmium removal

To investigate the Cd uptake under the effect of organic matter, humic acid was added to AGW at pH 7.00. The adsorption of Cd by humic acid was observed as the amounts of Cd at zero time showed within an average of 24 nmol per g of dry biomass, which is lower than the amounts of Cd at zero time recorded in previous experiments (see results section 5-3-2). It was determined that there were reductions in the amounts of Cd from AGW by all beads, but their responses were different (Figures 72, 73, 74, 75, 76). Ca-alginate beads containing live cells of *B. agri* C15 or *B. agri* C15 Cd^R reduced the amounts of Cd within the first few hours of operating the reactor (Figures 73, 74, 75). However, Ca-alginate beads without bacterial cells or containing killed-control cells of *B. agri* C15 or *B. agri* C15 Cd^R initially showed the slow removal of Cd (Figures 72, 75, 76).

The released amounts of Na, Ca, and Mg into the AGW were higher than the amounts obtained without adding the humic acid (see results section 5-3-2). The released amounts were up to 230 μmol per g of dry biomass for Ca and 180 μmol per g of dry biomass for Na. The amounts of these elements in the beads before and after adding the humic acid in this process were similar to the amounts found in the previous experiments (see results section 5-3-2).

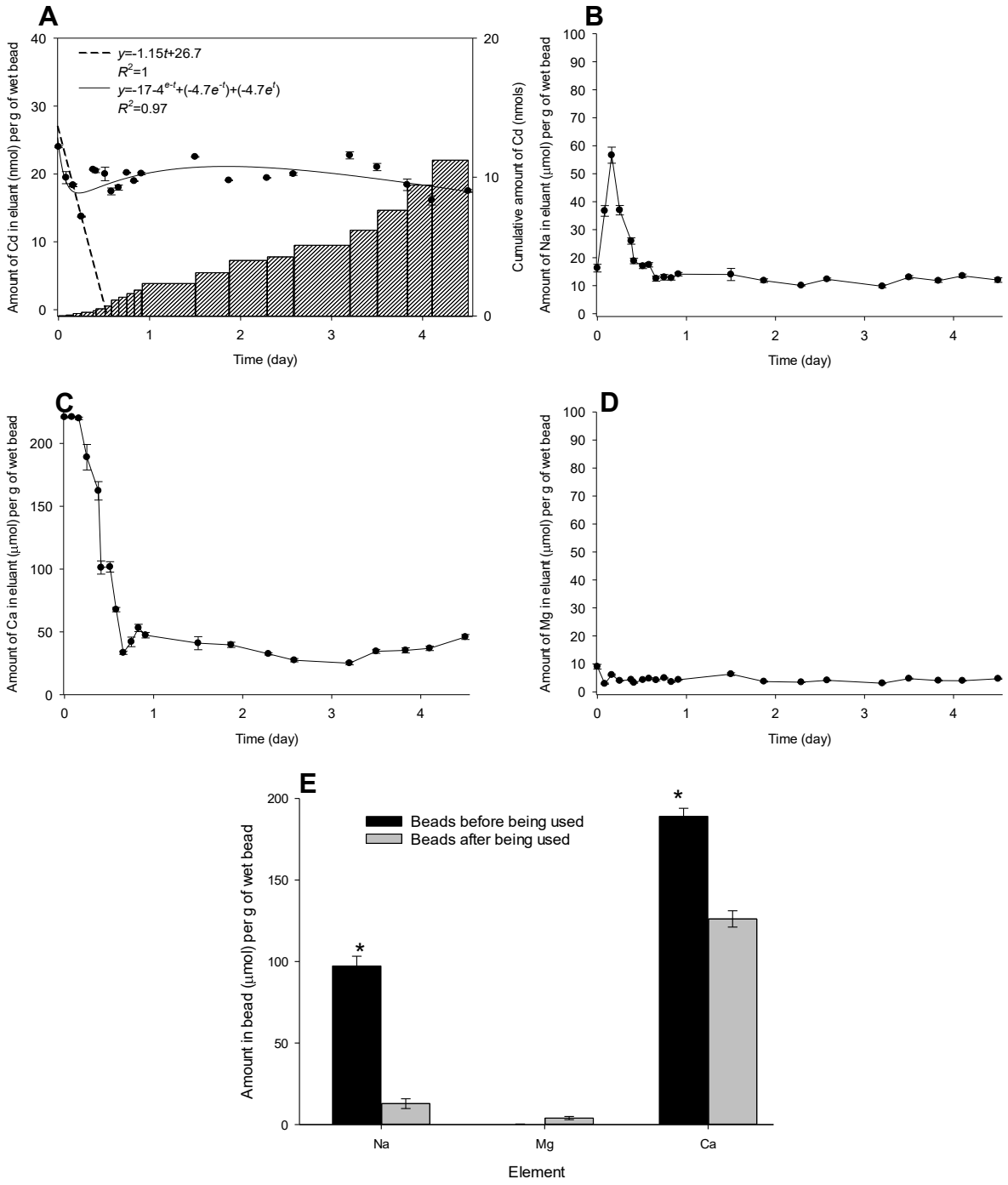

Figure 72. (A) Amounts of the remaining Cd in the AGW and Cd accumulated by Ca-alginate beads without bacterial cells from 100 mL of AGW, with a nominal concentration of 10 µM Cd at pH 7.00, under the effect of humic acid (10 mg/L). Amounts of **(B)** Na, **(C)** Ca, and **(D)** Mg released from the beads and measured in the AGW. **(E)** Respective amounts of Ca, Na, and Mg in the beads, measured after *aqua regia* digestion, before and after being used in the process. The error bars represent the standard error of the mean of three independent reactors. *Significant difference between beads before and after being used.

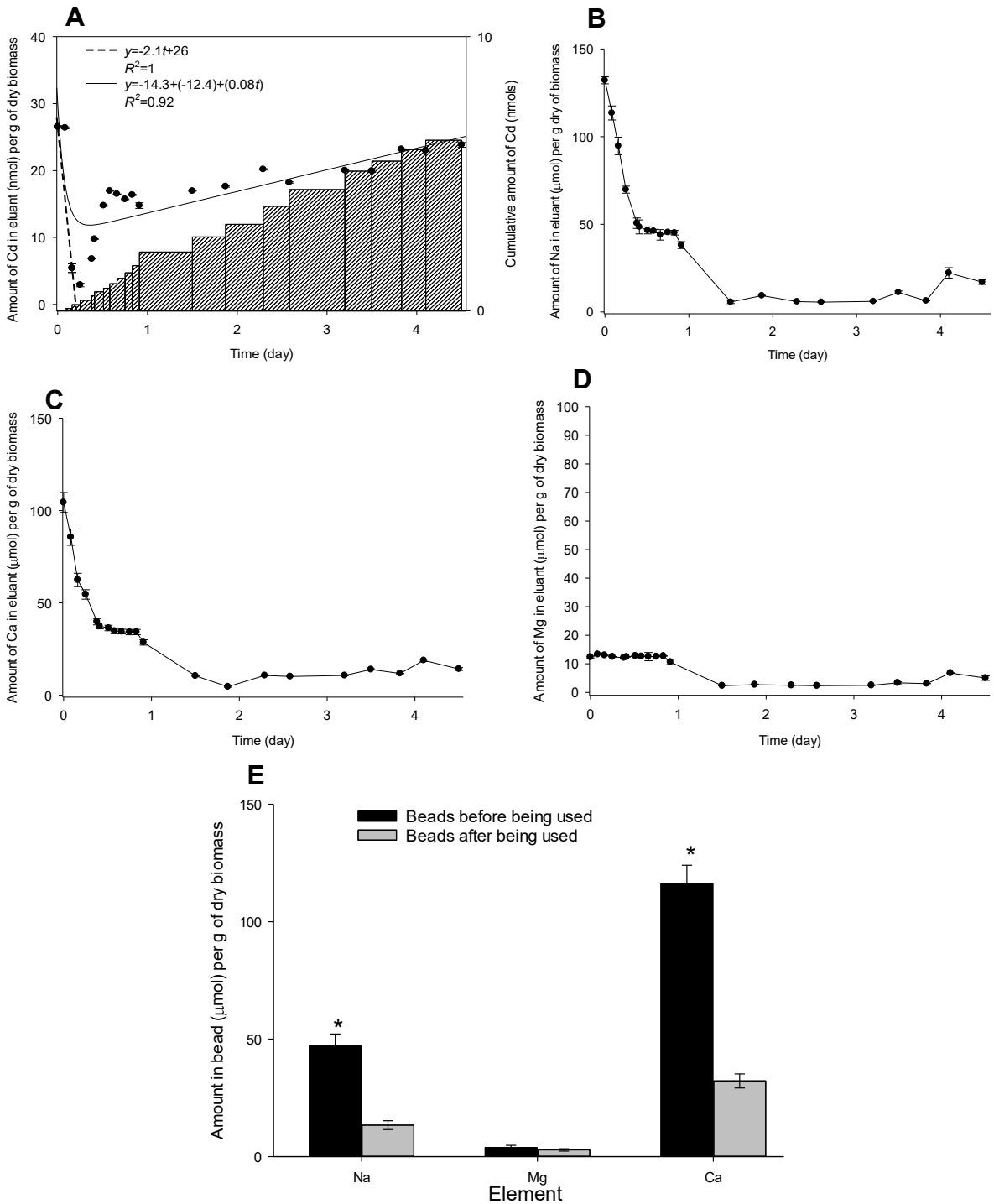

Figure 73. **(A)** Amounts of the remaining Cd in the AGW and Cd accumulated by Ca-alginate beads containing live cells of *B. agri* C15 from 100 mL of AGW with a nominal concentration of 10 µM Cd at pH 7.00, under the effect of humic acid (10 mg/L). Amounts of **(B)** Na, **(C)** Ca, and **(D)** Mg released from the beads and measured in the AGW. **(E)** Respective amounts of Ca, Na, and Mg in the beads, measured after *aqua regia* digestion, before and after being used in the process. The error bars represent the standard error of the mean of three independent reactors.*Significant difference between beads before and after being used.

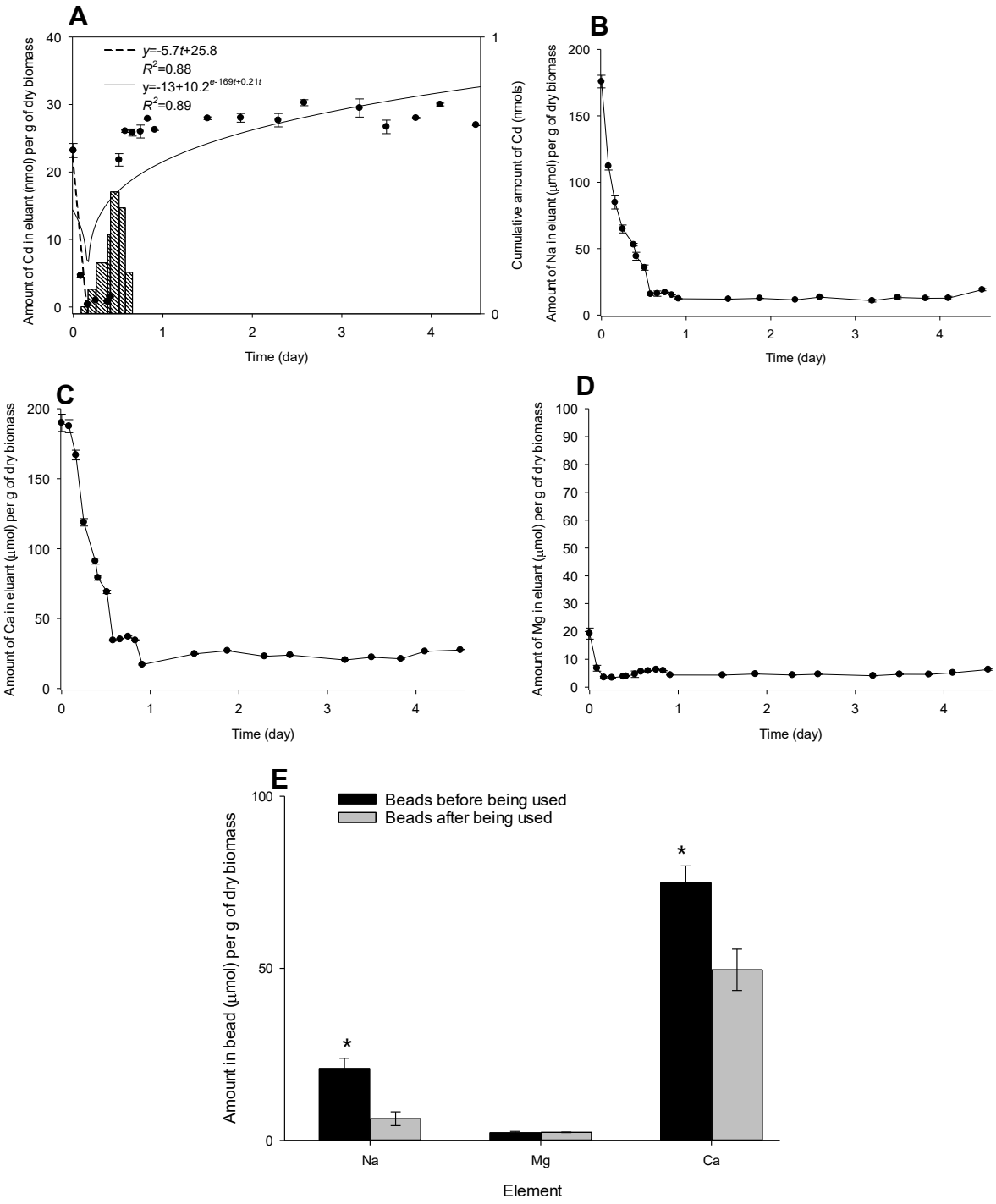

Figure 74. **(A)** Amounts of the remaining Cd in the AGW and Cd accumulated by Ca-alginate beads containing live cells of *B. agri* C15 Cd^R from 100 mL of AGW, with a nominal concentration of 10 µM Cd at pH 7.00, under the effect of humic acid (10 mg/L). Amounts of **(B)** Na, **(C)** Ca, and **(D)** Mg released from the beads and measured in the AGW. **(E)** Respective amounts of Ca, Na, and Mg in the beads, measured after *aqua regia* digestion, before and after being used in the process. The error bars represent the standard error of the mean of three independent reactors. *Significant difference between beads before and after being used.

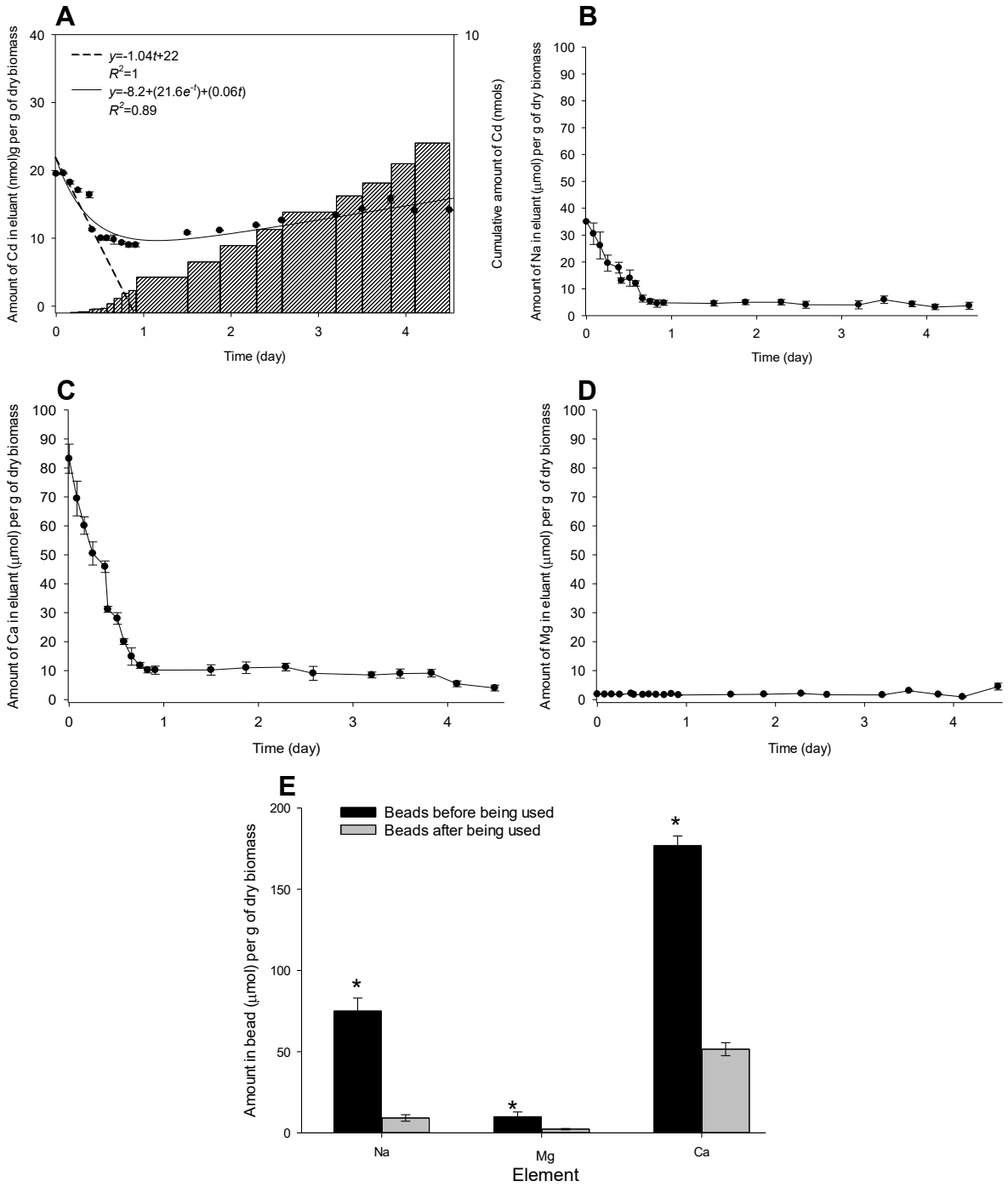

Figure 75. (A) Amounts of the remaining Cd in the AGW and Cd accumulated by Ca-alginate beads containing killed-control cells of *B. agri* C15 from 100 mL of AGW, with a nominal concentration of 10 µM Cd at pH 7.00, under the effect of humic acid (10 mg/L). Amounts of **(B)** Na, **(C)** Ca, and **(D)** Mg released from the beads and measured in the AGW. **(E)** Respective amounts of Ca, Na, and Mg in the beads, measured after *aqua regia* digestion, before and after being used in the process. The error bars represent the standard error of the mean of three independent reactors. *Significant difference between beads before and after being used.

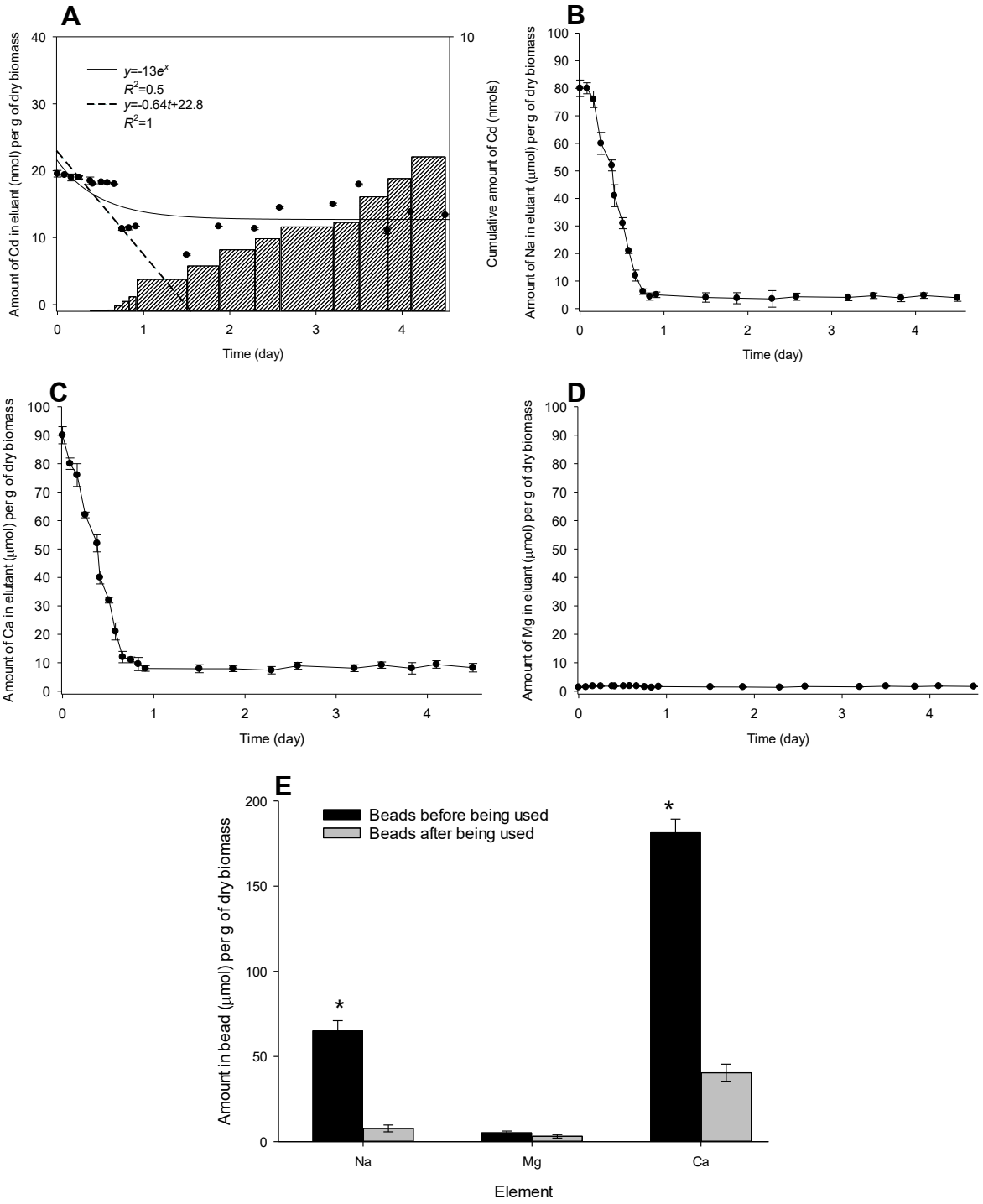

Figure 76. (A) Amounts of the remaining Cd in the AGW and Cd accumulated by Ca-alginate beads containing killed-control cells of *B. agri* C15 Cd^R from 100 mL of AGW, with a nominal concentration of 10 µM Cd at pH 7.00, under the effect of humic acid (10 mg/L). Amounts of **(B)** Na, **(C)** Ca, and **(D)** Mg released from the beads and measured in the AGW. **(E)** Respective amounts of Ca, Na, and Mg in the beads, measured after *aqua regia* digestion, before and after being used in the process. The error bars represent the standard error of the mean of three independent reactors. *Significant difference between beads before and after being used.

The removal rates of Cd by the beads from AGW under the effect of humic acid were obtained (Figure 77), and Ca-alginate beads containing live cells of *B. agri* C15 Cd^R showed a significant removal rate of Cd ($^a p<0.05$) compared to other beads.

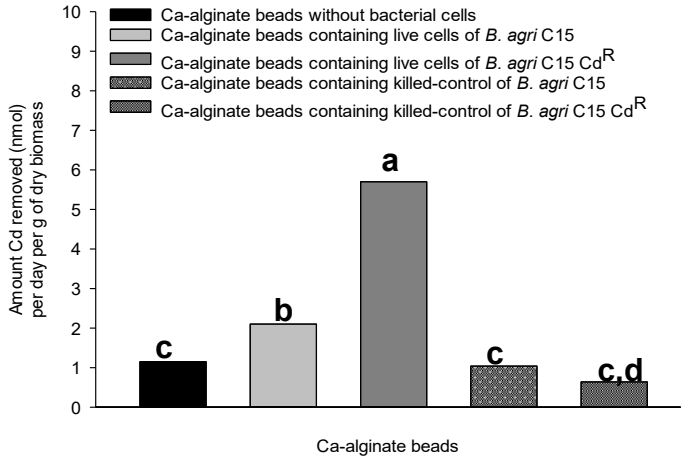

Figure 77. Respective maximum initial rates of Cd removed under the effect of humic acid (10 mg/L). The rate of each group was obtained from one tangent line; therefore, error bars are not displayed. The rates were subjected to two-way ANOVA, Tukey *post hoc* test, and a different letter indicates a significant difference in the rates between the groups.

The effect of humic acid on the accumulation of Cd in the beads was obtained by measuring the concentrations of Cd in the beads after *aqua regia* digestion (Figure 78). Under this effect, the Ca-alginate beads without bacterial cells ($^a p<0.05$), or containing killed-control cells of *B. agri* C15 ($^c p<0.05$) or *B. agri* C15 Cd^R ($^b p<0.05$), showed significantly higher cumulative amounts of Cd than those containing live cells.

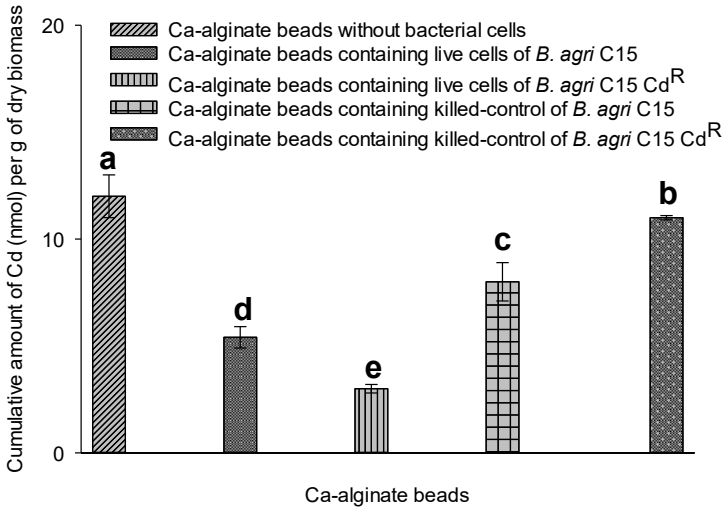

Figure 78. Cumulative amounts of Cd by the beads from AGW under the effect of the humic acid (10 mg/L), measured after *aqua regia* digestion. The amounts are the mean, and the error bars represent the standard error of the mean between the reactors (n = 3). The amounts were subjected to two-way ANOVA, Tukey *post hoc* test, and a different letter indicates a significant difference in the amounts between the groups.

5-3-6 Cadmium removal from NRW

The Cd removal from NRW was carried out, as shown in Figures 79, 80, 81, 82, 83. The beads accumulated Cd, as there were reductions in the amounts of Cd in the NRW, and their response was slightly different. The released amounts of Na and Ca into the NRW were higher than the amounts into AGW (as shown in section 5-3-3). The released amounts were up to 120 per g of dry biomass for Ca and 80 per g of dry biomass μmol per g of dry biomass for Na. The amounts of these elements in the beads before and after being used in this process showed similar released amounts to those from AGW (as shown in section 5-3-3).

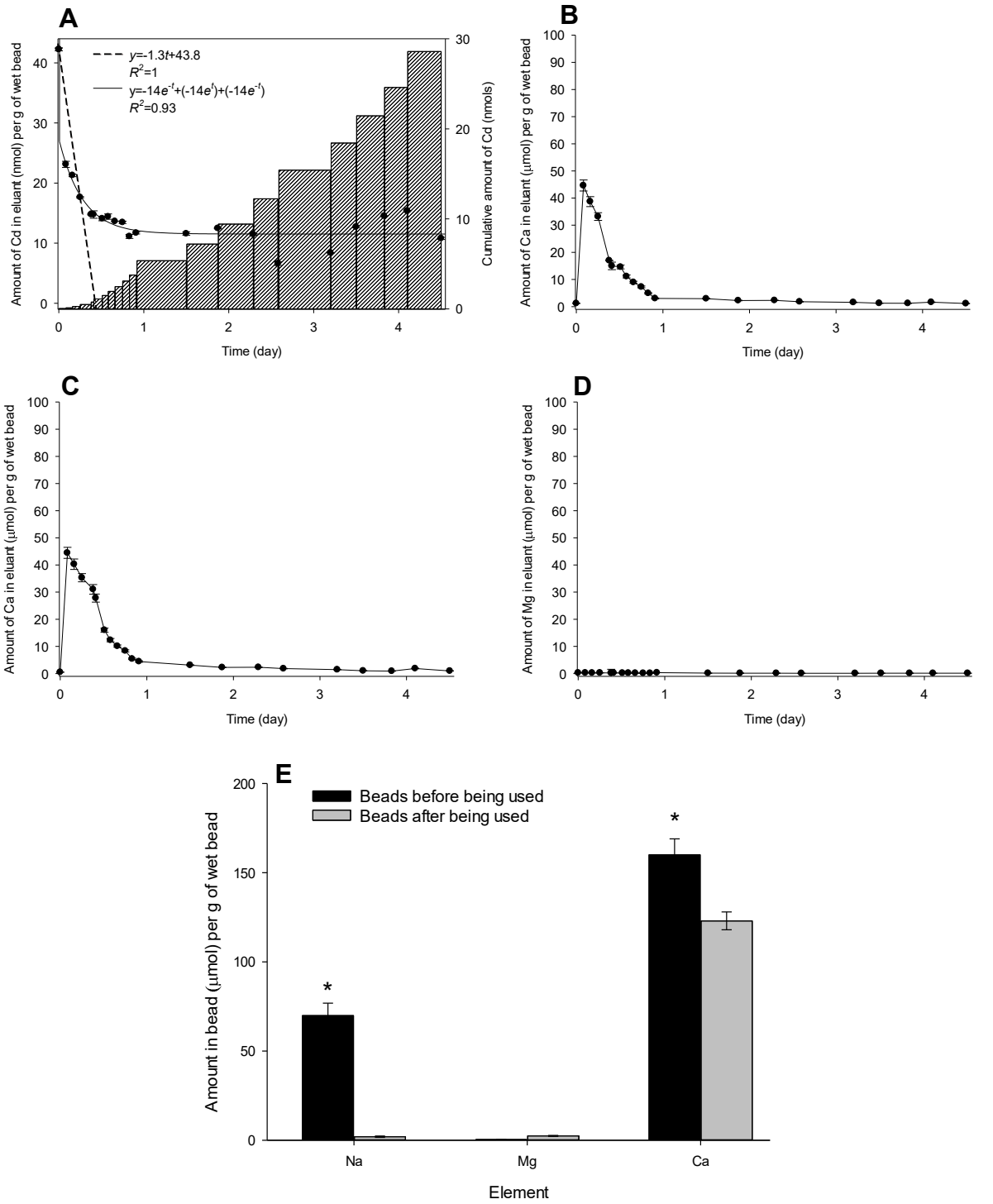

Figure 79. **(A)** Amounts of the remaining Cd in the NRW and Cd accumulated by Ca-alginate beads without bacterial cells from 100 mL of NRW, with a nominal concentration of 10 µM Cd. Amounts of **(B)** Na, **(C)** Ca, and **(D)** Mg released from the beads measured in the NRW. **(E)** Respective amounts of Ca, Na, and Mg in the beads, measured after *aqua regia* digestion, before and after being used in the process. The error bars represent the standard error of the mean of three independent reactors. *Significant difference between beads before and after being used.

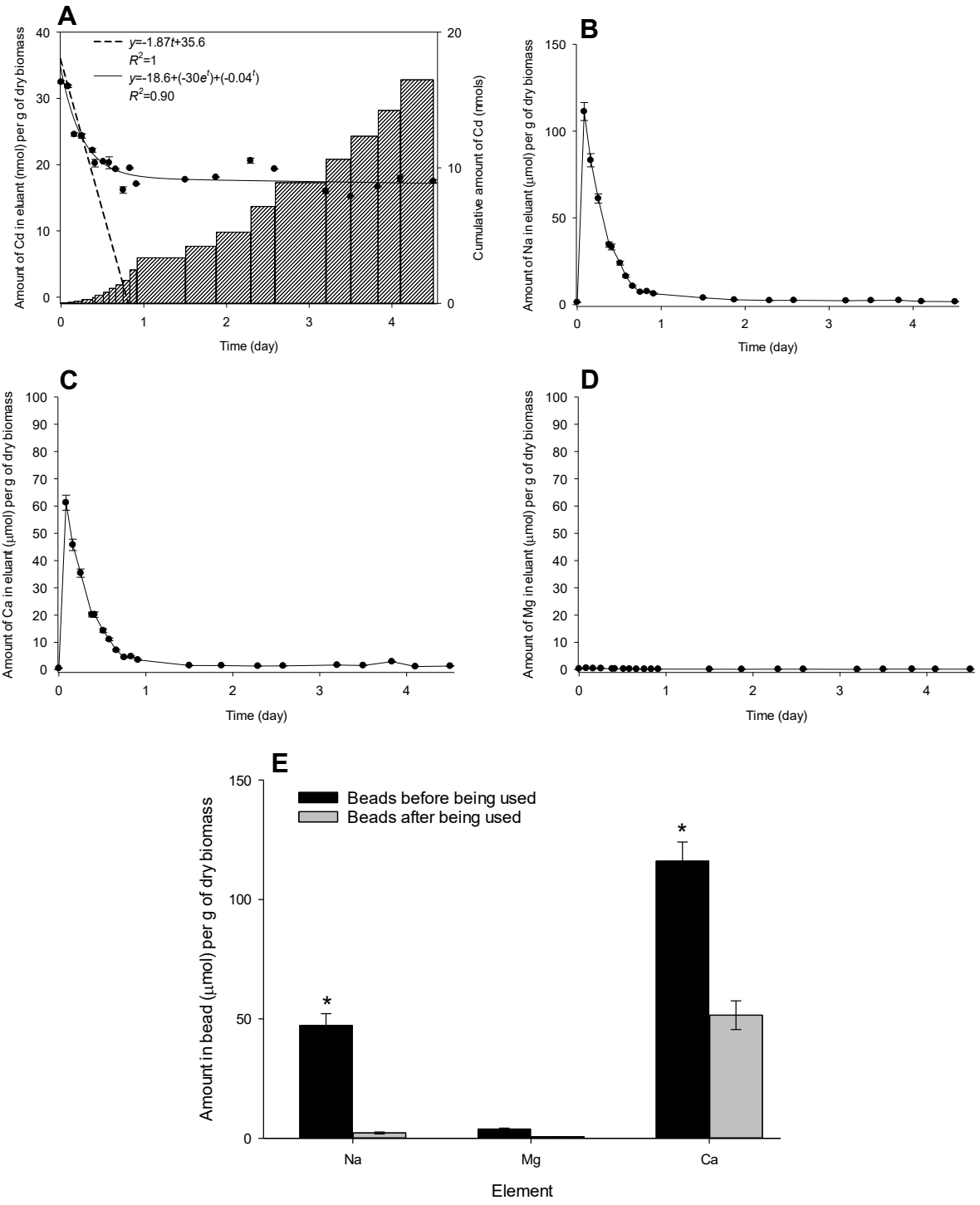

Figure 80. (A) Amounts of the remaining Cd in the NRW and Cd accumulated by Ca-alginate beads containing live cells of *B. agri* C15 from 100 mL of NRW, with a nominal concentration of 10 µM Cd. Amounts of **(B)** Na, **(C)** Ca, and **(D)** Mg released from the beads measured in the NRW. **(E)** Respective amounts of Ca, Na, and Mg in the beads, measured after *aqua regia* digestion, before and after being used in the process. The error bars represent the standard error of the mean of three independent reactors. *Significant difference between beads before and after being used.

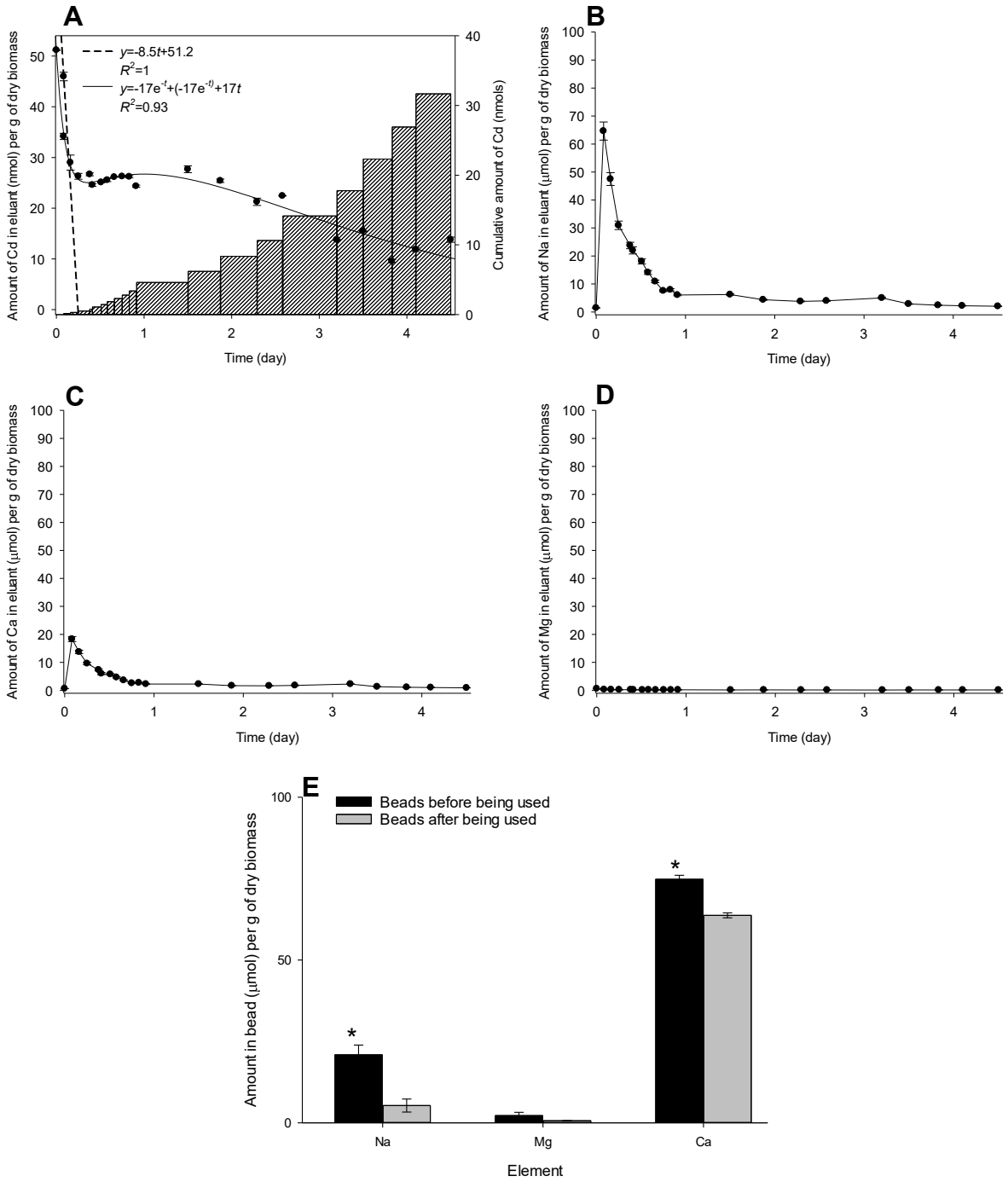

Figure 81. (A) Amounts of the remaining Cd in the NRW and Cd accumulated by Ca-alginate beads containing live *B. agri* C15 Cd^R from 100 mL of NRW, with a nominal concentration of 10 µM Cd. Amounts of **(B)** Na, **(C)** Ca, and **(D)** Mg released from the beads measured in the NRW. **(E)** Respective amounts of Ca, Na, and Mg in the beads, measured after *aqua regia* digestion, before and after being used in the process. The error bars represent the standard error of the mean of three independent reactors. *Significant difference between beads before and after being used.

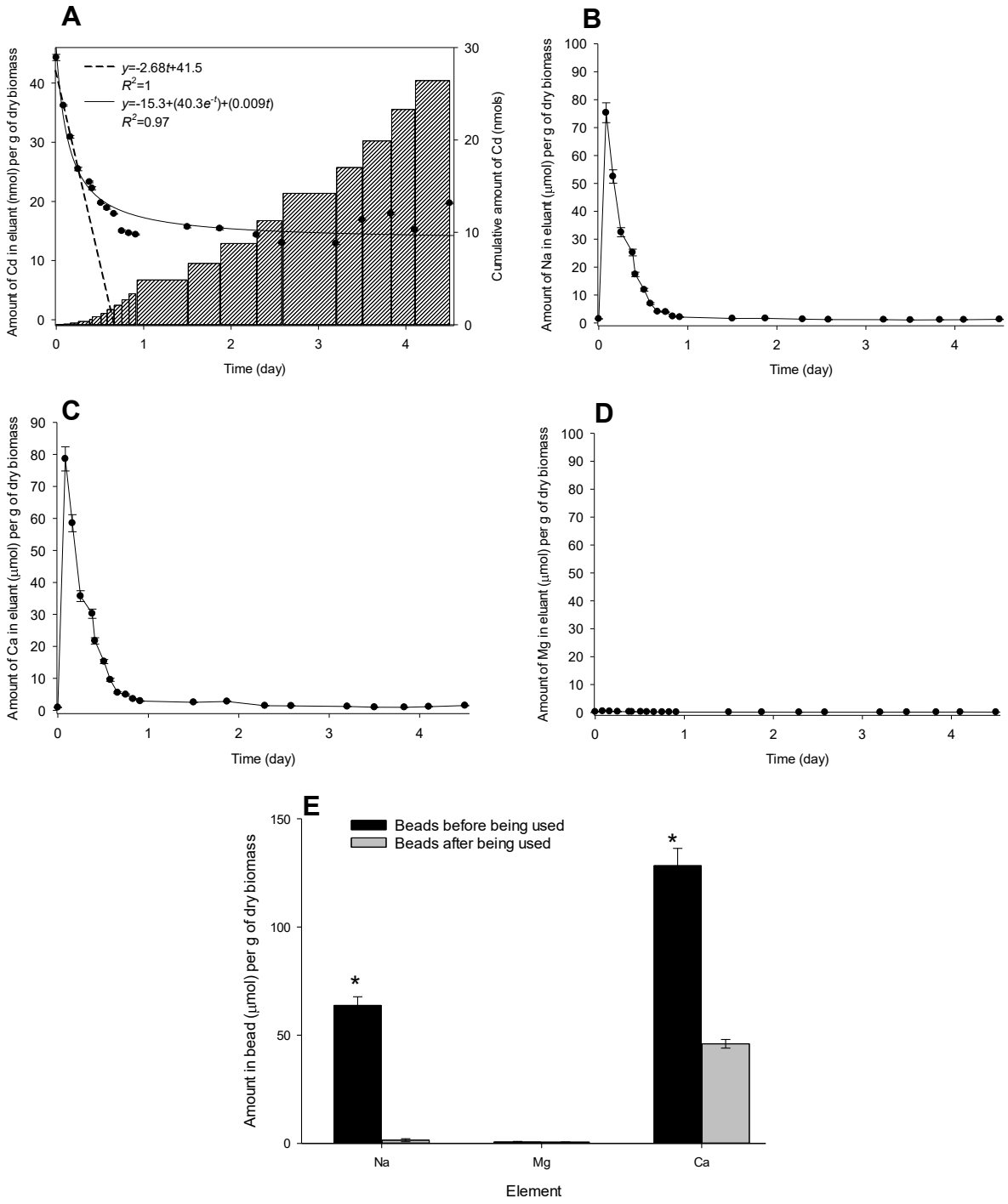

Figure 82. (A) Amounts of the remaining Cd in the NRW and Cd accumulated by Ca-alginate beads containing killed-control cells of *B. agri* C15 from 100 mL of NRW, with a nominal concentration of 10 µM Cd. Amounts of **(B)** Na, **(C)** Ca, and **(D)** Mg released from the beads measured in the NRW. **(E)** Respective amounts of Ca, Na, and Mg in the beads, measured after *aqua regia* digestion, before and after being used in the process. The error bars represent the standard error of the mean of three independent reactors.*Significant difference between beads before and after being used.

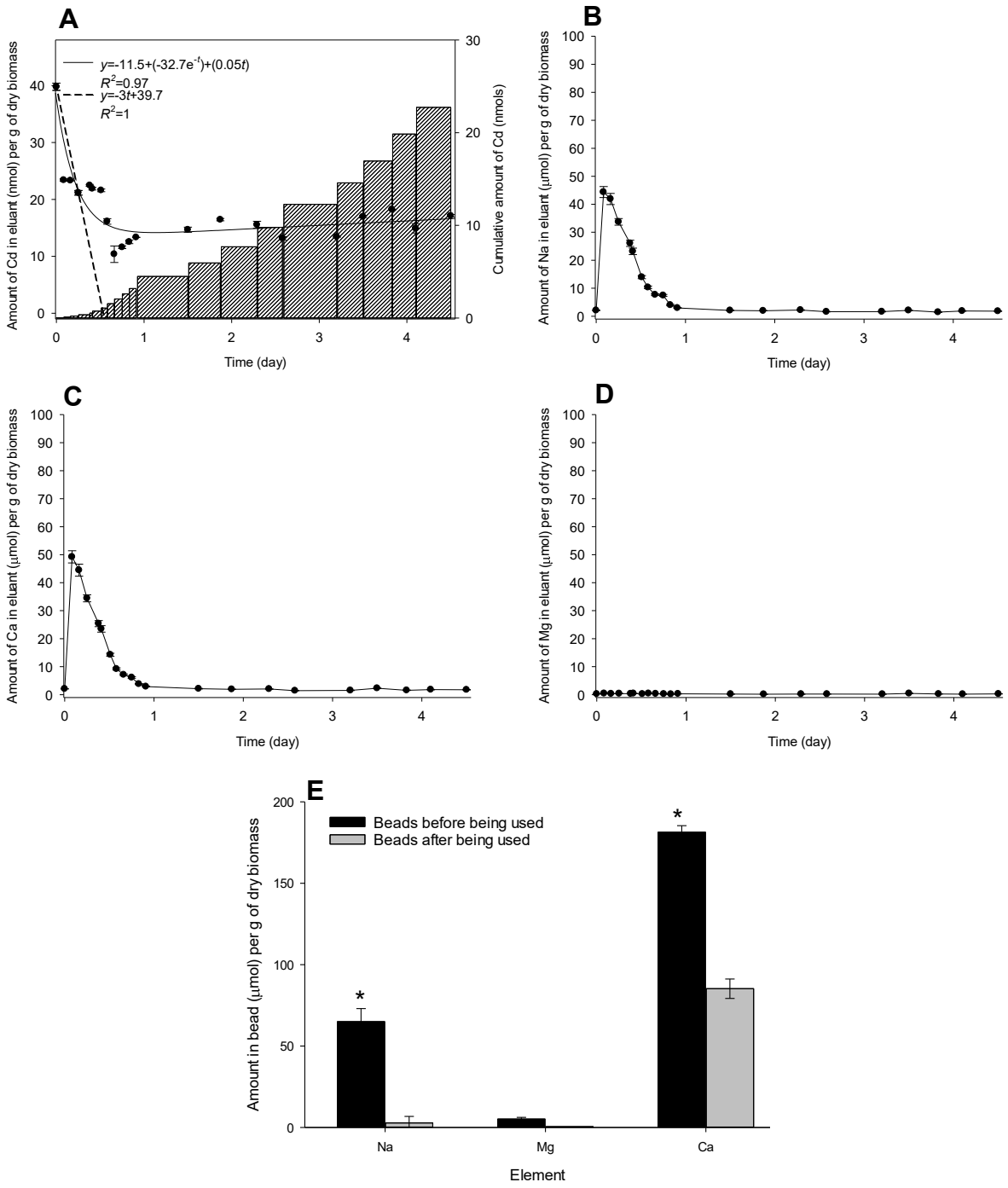

Figure 83. (A) Amounts of the remaining Cd in the NRW and Cd accumulated by Ca-alginate beads containing killed-control cells of *B. agri* C15 Cd^R from 100 mL of NRW, with a nominal concentration of 10 µM Cd. Amounts of **(B)** Na, **(C)** Ca, and **(D)** Mg released from the beads measured in the NRW. **(E)** Respective amounts of Ca, Na, and Mg in the beads, measured after *aqua regia* digestion, before and after being used in the process. The error bars represent the standard error of the mean of three independent reactors.*Significant difference between beads before and after being used.

The removal rates of Cd from NRW by the beads were achieved (Figure 84), and Ca-containing live cells of *B. agri* C15 Cd^R showed significantly higher rates ($^a p<0.05$), compared to the other beads. The cumulative amounts of Cd from NRW in the (Figure 85) were significantly higher ($^a p<0.05$) in the Ca-alginate beads containing live cells of *B. agri* C15 Cd^R.

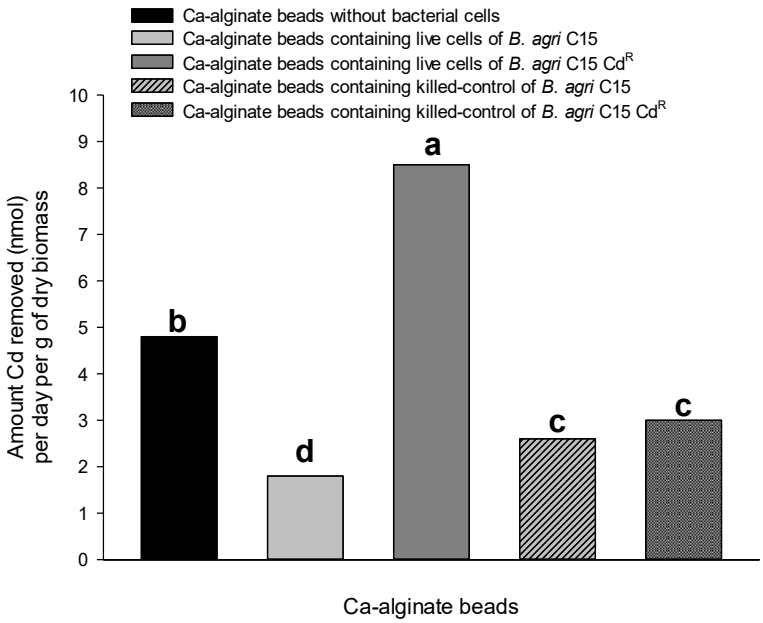

Figure 84. Respective maximum initial rates of Cd removed by the beads from NRW. The rate of each group was obtained from one tangent line; therefore, error bars are not displayed. The rates were subjected to two-way ANOVA, Tukey *post hoc* test, and a different letter indicates a significant difference between the groups.

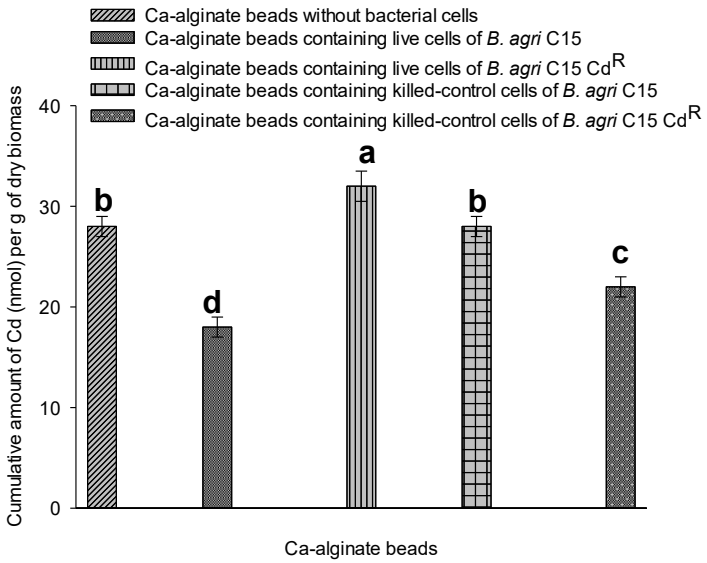

Figure 85. Cumulative amounts of Cd by the beads from NRW. The amounts are the mean, and the error bars represent the standard error of the mean of three independent reactors. The amounts were subjected to two-way ANOVA, Tukey *post hoc* test, and a different letter indicates a significant difference between the groups.

The summarised uptake rates of Cd by all Ca-alginate beads under a different matrix showed that each bead responds differently (Figure 86). The effects of cation/anion and humic acid were apparent on the majority of the beads. The rate of Cd uptake from AGW showed different amounts by all of the beads. The highest uptake was obtained by Ca-alginate beads containing live cells of *B. agri* C15 Cd^R from AGW at pH 4.00 (9.6 nmol per day per g of dry biomass) and NRW (8.9 nmol per day per g of dry biomass) (Figure 86C, $^a p<0.05$).

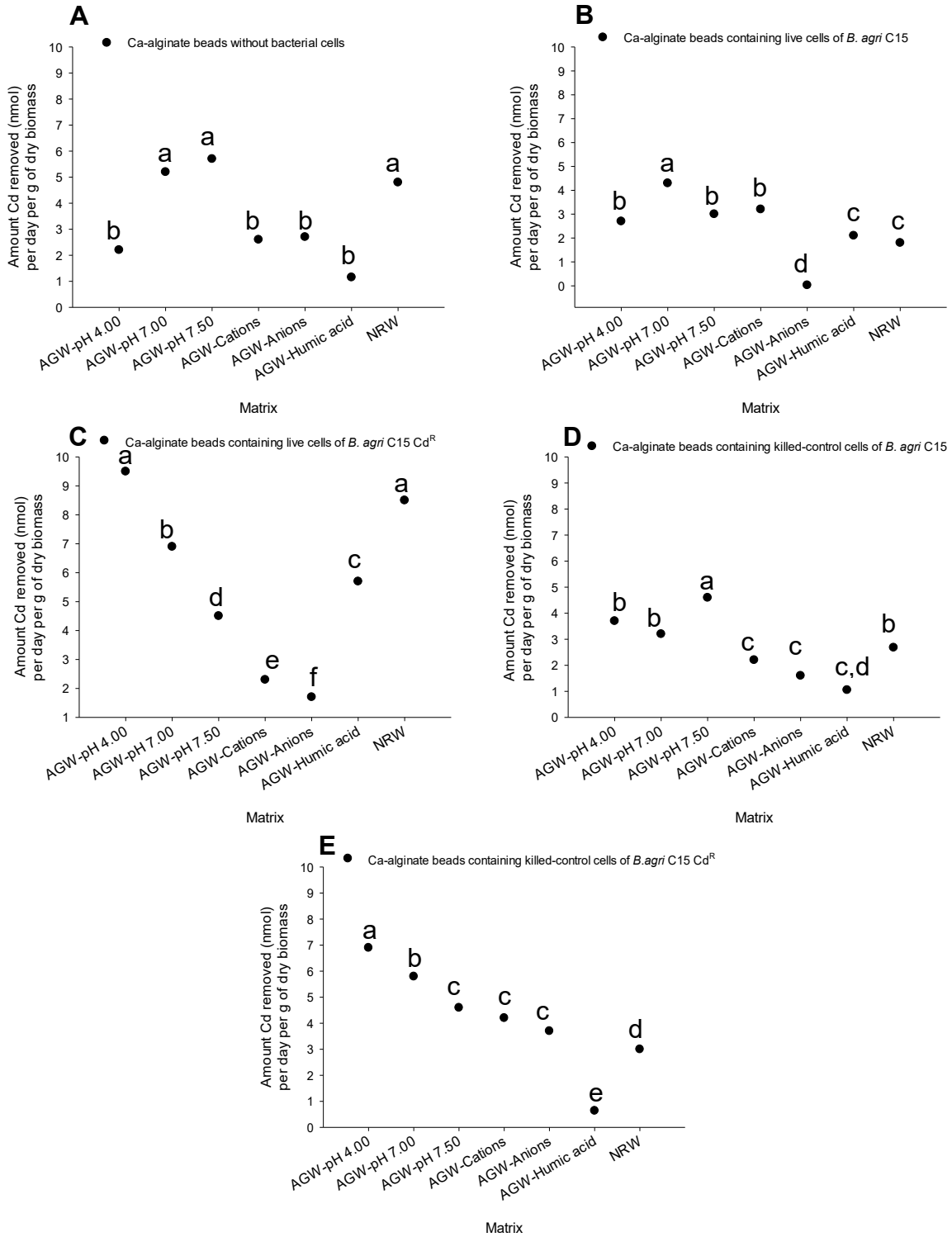

Figure 86. The uptake rates of Cd by all the beads under different matrix. **(A)** Ca-alginate beads without bacterial cells, Ca-alginate beads containing live cells of **(B)** *B. agri* C15, and **(C)** *B. agri* C15 Cd^R or containing killed-control cells of **(D)** *B. agri* C15 and **(E)** *B. agri* C15 Cd^R. The rate of each group was obtained from one tangent line; therefore, error bars are not displayed. The rates were subjected to two-way ANOVA, Tukey *post hoc* test, and a different letter indicates a significant difference between the groups.

5-3-7 Hazard classification of the cadmium-loaded bead

The amounts of Cd, which accumulated in all types of Ca-alginate beads, were used to quantify their hazards. Escudero *et al.* (2009) classified the As-loaded sorbent after obtaining the removal process, according to US EPA (1999). US EPA established that the waste extract is considered non-hazardous if the concentration of extracted metal does not exceed 100 times the Maximum Contaminant Level (MCL) in drinking water. MCL of Cd in drinking water is 5 μg/L. According to the cumulative amounts of Cd obtained from all experiments in this study (Figures 57, 64, 78, 85), the highest amount was 67 nmol per g of dry biomass, which was extracted using Ca-alginate beads containing live cells of *B. agri* C15 Cd^R from AGW at pH 4.00 (Figure 57 C). This amount was used for evaluating the hazard per weight. The assessment revealed that Cd extracted concentration was below the standards of 100 times the MCL.

5-4 Discussion

Ca-alginate beads containing bacterial cells have been extensively used to remove cadmium from water or wastewater (Krystyna, 2019). Since this a biological method, it is not clear whether the removal mechanisms of the beads would be responsible for ion exchange, precipitation, or bioaccumulation. In this study, the ion exchange process of Cd with Ca from the Ca-alginate beads under various groundwater geochemical conditions was tested, followed by an investigation of the process in NRW. The removal of Cd was studied during the operation of the reactor, and the total concentrations of Cd, Na, Ca, and Mg in eluants were determined. The released amounts of Na and Ca were obtained during the ion exchange process between Cd in the AGW and Na and Ca from the beads.

In contrast to the ion exchange process, the amounts of Na, Ca, and Mg were measured in the Ca-alginate beads before and after being used in this process. These

amounts must be high in the beads before use; however, in some of the results, the amount of Ca was high after being used in Cd removal due to the accumulation of calcium from the AGW in the bacterial cells. Handley-Sidhu *et al.* (2011) reported that bacteria could accumulate Ca and form nano-crystalline hydroxyapatite when Ca is available in the solution. The accumulation capacity of Cd, which ranged between 39 and 45 nmol per g of dry biomass on all beads, was observed at a pH level of 7.00. From these experiments, it seems that the ion exchange of Cd with Ca and Na could have occurred, as the decreasing Cd amounts in eluants were compatible with the release of Ca and Na (Carro *et al.*, 2015).

Due to this uncertainty of the ion exchange process, the process was studied at different pH levels of AGW to gain knowledge of other mechanisms such as adsorption and precipitation that might occur. It is reported previously that the Cd uptake by an absorbent depends on the pH of the solution (Liu *et al*., 2010). The theoretical prediction of Cd in AGW, using the thermodynamic calculations (MINTEQ program) showed that Cd was precipitated at pH 7.00 and 7.50. It has been recently reported by Siswoyo *et al*. (2019) that cadmium could be precipitated at alkaline pH (>8.00). The influence of the pH on the Cd uptake of all beads was different. The Cd accumulated in the beads was higher at pH 4.00 than at higher pH values. The accumulation capacity of Cd of 28 to 68 nmol per g of dry biomass onto all beads was observed at the pH 4.00, with the highest capacity obtained by the Ca-alginate beads containing live cells of *B. agri* C15 Cd^R. At pH 4.00, the increase of H^+ concentrations competes for the ion exchange of Cd with Ca and Na or the cation coordination on the surface of beads. The prediction of the Cd fractions in AGW at pH 4.00 (MINTEQ program), showed that the free Cd^{2+} was the dominant species. Cd^{2+} is the free ion that can exchange with Ca and Na on the beads. Also, Cd^{2+} ion can coordinate with

the negative charges of the functional groups, which are available from the alginate or the bacterial cell wall. Recently, Yang *et al.* (2019b) revealed that the efficiency of Cd removal increased when the pH was at 4.00. Therefore, it seems that competition from the protonation of the functional groups of the alginate beads due to increasing H^+ concentrations at low pH was not preventing efficient removal of Cd from AGW.

On the contrary, other researchers found that Cd uptake increases with the increase of pH (Yang *et al.*, 2019b). This prediction was not found in this study, as some beads had an uptake of the same Cd amounts at pH 7.50, compared to their uptakes at pH 4.00. The accumulation capacity of Cd at a range of between 22 and 58 nmol per g of dry biomass onto all beads was observed at pH 7.50. The assumption for this uptake was due to the ion exchange of Cd free ions with Ca rather than the formation and precipitation of $Cd(OH)_2$, with a solubility product constant (K_{sp}) 7.2 $X10^{-15}$ (Rumble, 2018). Indeed, in the thermodynamic calculations (MINTEQ program), $Cd(OH)_2$ was not predicted under experimental conditions. Therefore, the related effects of pH on the beads' surface, the electrostatic forces, and the coordination of Cd could control the uptake amounts. Recently, Hu *et al*. (2019) revealed an inappropriate relationship between the predicted species and precipitation, which affected this study. Considering the above facts, it can be predicted that the ion exchange was responsible for the Cd uptake that occurred at different pH values, because of the distribution of Cd^{2+} ions and the released amounts of Ca and Na in the AGW at different pH were similar. However, at an alkaline pH, more OH^- was present, resulting in more negative functional groups, which provide an electrostatic surface for higher coordination with Cd.

It has been seen that the beads were different in their abilities regarding Cd uptake; the Ca-alginate beads containing killed-control cells (inactive cells) had higher uptake

rates, under some conditions than the alginate beads without bacterial cells or those containing live cells of *B. agri* C15. It is well known that dormant bacterial cells are capable of uptaking more Cd compared to the active cells, notably when the enzymatic or bioaccumulation process is absent. Previously, Katırcıoğiu *et al.* (2008) found that the ability of the immobilised heat-inactivated cells of *Oscillatoria* sp. H1, a *cyanobacterium* for Cd removal, was higher than in their live cells. The high Cd removal ability was possible due to the increase in the negative charges of the dormant bacterial cells and the irreversible denaturation of the cell compounds during the inactivation process. However, Ca-alginate beads containing live cells of *B. agri* C15 Cd^R showed a high uptake ability compared to the *B. agri* C15. Therefore, it can be suggested that bioaccumulation and surface complexation mechanisms were more active in the live cells of *B. agri* C15 Cd^R than in the live cells of *B. agri* C15 (as discussed in Chapter Four).

Mechanisms of Ca-alginate beads for the uptake of Cd were also investigated under selected individual constituents (cation, anion, and humic acid) present in AGW. These experiments were carried out to understand the impact of these constituents on the rates of Cd uptake and the accumulative amounts of Cd in the beads. The influence of calcium (cation) on Cd removal was used as this element is the primary ion of the hardness and is a known antagonist of Cd. The Cd uptake decreased significantly under the effect of calcium. The accumulation capacity in the range between 18 to 23 nmol per g of dry biomass Cd onto all types of beads was observed under the effect of cation, with the highest capacity obtained by the Ca-alginate beads containing live cells of *B. agri* C15 Cd^R. The thermodynamic calculations predicted the species of Cd^{2+} (53%) and $CdCl^+$ (41%) occurred in AGW under this effect. The occurrence of a high fraction of $CdCl^+$ diminished the Cd ion exchange or adsorption, due to its low

affinity compared with the fraction of Cd^{2+} ion (Boparai *et al*., 2013). Ca-alginate beads have a negative charge; therefore, Ca is competitive with Cd in the coordination with this charge or with ion exchange with Ca and Na from the beads, reducing the Cd uptake amount.

Similarly, under the influence of anion (phosphate), the Cd uptake was hindered significantly as the accumulation capacity of Cd in the range between 3 to 20 nmol per g of dry biomass onto all beads was observed. The addition of phosphate into AGW leads to the formation of $CdHPO_4$ (89% of total Cd in AGW), which was predicted using the thermodynamic calculations (MINTEQ program). $CdHPO_4$ cannot be adsorbed into the beads due to its low affinity (Aujard-Catot *et al*., 2018). Also, this fraction prevented the ion exchange process of Cd with Ca in the beads, as the process mainly occurred with free ion Cd^{2+}. A comparison with another adsorption study under the presence of co-existing ions indicated that these cations/anions were the most inhibiting ions in the process (Kanematsu *et al*., 2013). In this study, the occurrence of calcium or phosphate in the AGW inhibited the Cd uptake.

The complexation of Cd with humic acid (Cd-HA) was predicted in the thermodynamic calculations, (MINTEQ program), as this complex is the most formed complex with Cd (Datta *et al*., 2001), therefore this type of complexation affects the Cd removal process. As the complexation of Cd-HA occurs, the blocking of the functional groups on the beads could take place through the Cd-HA complex. The secondary effect of humic acid on the Cd uptake was also observed due to the release of Ca, Mg, and Na from the humic acid. This effect began after 10 hours of operating the reactor, for which the competitive effects started on the Cd uptake. It is well known that the humic acid, abundant with these ions, is due to the complexation of these ions with its functional groups, carboxylate, and phenolate (Tianzi and Weimin, 2019). A low accumulation

range of Cd capacity of between 4 and 13 nmol per g of dry biomass onto all beads was observed under the effect of the humic acid.

For the investigation, the Cd uptake from NRW, a sample of Walkham River, was collected and analysed. The environmental parameters of the analysed sample were obtained similar to the values of the Walkham River that were recorded previously (Handy *et al*., 2002). As the Walkham River is being monitored for water quality, the concentration of Cd in the analysed sample was low (0.4 $\pm$ 0.06 nM), below the limit concentration of Cd in drinking water (EPA, 2011). Therefore, to achieve the Cd uptake in NRW, a final nominal concentration of 10 mM Cd in the NRW was added. Ca-alginate beads without bacterial cells and Ca-alginate beads containing *B. agri* C15 Cd^R showed higher removal rates of Cd from NRW. The preferential accumulation capacity of Cd in the range between 17 to 32 nmol per g of dry biomass onto all beads were observed. It seems that the NRW parameters did not affect the ability of the beads for Cd removal. The concentrations of Na, Mg, and Ca and the hardness overall were low in NRW compared to AGW. In terms of classifying the Cd-loaded sorbent after obtaining the removal process, the hazard classification of the cadmium-loaded bead estimated that the waste is not hazardous and can enter the ordinary waste system without further treatment.

5-5 Conclusion

The removal of Cd with different types of Ca-alginate beads holds the potential for AGW treatment, while their ability varies depending on the pH of the AGW. However, when cations/anions and humic acid that form Cd-complexes exist, the efficiency of Cd removal could be reduced. The precipitation of Cd species and the formation of Cd minerals are important responses to the change in pH, and adding cations/anions and humic acid into the AGW reduces the efficiency of the ionic exchange of Cd with

Ca-alginate beads. Ca-alginate beads containing live cells of mutant *B. agri* C15 Cd^R showed a considerable accumulation of Cd from AGW at pH 4.00 and NRW. The performance of the mutant strain at low pH provides opportunities for the treatment of ground or surface waters that are affected by acid (mine) drainage or are naturally low in pH. The hazard classification showed that its beads were a non-hazardous waste. Hence, alternative bioremediation may interfere with its environmental qualities, which may generate secondary products that are harmful to humans. The toxicity of waste during this process still requires further research.

Chapter 6. *In vitro* bioaccessibility assessment as a tool to predict the toxicity of bioremediation products

Abstract

The demand for the development of bioremediation processes designed to maintain healthy environments has increased; however, evaluation of the toxicity of its products is needed. Therefore, the toxicity of the Cd-loaded beads of the bioremediation approach developed in this thesis was evaluated by using *in vitro* human gastrointestinal simulation (BARGE method). Cd-loaded beads were obtained from adsorption experiments of Cd from artificial groundwater (AGW) and natural river water (NRW, Walkham River) using Ca-alginate beads containing live cells of the mutant *B. agri* C15 Cd^R or its wild type *B. agri* C15, in batch flasks. The results showed that the Ca-alginate beads containing the mutant adsorped a significant concentration of Cd (1700 mmolal), related to its adsorption capacity. Cd-loaded beads had higher concentrations of Ca and Na (2030 ± 40 and 4300 ± 18 molal, respectively), related to its composition. The effects of the gastrointestinal simulation showed that Ca had the highest bioaccessible concentrations from Cd-loaded beads of all tested elements (Al, Ca, Co, Cu, Fe, K, Mg, Na, and Zn) from (1280 ± 13.00 molal), while some other elements were not detected at the end of the gastrointestinal system. Cd bioaccessibility was significantly lower in the Cd-loaded beads containing the mutant (0.17 and 0.14 molal in the gastric and gastrointestinal phases, respectively), compared to the wild type (0.23 and 0.19 molal, respectively). The bioaccessible fractions (BAFs) of Cd were significantly lower in the Cd-loaded beads containing the mutant at the gastric and gastrointestinal phase, with the mean of 4.85% and 2.95%, respectively. The low percentages of BAFs of Cd suggested that the products of the bioremediation process developed in this project might not be relevant as a human health risk.

6-1 Introduction

Entrapment is used as a method to improve the stability and bioavailability of some bioactive materials, such as bacteria. A variety of natural matrixes have been used as entrapment carriers such as cellulose, starch, pectin, agarose gel, collagen, carrageenan, chitin, chitosan, agar-agar, and alginate. Alginate is naturally extracted from brown seaweed and bacteria. The gelation of alginate in calcium forms ca-alginate beads with a shape that is generally known as a cylindrical shape with rounded ends. Ca-alginate beads are used as an entrapment method in pharmaceutical (Hoare and Kohane, 2008), plant (Wang *et al.*, 2018), medical (Bhujbal *et al.*, 2014) and adsorption (Bilal and Iqbal, 2019) applications. Ca-alginate beads possess some unique properties, such as being cost-effective, non-toxic, and biodegradable (Calvo *et al.*, 2018) and the design and development of bioremediation processes using Ca-alginate beads take advantage of their adequate metal – binding capacity (Draget and Taylor, 2011). The evaluation of designed bioremediation processes typically focuses on the estimation of their efficiency. However, the adsorbed concentrations of contaminates within the Ca-alginate beads may present an environmental or toxicological challenge. Therefore, the Ca-alginate beads produced by the bioremediation processes must be investigated, as their ultimate purpose is to reduce environmental contamination and toxicity in terms of using absorbent material and its secondary products. To evaluate the toxicity of the bioremediation products, bioaccessibility determination instead of the total concentration is necessary. A range of methods are available, each of them representing a different and operationally defined, evaluation of bioavailability to ether specific receptors (e.g., bioassay (Altenburger *et al*., 2019)) or biogeochemical setting as a proxy (e.g., redox condition (Rajpert *et al*., 2018)). Useful Ca-alginate beads are

defined as absorbents that have no toxicity or health risk in case of accidental ingestion. For this purpose, they should be appraised using in vivo or in vitro assays to interpret their toxic effects under the gastrointestinal system of the human body. The bioaccessibility of metal in used Ca-alginate beads could be defined as the fraction of the adsorbed metal released from the beads into the gastrointestinal system to be accessible for intestinal adsorption. This metal fraction contributes to evaluating the beads' toxicity. In vitro assays are being used as a standard regulatory purpose rather than in vivo assays, due to their operability, efficiency, and accessibility.

Most importantly, in vitro assays are the most effective way to determine the bioaccessibility when it is impossible to assess the bioaccessibility of a matrix in oral human studies and to reduce the need for animal models due to ethical considerations. Specifically, the bioaccessibility can be determined through an *in vitro* human gastrointestinal simulation. This approach mimics the physiological conditions of the stomach and the small intestine in the human digestive system, while also taking into consideration the retention time and pH of each section of the system (Sharafi *et al*., 2019). Various in vitro human gastrointestinal simulation assays have been used to evaluate the bioaccessibility of metals in the soil, including the physiological based extraction test (PBET), in vitro gastrointestinal (IVG), solubility bioaccessibility research consortium (SBRC) and the bioaccessibility research group of Europe (BARGE, called unified bioaccessibility method (UBM)) (Tang *et al*., 2018). The BARGE method was designed to determine bioaccessibility for the assessment of the health risk to humans from metal contamination in soils and secondary products, such as food (Cámara-Martos *et al*., 2019; da Silva Haas *et al*., 2019). By this method, the bioaccessible fraction of Cd has been determined previously in soils (Xie *et al*., 2019), particulate matter (Xing *et al*., 2019), fish (Marval-León *et al*., 2014) and food (Cámara-

Martos *et al*., 2019), showing the possibility for determining the bioaccessible fractions in different products. Therefore, this chapter aims to evaluate the risk to human health arising from the products of the bioremediation process developed in this thesis by estimating the bioaccessible fraction (BAFs) of Cd of Cd-loaded beads using the BARGE method. The objectives of this study were firstly to achieve Cd adsorption on the beads from AGW and NRW by Ca- alginate beads containing live cells of the mutant *B. agri* C15 Cd^R or its wild type *B. agri* C15, in batch flasks. Secondly, the determination of the adsorped concentration of Cd was estimated after aqua regia acid digestion using ICP-MS or ICP-OES, in addition to the elements of Al, Ca, Co, Cu, Fe, K, Mg, Na, and Zn. Thirdly, the element bioaccessibility within beads in the gastrointestinal tract was estimated using synthetic simulation solutions for gastric and gastrointestinal digestion. Finally, the BAFs of Cd was calculated from the total (after aqua regia acid digestion) and bioaccessible (after the gastric or gastrointestinal digestion) concentrations.

6-2 Methodology

6-2-1 Preparation of Ca-alginate beads and adsorption of cadmium

Ca-alginate beads containing either *B. agri* C15 or *B. agri* C15 Cd^R were prepared using the entrapment method of calcium alginate gel, as described in Chapter Two. In order to compare bead properties after adsorption of Cd from AGW or NRW, the beads of each strain were divided into two parts. One part was used for Cd adsorption obtained from AGW. The second part of the beads was used for Cd adsorption obtained from NRW (Walkham River). The elemental composition of AGW and NRW are provided in Table 18.

Table 18. The composition of AGW and NRW (Walkham River) was used in this experiment. ± presents the standard error of the mean (SEM) (*n* = 3 replicates).

Element	AGW: concentration, unit	NRW: concentration, unit
Al	**	2 ± 0.03 μM
Ca	1.75 mM	83 ± 0.2 μM
Cl	1.75 mM	*
Cd	**	0.1 ± 0.02 nM
Cu	**	31 ± 0.8 nM
K	103 μM	4 ± 0.1 μM
Fe	**	2 ± 0.02 μM
Mg	448 μM	58 ± 0.6 μM
Na	1.14 mM	202 ± 6 μM
NO	44 μM	*
Pb	**	0.4 ± 0.06 nM
SO	448	*
DOC	**	0.037 ± 0.03 mg/L
Zn	**	8 ± 0.05 nM

DOC: Dissolved organic matter.
*Not measured.
** No component added.

The batch adsorption experiments were carried out in flasks (250 mL Erlenmeyer flasks) to adsorb Cd into Ca-alginate beads, before the determination of the bioaccessible element fractions in loaded Cd-beads using the BARGE method. To acquire a constant adsorption level of Cd by the beads, the adsorption was carried out in a single batch experiment. The tests were performed separately for Cd adsorption from 100 mL of AGW or NRW, respectively, with a nominal concentration of 10 μM of $Cd(NO_3)_2 \cdot 4H_2O$ (Sigma-Aldrich) using the beads (100 g). The flasks were covered with aluminium foil and incubated at room constant temperature (22 °C) for five days, which were stirred twice a day using a glass rod.

6-2-2 Ca- alginate bead samples and pretreatment

After five days of the adsorption period, the Ca-alginate beads were collected from each batch using a plastic sieve, rinsed quickly with ddH_2O, and transferred into acid-washed and deionised ceramic drying boats. The bead samples were then

weighted and dried to constant mass at 90 °C (Gallenkamp OV-160). The dry Cd-loaded beads were then ground and sieved to a fraction (< 250 μm particle size, using a mesh sieve) that is expected to be available for children`s hand-to-mouth contact (Rodriguez *et al.*, 1999).

6-2-3 *Aqua regia* acid digestion of Ca-alginate beads

The element concentration contained in the dried, sieved beads (0.6 g, *n* = 3, from each batch) was determined using an *aqua regia* acid digestion (as described in Chapter Two). The results were used to determine the total concentrations of elements and to calculate the percentage of BAFs of Cd, which results from the *in vitro* human gastrointestinal simulation.

The accuracy of the acid digestion for the beads was evaluated using a spike recovery test, according to the method described by Xu *et al.* (2012) as there is no certified reference material for Ca-alginate beads. The spike recovery test was carried out by spiking the dried, sieved beads with Cd (0.6 g, *n* = 3 samples). The amount of 50 mg Cd was added to the samples (Ca-alginate beads without bacterial mass) as 0.6 mL of 89.28 mM Cd to 0.6 g of the beads in a Falcon tube (50 mL). The beads were mixed with the Cd using a class rode and left for 48 h, mixing frequently. Then, the beads were dried at room constant temperature (22 °C) before the *aqua regia* acid digestion. Comparably, *aqua regia* acid digestion was carried out with the same dried sieved bead before being spiked with Cd. The spike recovery was determined using the equation:

$$\text{Spike recovery (\%)} = \frac{(\text{Cd measured in spiked sample} - \text{Cd measured in unspiked sample})}{\text{Cd spiked}} \times 100$$

The Cd measured in the spiked sample is the total amount of Cd determined at the end of the spike recovery test. In contrast, the Cd concentration determined in the

unspiked sample is the total amount of Cd measured before the addition of Cd, and the Cd spiked is the nominated amount of Cd spiked into the beads.

6-2-4 Elements analyses

The total concentrations of Al, Ca, Cd, Co, Cu, Fe, K, Mg, Na, and Zn in *aqua regia* acid digestion extracts of Ca-alginate beads before *in vitro* human gastrointestinal digestion and digestive fluids after the gastrointestinal digestion were analysed using ICP-MS (Thermo Scientific, X Series 2) or ICP-OES (Thermo Scientific, iCAP 700 Series). The instruments' limited detection (LOD) are reported in Table 19 as five times the standard deviation (SD) of multiple (n =10) analysis of the lowest calibration standard. Table 19 also presents the results of the procedural blank samples (without any beads, n = 3 blanks). The digestive fluids after the gastrointestinal digestion were analysed for determining the total concentrations of elements.

Table 19. The LOD (derived from 5 X SD of *n* = 10 analyses) and procedural blank (*n* = 3), and analytical techniques for each element.

Element	Analytical technique	LOD	Procedural blank ± SEM	Unit
Al	ICP-MS	0.13	< LOD	μM
As	ICP-OES	0.01	0.02 ± 0.008	mM
Ca	ICP-OES	0.01	< LOD	mM
Cd	ICP-MS	0.02	0.003 ± 0.0004	μM
Co	ICP-OES	0.06	< LOD	mM
Cu	ICP-OES	0.01	< LOD	mM
Fe	ICP-OES	0.3	< LOD	μM
Pb	ICP-OES	0.01	< LOD	mM
K	ICP-OES	0.9	< LOD	μM
Mg	ICP-OES	0.8	< LOD	μM
Na	ICP-OES	0.04	< LOD	mM
Zn	ICP-OES	0.06	< LOD	mM

The recovery of the *aqua regia* acid digestion of the British geological society reference soil (BGS-102, Wragg, 2009) was evaluated for Cd and other elements. The accuracy was low for some elements (Table 20): Ca (65.5%), Co (60%), Cu (67.5%) and Fe (48%). However, significant recovery percentages ($^{*}p<0.05$) of the other elements were as follows: K (100%), Cd (95%), and Zn (96%). The good accordance between the measured and the certified values for K, Cd, and Zn indicates that losses during experimental or analytical procedures were not responsible for the poor recovery of Ca, Co, Cu, and Fe.

Table 20. Results of *aqua regia* acid digestion, certified value, and recovery percentage of soil BGS-102. The recoveries were estimated from the mean of the recorded, and certified values and ± presents the standard error of the mean (SEM) (*n* = 3 experimental replicates). *Significant differences between recoveries.

Element	Concentration (molal)		Recovery (%)
	Recorded value	Certified value	
Ca	459 ± 0.2	700 ± 7.5	65.5 ± 1.8
Co	0.40 ± 0.005	0.67 ± 0.001	60 ± 3.0
Cu	0.27 ± 0.002	0.40 ± 0.02	67.5 ± 2.2
Fe	115 ± 13.5	236 ± 14.3	48 ± 1.7
K	30.3 ± 0.6	30 ± 2	100 ± 1.4*
Cd	2.35 ± 0.04*	2.45 ± 1.60*	95 ± 1.8*
Zn	2.8 ± 0.05	2.9 ± 0.03	96 ± 1.3*

Results of the Cd spike test (nominated amount of Cd = 50 mg) for the Ca-alginate beads was with the recovery of 00.08 ± 0.2 %, which was calculated from the Cd amount measured in spiked beads (50.08 ± 0.2 mg) and Cd amount measured in unspike beads (0.04 ± 0.0002 mg).

6-2-5 *In vitro* human gastrointestinal evaluation of Cd-loaded beads

The BARGE-*in vitro* human gastrointestinal simulation was carried out to determine the BAFs of Cd in the products, Ca-alginate beads, of the bioremediation process. The *in vitro* simulation consisted of two digestion phases, gastric and gastrointestinal. Four synthetic gastric -intestinal digestive fluids (saliva, gastric, duodenal, and bile) were prepared separately in sterile ddH_2O from analytical reagents in two different solutions, inorganic (I) and organic (O) according to masses and volumes specified in the BARGE (2010) protocol. Then, the solution I and solution O of each type of fluid (i.e., saliva, gastric, *etc*.) were mixed, and the appropriate enzymes were added into

the final volume of 500 mL. The fluids were stirred for at least three h using magnetic stirring (IKA-WERKE R015), and the pH of each fluid was adjusted with a pH meter (Thermo Scientific Orion Star Plus, calibrated at pH 4.0, 7.0 and 10.0). The fluids were used within 24 h of the day of preparation.

For the gastric phase, 0.6 g of dried, sieved bead was added to a polypropylene tube (50 mL, n = 4, from each batch), salivary fluid at pH 6.5 ± 0.5 and gastric fluid at pH 1.1 ± 0.1, were added sequentially and shaken by hand for 10 s. The pH at this step was adjusted with NaOH (1 M) or HCl (~37 %) to 1.20 ± 0.05 (pH meter as above), followed by 10 s of shaking by hand, repeating three times until the pH remained stable. Then, the tubes were incubated at 37 °C for an hour and shaken using an end-over-end rotator (Grant-bio, PTR-60). After the incubation time, the pH was checked to be < 1.50. Two tubes from this phase were centrifuged for 15 mins at 4500 g; then, the supernatants were collected by prudently pipetting and acidified with 0.5 mL of concentrated HNO_3 (> 68 %). The procedural blank sample of the gastric phase (G_{C0}) was the salivary and gastric fluids without any beads (n = 2 blanks). The other two tubes of gastric phases were then processed to the intestinal phase by the addition of the duodenal fluid at pH 7.4 ± 0.2 and bile fluid at pH 8.0 ± 0.2. The pH at this phase was adjusted to 6.30 ± 0.5, as mentioned above. Then, the tubes were incubated at 37 °C for 4 h and shaken using the end-over-end rotator. The pH of the samples was noted at the end of the incubation, followed by the centrifugation at 4500 g for 15 mins. The supernatants were collected to be acidified with 1.0 mL of concentrated HNO_3 (> 68 %). The procedural blank sample of the gastrointestinal phase (Ist_0) consisted of the salivary, gastric, duodenal, and bile fluids, respectively, without any beads (n = 2 blanks). Soil BGS-102 was used to validate the analytical chemistry.

6-2-6 Cadmium speciation and precipitation during BARGE experiments

The speciation and potential for precipitation of Cd within during the BARGE experiments were evaluated with thermodynamic equilibrium calculations. To this end, the inorganic chemical speciation at 22 °C was calculated using the geochemical speciation software Visual MINTEQ, version 3.1 (Gustafsson, 2011). The input files contained the inorganic components and concentrations of the gastric (pH 1.5) and intestinal fluids (pH 6.3), respectively, as well as Cd, Al, and Zn concentrations after incubation of the Ca-alginate beads containing the mutant and exposed to AGW, as specified in Table 21 The organic components contained in the BARGE fluids are assumed to form complexes that maintain Cd in solution and therefore, the inorganic speciation provides a worst-case scenario for precipitation. Oversaturated solids were allowed to precipitate, pH was fixed, ionic strength was calculated, the experiment was open to the atmosphere, and activity corrections were performed after Davies. The redox potential was fixed at *E*h = -200 mV, 0 mV +200 mV and 400 mV in separate calculations.

Table 21. The input files for Visual MINTEQ contained the inorganic components and their concentrations in gastric and intestinal BARGE fluids. The inorganic components of the BARGE solutions were entered, as well as the determined concentrations of Cd, Al, and Zn after incubation of the Ca-alginate beads containing the *B. agri* C15 or *B. agri* C15 Cd^R and exposed to AGW.

Component	Concentration (μM)	
	Gastric (pH 1.5)	Intestinal (pH 6.3)
Cd^{2+}	563	0.25
Al^{3+}	1.0	0.17
Zn^{2+}	0.68	150
Ca^{2+}	5300	*
Cl^-	34500	12600
CO_3^{2-}	*	104500
K^+	25500	13200
Mg^{2+}	*	0.9
Na^+	47100	255200
NO_3^-	2100	*
NH_4^+	6100	*
PO_4^{3-}	9600	*
SO_4^{2-}	37500	150000

* No component added.

6-2-7 Statistical analysis

The results were subjected to statistical analysis using one-way analysis of variance (ANOVA), followed by Tukey *post hoc* test in IBM SPSS statistics 22 software. This analysis helped to evaluate whether total and bioavailable concentrations of each element were significantly different. The bioaccessible fractions of Cd of each bead in each adsorption matrix were compared between gastric and gastrointestinal phases. SigmaPlot (version 13) was used to illustrate the data of bar charts. The data were expressed as mean ± standard error of the mean (SEM).

6-2-8 Calculation of bioaccessibility index for cadmium

The outcome of *in vitro* human gastrointestinal digestion on the Cd-loaded beads was expressed in terms of the BAF using the equation:

$$\text{BAF (\%)} = \frac{(\text{Cd}_{\text{bioaccessible}}\ [\text{Cd mol per kg beads}])}{\text{Cd}_{\text{total}}\ [\text{Cd mol per kg beads}]} \times 100$$

The $\text{Cd}_{\text{bioaccessible}}$ is the total Cd concentration in digestive fluids at the end of both gastric and gastrointestinal phases. In contrast, the Cd_{total} is the total Cd concentration in the bead before using *in vitro* digestion (measured from the *aqua regia* acid digestion). The results of this experiment were expressed as molal.

6-3 Results

6-3-1 Adsorption of cadmium onto Ca-alginate beads

The adsorption of Cd by the beads was determined by measuring the concentrations of Cd, adsorbed from the different matrixes (five days), after extraction using *aqua regia* acid digestion of the dried sieved beads. The adsorption experiments revealed higher total concentrations of Cd were adsorbed from water by the Ca-alginate beads containing live cells of *B. agri* C15 Cd^{R} (1700 mmolal), than by those containing live cells of *B. agri* C15 (1100 mmolal). The results showed no significant differences (Figure 87, $^{\#}p<0.05$) in Cd concentrations adsorbed from the different matrixes of AGW and NRW.

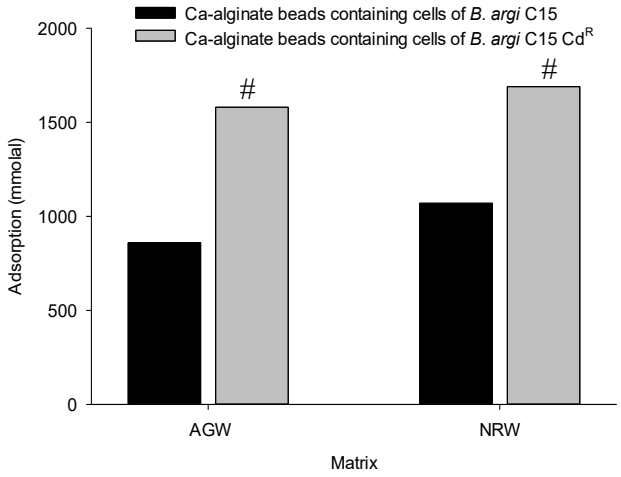

Figure 87. Concentrations of Cd adsorbed from AGW or NRW, with a nominal concentration of 10 μM Cd, onto Ca-alginate beads containing live cells of *B. agri* C15 or *B. agri* C15 Cd^R. The adsorption concentrations were measured after *aqua regia* acid digestion of the dried sieved beads. # Significant differences between strains.

6-3-2 Total concentrations of elements in Ca-alginate beads

Concentrations of Ca and Na (2030 ± 40 and 4300 ± 18 molal, respectively) in both types of beads and both adsorption matrixes were higher than other elements analysed (Figures 88A, 89A), and this is related to Ca and Na being components released from the alginate beads. There were no significant differences between Ca concentrations in Ca-alginate beads containing *B. agri* C15 used in either AGW or NRW (Figure 88A, $^a p<0.05$). In contrast, the concentrations of Ca in the Ca-alginate beads containing live cells of *B. agri* C15 Cd^R used in NRW was significantly higher (Figure 89A, $^a p<0.05$) than those used in AGW.

Similarly, the concentration of K in the Ca-alginate beads containing *B. agri* C15 was significantly higher when used in NRW ($^a p<0.05$) than AGW (Figure 88B). In Ca-alginate beads containing *B. agri* C15 Cd^R, the K concentration was similar in the beads used in either water (Figure 89B, $^a p<0.05$). The total concentrations of Al, Cd, Co, Cu, Fe, and Zn in both types of Ca-alginate beads were at least one order of magnitude below those of Ca (Figures 88B, C, 89B, C). More Al, Cd, and Fe recorded

in Ca-alginate beads containing *B. agri* C15 Cd^R (Figure 89C), compared to the Ca-alginate beads containing *B. agri* C15 (Figures 88C), and more Mg detected significantly in the adsorption from AGW than from NRW (Figures 88B, 89B, $^a p<0.05$) for either strain.

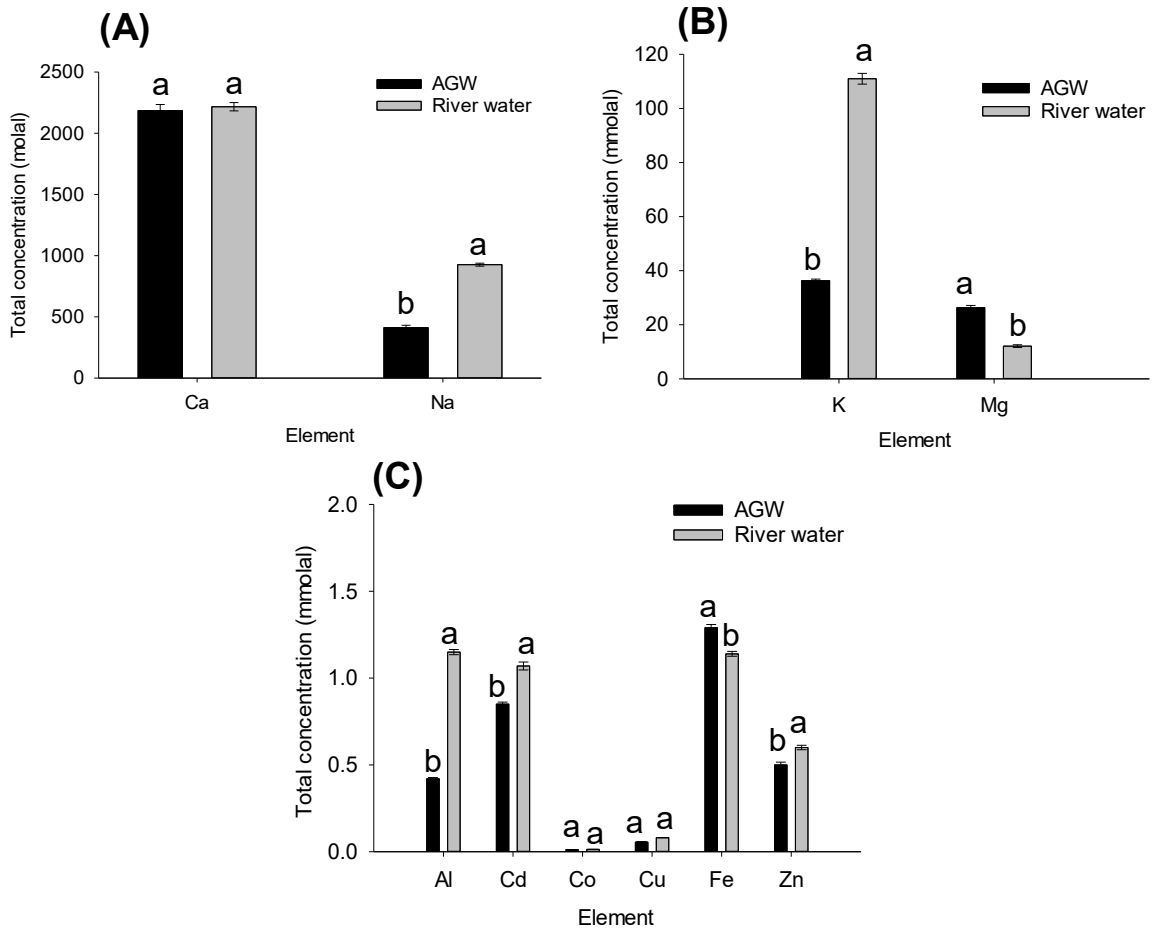

Figure 88. The total element concentrations of **(A)** Ca and Na, **(B)** K and Mg, and **(C)** Al, Cd, Co, Cu, Fe and Zn in the dried sieved Ca-alginate beads containing live cells of *B. agri* C15 after adsorption of Cd from AGW or NRW, determined after *aqua regia* acid digestion. The concentrations are mean, and the error bars indicate the standard error of the mean (n = 3). The concentrations were subjected to two-way ANOVA, Tukey *post hoc* test, and a different letter indicates a significant difference in the element concentrations between water, AGW and NRW.

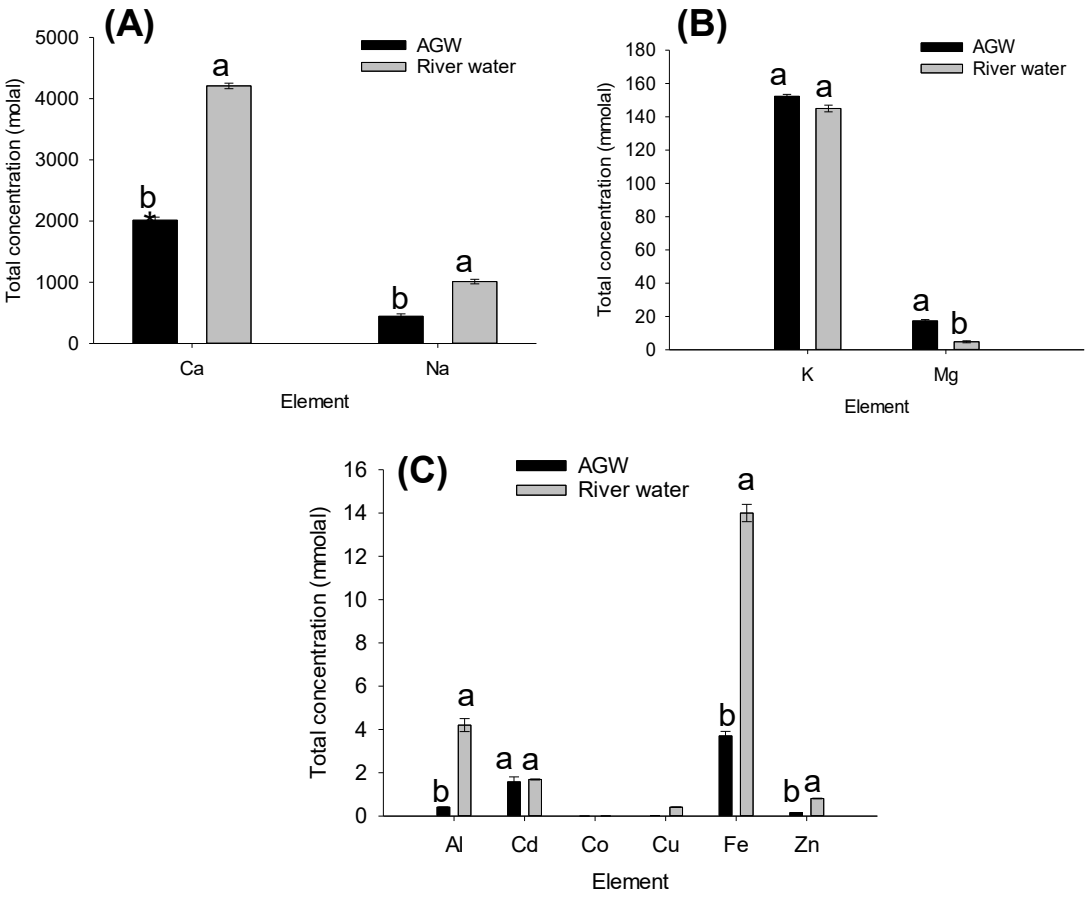

Figure 89. The total element concentrations **(A)** Ca and Na, **(B)** K and Mg, and **(C)** Al, Cd, Co, Cu, Fe and Zn in the dried sieved Ca-alginate beads containing live cells of *B. agri* C15 Cd^R after adsorption of Cd from AGW or NRW, determined after *aqua regia* acid digestion. The concentrations are mean, and the error bars indicate the standard error of the mean (n = 3). The concentrations were subjected to two-way ANOVA, Tukey *post hoc* test, and a different letter indicates a significant difference in the element concentrations between water, AGW, NRW.

6-3-3 *In vitro* bioaccessibility of cadmium in Ca-alginate beads of two phases of the human gastrointestinal system

The bioaccessibility of Cd and other elements adsorbed by Ca-alginate beads from either AGW or NRW was evaluated by determining the element concentrations in different Ca-alginate beads in each digestion phase (gastric and gastrointestinal phases). As was the case for *aqua regia* acid digestion, Figures 90A, 91A, 92A, and 93A show that Ca concentrations dominated the element distribution in gastric and gastrointestinal phases. Generally, higher element concentrations were recorded in

the gastric phase than the gastrointestinal phase (Na, K, and Mg, Figure 91A and B; K and Mg, Figure 92B; Al, K and Mg, Figure 93B). Lowest total concentrations were recorded for Al, Co, Cu, Fe, Mg, Na, and Zn, and these were not detectable in either of the gastric or of the gastrointestinal phase.

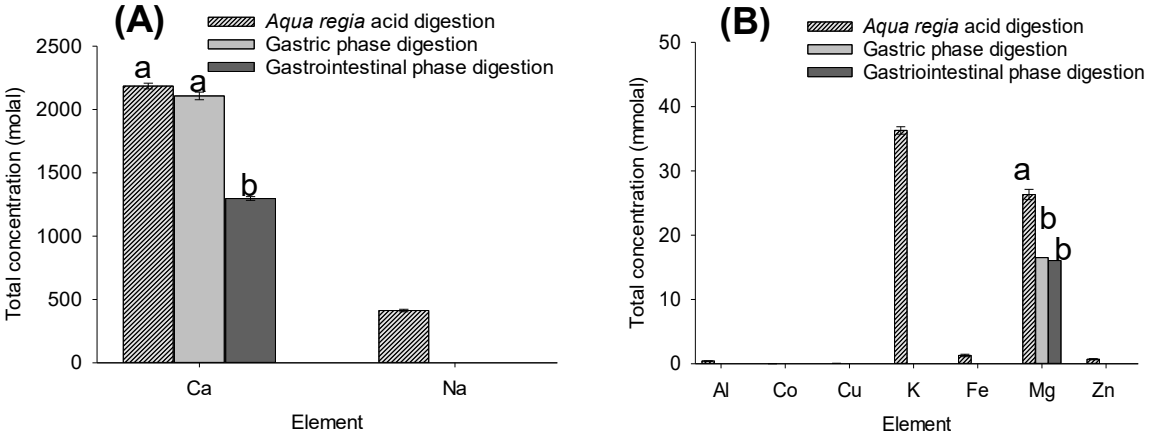

Figure 90. The total (determined after *aqua regia* acid digestion) and the bioavailable (determined after the gastric and the gastrointestinal digestions) of the element concentrations of **(A)** Ca and Na, and **(B)** Al, Co, Cu, K, Fe, Mg and Zn in the dried sieved Ca-alginate beads containing live cells of *B. agri* C15 after adsorption of Cd from AGW. All concentrations are mean, and the error bars indicate the standard error of the mean (*n* = 2). The concentrations were subjected to two-way ANOVA, Tukey post hoc test, and a different letter indicates a significant difference in the element concentrations between digestions.

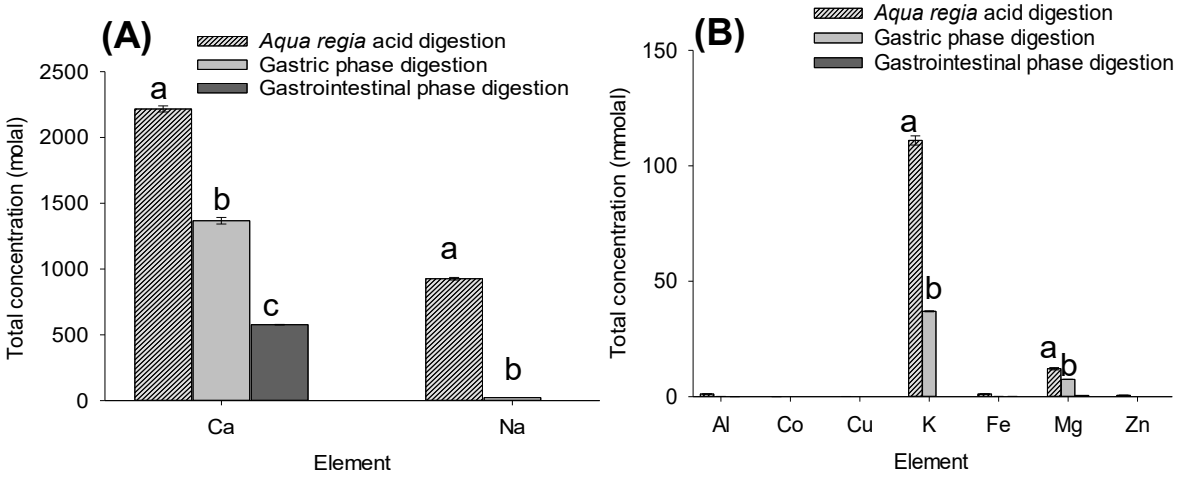

Figure 91. The total (determined after *aqua regia* acid digestion) and the bioavailable (determined after the gastric and the gastrointestinal digestions) of the element concentrations of **(A)** Ca and Na, and **(B)** Al, Co, Cu, K, Fe, Mg and Zn in the dried sieved Ca-alginate beads containing live cells of *B. agri* C15 after adsorption of Cd from NRW. All concentrations are mean, and the error bars indicate the standard error of the mean (*n* = 2). The concentrations were subjected to two-way ANOVA, Tukey *post hoc* test, and a different letter indicates a significant difference in the element concentrations between digestions.

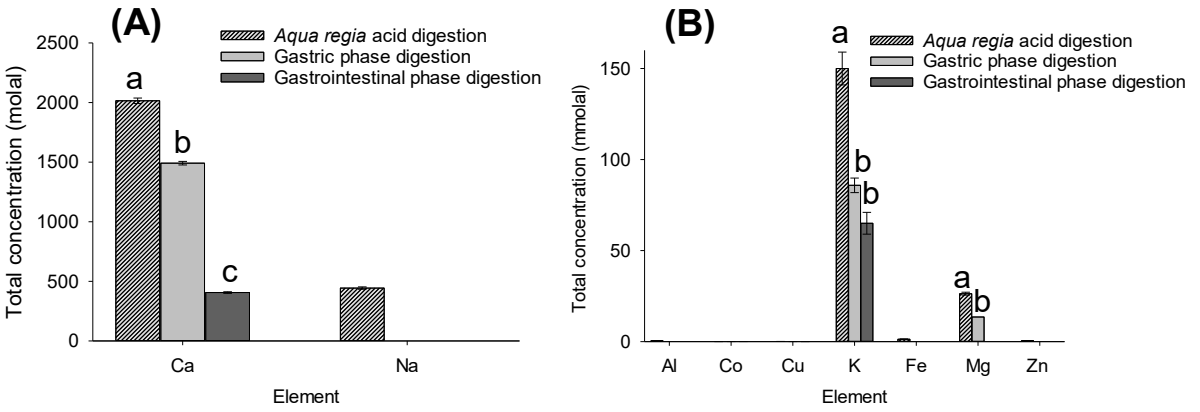

Figure 92. The total (determined after *aqua regia* acid digestion) and the bioavailable (determined after the gastric and the gastrointestinal digestions) of the element concentrations of **(A)** Ca and Na, and **(B)** Al, Co, Cu, K, Fe, Mg and Zn in the dried sieved Ca-alginate beads containing live cells of *B. agri* C15 Cd^R after adsorption of Cd from AGW. All concentrations are mean, and the error bars indicate the standard error of the mean (n = 2). The concentrations were subjected to two-way ANOVA, Tukey post hoc test, and a different letter indicates a significant difference in the element concentrations between digestions.

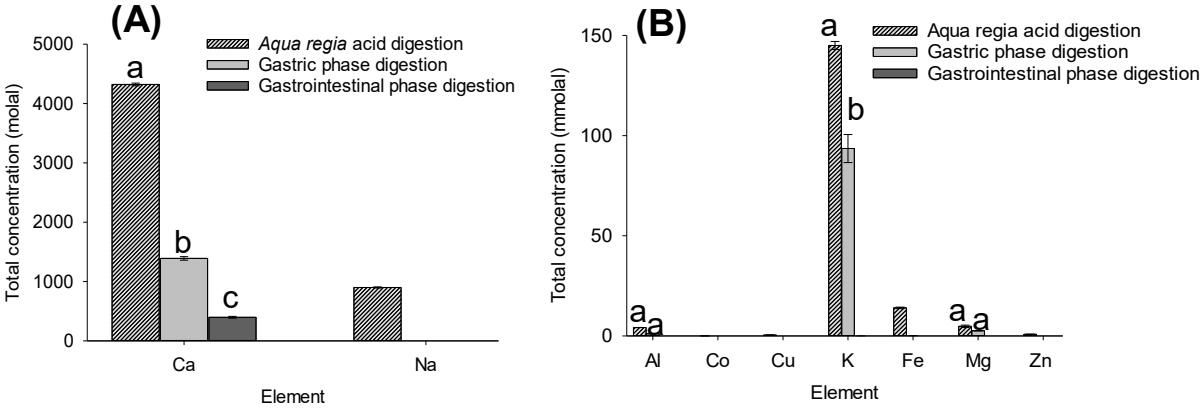

Figure 93. The total (determined after *aqua regia* acid digestion) and the bioavailable (determined after the gastric and the gastrointestinal digestions) of the element concentrations of **(A)** Ca and Na, and **(B)** Al, Co, Cu, K, Fe, Mg and Zn in the dried sieved Ca-alginate beads containing live cells of *B. agri* C15 Cd^R after adsorption of Cd from NRW. All concentrations are mean, and the error bars indicate the standard error of the mean (n = 2). The concentrations were subjected to two-way ANOVA, Tukey *post hoc* test, and a different letter indicates a significant difference in the element concentrations between digestions.

The concentrations of Cd in the dried sieved beads digested *aqua regia* ranged between 0.83 and 1.7 molal (Figure 94A and B, respectively), and much lower Cd concentrations in the gastric (0.23 – 0.17 molal) and gastrointestinal (0.19 – 0.14 molal) phases were only slightly different from each other.

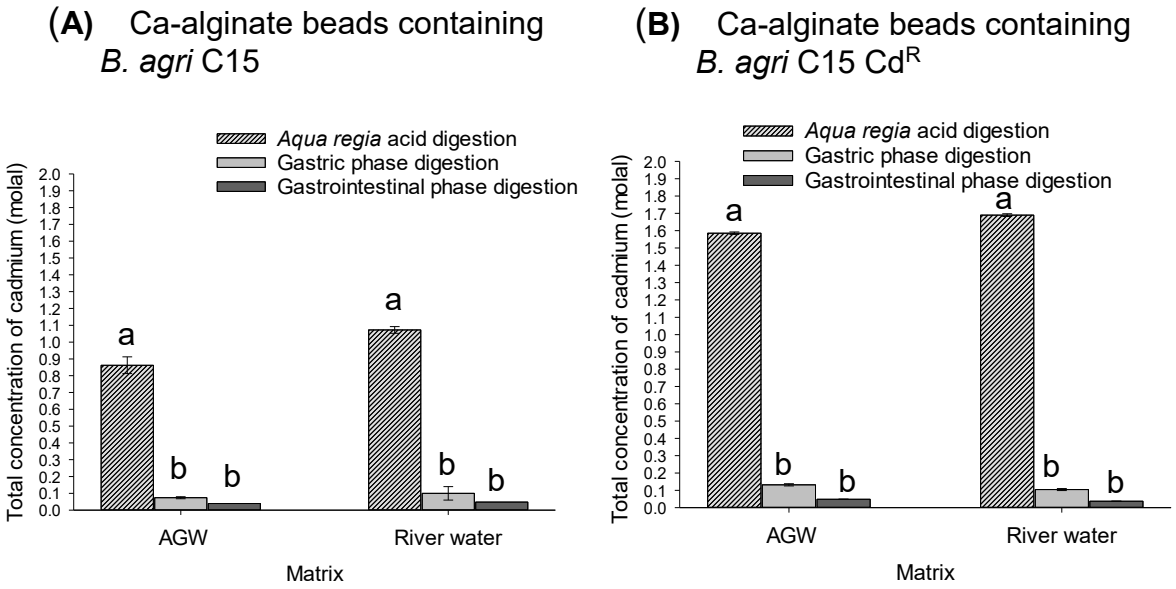

Figure 94. The total (determined after *aqua regia* acid digestion) and the bioavailable (determined after the gastric and the gastrointestinal digestions) of the concentrations of Cd in the dried sieved Ca-alginate beads containing live cells of **(A)** *B. agri* C15 and **(B)** *B. agri* C15 Cd^R after adsorptions of Cd from AGW and NRW. All concentrations are mean, and the error bars indicate the standard error of the mean (n = 2). The concentrations were subjected to two-way ANOVA, Tukey *post hoc* test, and a different letter indicates a significant difference in the element concentrations between digestions.

The BAFs of Cd was significantly higher (Figure 95, $^{\#}p<0.05$) in Ca-alginate beads containing *B. agri* C15 than *B. agri* C15 Cd^R. The BAFs of Cd from Ca-alginate beads containing *B. agri* C15 Cd^R were lower for both gastric and gastrointestinal phases than beads containing *B. agri* C15, and lower when used for Cd adsorption from NRW than from AGW.

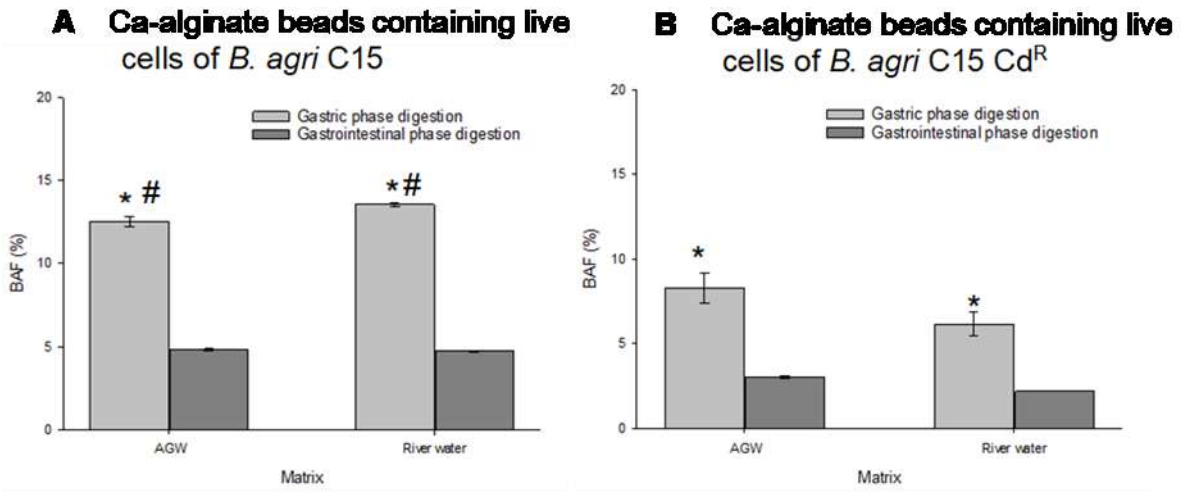

Figure 95. BAFs of Cd in the Ca-alginate beads containing live cells of **(A)** *B. agri* C15 and **(B)** *B. agri* C15 Cd^R from different adsorptions, in two phases of human gastrointestine, the gastric and gastrointestinal phases. All percentages are mean, and the error bars indicate the standard error of the mean (n = 2). *Significant difference in the percentages of BAFs. # Significant difference between strains (A and B).

6-4 Discussion

The BAFs of Cd in the secondary products of an adsorptive water remediation process, using *B. agri* C15 and *B. agri* C15 Cd^R entrapped in calcium alginate gel, were estimated to evaluate the effects of accidental ingestion by humans. The Ca-alginate beads were exposed to Cd within AGW or NRW for five days, after which Cd adsorption, as shown in previous Chapters, has been confirmed.

Aqua regia acid digestion of the sieved dried beads showed effective disintegration of the solid, with releases of high total concentrations of Ca and Na, which are the main components of the Ca-alginate beads (see Chapter Five), followed with the release of total concentrations of K and Mg due to their concentrations in AGW or NRW. Al, Cu, Fe, and Zn were recorded in lower concentrations in the digested Cd-loaded beads. These elements were not integral components of the bead structure and were not added to the AGW or recorded in the NRW (Table 18).

The Cd concentrations released from the beads determined after *aqua regia* acid digestion were between 0.83 and 1.7 molal, and the significant concentration recorded from Ca-alginate beads containing cells of *B. agri* C15 Cd^R, which were related to its adsorption capacity. The binding strength of metals with the Ca-alginate beads determines their bioaccessibility in the gastro/gastrointestinal system. Metal has a weaker binding strength to Ca-alginate beads, which causes a higher bioaccessibility and, consequently, a risk to human health upon ingestion. There was no statistically significant difference between AGW and NRW in the bioaccessible concentrations determined, and hence, the two matrixes will not be discussed separately in the following paragraphs.

It was important to determine the bioaccessible concentrations of Cd as well as of the elements, which are the main component in Ca-alginate beads, mainly Ca and Na. Studies have reported the relationship between calcium and sodium and hypertension in humans, whereas potassium is well known for its effects on electrolyte concentrations in cardiac electrophysiology (Noordam *et al*., 2019). For all elements in the Cd-loaded beads, the total concentrations (*aqua regia*) were higher than the bioaccessible concentrations. Under the effects of gastrointestinal simulation on element bioaccessibility, higher element concentrations were released in the gastric phase, than in the intestinal phase. Al, Co, Cu, Fe, K, Na, and Zn were not detected in either of the gastric or of the gastrointestinal phase. These results are comparable with previous studies, which showed that the BAFs of Al, Cu, Fe, and Zn in infant cereal samples were <LOD, 0.84%, 28%, and 1.1%, respectively (de Souza *et al*., 2019). The bioaccessible concentrations of Ca, K and Mg, were low in the intestinal phase than in the gastric phase, and these results are analogous with the study of evaluation of these elements in linseed and sesame, which showed that significant effects of the

intestinal phase on these elements (Souza *et al*., 2018). These differences in element bioaccessibility are associated with the characteristics of the Ca-alginate beads and digestive fluids. The elements were more prone to release under the stomach conditions (pH 1.5); as hydrogen ion concentrations increase, the acidic environment in the gastric phase increases the solubility of the divalent cations (Mortazavian *et al.*, 2008).

On the other hand, the human gastrointestinal phase is a less acidic (pH 6.3) environment, which may provide lower solubility. Thermodynamic equilibrium calculations (VMINTEQ 3.11) provided no evidence that precipitation took place in either gastric (pH 1.5) or intestinal fluids (pH 6.3) after BARGE over a wide range of redox conditions (*E*h -200 to +400 mV). The calculated speciation shows Cd^{2+} (~37%) and $CdCl^{-}$ (~43%) as dominant species in the gastric experiment, owing to the high stability constant of Cd-chloro complexes and high Cl^{-} concentration in the solution. In the intestinal experiment, Cd-sulfate complexes (total of 67%) dominated, due to high sulfate concentrations in the solution, with ~13% present as free Cd^{2+} ion. This indicates that re-adsorption of elements from the synthetic digestive fluids may have caused the reduction of the estimated bioaccessible concentrations and a decrease in intestinal absorption, rather than precipitation.

In confirmation of the above results, the BAFs of Cd in the gastric portions were higher (14.3 – 6.2%) than in the intestinal phase (4.85 – 2.95%). These results are comparable with previous studies, which showed that the BAFs of Cd decreased from the gastric phase (83.6%) to the intestinal phase (19.9%) (Tang *et al.*, 2018). The BAFs of Cd varied in the human gastrointestine mainly due to the differences in the pH, as noted above. The differences in the pH change the solubility of Cd, and its solubility depends on its potential precipitation mineralogy. So far, few bioaccessibility

studies have investigated the impact of mineralogy on BAFs of metals. Recently, Xing *et al.* (2019) reported that the PbS and $Pb_3(PO_4)_2$ contribute to the low bioaccessibility of Pb due to their low solubility product constants (K_{sp}) and consequently, precipitation from the synthetic digestive fluids. Ollson *et al*. (2016) observed that the BAFs of As increased in the gastric phase due to the presence of sulphides, sulphates, and hydroxides of As, which have high K_{sp} values, preventing precipitation and increasing their bioaccessibility. Results from this study suggest that the high BAFs of Cd in the gastric phase were possibly due to the formation of the mineral CdS (greenockite and hawleyite) in response to the acidic conditions. The K_{sp} of CdS is high (8×10^{-7}) (Rumble, 2018), which is enough to contribute to the increase in Cd bioaccessibility.

Conversely, when the pH was raised in the intestinal phase, the BAFs of Cd were lower, possibly due to the formation of minerals with low K_{sp}, in addition to CdS such as $Cd(OH)_2$ (7.2×10^{-15}), causing the precipitation and the decreasing of Cd bioaccessibility. In addition, the intestinal phase was extracted after the gastric phase. Hence, the total Cd concentration remaining in the experiment had been lowered, compared to the start of the experiment. The BAFs of Cd resulting from using Ca-alginate beads containing the *B. agri* C15 Cd^R were lower for both gastric and intestinal phases than the *B. agri* C15. This suggests that Ca-alginate beads containing cells of *B. agri* C15 Cd^R bond Cd more firmly due to the coordination of Cd with functional groups on its cell surface that were not available in *B. agri* C15.

6-5 Conclusion

Newly designed bioremediation processes must be evaluated for the toxicity of their absorbent materials and their secondary products, to satisfy the desire to use eco-friendly methods, and especially for regulatory toxicological values. Among the *in*

vitro human gastrointestinal stimulation assay, the BARGE method plays a significant role in overcoming a current limitation of performing ecotoxicological experiments evaluating human health risks of contaminants in soils or secondary products. In this study, BAFs of the bioremediation products were evaluated using the BARGE method, which has been validated for Cd for the gastric and gastrointestinal extraction phases. BAFs of Cd significantly decreased at the end of the gastrointestinal system, and researchers use this reduction as a guide that oral exposure to Cd (within beads) does not pose a risk to human health. This method was considered in this study without food, indicating the worst incident situation for the possible absorption. This study suggested that BAFs of Cd could be figured as a real scenario when children accidentally ingest Ca-alginate beads, which contain Cd.

Chapter 7. General discussion, conclusions and future work

7-1 General discussion

This study has sought to develop a novel process for the bioremediation of metal-contaminated water. Specifically, Cd was selected as the source of water contamination, due to its high toxicity and the ease of determining its concentration in aqueous solution using inductively coupled plasma spectrometry. The study was based on microbe-mediated bioremediation using Cd-resistant bacteria that were subjected to mutagenesis to increase their tolerance to the metal. The results of this work successfully applied a new bioremediation process to treat Cd in artificial groundwater (AGW) and natural river water (NRW) using *B. agri* C15 Cd^R that is a UV light-mutant of isolated *B. agri* C15. From a biotechnology perspective, the resistance of bacteria is an important feature that influences the abilities of bacteria in the bioremediation process.

7-1-1 Improvement of *B. agri* C15 using UV-light mutagenesis

From eight Cd-resistant isolates, *B. agri* C15 was resistant to 15 mM of Cd; therefore, it was chosen to improve its Cd resistant ability. It was necessary to investigate the growth of *B. agri* C15 under exposure to cadmium. The results showed that the increase in cadmium concentrations significantly inhibited the growth of *B. agri* C15. Similar findings of cadmium toxicity on bacterial growth were reported (McEldowney, 2000; Peptides, 2009; Chudobova *et al.*, 2015; Ramos-Zúñiga *et al.*, 2019).

UV-light mutagenesis was used to improve the resistance ability of wild type *B. agri* C15 to cadmium by the generation of a mutant in EBS growth medium that contained cadmium at a higher concentration than the resistant ability of *B. agri* C15. The mutant *B. agri* C15 Cd^R was generated with a tolerance of 20.00 mM of Cd. This work confirmed the principle reported in the literature (e.g., Wu *et al.* 2019) that the growth of a bacterium with Cd induces a mutant with elevated resistance to Cd. It has also

been shown that genetic engineering methods can be used for the enhancement of the Cd-resistance of *P. putida* 06909 to 1.7 mM of Cd (Wu *et al.*, 2009), and chemical mutagenesis was used to enhance the Cd-resistance of *P. aeruginosa* to 7 mM of Cd (Jabbari *et al.*, 2010). The current study proves the success of using UV-mutagenesis of *B. agri* C15 to increase its resistance to Cd, which is a desirable outcome due to the low-tech nature of this technique and its limited requirement for toxic reagents. In addition, there is no need to know a genetic system for the reference organism, which may be useful when used to create mutations of a newly isolated strain. The MIC value of Cd for the wild type *B. agri* C15 was 16 ± 0.7 mM, and for mutant *B. agri* C15 Cd^R was 21 ± 0.4 mM. No new cultural or cellular morphological characterisations were observed of the mutant *B. agri* C15 Cd^R compared to the wild type *B. agri* C15.

The mutant *B. agri* C15 Cd^R exhibited 25% increase in resistance to Cd compared to the wild type *B. agri* C15. This was considered as a small improvement, compared to the mutant of *B. subtilis* 38 (Jiang *et al*., 2009), generated by UV mutagenesis, which exhibited a 12 – fold increase of resistance to Cd; however, the wild type from which *B. subtilis* 38 was generated had a low MIC (0.25 mM Cd), from which resistance was increased to 3 mM Cd. The higher concentrations used in the present study presented a greater toxic challenge to the organisms.

The influence of cadmium stress on bacteria can introduce some Cd-tolerance, as Wu *et al.* (2019), in their study, showed the development of a mutant strain of *Bacillus megaterium* 'BM18' with a tolerance of 60 mM Cd. Similarly, the effect of UV in this study generated a mutant with high Cd resistance. El-Bestawy *et al*. (1998) in their study of enhancement of bacterial efficiency for metal removal using two separate mutation techniques (UV irradiation or 1% ethidium bromide) found that mutants of *Staphylococcus aureus, Bacillus Sphaericus, B. licheniformis* and *Arthrobacter* sp

exhibited higher removal efficiency when induced by UV than when induced by ethidium bromide. From these generation process it is possible to get mutants resist to cadmium. It has been reported that the *cadA* operon in many Cd resistant bacteria (Lee *et al*., 2001) and the variations in the *cadA* sequence or in its expression could contribute to the observed difference in MIC between the wild type and mutant.

An indication of this was observed when the effect of Cd on the specific growth rate and the amount of biomass of both strains were determined. At higher Cd concentration, the mutant *B. agri* C15 Cd^R exhibited a lower growth rate and biomass, and this result was similar to the result obtained of the mutant of *P. aeruginosa* G-1 (Horitsu and Kato, 1980).

The investigations using SEM and TEM showed no major differences in the cell morphology and structure before and after the exposure to Cd. The endospore and electrondense granules (poly-*β*-hydroxybutyrate (P*β*HB)) within the cells were confirmed in the cells of both strains. However, exposure to Cd increased the production of extracellular polymeric substances (EPS) by both strains, which is likely to be a detoxification strategy through adsorption/ complexation of Cd by EPS on the outside of the cell, preventing it from entering Cd the cells (Zhou *et al*., 2009).

7-1-2 Evaluation of cadmium removal from AGW

From a biotechnology perspective, the resistance of bacteria is an important feature that influences the abilities of bacteria during the bioremediation process. As the Cd resistance of bacteria increases, their relative removal ability increases, this ability results in the adsorption of the Cd at the surface of the cell wall, instead of inside the bacteria (Zhang *et al*., 2019b). The initial hypothesis of this study considered that the

creation of a mutant high in resistance to Cd must fundamentally lead to advancement in the bioremediation of Cd.

The experiments comparing the ability for Cd removal from AGW of the mutant *B. agri* C15 Cd^R entrapped in calcium alginate beads with that of the wild type *B. agri* C15 investigations confirmed, in general, the hypothesis' expectation. The mutant *B. agri* C15 Cd^R was found to have a significantly higher Cd removal rate at different initial concentrations (4.4 – 17.4 μM), compared to the wild type strain. This finding was consistent with the study of Wu *et al.* (2019), who reported that the mutant BM18-2 of *Bacillus megaterium* BM18-2 performed a higher uptake of Cd than the wild type.

The present work also assessed the potential mechanism of the Cd uptake by entrapped bacterial cells in Ca-alginate beads. SEM images of the beads showed the impurities on the surface of the Cd-loaded beads of both strains that confirmed that the initial uptake of Cd was due to the ion exchange with the Ca of the beads, in addition to the precipitation process. These suggestions were consistent with the studies of Zou *et al.* (2007) and Shim *et al.* (2019). Uptake of Cd into the bacterial cells was indicated by the distribution of Cd-dithizone complexes in stained beads that revealed that Cd was adsorbed within the beads, particularly in the bioremediation process that occurred with entrapped bacterial cells within the Ca-alginate beads.

7-1-3 Evaluation of the cadmium removal from AGW under different conditions and from NRW, Walkham River

The effect of different groundwater conditions on Cd removal efficiency by the Ca-alginate beads containing live cells of *B. agri* C15 Cd^R was investigated with alteration of pH and addition of calcium, phosphate, and humic acid to the AGW. Under these experimental conditions, it was essential to theoretically predict Cd precipitation and speciation (Boparai *et al*., 2013) in AGW using thermodynamic calculations

(MINTEQ program). The dominant speciation of Cd with the decreasing pH was free Cd^{2+}. It can be suggested that the free Cd^{2+} replaced Ca^{2+} in the Ca-alginate beads, in accordance with similar expectations in a recent study (Yang *et al.*, 2019). When pH increased to 7.50, OH- ions react with Cd to generate $Cd(OH)_2$; therefore, Cd precipitation becomes more likely to occur on the beads. The formation of $CdCl^+$, $CdHPO_4$ and/or Cd complexes with humic acids was found to hinder the Cd uptake. Kanematsu *et al*. (2013) also reported the inhibition effect of cations or anions on the removal process. High rates of Cd removal by mutant *B. agri* C15 Cd^R from AGW at pH 4.00 and NRW (Walkham River) were obtained.

Based on the hazard classification of the cadmium-loaded beads that were used in the removal experiments, even with the highest amount accumulated by mutant *B. agri* C15 Cd^R, the beads were classified as non-hazardous waste. This classification, showing the beads do not need any treatments, leads to producing a process that is cost-effective and eco-friendly.

7-1-4 The human health risk arising from products of the bioremediation process in this project

Once Cd removal has been achieved, non-hazardous waste (Cd-loaded beads) must be managed through land disposal units such as landfills, land treatment or land farming, and this disposal way puts the human under the risk from Cd toxicity (US EPA, 2018). To investigate this risk of the developed removal process in case of the accidental digestion of Cd-loaded beads by humans, the BARGE procedure was used. It is the standard method for estimating the human risk of contaminated soil, tested on children aged ten years, and based on the BAFs of Cd *in vitro* human gastrointestinal simulation. The procedure showed that BAFs were low during two gastrointestinal phases, gastric and gastrointestinal, and the lowest value of BAFs was during the

gastrointestinal phase. This investigation indicated that the Cd-loaded beads, which contained live cells of *B. agri* C15 Cd^R, were not representing risks to humans.

7-2 Conclusions

- The aim of the study, to develop a novel method for the bioremediation of Cd form water, was achieved through successful UV mutagenesis of a wild strain bacterium that generated *B. agri* C15 Cd^R with a MIC of 21 ± 0.4 mM Cd and its application to treat Cd contaminated water in a bench-scale reactor.
- The study provided evidence to underpin the hypothesis that Cd removal from water can be improved with a developed Cd-resistant bacterium, whereby the mutant *B. agri* C15 Cd^R out-performed the wild-type in removal rate and accumulation capacity.
- The novel bioremediation has been developed in environmentally sustainable ways: using UV mutagenesis for creating a mutant with elevated resistance to Cd, which results in non-toxic bead wastes that are not related to the risks to humans.

7-3 Future work and recommendations

The study carried out in this thesis has demonstrated that it is possible to obtain the mutant *B. agri* C15 Cd^R with elevated resistance to Cd and that it has potential in the removal of Cd from freshwater. However, further research needs to be conducted to support the current study. There are many areas of research that could be followed in the future.

It is proposed in this study that the introduction of –SH (sulfhydryl) compounds (Cooley *et al*., 1986; García *et al*., 2002) in the mutant leads to an increase in its resistance toward Cd and its ability in uptake Cd. A quantitative study of thiols compounds in the wild type and mutant under Cd stress (Wu *et al*., 2016) could assert this suggestion.

Single nucleotide polymorphisms (SNPs) could be used (Binet and Poole, 2000) to analyse gene expression of P-type ATPase ZntA, which could confer Cd resistance and is related to Cd efflux pump in the wild type and mutant. Wu *et al.* (2019) used the full genome sequencing for the comparison of DNA sequences for *Bacillus megaterium* strain 'BM18', and its mutant 'BM18-2 and the sequencing revealed that six different genes between both.

Also, an investigation of a plasmid efflux system of both strains could be studied. Zheng *et al.* (2019) investigated the plasmids associated with the Cd tolerance of the isolated DNA from soil microbes using metagenomic analysis.

Polyphosphate metabolism analyses and genome sequencing of both strains, grown at Cd stress, could be suggested. Associated work was carried out by Jasso-Chávez *et al.* (2019) as they investigated whether the polyphosphate level or genome mutations in the Cd resistant mutants of *Methanosarcina acetivorans* were responsible for the resistance. The Cd stress caused the metabolic adaptation of increased polyphosphate synthesis rather than inducing mutation in the genome as a mechanism to cope with Cd toxicity. Therefore, if this analysis was performed and the studied strains showed the response metabolism of polyphosphate, it would be possible to use these strains for Cd removal and phosphate from waters as the polyphosphate synthesis is mainly the sink for phosphate.

As no differences of the bacterial cell were observed in response to the effects of the Cd exposure, analysis of the functional groups (Fourier transform infrared spectroscopy, FTIR) of the bacterial cells before and after the exposure to Cd could indicate the complex interaction between these groups and Cd (Das *et al.*, 2014).

High angle annular dark-field scanning–transmission electron microscopy (HAADF-STEM) on bacterial cells are grown under exposure to Cd could be studied.

Lira-Silva *et al.* (2012) observed the intracellular accumulation of Cd in the cells of *Methanosarcina acetivorans* after they were grown with Cd, using HAADF-STEM.

EPS were observed more in the cells of both strains under exposure to Cd; therefore, the isolation of EPS (Gupta and Diwan, 2017) from the cells and the investigation of its role in Cd uptake could provide an alternative process of Cd removal rather than using whole bacterial cells.

The observations of the extracellular EPS and the intracellular P*β*HB molecules of the strains under SEM and TEM, respectively, allowed the proposal of their contributions in the Cd detoxification system. A more in-depth study of the investigation of the production of these molecules under Cd stress (Leonel *et al*., 2019) could provide additional knowledge about their roles during bacterial exposures to Cd. In addition, the observations of the morphological changes of these molecules using TEM images could indicate the Cd stress effect on their structures, the distribution of EPS around the bacterial cells, the size of P*β*HB granules, and the concentration of Cd inside the granules.

During the removal experiments of Cd in the column reactors, the mutant *B. agri* C15 Cd^R was able to absorb more Cd. It was not understood, whether the absorption was due to the exchange of ions, precipitation or complexation of Cd with the composition of Ca-alginate beads or due to the bioremediation of the biomass, bioaccumulation of Cd inside the cells (intracellular) or adsorption outside of the cell (extracellular). FTIR (Chand *et al.*, 2014) of the Cd-loaded Ca-alginate beads without bacterial cells, containing live cells of *B. agri* C15 or live cells of *B. agri* C15 Cd^R and the determination of the functional groups present on the surface of the beads will explain the binding mechanisms of Cd.

It is possible to investigate the surface complexation of Cd in *B. agri* C15 and *B. agri* C15 Cd^R for determining the model of the Cd adsorption reaction (Fein *et al*., 2001). Staining of Cd-loaded Ca-alginate beads with dithizone stain showed the distribution of Cd-dithizone complexes within the beads. Alternatively, using SEM imaging, EDX mapping, and X-ray photoelectron spectroscopy (XPS) (Boparai *et al*., 2013) could observe the distribution of Cd and predict the mechanism of absorbing Cd.

It is possible to run the reactor for an extended period (Gaza *et al.*, 2019) and depending on the removal rate during the operation time, the flow rate and the concentration of Cd could be altered. Therefore, the rate decreased at a specific time; the flow rate and the concentration of Cd must be reduced to less.

In this study, a constant room temperature of 22 °C was used for all the Cd removal experiments. This temperature allows the process to be implemented in an area with the same temperature. This process could be applied at groundwater temperature after investigating the process at temperatures ranging from 4 to 15 °C (Mosmeri *et al.*, 2017).

It would be possible to determine the absorption mechanism of Cd by the Ca-alginate beads, even if the ion exchange process is performed X-ray diffraction (XRD) or co-precipitation using FTIR (Yang *et al.*, 2019).

The ion exchange process of Cd with Ca in the Ca-alginate beads was estimated by measuring the concentrations of Ca in the beads before and after the process. The concentrations of Ca were high in some beads after the process, which reflected the ability of the studied strains to accumulate Ca (Handley-Sidhu *et al.*, 2011), and it could be applied for Ca accumulation.

The BARGE procedure has been applied to the Cd-loaded beads; however, this procedure can be applied to Cd-loaded beads and mixed with the soil to understand the accidental scenario of children's hand-to-mouth contact.

It would be possible to determine the Cd mineralogy in gastric and gastrointestinal phases under the BARGE assay (Ollson *et al*., 2016) to investigate the differences of the BAFs of Cd in the gastrointestinal system between the strains and matrixes.

8- References

Alonso, A., Sanchez, P., Martínez, J. L. (2000) *'Stenotrophomonas maltophilia* D457R contains a cluster of genes from gram-positive bacteria involved in antibiotic and heavy metal resistance'. *Antimicrob Agents Chemother*, 44:1778-1782.

Al Sadat Shafiof, M., Nezamzadeh-Ejhieh, A. (2020) 'A comprehensive study on the removal of Cd (II) from aqueous solution on a novel pentetic acid-clinoptilolite nanoparticles adsorbent: Experimental design, kinetic and thermodynamic aspects'. *Solid State Sci*, 99: 106071.

Al-Rashdi, B., Somerfield, C., Hilal, N. (2011) 'Heavy metals removal using adsorption and nanofiltration techniques'. *Sep Purif Rev*, 40: 209-259.

Angelim, A. L., Costa, S. P., Farias, B. C. S., Aquino, L. F., Melo, V. M. M. (2013). 'An innovative bioremediation strategy using a bacterial consortium entrapped in chitosan beads'. *J Environ Manage*, 127:10-17.

Altenburger, R., Brack, W., Burgess, R. M., Busch, W., Escher, B. I., Focks, A., Hewitt, L. M., Jacobsen, B. N., de Alda, M. L., Ait-Aissa, S. (2019). 'Future water quality monitoring: improving the balance between exposure and toxicity assessments of real-world pollutant mixtures'. *EnvironSci Eur*, 31:12-20.

Alviz Gazitua, P., Fuentes, S., Rojas, L. A., Turner, R. J., Guiliani, N. & Seeger, M. (2019) 'The response of *Cupriavidus metallidurans* CH34 to cadmium involves inhibition of the initiation of biofilm formation, decrease in intracellular c-di-GMP levels and a novel metal regulated phosphodiesterase'. *Front Microbiol*, 10:1499.

Al-Dahhan, M., Highfill, W. (1999). 'Liquid holdup measurement techniques in laboratory high pressure trickle bed reactors', *Can J Chem Eng*, 77: 759-765.

Anayurt, R. A., Sari, A., Tuzen, M. (2009). 'Equilibrium, thermodynamic and kinetic studies on biosorption of Pb (II) and Cd (II) from aqueous solution by macrofungus (*Lactarius scrobiculatus*) biomass'. *Chem Eng J*, 151: 255-261.

António, D. C., Cascio, C., Gilliland, D., Nogueira, A. J., Rossi, F., Calzolai, L. (2016). 'Characterization of silver nanoparticles-alginate complexes by combined size separation and size measurement techniques'. *Biointerphases*, 11:04B309.

Aujard-Catot, J., Nguyen, M., Bijani, C., Pratviel, G., Bonduelle, C. (2018). 'Cd^{2+} coordination: an efficient structuring switch for polypeptide polymers'. *Polym Chem*, 9: 4100-4107.

Arıca, M. Y., Kacar, Y., Genç, Ö. (2001). 'Entrapment of white-rot fungus *Trametes versicolor* in Ca-alginate beads: preparation and biosorption kinetic analysis for cadmium removal from an aqueous solution'. *Bioresou tech*, 80: 121-129.

Asokbunyarat, V., Lens, P. N., Annachhatre, A. P. (2017). 'Permeable Reactive Barriers for Heavy Metal Removal', *Sustainable Heavy Metal Remediation.* Springer: 65-100.

Aspinall, G. O. (2014) *The polysaccharides.* Academic Press.

ATSDR, Agency for Toxic Substances and Disease Registry, Faroon, O., Ashizawa, A., Wright, S., Tucker, P., Jenkins, K., Ingerman, L., Rudisill, C. (2012). 'Toxicological profile for cadmium, '. *Atlanta, Georgia*,

Azouaou, N., Sadaoui, Z., Mokaddem, H. (2008). 'Removal of cadmium from aqueous solution by adsorption on vegetable wastes'. *Applied Sci*, 8: 4638-4643.

Bang, S.-W., Clark, D. S. and Keasling, J. D. (2000a) 'Engineering hydrogen sulfide production and cadmium removal by expression of the thiosulfate reductase gene

Bang, S.-W., Clark, D. S., Keasling, J. D. (2000b) 'Cadmium, lead, and zinc removal by expression of the thiosulfate reductase gene from *Salmonella typhimurium* in *Escherichia coli'*. *Biotechnol Lett*, 22:1331-1335.

Banjerdkij, P., Vattanaviboon, P., Mongkolsuk, S. (2005). 'Exposure to cadmium elevates expression of genes in the *OxyR* and *OhrR* regulons and induces cross-resistance to peroxide killing treatment in *Xanthomonas campestris'*. *Appl Environ Microbiol*, 71: 1843-2049.

Banks, D. (1997). 'Hydrogeochemistry of millstone grit and coal measures groundwaters, south Yorkshire and north Derbyshire, UK'. *Q J Eng Geol*, 30: 237-256.

Bar, N., Das, S. K. (2016). 'Applicability of ANN in adsorptive removal of Cd (II) from aqueous solution', *Handbook of Research on Natural Computing for Optimization Problems.* IGI Global: 523-560.

Batu, V. (2005). Applied flow and solute transport modeling in aquifers: fundamental principles and analytical and numerical methods. CRC Press.

Bayramoglu, G., Denizli, A., Bektas, S., Arica, M. Y. (2002). 'Entrapment of *Lentinus sajorcaju* into Ca-alginate gel beads for removal of Cd (II) ions from aqueous solution: preparation and biosorption kinetics analysis'. *Microchem J*, 72: 63-76.

Bedessem, J., Cardoso, A., Darby, J., Forbort, J., Henderson, T., May, W., Molnaa, B., Nair, V., Spooner, C., Suarez, G. (2009). *In*: Evan K. Nyer (*ed*). Groundwater treatment technology, J. Wiley & Son.

Beisner, K. R., Paretti, N. V., Tillman, F. D., Naftz, D. L., Bills, D. J., Walton-Day, K., Gallegos, T. J. (2017). 'Geochemistry and hydrology of perched groundwater springs: assessing elevated uranium concentrations at Pigeon Spring relative to nearby Pigeon Mine, Arizona (USA)'. *Hydrogeol J,* 25: 539-556.

Berg, J. A., Merrill, B. D., Crockett, J. T., Esplin, K. P., Evans, M. R., Heaton, K. E., Hilton, J. A., Hyde, J. R., McBride, M. S., Schouten, J. T. (2016). 'Characterization of five novel *Brevibacillus* bacteriophages and genomic comparison of *Brevibacillus* phages'. *PloS one*, 11: e0156838.

Bhujbal, S. V., de Vos, P., Niclou, S. P. (2014). 'Drug and cell encapsulation: alternative delivery options for the treatment of malignant brain tumors'. *Adv Drug Deliv Rev*, 67:142-153.

Bilal, M., Iqbal, H. M. (2019). 'Lignin peroxidase immobilization on Ca-alginate beads and its dye degradation performance in a packed bed reactor system'. *Biocatal Agric Biotechnol*,101205:1-8.

Binet, M. R., Poole, R. K. (2000). 'Cd (II), Pb (II) and Zn (II) ions regulate expression of the metal-transporting P-type ATPase ZntA in *Escherichia coli*'. *FEBS letters*, 473: 67-70.

Boden, R., Thomas, E., Savani, P., Kelly, D.P., Wood, A.P., (2008). Novel methylotrophic bacteria isolated from the River Thames (London, UK*). Environ Microbiol,* 10: 3225-36.

Boden R., Hutt L.P. (2018). Determination of Kinetic Parameters and Metabolic Modes Using the Chemostat. *In*: Steffan R. (*eds*) Consequences of Microbial Interactions with Hydrocarbons, Oils, and Lipids: Biodegradation and Bioremediation. Handbook of Hydrocarbon and Lipid Microbiology. Springer, Cham:1-42.

Boyd, C. E. 2020. 'Dissolved solids', *Water Quality.* Springer: 83-118.

Boparai, H. K., Joseph, M., O'Carroll, D. M. (2013). 'Cadmium (Cd 2+) removal by nano zerovalent iron: surface analysis, effects of solution chemistry and surface complexation modeling'. *Environ Sci Pollut Res*, 20: 6210-6221.

Bozzola, J. J. (2007). 'Conventional specimen preparation techniques for transmission electron microscopy of cultured cells', *Electron Microscopy.* Springer: 1-20.

Brena B., González-Pombo P., Batista-Viera F. (2013). Immobilization of Enzymes: A Literature Survey. *In*: Guisan J. *(ed*), Immobilization of Enzymes and Cells. Methods in Molecular Biology (Methods and Protocols), vol 1051. Humana Press, Totowa, NJ: 15-31.

Bernard, A. (2008). 'Cadmium and its adverse effects on human health'**.** *Indian J Med Res*, 128: 557.

Brown T, Idoine N, Raycraft E, Shaw R, Hobbs S, Everett E .2018. World Mineral Production 2012-16: British Geological Survey. Accssed on March 17 2019. http://nora.nerc.ac.uk/id/eprint/519784/1/WMP_2012-2016_complete.pdf.

Bruins, M. R., Kapil, S., Oehme, F. W. (2000). 'Microbial resistance to metals in the environment'. *Ecotoxicol Environ Saf*, 45:198-207.

Bruins, M., Kapil, S., Oehme, F. (2001). 'Plasmid and chromosomal basis of tolerance to cadmium and resistance to antibiotics in normal bovine duodenal bacterial flora'. *Vet Hum Toxicol*, 43:129-133.

Brusseau, M. L. (2019). 'Soil and groundwater remediation', *Environmental and Pollution Science.* Elsevier: 329-354.

Bulut, Y. (2007). 'Removal of heavy metals from aqueous solution by sawdust adsorption'. *J Environ Sci*, 19:160-166.

Buragohain, M., Bhuyan, B., Sarma, H. P. (2010). 'Seasonal variations of lead, arsenic, cadmium and aluminium contamination of groundwater in Dhemaji district, Assam, India'. *Environ Assess Manag*, 170: 345-351.

Busenlehner, L. S., Weng, T.-C., Penner-Hahn, J. E., Giedroc, D. P. (2002). 'Elucidation of primary (α 3 N) and vestigial (α 5) heavy metal-binding sites in *Staphylococcus aureus* pI258 CadC: evolutionary implications for metal ion selectivity of ArsR/SmtB metal sensor proteins'. *J Mol Biol*, 319: 685-701.

Buszewski, B., Dziubakiewicz, E., Pomastowski, P., Hrynkiewicz, K., Ploszaj-Pyrek, J., Talik, E., Kramer, M., Albert, K. (2015). 'Assignment of functional groups in Gram-positive bacteria'. *J Anal Bioanal Tech*, 6:1-7.

Calvo, T. R. A., Perullini, M., Santagapita, P. R. (2018). 'Encapsulation of betacyanins and polyphenols extracted from leaves and stems of beetroot in Ca (II)-alginate beads: A structural study'. *J. Food Eng*, 235: 32-40.

Cámara-Martos, F., Ramírez-Ojeda, A., Jiménez-Mangas, M., Sevillano-Morales, J., Moreno-Rojas, R. (2019). 'Selenium and cadmium in bioaccessible fraction of organic weaning food: Risk assessment and influence of dietary components'. *JTEMB*, 56: 116-123.

Camargo, F., Okeke, B., Bento, F., Frankenberger, W. (2004). 'Hexavalent Chromium Reduction by Immobilized Cells and the Cell-Free Extract of *Bacillus* sp. ES 29'. *Bioremediat J*, 8: 23-30.

Cánovas, D., Cases, I., De Lorenzo, V. (2003). 'Heavy metal tolerance and metal homeostasis in *Pseudomonas putida* as revealed by complete genome analysis'. *Environ Microbiol*, 5:1242-1256.

Carro, L., Barriada, J. L., Herrero, R., de Vicente, M. E. S. (2015). 'Interaction of heavy metals with Ca-pretreated *Sargassum muticum* algal biomass: characterization as a cation exchange process'. *Chem Eng J*, 264:181-207.

Carrasco, J., Liu, W., Michaelides, A., Tkatchenko, A. (2014). 'Insight into the description of van der Waals forces for benzene adsorption on transition metal (111) surfaces'. *J Chem Phys*, 140: 084704.

Chakraborti, D., Rahman, M. M., Das, B., Murrill, M., Dey, S., Mukherjee, S. C., Dhar, R. K., Biswas, B. K., Chowdhury, U. K., Roy, S. (2010). 'Status of groundwater arsenic contamination in Bangladesh: a 14-year study report'. *Water Res*, 44: 5789-5802.

Chand, P., Shil, A. K., Sharma, M., Pakade, Y. B. (2014). 'Improved adsorption of cadmium ions from aqueous solution using chemically modified apple pomace: mechanism, kinetics, and thermodynamics.' *Int Biodeterior Biodegradation*, 90: 8-16.

Chao, Y., Zhang, T. (2011). 'Optimization of fixation methods for observation of bacterial cell morphology and surface ultrastructures by atomic force microscopy'. *Appl Microbiol Biotechnol*, 92:381-389.

Chen, B.-Y., Chen, C.-Y., Guo, W.-Q., Chang, H.-W., Chen, W.-M., Lee, D.-J., Huang, C.-C., Ren, N.-Q., Chang, J.-S. (2014). 'Fixed-bed biosorption of cadmium using immobilized *Scenedesmus obliquus* CNW-N cells on loofa (*Luffa cylindrica*) sponge'. *Bioresour. Technol*, 160: 175-201.

Choi, W.-J., Kang, S.-k., Wookyung, C. (2018). Chronic cadmium intoxication with renal injury among workers in a small-sclaed silver soldering company'.[in BMJ Publishing Group Ltd.

Chrestensen, C. A., Starke, D. W., Mieyal, J. J. (2000). 'Acute cadmium exposure inactivates thioltransferase (Glutaredoxin), inhibits intracellular reduction of protein-glutathionyl-mixed disulfides, and initiates apoptosis'. *J Biol Chem*, 275: 26556-26565.

Christensen, J. B., Jensen, D. L., Christensen, T. H. (1996). 'Effect of dissolved organic carbon on the mobility of cadmium, nickel and zinc in leachate polluted groundwater'. *Water Res*, 30: 3037-3049.

Chudobova, D., Dostalova, S., Ruttkay-Nedecky, B., Guran, R., Rodrigo, M. A. M., Tmejova, K., Krizkova, S., Zitka, O., Adam, V., Kizek, R. (2015). 'The effect of metal ions on *Staphylococcus aureus* revealed by biochemical and mass spectrometric analyses'. *Microbiol Res*, 170:147-156.

Chapman, P. M., Anderson, J. (2005). 'A decision-making framework for sediment contamination'. *Integr Environ Assess Manag*, 1: 163-173.

Clément, B., Lamonica, D. (2018). 'Fate, toxicity and bioconcentration of cadmium on Pseudokirchneriella subcapitata and Lemna minor in single mid-term tests'. *Ecotoxicol*, 27: 132-143.

Coker, A. K. (2001) Modeling of chemical kinetics and reactor design. vol. 1. Gulf Professional Publishing.

Cole, R., Frederick, R., Healy, R., Rolan, R. (1984). 'Preliminary findings of the priority pollutant monitoring project of the nationwide urban runoff program'. *J Water Pollut Control Fed,* 14: 898-908.

Colli-Serrano, M., Midoux, N. (2000). 'Hydrodynamics and heat transfer in packed bed with co-current up flow for coalescing and non-coalescing liquids. A simple model'. *Chem Eng Sci*, 55: 4149-4157.

Cooley, R. N., Haslock, H. R., Tomsett, A. B. (1986) 'Isolation and characterization of cadmium-resistant mutants of *Aspergillus nidulans'*. *Curr Microbiol*, 13:265-268.

Costa, F.,Tavares, T. (2016). 'Biosorption of nickel and cadmium in the presence of diethylketone by a *Streptococcus equisimilis* biofilm supported on vermiculite'. *Int Biodeterior Biodegradation*, 115:119-132.

Costa E, Teixido N, Usall J, Atares E, Vinas I (2002). The effect of nitrogen and carbon sources on growth of the biocontrol agent *Pantoea agglomerans* strain CPA-2. *Lett Appl Microbiol* 35:117–120.

Corbett, J. D., Burkhard, W. J., Druding, L. F. (1961). 'Stabilization of the Cadmium (I) Oxidation State. The System Cd-Cd2I (AlCl4) 2-Cd2 (AlCl4) 2'. *J Am Chem Soc*, 83: 76-80.

Clark, M., Walsh, S., Smith, J. (2001). 'The distribution of heavy metals in an abandoned mining area; a case study of Strauss Pit, the Drake mining area, Australia: implications for the environmental management of mine sites'. *Environ Geol*, 40: 655-663.

Croué, J.-P. (2004). 'Isolation of humic and non-humic NOM fractions: structural characterization'. *Environ Monit Assess*, 92:193-207.

Cunningham, D. P., Lundie, L. (1993). 'Precipitation of cadmium by *Clostridium thermoaceticum'*. *Appl Environ Microbiol*, 59:7-14.

da Silva Haas, I. C., Toaldo, I. M., Gomes, T. M., Luna, A. S., de Gois, J. S., Bordignon-Luiz, M. T. (2019). 'Polyphenolic profile, macro-and microelements in bioaccessible fractions of grape juice sediment using *in vitro* gastrointestinal simulation'. *Food Biosci*, 27: 66-74.

Das, D., Salgaonkar, B. B., Mani, K., Braganca, J. M. (2014). 'Cadmium resistance in extremely halophilic archaeon *Haloferax* strain BBK2'. *Chemosphere*,112: 385-392.

Das, S., Dash, H. R. (2017). Handbook of Metal-microbe Interactions and Bioremediation. CRC Press.

Datta, A., Sanyal, S., Saha, S. (2001). 'A study on natural and synthetic humic acids and their complexing ability towards cadmium'. *Plant Soil*, 235:115-125.

Davis, A., Heatwole, K., Greer, B., Ditmars, R., Clarke, R. (2010). 'Discriminating between background and mine-impacted groundwater at the Phoenix mine, Nevada USA'. *Appl Geochem*, 25: 400-417.

Davis, T. A., Volesky, B., Mucci, A. (2003). 'A review of the biochemistry of heavy metal biosorption by brown algae'. *Water Res*, 37: 4311-4330.

de Vos, P., Bučko, M., Gemeiner, P., Navrátil, M., Švitel, J., Faas, M., Strand, B. L., Skjak-Braek, G., Morch, Y. A., Vikartovská, A. (2009). 'Multiscale requirements for bioencapsulation in medicine and biotechnology'. *Biomaterials*, 30: 2559-2570.

de Souza, A. O., Pereira, C. C., Heling, A. I., Oreste, E. Q., Cadore, S., Ribeiro, A. S., Vieira, M. A. (2019). 'Determination of total concentration and bioaccessible fraction of metals in infant cereals by MIP OES'. *J Food Compost Anal*, 77:60-65.

Deng, X., Yi, X., Liu, G. (2007). 'Cadmium removal from aqueous solution by gene-modified *Escherichia coli* JM109'. *J Hazard Mater*, 139: 340-344.

Dixit, R., Malaviya, D., Pandiyan, K., Singh, U., Sahu, A., Shukla, R., Singh, B., Rai, J., Sharma, P., Lade, H. (2015). 'Bioremediation of heavy metals from soil and aquatic environment: an overview of principles and criteria of fundamental processes'. *Sustainability*, 7: 2189-2212.

Deng, Y., Ediriwickrema, A., Yang, F., Lewis, J., Girardi, M., Saltzman, W. M. (2015). 'A sunblock based on bioadhesive nanoparticles'. *Nat. Mater*, 14: 1278-1283.

Deze, E. G., Papageorgiou, S. K., Favvas, E. P., Katsaros, F. K. (2012). 'Porous alginate aerogel beads for effective and rapid heavy metal sorption from aqueous solutions: Effect of porosity in Cu^{2+} and Cd^{2+} ion sorption'. *Chem Eng J*, 209: 537-546.

Dippong, T. M, Cristina, Hoaghia, M, Cical, E, Cosma, A. (2019). Chemical modeling of groundwater quality in the aquifer of Seini town–Someș Plain, Northwestern Romania. *Ecotoxicol Environ Saf*, 168: 88-101.

Dirbaz, M.,Roosta, A. (2018). 'Adsorption, kinetic and thermodynamic studies for the biosorption of cadmium onto microalgae *Parachlorella* sp'. *J Environ Chem Eng*: 2302-2309.

Draget, K. I., Taylor, C. (2011). 'Chemical, physical and biological properties of alginates and their biomedical implications'. *Food Hydrocoll*, 25: 251-256.

Du, J., Qiu, B., Gomes, M. P., Juneau, P., Dai, G. (2019) 'Influence of light intensity on cadmium uptake and toxicity in the cyanobacteria *Synechocystis* sp. PCC6803'. *Aquat Toxicol*, 211:163-172.

Du, Y.-L., He, M.-M., Xu, M., Yan, Z.-G., Zhou, Y.-Y., Guo, G.-L., Nie, J., Wang, L.-Q., Hou, H., Li, F.-S. (2014). 'Interactive effects between earthworms and maize plants on the accumulation and toxicity of soil cadmium'. *Soil Biol Biochem*, 72:193-202.

Duan, J., Su, B. (2014). 'Removal characteristics of Cd (II) from acidic aqueous solution by modified steel-making slag'. *Chem Eng J*, 246:160-167.

Du Laing, G., Chapagain, S., Dewispelaere, M., Meers, E., Kazama, F., Tack, F., Rinklebe, J., Verloo, M. (2009). 'Presence and mobility of arsenic in estuarine wetland soils of the Scheldt estuary (Belgium)'. *J Environ Monit*, 11: 873-881.

Dzionek, A., Wojcieszyńska, D., Guzik, U. (2016). 'Natural carriers in bioremediation: A review'. *EJB*, 23: 28-36.

Edwards, D. E., Adams, W. J., Heitkamp, M. A. (1994). 'Laboratory-scale evaluation of aerobic fluidized bed reactors for the biotreatment of a synthetic, high-strength chemical industry waste stream'. *Water Environ Res*, 66:70-83.

El-Bestawy, E., El-KHeir, E. A., El-Fatah, H. A. & Hassouna, S. (1998). 'Enhancement of bacterial efficiency for metal removal using mutation techniques'. *World J Microbiol Biotechnol*, 14: 853.

El-Naggar, N. E.-A., Hamouda, R. A., Mousa, I. E., Abdel-Hamid, M. S., Rabei, N. H. (2018). 'Statistical optimization for cadmium removal using *Ulva fasciata* biomass: characterization, immobilization and application for almost-complete cadmium removal from aqueous solutions'. *Sci Rep*, 8:12456-12461.

Escudero, C., Fiol, N., Villaescusa, I., Bollinger, J.-C. (2009). 'Arsenic removal by a waste metal (hydr) oxide entrapped into calcium alginate beads'. *J Hazard Mater*, 164: 533-541.

EA (2015) Contaminated land exposure assessment (CLEA) tool. CLEA Software Version 1.071. [available on-line]

https://www.gov.uk/government/publications/contaminated-land-exposure-assessment-clea-tool.

Etchie, A. T., Etchie, T. O., Adewuyi, G. O. (2012). 'Systemic chronic health risk assessment of residential exposure to Cd^{2+} and Cr^{6+} in groundwater'. *Toxicol Environ Chem*, 94:181-194.

Evans, G. M., Furlong, J. C. (2003). Environmental biotechnology: theory and application. IK International Pvt Ltd.

EC (2000). Directive 2000/60/EC of the European Parliament and of the Council of 23 October 2000 establishing a framework for community action in the field of Water Policy. In: L327/1, pp. 72. Official Journal of the European Communities (22/12/2000).

Fawcett, H. S. (1925). 'MAINTAINED GROWTH RATES IN FUNGUS CULTURES OF LONG DURATION 1'. *Ann Appl Biol*, 12:191-198.

Fein, J. B., Martin, A. M., Wightman, P. G. (2001). 'Metal adsorption onto bacterial surfaces: development of a predictive approach'. *Geochim Cosmochim Acta*, 65: 4267-4273.

Feng, M., Chen, X., Li, C., Nurgul, R., Dong, M. (2012). 'Isolation and identification of an Exopolysaccharide-Producing lactic acid bacterium strain from chinese paocai and biosorption of Pb (II) by its exopolysaccharide' *J Food Sci*., 6: 77-83.

Ferreira, L., Rosales, E., Sanromán, M., Pazos, M. (2014). 'Preliminary testing and design of permeable bioreactive barrier for phenanthrene degradation by *Pseudomonas stutzeri* CECT 930 immobilized in hydrogel matrices'. *Chem Technol Biotechnol,* 90:500-506.

Fetter, C.W. (1999). Contaminant hydrogeology. 2. edition. United States.

Fitch, M. W., Pearson, N., Richards, G., Burken, J. G. (1998). 'Biological fixed-film systems'. *Water Environ Res*, 70: 495-518.

Fischer, E.R, Hansen B.T, Nair V. (2012). Scanning electron microscopy. *Curr Prot in Microbiol*. 25: 2B.2.1- 2B.2.47.

Freeman, D.J, Falkiner, F.R, Keane, C.T. (1989). New method for detecting slime production by coagulase negative *staphylococci*. *J Clin Pathol*. 42: 872-874.

Fu, D., Singh, R. P., Yang, X., Ojha, C., Surampalli, R. Y., Kumar, A. J. (2018). 'Sediment in-situ bioremediation by immobilized microbial activated beads: Pilot-scale study'. *J Environ Manage*, 226: 62-69.

Fu, F., Wang, Q. (2011). 'Removal of heavy metal ions from wastewaters: a review'. *J Environ Manage*, 92:407-418.

Food and Agriculture Organization/World Health Organization (FAO/WHO). 2010. Seventy-third Meeting, Geneva, 8–17 June 2010. Summary and Conclusions. JECFA/73/SC

García, S., Prado, M., Dégano, R., Domínguez, A. (2002). 'A copper-responsive transcription factor, CRF1, mediates copper and cadmium resistance in *Yarrowia lipolytica*'. *J Biol Chem*, 277: 37359-37368.

Gaza, S., Schmidt, K. R., Weigold, P., Heidinger, M., Tiehm, A. (2019). 'Aerobic metabolic trichloroethene biodegradation under field-relevant conditions'. *Water Res*, 151: 343-348.

Geng, Y., Deng, Y., Chen, F., Jin, H., Hou, T., Tao, K. (2016). 'Isopropanol biodegradation by immobilized *Paracoccus denitrificans* in a three-phase fluidized bed reactor'. *Prep Biochem Biotechno*, 46:747-754.

Geisler, E., Bogler, A., Rahav, E., Bar-Zeev, E. (2019). 'Direct Detection of Heterotrophic Diazotrophs Associated with Planktonic Aggregates'. *Sci Rep*, 9: 1-9.

Ghosh, S., Debsarkar, A., Dutta, A. (2018). 'Technology alternatives for decontamination of arsenic-rich groundwater—A critical review'. *Environ Technol Innov*, 13:76-54.

Ghosh, S., Mahapatra, N., Banerjee, P. (1997). 'Metal resistance in Acidocella strains and plasmid-mediated transfer of this characteristic to Acidiphilium multivorum and *Escherichia coli*'. *Appl Environ Microbiol*, 63: 4523-4527.

Glendinning, K., Macaskie, L., Brown, N. (2005). 'Mercury tolerance of *thermophilic Bacillus* sp. and *Ureibacillus* sp'. *Biotechnol Lett*, 27: 1657-1662.

Gokhale, S. V., Tayal, R. K., Jayaraman, V. K., Kulkarni, B. D. (2005). 'Microchannel reactors: applications and use in process development'. *IJCRE*, 3:34-42.

Gomri, M. A., Rico-Díaz, A., Escuder-Rodríguez, J.-J., El Moulouk Khaldi, T., González-Siso, M.-I., Kharroub, K. (2018) 'Production and Characterization of an Extracellular Acid Protease from *Thermophilic Brevibacillus* sp. OA30 Isolated from an Algerian Hot Spring'. *Microorganisms*, 6: 31-39

Gondar, D., López, R., Fiol, S., Antelo, Arce, F. (2006) 'Cadmium, lead, and copper binding to humic acid and fulvic acid extracted from an ombrotrophic peat bog'. *Geoderma*, 135:196-203.

Grass, G., Wong, M. D., Rosen, B. P., Smith, R. L., Rensing, C. (2002). 'ZupT is a Zn (II) uptake system in *Escherichia coli'*. *JB*, 184: 864-866.

Green-Ruiz, C., Rodriguez-Tirado, V., Gomez-Gil, B. (2008). 'Cadmium and zinc removal from aqueous solutions by *Bacillus jeotgali*: pH, salinity and temperature effects'. *Bioresour Technol*, 99: 3864-3870.

Grau, J. M., Bisang, J. M. (2001). 'Electrochemical removal of cadmium using a batch undivided reactor with a rotating cylinder electrode'. *J. Chem Technol Biotechnol*, 76: 161-168.

Grillo-Puertas, M., Schurig-Briccio, L. A., Rodríguez-Montelongo, L., Rintoul, M. R., Rapisarda, V. A. (2014). 'Copper tolerance mediated by polyphosphate degradation and low-affinity inorganic phosphate transport system in *Escherichia coli*'. *BMC microbiol*, 14: 72-78.

Groschen, G. E., Arnold, T. L., Morrow, W. S., Warner, K. L. (2009). 'Occurrence and distribution of iron, manganese, and selected trace elements in ground water in the glacial aquifer system of the Northern United States'. U. S. Geological Survey.

Gupta, P., Diwan, B. (2017). 'Bacterial Exopolysaccharide mediated heavy metal removal: a review on biosynthesis, mechanism and remediation strategies'. *Biotechnol Rep*, 13: 58-71.

Gupta, C., Prakash, D. (2020). 'Novel bioremediation methods in waste management: Novel bioremediation methods', *Waste Management: Concepts, Methodologies, Tools, and Applications. IGI Global*: 1627-1643.

Gustafsson, J. (2011). 'Visual MINTEQ Version 3.1: A Windows version of MINTEQA2'.

Gyamfi, A. A., Al Shaikhly, M., Al-Assaf, S., Al-Dahhan, M., Bandeira, J. V., Abdelouahed, H. B., Bjørnstad, T., Boutaine, J.-L., Bryazgin, A., Chaouki, J. (2017). *ICARST,* IAEA: 218-223.

Haas, J. R., Dichristina, T. J., Wade Jr, R. (2001). 'Thermodynamics of U (VI) sorption onto *Shewanellaputrefaciens*'. *Chem Geol*, 180: 33-54.

Handley-Sidhu, S., Renshaw, J. C., Yong, P., Kerley, R., Macaskie, L. E. (2011) .'Nano-crystalline hydroxyapatite bio-mineral for the treatment of strontium from aqueous solutions'. *Biotechnol Lett*, 33: 79-87.

Hashim, M. A., Mukhopadhyay, S., Sahu, J. N., Sengupta, B. (2011). 'Remediation technologies for heavy metal contaminated groundwater'. *J Environ Manage*, 92: 2355-2388.

Handy, R., Runnalls, T., Russell, P. (2002). 'Histopathologic biomarkers in three spined sticklebacks, Gasterosteus aculeatus, from several rivers in Southern England that meet the freshwater fisheries directive'. *Ecotoxicology*, 11: 467-479.

Han, R., Wang, Y., Zou, W., Wang, Y., Shi, J. (2007). 'Comparison of linear and nonlinear analysis in estimating the Thomas model parameters for methylene blue adsorption onto natural zeolite in fixed-bed column'. *J Hazard Mater*, 145: 331-335.

Hao, Z., Reiske, H. R., Wilson, D. B. (1999). 'Characterization of cadmium uptake in *Lactobacillus plantarum* and isolation of cadmium and manganese uptake mutants'. *Appl Environ Microbiol*, 65: 4741-4745.

Harland, C. E. (2007). *Ion exchange: theory and practice.* Royal Society of Chemistry.

Helbig, K., Grosse, C., Nies, D. H. (2008). 'Cadmium toxicity in glutathione mutants of *Escherichia coli*'. *JB*. 190: 5439-5454.

Hellström, L., Elinder, C.-G., Dahlberg, B., Lundberg, M., Järup, L., Persson, B, Axelson, O. (2001). 'Cadmium exposure and end-stage renal disease'. *Am J Kidney Dis*, 38:1001-1008.

Henderson, A. D., Demond, A. H. (2007). 'Long-term performance of zero-valent iron permeable reactive barriers: a critical review' *Environ Eng Sci*, 24: 401-423.

Henry, J. R. (2000). An overview of the phytoremediation of lead and mercury. US Environmental Protection Agency, Office of Solid Waste and Emergency Response, Technology Innovation Office Washington, DC.

Herreros-Chavez, L., Cervera, M., Morales-Rubio, A. (2019). 'Direct determination by portable ED-XRF of mineral profile in cocoa powder samples'. *Food Chem*, 278: 373-379.

Herrmann, L., Schwan, D., Garner, R., Mobley, H. L., Haas, R., Schäfer, K. P., Melchers, K. (1999). *'Helicobacter pylori cadA* encodes an essential Cd (II)–Zn (II)–Co (II) resistance factor influencing urease activity'. *Mol Microbiol*, 33: 524-536.

Hetzer, A., Daughney, C. J., Morgan, H. W. (2006). 'Cadmium ion biosorption by the thermophilic bacteria *Geobacillus stearothermophilus* and *G. thermocatenulatus'*. *Appl Environ Microbiol*, 72: 4020-4027.

Higham, D. P., Sadler, P. J., Scawen, M. D. (1984). 'Cadmium-resistant *Pseudomonas putida* synthesizes novel cadmium proteins'. *Science*, 225: 1043-1046.

Hoare, T. R., Kohane, D. S. (2008). 'Hydrogels in drug delivery: Progress and challenges'. *Polymer*, 49: 1993-2007.

Hobley, L., Harkins, C., MacPhee, C. E., Stanley-Wall, N. R. (2015). 'Giving structure to the biofilm matrix: an overview of individual strategies and emerging common themes'. *FEMS Microbiol Rev*, 39:649-669.

Hochstrat, R., Wintgens, T., Corvini, P. (2015). '*Immobilised biocatalysts for bioremediation of groundwater and wastewater'.* Iwa Publishing.

Hong, W., Pang, B., West-Barnette, S., Swords, W. E. (2007). 'Phosphorylcholine expression by *nontypeable Haemophilus influenzae* correlates with maturation of biofilm communities in vitro and in vivo'. *JB*, 189: 8300-8307.

Horitsu, H., Kato, H. (1980). 'Comparisons of characteristics of cadmium-tolerant bacterium, *Pseudomonas aeruginosa* G-1 and its cadmium-sensitive mutant strain'. *Agri Biol Chem*, 44: 777-782.

Hossain, A., Bhattacharyya, S. R., Aditya, G. (2015). 'Biosorption of cadmium from aqueous solution by shell dust of the freshwater snail *Lymnaea luteola'*. *Environ Technol and Innovation*, 4: 82-91.

Howard, A. J., Kincey, M., Carey, C. (2015). 'Preserving the legacy of historic metal-mining industries in light of the water framework directive and future environmental change in Mainland Britain: challenges for the heritage community'. *The Historic Environment: Policy & Practice*, 6: 3-15.

Houben, G. J., Sitnikova, M. A., Post, V. E. (2017). 'Terrestrial sedimentary pyrites as a potential source of trace metal release to groundwater–A case study from the Emsland, Germany'. *Appl Geochem*, 76: 99-111.

Holman, I. P., Howden, N. J., Bellamy, P., Willby, N., Whelan, M. J., Rivas-Casado, M. (2010). 'An assessment of the risk to surface water ecosystems of groundwater P in the UK and Ireland'. *Sci Total Environ*, 408:1847-1857.

Huang, F., Dang, Z., Guo, C.-L., Lu, G.-N., Gu, R. R., Liu, H.-J., Zhang, H. (2013) 'Biosorption of Cd (II) by live and dead cells of *Bacillus cereus* RC-1 isolated from cadmium-contaminated soil'. *Colloids Surf B*, 107:11-20.

Huang, Z., Liu, D., Zhao, H., Zhang, Y., Zhou, W. (2017). 'Performance and microbial community of aerobic dynamic membrane bioreactor enhanced by Cd (II)-accumulating bacterium in Cd (II)-containing wastewater treatment'. *Chem Eng J*, 317: 368-375.

Hudson, N., Baker, A., Reynolds, D. (2007). 'Fluorescence analysis of dissolved organic matter in natural, waste and polluted waters—a review'. *River Res Appl*, 23: 631-649.

Hugouvieux, V., Dutilleul, C., Jourdain, A., Reynaud, F., Lopez, V., Bourguignon, J. (2009). 'Arabidopsis putative selenium-binding protein1 expression is tightly linked to cellular sulfur demand and can reduce sensitivity to stresses requiring glutathione for tolerance'. *Plant Physiol*, 151: 768-781.

Hynninen, A., Tõnismann, K., Virta, M. (2010). 'Improving the sensitivity of bacterial bioreporters for heavy metals'. *Bioeng Bugs*, 1:132-138.

Ike, A., Sriprang, R., Ono, H., Murooka, Y., Yamashita, M. (2007). 'Bioremediation of cadmium contaminated soil using symbiosis between leguminous plant and recombinant rhizobia with the MTL4 and the PCS genes'. *Chemosphere*, 66: 1670-1676.

Ireland, N., Vincent, K., Passant, N. (2006). 'Assessment of Heavy Metal Concentrations in the United Kingdom'. Report to the Department for Environment, Food and Rural Affairs, Welsh Assembly Government, the Scottish Executive and the Department of the Environment for Northern Ireland.

Jaafari, J., Yaghmaeian, K. (2019). 'Optimization of heavy metal biosorption onto freshwater algae (*Chlorella coloniales*) using response surface methodology (RSM)'. *Chemosphere*, 217: 447-455.

Jain, S., Arnepalli, D. (2019). 'Biominerlisation as a remediation technique: A critical review', *Geotechnical Characterisation and Geoenvironmental Engineering.* Springer: 155-162.

Jasso-Chávez, R., Lira-Silva, E., González-Sánchez, K., Larios Serrato, V., Mendoza-Monzoy, D. L., Pérez-Villatoro, F., Morett, E., Vega-Segura, A., Torres-Márquez, M. E., Zepeda-Rodríguez, A. (2019). 'Marine archaeon *Methanosarcina acetivorans*

enhances polyphosphate metabolism under persistent cadmium stress'. *Front Microbiol*, 10: 2432.

Jiang, C, Sun H, Sun T, Zhang Q, Zhang Y. (2009). 'Immobilization of cadmium in soils by UV-mutated *Bacillus subtilis* 38 bioaugmentation and NovoGro amendment'. *J Hazard Mater*,167:1170-7.

Jiang, W., Saxena, A., Song, B., Ward, B. B., Beveridge, T. J., Myneni, S. C. (2004). 'Elucidation of functional groups on gram-positive and gram-negative bacterial surfaces using infrared spectroscopy'. *Langmuir*, 20:11433-11442.

Kacar, Y., Arpa, Ç., Tan, S., Denizli, A., Genç, Ö., Arıca, M. Y. (2002). 'Biosorption of Hg (II) and Cd (II) from aqueous solutions: comparison of biosorptive capacity of alginate and immobilized live and heat inactivated *Phanerochaete chrysosporium*'. *Process Biochem*, 37: 601-610.

Kadirvelu, K., Namasivayam, C. (2003). 'Activated carbon from coconut *coirpith* as metal adsorbent: adsorption of Cd (II) from aqueous solution'. *Adv. Environ. Res*, 7: 471-478.

Kaewsarn, P.,Yu, Q. (2001). 'Cadmium (II) removal from aqueous solutions by pre-treated biomass of marine alga *Padina* sp'. *Environ Pollut*, 112:209-213.

Kanematsu, M., Young, T. M., Fukushi, K., Green, P. G., Darby, J. L. (2013). 'Arsenic (III, V) adsorption on a goethite-based adsorbent in the presence of major co-existing ions: modeling competitive adsorption consistent with spectroscopic and molecular evidence'.*Geochim Cosmochim Acta*, 106: 404-428.

Katırcıoğiu, H., Aslım, B., Türker, A. R., Atıcı, T., Beyatlı, Y. (2008). 'Removal of cadmium (II) ion from aqueous system by dry biomass, immobilized live and heat-

inactivated *Oscillatoria* sp. H1 isolated from freshwater (Mogan Lake)'. *Bioresour Technol*, 99: 4185-4191.

Kazemipour, M., Ansari, M., Tajrobehkar, S., Majdzadeh, M., Kermani, H. R. (2008). 'Removal of lead, cadmium, zinc, and copper from industrial wastewater by carbon developed from walnut, hazelnut, almond, pistachio shell, and apricot stone'. *J Hazard Mater*, 150: 322-327.

Kehres, D. G., Janakiraman, A., Slauch, J. M. & Maguire, M. E. (2002). 'SitABCD is the alkaline Mn^{2+} transporter of *Salmonella enterica serovar Typhimurium'*. *J Bacteriol*, 184: 3159-3166.

Khairnar, N. P., Joe, M.-H., Misra, H., Lim, S.-Y., Kim, D.-H. (2013). 'FrnE, a Cadmium-Inducible Protein in *Deinococcus radiodurans*, Is Characterized as a Disulfide Isomerase Chaperone In Vitro and for Its Role in Oxidative Stress Tolerance *In Vivo'*. *J Bacteriol*, 195: 2880-2886.

Khan, Z., Nisar, M. A., Hussain, S. Z., Arshad, M. N., Rehman, A. (2015). 'Cadmium resistance mechanism in *Escherichia coli* P4 and its potential use to bioremediate environmental cadmium'. *Appl Microbiol Biotechnol*, 99: 10745-10757.

Khan, Z., Rehman, A., Hussain, S. Z., Nisar, M. A., Zulfiqar, S,Shakoori, A. R. (2016). 'Cadmium resistance and uptake by bacterium, *Salmonella enterica* 43C, isolated from industrial effluent'. *AMB Express*, 6: 54-64.

Kiernan, J. A. (2008). Methods for inorganic ions, *Histological and histochemical methods: theory and practice.* 4th ed, Bloxham, United Kingdom, 344-347.

Kim, Y., Bae, J., Park, H., Suh, J.-K., You, Y.-W., Choi, H. (2016). 'Adsorption dynamics of methyl violet onto granulated mesoporous carbon: Facile synthesis and adsorption kinetics'. *Water Res*, 101:187-194.

Knobel, L., Bartholomay, R., Cecil, L., Tucker, B., Wegner, S. (1992). Chemical constituents in the dissolved and suspended fractions of ground water from selected sites, Idaho National Engineering Laboratory and vicinity, Idaho, 1989. Geological Survey, Idaho Falls, ID (United States). Available at:

https://pubs.usgs.gov/of/1992/0051/report.pdf.

Kocaoba, S. (2007). 'Comparison of Amberlite IR 120 and dolomite's performances for removal of heavy metals'. *J Hazard Mater*, 147: 488-496.

Kolev, N. (2006) *Packed bed columns: for absorption, desorption, rectification and direct heat transfer.* 1st ed. Elsevier Science.

Kotrba, P., Dolečková, L., de Lorenzo, V., Ruml, T. (1999). 'Enhanced bioaccumulation of heavy metal ions by bacterial cells due to surface display of short metal binding peptides'. *Appl Environ Microbiol*, 65: 1092-1098.

Konhauser, K. O. (2009). *Introduction to geomicrobiology.* John Wiley & Sons.

Kuiper, N., Rowell, C., Shomar, B. (2015). 'High levels of molybdenum in Qatar's groundwater and potential impacts'. *J Geochem Explor*, 150:16-24.

Kumar, S., Stecher, G., Tamura, K. (2016). 'MEGA7: molecular evolutionary genetics analysis version 7.0 for bigger datasets'. *Mol Biol Evol.*, 33: 1870-2074.

Kuppusamy, S., Palanisami, T., Megharaj, M., Venkateswarlu, K., Naidu, R. (2016). 'In-situ remediation approaches for the management of contaminated sites: a comprehensive overview', *Rev Environ Contam Toxicol.* 236:1-115.

Kuroda, M., Ohta, T., Uchiyama, I., Baba, T., Yuzawa, H., Kobayashi, I., Cui, L., Oguchi, A., Aoki, K.-i., Nagai, Y. (2001). 'Whole genome sequencing of meticillin-resistant *Staphylococcus aureus'*. *The Lancet*, 357: 1225-1240.

Krystyna, P. (2019). Removal of cadmium from wastewaters with low-cost adsorbents, *J Environ Chem Eng*, 7: 102795,

Langwaldt, J., Puhakka, J. (2000). 'On-site biological remediation of contaminated groundwater: a review'. *Environ Pollut*, 107: 187-197.

Lebrun, M., Audurier, A., Cossart, P. (1994). 'Plasmid-borne cadmium resistance genes in *Listeria monocytogenes* are similar to *cadA* and *cadC* of *Staphylococcus aureus* and are induced by cadmium'. *JB*. 176:3040-3048.

Lee, S.-W., Glickmann, E., Cooksey, D. A. (2001) 'Chromosomal locus for cadmium resistance in *Pseudomonas putida* consisting of a cadmium-transporting ATPase and a MerR family response regulator'. *Appl Environ Microbiol.*, 67:1437-1444.

Leedjärv, A., Ivask, A., Virta, M. (2008). 'Interplay of different transporters in the mediation of divalent heavy metal resistance in *Pseudomonas putida* KT2440'. *JB*, 190: 2680-2689.

Leonel, T. F., Moretto, C., Castellane, T. C. L., da Costa, P. I., de Macedo Lemos, E. G. (2019). 'The Influence of Cooper and Chromium Ions on the Production of Exopolysaccharide and Polyhydroxybutyrate by *Rhizobium tropici* LBMP-C01'. *J Polym Environ*, 27: 445-455.

Leyva-Ramos, R., Bernal-Jacome, L., Acosta-Rodriguez, I. (2005). 'Adsorption of cadmium (II) from aqueous solution on natural and oxidized corncob'. *Sep Purif Technol*, 45: 41-49.

Lehninger AL, Nelson DL, & Cox MM (2008). Lehninger principles of biochemistry, W.H. Freeman, New York, 5th Ed.

Li, Y.-H., Wang, S., Luan, Z., Ding, J., Xu, C. & Wu, D. (2003) 'Adsorption of cadmium (II) from aqueous solution by surface oxidized carbon nanotubes'. *Carbon*, 41: 1057-1062.

Lira-Silva, E., Santiago-Martínez, M. G., Hernández-Juárez, V., García-Contreras, R., Moreno-Sánchez, R., Jasso-Chávez, R. (2012). 'Activation of methanogenesis by cadmium in the marine archaeon Methanosarcina acetivorans'. *PloS one*, 7: e48779.

Liu, J., Qu, W., Kadiiska, M. B. (2009). 'Role of oxidative stress in cadmium toxicity and carcinogenesis'. *Toxicol Appl Pharmacol*, 238: 209-214.

Liang, X., Han, J., Xu, Y., Sun, Y., Wang, L., Tan, X. (2014). 'In situ field-scale remediation of Cd polluted paddy soil using sepiolite and palygorskite'. *Geoderma*, 235: 9-18.

Liu, W., Luo, Y., Teng, Y., Li, Z., Ma, L. Q. (2010). 'Bioremediation of oily sludge-contaminated soil by stimulating indigenous microbes'. *Environ Geochem Health* , 32: 23-29.

Liu, C., Bai, R., Hong, L., Liu, T. (2010). 'Functionalization of adsorbent with different aliphatic polyamines for heavy metal ion removal: Characteristics and performance'. *J Colloid Interface Sci*, 345: 454-460.

Li, Z. and Zhou, L. (2010). 'Cadmium transport mediated by soil colloid and dissolved organic matter: a field study'. *J Environ Sci*, 22: 106-115.

Li, X., Islam, M. M., Chen, L., Wang, L. & Zheng, X. (2020) 'Metagenomics-guided discovery of potential bacterial metallothionein genes conferring Cu/Cd resistance from soil microbiome'. *Appl. Environ. Microbiol*, 86: e02907-19

Lv, Y., Ezemaduka, A. N., Wang, Y., Xu, J., Li, X. (2019). 'AgsA response to cadmium and copper effects at different temperatures in *Escherichia coli*'. *J Biochem Mol Toxicol*.,e22344:10-7.

Locatelli, L., Binning, P. J., Sanchez-Vila, X., Søndergaard, G. L., Rosenberg, L., Bjerg, P. L. (2019). 'A simple contaminant fate and transport modelling tool for management and risk assessment of groundwater pollution from contaminated sites'. *J Contam Hydrol*, 221:35-49.

Lu, W.-B., Shi, J.-J., Wang, C.-H. and Chang, J.-S. (2006) 'Biosorption of lead, copper and cadmium by an indigenous isolate *Enterobacter* sp. J1 possessing high heavy-metal resistance'. *J Hazard Mater*, 134: 80-86.

Macaskie, L. E., Dean, A. (1982) 'Cadmium accumulation by micro-organisms'. *Environ Technol*, 3: 49-56.

Mahapatra, N. R., Banerjee, P. (1996). 'Extreme tolerance to cadmium and high resistance to copper, nickel and zinc in different Acidiphilium strains'. *Lett Appl Microbiol*, 23: 393-397.

Mao, J., Won, S. W., Yun, Y.-S. (2013) 'Development of poly (acrylic acid)-modified bacterial biomass as a high-performance biosorbent for removal of Cd (II) from aqueous solution'. *Ind Eng Chem Res*, 52: 6446-6452.

Marche, M. G., Mura, M. E., Falchi, G., Ruiu, L. (2017) 'Spore surface proteins of *Brevibacillus laterosporus* are involved in insect pathogenesis'. *Sci. Rep*, 7: 43805-43811.

Marques, P., Pinheiro, H. M., Rosa, M. F. (2007). 'Cd (II) removal from aqueous solution by immobilised waste brewery yeast in fixed-bed and airlift reactors'. *Desalination*, 214: 343-351.

Marusak, K., Feng, Y., Eben, C., Payne, S., Cao, Y., You, L., Zauscher, S. (2016). 'Cadmium sulphide quantum dots with tunable electronic properties by bacterial precipitation'. *RSC Advances*, 6: 76158-76166.

Marval-León, J. R., Cámara-Martos, F., Amaro-López, M. A., Moreno-Rojas, R. (2014) 'Bioaccessibility and content of Se in fish and shellfish widely consumed in Mediterranean countries: influence of proteins, fat and heavy metals'. *Int J Food Sci Nutr*, 65: 678-685.

Masoudzadeh, N., Zakeri, F., bagheri Lotfabad, T., Sharafi, H., Masoomi, F., Zahiri, H. S., Ahmadian, G., Noghabi, K. A. (2011) 'Biosorption of cadmium by *Brevundimonas* sp. ZF12 strain, a novel biosorbent isolated from hot-spring waters in high background radiation areas'. *J Hazard Mater*, 197: 190-198.

Massaccesi, G., Romero, M. C., Cazau, M. C., Bucsinszky, A. M. (2002). 'Cadmium removal capacities of filamentous soil fungi isolated from industrially polluted sediments, in La Plata (Argentina)'. *World J Microbiol Biotechnol*, 18: 817-820.

Mateo, C., Palomo, J. M., Van Langen, L. M., Van Rantwijk, F., Sheldon, R. A. (2004). 'A new, mild cross-linking methodology to prepare cross-linked enzyme aggregates'. *Biotechnol Bioeng,* 8: 273-276.

Matlock, M. M., Henke, K. R., Atwood, D. A. (2002). 'Effectiveness of commercial reagents for heavy metal removal from water with new insights for future chelate designs'. *J Hazard Mater*, 92:129-142.

Mattiasson, B. (2018). 'Immobilization methods'. *Immobilized cells and organelles.* Vol. 1, CRC Press, Boca Raton : 3-26.

Matyar, F., Kaya, A., Dinçer, S. (2008). 'Antibacterial agents and heavy metal resistance in Gram-negative bacteria isolated from seawater, shrimp and sediment in Iskenderun Bay, Turkey'. *Sci Total Environ*, 407: 279-285.

McBride, M. B., Spiers, G. (2001). TRACE ELEMENT CONTENT OF SELECTED FERTILIZERS AND DAIRY MANURES AS DETERMINED BY ICP–MS*, Commun Soil Sci Plant Anal*, 32:139-156.

McEldowney, S. (2000) 'The impact of surface attachment on cadmium accumulation by *Pseudomonas fluorescens* H2'. *FEMS Microbiol Ecol*, 33: 121-128.

Mergeay, M., Nies, D., Schlegel, H., Gerits, J., Charles, P., Van Gijsegem, F. (1985). '*Alcaligenes eutrophus* CH34 is a facultative chemolithotroph with plasmid-bound resistance to heavy metals'. *Jb*, 162:328-334.

Mendes, A. A., Oliveira, P. C., Vélez, A. M., Giordano, R. C., de LC Giordano, R., de Castro, H. F. (2012). 'Evaluation of immobilized lipases on poly-hydroxybutyrate beads to catalyze biodiesel synthesis'. *Int J BiolMacromol*. 50: 503-511.

Missiakas, D., Raina, S. (1997). 'Protein folding in the bacterial periplasm'. *J Bacteriol*, 179: 2465.

Ming, L., Li, L., Zhang, Y., Lin, W., Wang, G., Zhang, S., Guo, P. (2014). 'Effects of dissolved organic matter on the desorption of Cd in freeze–thaw treated Cd-contaminated soils'. *Chem Biol*, 30: 76-86.

Mobasherpour, I., Salahi, E., Pazouki, M. (2011). 'Removal of divalent cadmium cations by means of synthetic nano crystallite hydroxyapatite'. *Desalination*, 266:142-148.

Mohan, D., Singh, K. P. (2002). 'Single-and multi-component adsorption of cadmium and zinc using activated carbon derived from bagasse: an agricultural waste'. *Water Res*, 36: 2304-2318.

Mohapatra, R. K., Parhi, P. K., Pandey, S., Bindhani, B. K., Thatoi, H., Panda, C. R. (2019). 'Active and passive biosorption of Pb (II) using live and dead biomass of marine bacterium *Bacillus xiamenensis* PbRPSD202: Kinetics and isotherm studies'. *J Environ Manage*, 247:121-134.

Mohnen, D. (2008) 'Pectin structure and biosynthesis'. *Curr Opin Plant Biol*, 11: 266-277.

Morway, E. D., Thodal, C. E. & Marvin-DiPasquale, M. (2017). 'Long-term trends of surface-water mercury and methylmercury concentrations downstream of historic mining within the Carson River watershed'. *Environ Pollut*, 229: 1006-1018.

Moon, R. J., Martini, A., Nairn, J., Simonsen, J., Youngblood, J. (2011). 'Cellulose nanomaterials review: structure, properties and nanocomposites'. *Chem Soc Rev*, 40: 3941-3994.

Monod, J. (1949). 'The growth of bacterial cultures'. *Annu Rev Microbiol*, 3: 371-394.

Mor, S., Ravindra, K., Dahiya, R., Chandra, A. (2006). 'Leachate characterization and assessment of groundwater pollution near municipal solid waste landfill site'. *Environ Monit Assess*, 118: 435-456.

Morillo, J. A., Aguilera, M., Ramos-Cormenzana, A., Monteoliva-Sánchez, M. (2006). 'Production of a metal-binding exopolysaccharide by *Paenibacillus jamilae* using two-phase olive-mill waste as fermentation substrate'. *Curr Microbiol*, 53: 189-193.

Mortazavian, A., Azizi, A., Ehsani, M., Razavi, S., Mousavi, S., Sohrabvandi, S., Reinheimer, J. (2008). 'Survival of encapsulated probiotic bacteria in Iranian yogurt

drink (Doogh) after the product exposure to simulated gastrointestinal conditions'. *Milchwissenschaft*, 63: 427-433.

Mosmeri, H., Alaie, E., Shavandi, M., Dastgheib, S. M. M., Tasharrofi, S. (2017). 'Bioremediation of benzene from groundwater by calcium peroxide (CaO2) nanoparticles encapsulated in sodium alginate'. *J TAIWAN INST CHEM E*, 78:299-306.

Mueller, J. G., Lantz, S. E., Ross, D., Colvin, R. J., Middaugh, D. P., Pritchard, P. H. (1993). 'Strategy using bioreactors and specially selected microorganisms for bioremediation of groundwater contaminated with creosote and pentachlorophenol'. *Environ Sci Technol*, 27: 691-698.

Mulligan, C., Yong, R., Gibbs, B. (2001). 'Remediation technologies for metal-contaminated soils and groundwater: an evaluation'. *Eng Geol*, 60: 193-207.

Munataka, M., Kitagawa, S., Yagi, F. (1986). 'Cadmium-113 NMR of cadmium (II) complexes with ligands containing *N*-donor atoms. Dependence of the chemical shift upon the ligand basicity, chelate ring size, counteranion, and cadmium concentration'. *Inorg Chem*, 25:964-970.

Munkelt, D., Grass, G., Nies, D. H. (2004). 'The chromosomally encoded cation diffusion facilitator proteins DmeF and FieF from *Wautersia metallidurans* CH34 are transporters of broad metal specificity'. *JB*,186:8036-8043.

Naddafi, K., Nabizadeh, R., Saeedi, R., Mahvi, A. H., Vaezi, F., Yaghmaeian, K., Ghasri, A., Nazmara, S. (2007). 'Biosorption of lead (II) and cadmium (II) by protonated Sargassum glaucescens biomass in a continuous packed bed column'. *J Hazard Mater*, 147: 785-791.

Naddy, R. B., Cohen, A. S., Stubblefield, W. A. (2015). 'The interactive toxicity of cadmium, copper, and zinc to *Ceriodaphnia dubi*a and rainbow trout (*Oncorhynchus mykiss*)'. *Environ Toxicol Chem*, 34: 809-815.

Nagy, B., Măicăneanu, A., Indolean, C., Mânzatu, C., Silaghi-Dumitrescu, L., Majdik, C. (2014). 'Comparative study of Cd (II) biosorption on cultivated *Agaricus bisporus* and wild *Lactarius piperatus* based biocomposites. Linear and nonlinear equilibrium modelling and kinetics'. *J Taiwan Inst Chem Eng*, 45: 921-929.

Nazina, T., Tourova, T., Poltaraus, A., Novikova, E., Grigoryan, A., Ivanova, A., Lysenko, A., Petrunyaka, V., Osipov, G., Belyaev, S. (2001). 'Taxonomic study of aerobic thermophilic bacilli: descriptions of *Geobacillus subterraneus* gen. nov., sp. nov. and *Geobacillus uzenensis* sp. nov. from petroleum reservoirs and transfer of *Bacillus stearothermophilus*, *Bacillus thermocatenulatus*, *Bacillus thermoleovorans*, *Bacillus kaustophilus*, *Bacillus thermodenitrificans* to *Geobacillus* as the new combinations *G. stearothermophilus*, G. th'. *IntJ Syst Evol Microbiol*, 51:433-446.

Nei M, Kumar S. 2000. Molecular evolution and phylogenetics. Oxford: Oxford University Press.

Neiva, A. M. R., de Carvalho, P. C. S., Antunes, I. M. H. R., dos Santos, A. C. T., da Silva Cabral-Pinto, M. M. (2015). 'Spatial and temporal variability of surface water and groundwater before and after the remediation of a Portuguese uranium mine area'. *Chem Erde Geochemi*, 75: 345-356.

Nanda, M., Kumar, V., Sharma, D. (2019). 'Multimetal tolerance mechanisms in bacteria: The resistance strategies acquired by bacteria that can be exploited to ‘clean-up’heavy metals contaminants from water'. *Aquat Toxicol*, 212: 1-10.

Nies, D. H. (1995) 'The cobalt, zinc, and cadmium efflux system CzcABC from *Alcaligenes eutrophus* functions as a cation-proton antiporter in *Escherichia coli*'. *J Bacteriol*, 177: 2707-2712.

Nies, D. H. (2003). 'Efflux-mediated heavy metal resistance in prokaryotes'. *FEMS Microbiol Rev*, 27: 313-339.

Nies, D. H. (2013). 'RND efflux pumps for metal cations'. Microbial Efflux Pumps: *Curr Res*, 1: 79-121.

Nongkhlaw, M., Kumar, R., Acharya, C., Joshi, S. R. (2012). 'Occurrence of horizontal gene transfer of PIB-type ATPase genes among bacteria isolated from the uranium rich deposit of Domiasiat in North East India'. *PloS one*, 7: e48199.

Nouri, L., Ghodbane, I., Hamdaoui, O., Chiha, M. (2007). 'Batch sorption dynamics and equilibrium for the removal of cadmium ions from aqueous phase using wheat bran'. *J Hazard Mater*, 149: 115-125.

Noordam, R., Young, W. J., Salman, R., Kanters, J. K., van den Berg, M. E., van Heemst, D., Lin, H. J., Barreto, S. M., Biggs, M. L., Biino, G. (2019). 'Effects of calcium, magnesium, and potassium concentrations on ventricular repolarization in unselected individuals'. *J Am Coll Cardiol*, 73: 3118-3131.

Nucifora, G., Chu, L., Misra, T. K., Silver, S. (1989). 'Cadmium resistance from *Staphylococcus aureus* plasmid pI258 *cadA* gene results from a cadmium-efflux ATPase'. *Proc Natl Acad Sci* , 86: 3544-3548.

Okinaka, Y. (1985). 'Standard Potentials in Aqueous Solution '. *M. Dekker*, Bard, AJ

Ollson, C. J., Smith, E., Scheckel, K. G., Betts, A. R., Juhasz, A. L. (2016). 'Assessment of arsenic speciation and bioaccessibility in mine-impacted materials'. *J Hazard Mater*, 313:130-137.

Owojori, O. J., Ademosu, O. T., Jegede, O. O., Fajana, H. O., Kehinde, T. O., Badejo, M. A. (2019). 'Tropical oribatid mites in soil toxicity testing: Optimization of test protocol and the effect of two model chemicals (cadmium and dimethoate) on *Muliercula inexpectata*'. *Chemosphere*, 218: 948-954.

Ozdemir, G., Ceyhan, N., Manav, E. (2005a). 'Utilization in alginate beads for Cu (II) and Ni (II) adsorption of an exopolysaccharide produced by *Chryseomonas luteola* TEM05'. *World J Microbiol Biotechnol*, 21: 163-167.

Ozdemir, G., Ceyhan, N., Manav, E. (2005b). 'Utilization of an exopolysaccharide produced by *Chryseomonas luteola* TEM05 in alginate beads for adsorption of cadmium and cobalt ions'. *Bioresour. Technol*, 96: 1677-1682.

Ozdemir, G., Ceyhan, N., Ozturk, T., Akirmak, F., Cosar, T. (2004). 'Biosorption of chromium (VI), cadmium (II) and copper (II) by *Pantoea* sp. TEM18'. *Chem Eng J*. , 102: 249-253.

Ozdemir, G., Ozturk, T., Ceyhan, N., Isler, R., Cosar, T. (2003). 'Heavy metal biosorption by biomass of *Ochrobactrum anthropi* producing exopolysaccharide in activated sludge'. *Bioresour Technol*, 90: 71-74.

Pagnanelli, F., Viggi, C. C., Toro, L. (2010) 'Isolation and quantification of cadmium removal mechanisms in batch reactors inoculated by sulphate reducing bacteria: biosorption versus bioprecipitation'. *Bioresour Technol*, 101: 2981-2987.

Pakshirajan, K.,Swaminathan, T. (2006). 'Continuous biosorption of Pb, Cu, and Cd by *Phanerochaete chrysosporium* in a packed column reactor'. *Soil Sediment Contam*, 15: 187-197.

Palmer, L. D., Skaar, E. P. (2016). 'Transition metals and virulence in bacteria'. *Annu Rev Genet*, 50:. 67-91.

Pardo, R., Herguedas, M., Barrado, E., Vega, M. (2003). 'Biosorption of cadmium, copper, lead and zinc by inactive biomass of *Pseudomonas putida'*. *Anal Bioanal Chem*, 376: 26-32.

Patel, J., Zhang, Q., McKay, R. M. L., Vincent, R., Xu, Z. (2010). 'Genetic engineering of *Caulobacter crescentus* for removal of cadmium from water' *Appl Biochem Biotechnol*, 160: 232-243.

Pavlaki, M. D., Araújo, M. J., Cardoso, D. N., Silva, A. R. R., Cruz, A., Mendo, S., Soares, A. M., Calado, R., Loureiro, S. (2016). 'Ecotoxicity and genotoxicity of cadmium in different marine trophic levels'. *Environ Pollut*, 215: 203-212.

Pearson, H. B., Comber, S. D., Bungartt, C. B., Worsfold, P., Stockdale, A., Lofts, S. (2018). 'Determination and prediction of zinc speciation in estuaries'. *Environ Sci Technol.*, 52: 14245-14255.

Peptides, P. (2009). 'A Common Highly Conserved Cadmium Detoxification Mechanism from Bacteria to Humans'. *J Biol Chem*, 284: 4936-4943.

Pérez-Rama, M., Alonso, J. A., López, C. H., Vaamonde, E. T. (2002). 'Cadmium removal by living cells of the marine microalga *Tetraselmis suecica'*. *Bioresour. Technol*, 84: 265-270.

Philp, J. C., Atlas, R. M. (2005). 'Bioremediation of contaminated soils and aquifers', Bioremediation. *MBio*:139-236.

PHREEQC, 2017. Database PHREEQC.dat, PHREEQC Interactive Version 3.4.0.12927. Released November 9, 2017. USGS.

Pirt, S. (1967). 'A kinetic study of the mode of growth of surface colonies of bacteria and fungi'. *Microbiology*, 47:181-197.

Polettini, A., Pomi, R., Rolle, E., Ceremigna, D., De Propris, L., Gabellini, M., Tornato, A. (2006). 'A kinetic study of chelant-assisted remediation of contaminated dredged sediment'. *J Hazard Mater*, 137: 1458-1465.

Prapagdee, B., Chanprasert, M., Mongkolsuk, S. (2013). 'Bioaugmentation with cadmium-resistant plant growth-promoting rhizobacteria to assist cadmium phytoextraction by *Helianthus annuus'*. *Chemosphere*, 92: 659-666.

Prasad, B., Kumari, P., Bano, S., Kumari, S. (2014). 'Ground water quality evaluation near mining area and development of heavy metal pollution index'. *Appl Water Sci*, 4: 11-17.

Prasad, M. N. V., Sajwan, K. S., Naidu, R. (2006). Trace elements in the environment: biogeochemistry, biotechnology, and bioremediation. CRC Press.

Podrabsky, J. E., Somero, G. N. (2004). 'Changes in gene expression associated with acclimation to constant temperatures and fluctuating daily temperatures in an annual killifish *Austrofundulus limnaeus*'. *J Exp Biol*, 207: 2237-2254.

Qin, W., Liu, X., Yu, X., Chu, X., Tian, J.,Wu, N. (2017) 'Identification of cadmium resistance and adsorption gene from *Escherichia coli* BL21 (DE3)'. *RSC Adv*, 7: 51460-51465.

Qin, W., Yu, X., Liu, X., Chu, X., Tian, J., Wu, N. (2019). 'Improving Cadmium Resistance in *Escherichia coli* Through Continuous Genome Evolution'. *Front Microbiol*, 10: 278-282.

Raetz, C. R., Whitfield, C. (2002) 'Lipopolysaccharide endotoxins'. *Annu Rev Biochem*, 71: 635-700.

Rader, K. J., Carbonaro, R. F., van Hullebusch, E. D., Baken, S., Delbeke, K. (2019). 'The Fate of Copper Added to Surface Water: Field, Laboratory, and Modeling Studies'. *Environ Toxicol Chem*, 38: 1386–1399.

Raikova, S., Piccini, M., Surman, M. K., Allen, M. J., Chuck, C. J. (2019). 'Making light work of heavy metal contamination: the potential for coupling bioremediation with bioenergy production'. *J Chem Technol Biotechnol*: 94: 3064–3072.

Rajesh, V., Kumar, A. S. K., Rajesh, N. (2014) 'Biosorption of cadmium using a novel bacterium isolated from an electronic industry effluent'. *Chem Eng J*, 235: 176-205.

Rajpert, L., Schäffer, A., Lenz, M. (2018). 'Redox-stat bioreactors for elucidating mobilisation mechanisms of trace elements: an example of As-contaminated mining soils'. *Appl Microbiol Biotechnol*, 102:7635-7641.

Ramachandran, A., Krishnamurthy, R., Jayaprakash, M., Shanmugasundharam, A. (2018). 'Environmental impact assessment of surface water and groundwater quality due to flood hazard in Adyar River Bank'. *Acta Ecologica Sinica*, 13:23-32.

Ramos, O. E. R., Rötting, T. S., French, M., Sracek, O., Bundschuh, J., Quintanilla, J., Bhattacharya, P. (2014). 'Geochemical processes controlling mobilization of arsenic and trace elements in shallow aquifers and surface waters in the Antequera and Poopó mining regions, Bolivian Altiplano'. *J Hydrol*, 518: 421-433.

Ramos-Zúñiga, J., Gallardo, S., Martínez-Bussenius, C., Norambuena, R., Navarro, C. A., Paradela, A., Jerez, C. A. (2019). 'Response of the biomining *Acidithiobacillus ferrooxidans* to high cadmium concentrations'. *J Proteomics*, 198:132-144.

Rangsayatorn, N., Pokethitiyook, P., Upatham, E., Lanza, G. (2004) 'Cadmium biosorption by cells of *Spirulina platensis* TISTR 8217 immobilized in alginate and silica gel'. *Envi. I*, 30: 57-63.

Rao, K. S., Anand, S.,Venkateswarlu, P. (2010). 'Adsorption of cadmium (II) ions from aqueous solution by *Tectona grandis* LF (teak leaves powder)'. *Bio Resources*, 5: 438-454.

Rao, M. M., Ramesh, A., Rao, G. P. C., Seshaiah, K. (2006). 'Removal of copper and cadmium from the aqueous solutions by activated carbon derived from *Ceiba pentandra* hulls'. *J Hazard Mater*, 129: 123-129.

Rasulov, B. A., Yili, A., Aisa, H. A. (2013). 'Biosorption of metal ions by exopolysaccharide produced by *Azotobacter chroococcum* XU1'. *J Environ Prot* , 4: 989-993.

Ratnayake, K., Joyce, D. C., Webb, R. I. (2012) 'A convenient sample preparation protocol for scanning electron microscope examination of xylem-occluding bacterial biofilm on cut flowers and foliage'. *Sci Hort*, 140: 12-20.

Raungsomboon, S., Chidthaisong, A., Bunnag, B., Inthorn, D., Harvey, N. W. (2006). 'Production, composition and Pb^{2+} adsorption characteristics of capsular polysaccharides extracted from a cyanobacterium *Gloeocapsa gelatinosa*'. *Water Res*, 40: 3759-3766

Rensing, C., Mitra, B., Rosen, B. P. (1997). 'Insertional inactivation of dsbA produces sensitivity to cadmium and zinc in *Escherichia coli*'. *J Bacteriol*, 179:: 2769-2771.

Rensing C., Mitra B. (2007). Zinc, Cadmium, and Lead Resistance and Homeostasis. *In*: Nies D.H., Silver S. (*eds*) Molecular Microbiology of Heavy Metals. Microbiology Monographs, vol 6. Springer, Berlin, Heidelberg: 321-341.

Rindala, S., Jean-Ralph, Z., Carbonnelle, E., Lescat, M. (2019). 'Aerobic bacteria as *Escherichia coli* can survive in ESwabTM medium after a 3 month-freezing at-80° C but not after multiple thawing'. *bioRxiv*:537647.

Rinklebe, J., Shaheen, S. M., Yu, K. (2016). 'Release of As, Ba, Cd, Cu, Pb, and Sr under pre-definite redox conditions in different rice paddy soils originating from the USA and Asia'. *Geoderma*, 270: 21-32.

Rodriguez, R. R., Basta, N. T., Casteel, S. W., Pace, L. W. (1999) 'An in vitro gastrointestinal method to estimate bioavailable arsenic in contaminated soils and solid media'. *Environ. Sci. Technol*. 33: 642-649.

Romaniuk, J. A., Cegelski, L. (2015). 'Bacterial cell wall composition and the influence of antibiotics by cell-wall and whole-cell NMR'. *Philos Trans R Soc Lond B Biol Sci*, 370:201-500.

Romera, E., González, F., Ballester, A., Blázquez, M., Munoz, J. (2007). 'Comparative study of biosorption of heavy metals using different types of algae'. *Bioresour Technol*, 98: 3344-3353.

Rösner, U. (1998). 'Effects of historical mining activities on surface water and groundwater-an example from northwest Arizona'. *EnviroGeol*, 33: 224-230.

Ruangsomboon, S., Chidthaisong, A., Bunnag, B., Inthorn, D., Harvey, N. W. (2007). 'Lead (Pb^{2+}) adsorption characteristics and sugar composition of capsular polysaccharides of cyanobacterium *Calothrix marchica'*. *Songklanakarin J Sci Technol*, 29: 529-541.

Ruiz-Lozano, J. M. and Azcón, R. (2011). '*Brevibacillus*, arbuscular mycorrhizae and remediation of metal toxicity in agricultural soils'. *Endospore-forming Soil Bacteria.* Springer: 235-258.

Rumble, J. R. (2018) 'Solubility product constants of inorganic salts '. *CRC Handbook of Chemistry and Physics*, 99 th ed. Taylor & Francis Group, 5-208-209.

Sakimoto, K. K., Wong, A. B., Yang, P. (2016). 'Self-photosensitization of nonphotosynthetic bacteria for solar-to-chemical production'. *Science*, 351: 74-77.

Saha, N., Saha, L., Ji, -n., Zjao, J., Gregan, F., Ali A., Sajadi, A., Song, B., Sigel, H. 1996. Stability of metal ion complexes formed with methyl phosphate and hydrogen phosphate. *J Biol Inorg Chem*, 1: 231-238.

Salvadori, M. R., Ando, R. A., do Nascimento, C. A. O., Corrêa, B. (2014). 'Intracellular biosynthesis and removal of copper nanoparticles by dead biomass of yeast isolated from the wastewater of a mine in the Brazilian Amazonia'. *PloS one*, 9:e87968.

Sambrook, J., Russell, D. W. (2001) 'Molecular cloning: a laboratory manual. '.Cold Spring Harbor Laboratory Press, Cold Spring Harbor, New York.

Sandrin, T. R., Maier, R. M. (2002). 'Effect of pH on cadmium toxicity, speciation, and accumulation during naphthalene biodegradation'. *Int J Toxicol*, 21: 2075-2079.

Sartape, A. S., Mandhare, A. M., Salvi, P. P., Pawar, D. K., Kolekar, S. S. (2013). 'Kinetic and equilibrium studies of the adsorption of Cd (II) from aqueous solutions by wood apple shell activated carbon'. *Desalination Water Treat*, 51: 4638-4650.

Satarug, S., Baker, J. R., Reilly, P. E., Moore, M. R., Williams, D. J. (2002). 'Cadmium levels in the lung, liver, kidney cortex, and urine samples from Australians without occupational exposure to metals'. *Arch Environ Health*, 57:69-77.

Satarug, S., Garrett, S. H., Sens, M. A., Sens, D. A. (2009). 'Cadmium, environmental exposure, and health outcomes'. *Environ Health Perspect*, 118: 182-190.

Schirawski, J., Hagens, W., Fitzgerald, G. F., van Sinderen, D. (2002). 'Molecular characterization of cadmium resistance in *Streptococcus thermophilus* strain 4134: an example of lateral gene transfer'. *Appl Environ Microbiol.*, 68: 5508-5516.

Schmidt, T. Schlegel, H. G. 1994. Combined nickel-cobalt-cadmium resistance encoded by the ncc locus of *Alcaligenes xylosoxidans* 31A. *JB*,176: 7045-7054.

Scott, J., Palmer, S. (1990). 'Sites of cadmiun uptake in bacteria used for biosorption'. *Appl Microbiol Biotechnol*, 33: 221-225.

Scoullos, M. J., Vonkeman, G. H., Thornton, I., Makuch, Z. (2012). *Mercury—cadmium—lead handbook for sustainable heavy metals policy and regulation.* vol. 31. Springer Science & Business Media.

Sepa, U., Oswer, D. (2001). *Groundwater pump and treat systems: Summary of selected cost and performance information at superfund-financed sites.* EPA 542-R-01-021b.

Sharafi, K., Nodehi, R. N., Mahvi, A. H., Pirsaheb, M., Nazmara, S., Mahmoudi, B., Yunesian, M. (2019). 'Bioaccessibility analysis of toxic metals in consumed rice through an in vitro human digestion model–Comparison of calculated human health risk from raw, cooked and digested rice'. *Food Chem*, 299:125126.

Shahryari T, Mostafavi A., Afzali D., Rahmati M., (2019). Enhancing cadmium removal by low-cost nanocomposite adsorbents from aqueous solutions; a continuous system, Compos. *Part B Eng*. 173, 106963.

Sharma, J. (2019). 'Advantages and Limitations of In Situ Methods of Bioremediation'. *Recent Adv Biol Med*, 5:10941-10952.

Shen, Q., Yang, R., Hua, X., Ye, F., Zhang, W., Zhao, W. (2011). 'Gelatin-templated biomimetic calcification for β-galactosidase immobilization'. *Process Biochem*, 46: 1565-1571.

Sheng, Y., Wang, Y., Yang, X., Zhang, B., He, X., Xu, W., Huang, K. (2016). 'Cadmium tolerant characteristic of a newly isolated *Lactococcus lactis subsp. lactis*'. *Environ Toxicol Pharmacol* 48:183-190.

Shepherd, K. A., Ellis, P. A., Rivett, M. O. (2006). 'Integrated understanding of urban land, groundwater, baseflow and surface-water quality—The City of Birmingham, UK'. *Sci Total Environ*, 360: 180-195.

Shi, X., Zhou, G., Liao, S., Shan, S., Wang, G., Guo, Z. (2018). 'Immobilization of cadmium by immobilized *Alishewanella* sp. WH16-1 with alginate-lotus seed pods in pot experiments of Cd-contaminated paddy soil'. *J Hazard Mater*, 357:431-439.

Shim, J., Kumar, M., Mukherjee, S., Goswami, R. (2019). 'Sustainable removal of pernicious arsenic and cadmium by a novel composite of MnO_2 impregnated alginate beads: A cost-effective approach for wastewater treatment'. *J Environ Manage*, 234: 8-20.

Shriver, D.F; Atkins, P.W. (1999). *Inorganic Chemistry* (3rd ed.). Oxford University Press.

Sims, D. B., Hudson, A. C., Keller, J. E., Konstantinos, V. I., Konstantinos, M. P. (2017) .'Trace Element Scavenging in Dry Wash Surficial Sediments in an Arid Region of Southern Nevada, USA'. *Mine Water Environt*, 36: 124-132.

Siripornadulsil, S., Siripornadulsil, W. (2013). 'Cadmium-tolerant bacteria reduce the uptake of cadmium in rice: potential for microbial bioremediation'.*Ecotoxicol Environ Saf*, 94: 94-103.

Siswoyo, E., Qoniah, I., Lestari, P., Fajri, J. A., Sani, R. A., Sari, D. G., Boving, T. (2019). 'Development of a floating adsorbent for cadmium derived from modified drinking water treatment plant sludge'. *Environ Technol. Inno*, 14:32-43.

Sjöstedt, C. S., Gustafsson, J. P., Köhler, S. J. (2010). 'Chemical equilibrium modeling of organic acids, pH, aluminum, and iron in Swedish surface waters'. *Environ Sci Technol*, 44: 8587-8593.

Sochor, J., Zitka, O., Hynek, D., Jilkova, E., Krejcova, L., Trnkova, L., Adam, V., Hubalek, J., Kynicky, J., Vrba, R. (2011). 'Bio-sensing of cadmium (II) ions using *Staphylococcus aureus'*. *Sensors*, 11:10638-10663.

Soto-Hidalgo, K. T., Cabrera, C. R. (2018). 'Nanoscale Zero Valent Iron for Environmental Cadmium Metal Treatment', Green Chemistry. InTech.

Sousa, C., Cebolla, A., de Lorenzo, V. (1996). 'Enhanced metalloadsorption of bacterial cells displaying poly-His peptides'. *Nat Biotechnol*, 14: 1017-1020.

Souza, L. A., Souza, T. L., Santana, F. B., Araujo, R. G., Teixeira, L. S., Santos, D. C., Korn, M. G. A. (2018). 'Determination and in vitro bioaccessibility evaluation of Ca, Cu, Fe, K, Mg, Mn, Mo, Na, P and Zn in linseed and sesame'. *Microchem J*, 137: 8-14.

Stafford, S. J., Humphreys, D. P., Lund, P. A. (1999). 'Mutations in dsbA and dsbB, but not dsbC, lead to an enhanced sensitivity of *Escherichia coli* to Hg^{2+} and Cd^{2+}'. *FEMS Microbiol Lett*, 174: 179-204.

Stähler, F. N., Odenbreit, S., Haas, R., Wilrich, J., Van Vliet, A. H., Kusters, J. G., Kist, M., Bereswill, S. (2006). 'The novel Helicobacter pylori CznABC metal efflux pump is required for cadmium, zinc, and nickel resistance, urease modulation, and gastric colonization'. *Infect Immun*, 74: 3845-3852.

Stohs, S. J., Bagchi, D. (1995). 'Oxidative mechanisms in the toxicity of metal ions'. *Free Radic Biol Med*, 18: 321-336.

Subashchandrabose, S. R., Megharaj, M., Venkateswarlu, K., Naidu, R. (2015). 'Interaction effects of polycyclic aromatic hydrocarbons and heavy metals on a soil microalga, *Chlorococcum* sp. MM11'. *Environ Sci Pollut Res*, 22: 8876-8889.

Sun, G., Shi, W. (1998). 'Sunflower stalks as adsorbents for the removal of metal ions from wastewater'. *Ind Eng Chem Res*, 37 (4): 1324-1328.

Sun, J., Yin, L., Huang, K., Li, X., Ai, X., Huang, Y., Yin, Y., Liu, J. (2018). 'Removal of cadmium from a citrate-bearing solution by floatable microsized garlic peel'. *RSC Advances*, 8: 28284-28292.

Sutton, P.,Mishra, P. (1994). 'Activated carbon based biological fluidized beds for contaminated water and wastewater treatment: a state-of-the-art review'. *Wat Sci Tech*, 29: 309-317.

Suzuki, H., Koyanagi, T., Izuka, S., Onishi, A., Kumagai, H. (2005). 'The yliA,-B,-C, and-D genes of *Escherichia coli* K-12 encode a novel glutathione importer with an ATP-binding cassette'. *J Bacteriol*, 187: 5861-5867.

Takebe, F., Hirota, K., Nodasaka, Y., Yumoto, I. (2012) *'Brevibacillus nitrificans* sp. nov., a nitrifying bacterium isolated from a microbiological agent for enhancing microbial digestion in sewage treatment tanks'. *Int J Sys. Evol Microbiol*, 62: 2121-2126.

Tang, W., Xia, Q., Shan, B., Ng, J. C. (2018). 'Relationship of bioaccessibility and fractionation of cadmium in long-term spiked soils for health risk assessment based on four in vitro gastrointestinal simulation models'. *Sci Total Environ*, 631:1582-1589.

Tao, H. C., Li, P. S., Liu, Q. S., Su, J., Qiu, G. Y., Li, Z. G. (2016). 'Surface-engineered *Saccharomyces cerevisiae* cells displaying redesigned CadR for enhancement of adsorption of cadmium (II)'. *J Chem Technol Bio*, 91: 1889-2095.

Taty-Costodes, V. C., Fauduet, H., Porte, C., Delacroix, A. (2003). 'Removal of Cd (II) and Pb (II) ions, from aqueous solutions, by adsorption onto sawdust of Pinus sylvestris'. *J Hazard Mater*, 105: 121-142.

Taudte, N., Grass, G. (2010). 'Point mutations change specificity and kinetics of metal uptake by ZupT from *Escherichia coli*'. *Biometals*, 23: 643-656.

Tchounwou, P. B., Yedjou, C. G., Patlolla, A. K., Sutton, D. J. (2012). 'Heavy metal toxicity and the environment', *Mol Clin Env toxic.* Springer, 12: 33-164.

Tedd, K., Coxon, C., Misstear, B., Daly, D., Craig, M., Mannix, A., Williams, T. H. (2017). Assessing and Developing Natural Background Levels for Chemical Parameters in Irish Groundwater, Vol. 183. Environmental Protection Agency, Waxford, Ireland.

Thomas, P. (2006) 'Isolation of an ethanol-tolerant endospore-forming Gram-negative *Brevibacillus* sp. as a covert contaminant in grape tissue cultures'. *J Appl Microbiol*, 101: 764-774.

Tianzi, Y., Weimin, Z. (2019). 'Effects of Ionic strength, Inorganic Ions and Humic acids on U (VI) removal by HAP modified Quartz Sand'. 2019 6th International Conference on Machinery, Mechanics, Materials, and Computer Engineering (MMMCE 2019), 830-836.

Trzcinka-Ochocka, M., Jakubowski, M., Razniewska, G., Halatek, T., Gazewski, A. (2004). 'The effects of environmental cadmium exposure on kidney function: the possible influence of age'. *Environ Res*, 95:143-150.

Tsai, K.-J., Linet, A. L. (1993). 'Formation of a phosphorylated enzyme intermediate by the cadA Cd^{2+}-ATPase'. *Arch Biochem Biophys*, 305: 267-270

Tsai, K.-J., Yoon, K. P., Lynn, A. R. (1992). 'ATP-dependent cadmium transport by the *cadA* cadmium resistance determinant in everted membrane vesicles of *Bacillus subtilis*'. *JB*, 174: 116-121.

Tuovinen, O., Kelly, D., (1973). Studies on the growth of *Thiobacillus ferrooxidans*. I. Use of membrane filters and ferrous iron agar to determine viable numbers, and comparison with 14 CO_2 -fixation and iron oxidation as measures of growth. *Archiv für Mikrobiologie*, 88, 285-98.

Turner, A. (2019) 'Cadmium pigments in consumer products and their health risks'. *Sci Total Environ*, 657: 1409-1414.

Twarakavi, N. K., Kaluarachchi, J. J. (2005). 'Aquifer vulnerability assessment to heavy metals using ordinal logistic regression'. *Groundwater*, 43: 200-214.

United States Environmental Protection Agency (US EPA), (1999). Toxicity characteristics leaching procedure, Federal Register 55, 11798–11877.

United States Environmental Protection Agency (US EPA). (2018). Advancing Sustainable Materials Management: 2015 Fact Sheet. EPA530F180047.

United States Environmental Protection Agency (US EPA). (2018). Wastes | EPA's Report on the Environment (ROE). What are the trends in wastes and their effects on human health and the environment? https://www.epa.gov/report-environment/wastes.

UK Groundwater Forum 2011. “Groundwater Basics: Why is Groundwater Important?” [Online] Available at:

http://www.groundwateruk.org/Why-is-GroundwaterImportant.aspx Accessed on 3/02/2019.

United States Environmental Protection Agency (US EPA). (2011). Edition of the drinking water standards and health advisories. Washington, DC: U.S. Environmental Protection Agency, Office of Water. EPA822R06013. PB2007101258.

United Nations Environment Programme (UNEP). (2017). 'Global mercury supply, trade and demand. Chemicals and Health Branch. Geneva, Switzerland'.

US Geological Survey (US GS). 2019. Refinery production of cadmium in selected countries between 2013 and 2017 (in metric tons). [Online] Available at: https://www.statista.com/statistics/264983/production-of-cadmium/ Accessed on 6/02/2019.

US Geological Survey (US GS). 2011. “Where is the Earth’s Water Located?” [Online] Available at: http://ga.water.usgs.gov/edu/earthwherewater.html Accessed on13/04/2011 Accessed on3/02/2019.

Vaessen, V., Brentführer, R. (2014). 'Integration of groundwater management: into transboundary basin organizations in Africa'. https://cgspace.cgiar.org/bitstream/handle/10568/77070/00_Training_Manual_Intro_en.pdf?sequence=1.

Valdez, C., Perengüez, Y., Mátyás, B., Guevara, M. F. (2018). 'Analysis of removal of cadmium by action of immobilized *Chlorella* sp. micro-algae in alginate beads'. *F1000Research*, 7

Valencia, E. Y., Braz, V. S., Guzzo, C., Marques, M. V. (2013). 'Two RND proteins involved in heavy metal efflux in Caulobacter crescentus belong to separate clusters within proteobacteria'. *BMC microbiol*, 13: 79-84.

van der Lelie, D., Springael, D., Römling, U., Ahmed, N., Mergeay, M. (1999). 'Identification of a gene cluster, *czr*, involved in cadmium and zinc resistance in *Pseudomonas aeruginosa'*. *Gene*, 238: 417-425.

Van Nguyen, D., Ho, N. M., Hoang, K. D., Le, T. V. & Le, V. H. 2020. 'An investigation on treatment of groundwater with cold plasma for domestic water supply'. *Groundw Sustain Dev*, 10:100309.

Vilensky, M. Y., Berkowitz, B., Warshawsky, A. (2002). 'In situ remediation of groundwater contaminated by heavy-and transition-metal ions by selective ion-exchange methods'. *Environ Sci Technol*, 36: 1851-1855.

Vassilis, I. J. (2010). 'Ion exchange and adsorption fixed bed operations for wastewater treatment-Part I: modeling fundamentals and hydraulics analysis'. *JESR,* 16: 29-41.

Velásquez, L., Dussan, J. (2009). 'Biosorption and bioaccumulation of heavy metals on dead and living biomass of *Bacillus sphaericus'*. *J Hazard Mater*, 167: 713-716.

Veneu, D. M., Pino, G. A., Torem, M. L., Saint'Pierre, T. D. (2012). 'Biosorptive removal of cadmium from aqueous solutions using a *Streptomyces lunalinharesii* strain'. *Min Eng*, 29:112-120.

Veneu, D. M., Schneider, C. L., de Mello Monte, M. B., Cunha, O. G. C., Yokoyama, L. (2017). 'Cadmium Removal by Bioclastic Granules (*Lithothamnium calcareum*): Batch and Fixed-Bed Column Systems Sorption Studies'. *Environ Technol*, 4: 1-43.

Vieira, R. H.,Volesky, B. (2000). 'Biosorption: a solution to pollution?'. *In microbiol*, 3: 17-24.

Vinci A, Zoli L, Galizia P, Kütemeyer M, Koch D, Sciti D. Reactive melt infiltration of carbon fibre reinforced ZrB2/B composites with Zr2Cu. Compos. Part A Appl. Sci. Manuf. 2020; 137 (105973): 1-8.

Vijayaraghavan, K., Balasubramanian, R. (2015). 'Is biosorption suitable for decontamination of metal-bearing wastewaters? A critical review on the state-of-the-art of biosorption processes and future directions'. *J Environ Manage*, 160: 283-296.

Vos, P., Garrity, G., Jones, D., Krieg, N. R., Ludwig, W., Rainey, F. A., Schleifer, K.-H., Whitman, W. (2011) *Bergey's Manual of Systematic Bacteriology: Volume 3: The Firmicutes.* vol. 3. Springer Science and Business Media.

Waalkes, M. P., Klaassen, C. D. (1985). 'Concentration of metallothionein in major organs of rats after administration of various metals'. *Fundam Appl Toxicol*, 5: 473-477.

Waisberg, M., Joseph, P., Hale, B., Beyersmann, D. (2003). 'Molecular and cellular mechanisms of cadmium carcinogenesis'. *Toxicology*. 192: 95-117.

Wan, J., Meng, D., Long, T., Ying, R., Ye, M., Zhang, S., Li, Q., Zhou, Y., Lin, Y. (2015). 'Simultaneous removal of lindane, lead and cadmium from soils by rhamnolipids combined with citric acid'. *PloS one*, 10: e0129978.

Wang, F. Y., Wang, H., Ma, J. W. (2010). 'Adsorption of cadmium (II) ions from aqueous solution by a new low-cost adsorbent—Bamboo charcoal'. *J Hazard Mater*, 177: 300-306.

Wang, M.-R., Yang, W., Zhao, L., Li, J.-W., Liu, K., Yu, J.-W., Wu, Y.-F., Wang, Q.-C. (2018) 'Cryopreservation of virus: a novel biotechnology for long-term preservation of virus in shoot tips'. *Plant Methods*, 14: 47-53.

Wang, B., Wan, Y., Zheng, Y., Lee, X., Liu, T., Yu, Z., Huang, J., Ok, Y. S., Chen, J., Gao, B. (2019). 'Alginate-based composites for environmental applications: a critical review'. *Crit Rev Environ Sci Technol*, 49: 318-356.

Wawrik, B., Kerkhof, L., Kukor, J., & Zylstra, G. (2005). Effect of different carbon sources on community composition of bacterial enrichments from soil. *Appl Environ Microbiol*, *71*(11), 6776–6783.

Wu, J., Kamal, N., Hao, H., Qian, C., Liu, Z., Shao, Y., Zhong, X. & Xu, B. (2019) 'Endophytic *Bacillus megaterium* BM18-2 mutated for cadmium accumulation and improving plant growth in hybrid *Pennisetum*'. *Biotechnol Rep*, 24. e00374.

World Health Organization (WHO). (2011). 'Cadmium in Drinking-water Background document for development of WHO Guidelines for Drinking-water Quality

World Health Organization (WHO). (2008). Air quality and health — Fact sheet no 313 — Updated August 2008 (http://www.WHO.int/mediacentre/factsheets/fs313/en/), accessed 9 January 2019.

World Health Organisation International Agency for Research on Cancer (WHO IARC). (2004). IARC Monographs on the Evaluation of Carinogenic Risks to Humans, vol. 84,

William, S., Feil, H., Copeland, A. (2012). 'Bacterial genomic DNA isolation using CTAB'. *Sigma*, 50: 6876-6881.

Wilkin, R. T. (2007). Cadmium. In: Monitored Natural Attenuation of Inorganic Contaminants in Ground Water, Volume 2, Assessment for Non-Radionuclides Including Arsenic, Cadmium, Chromium, Copper, Lead, Nickel, Nitrate, Perchlorate, and Selenium *In*: R. G. Ford, R. T. Wilkin, R. W. Puls, (*eds*.), Vol. 2: 1-9. Environmental Protection Agency, Ada, Oklahoma.

Winkelmann, G. (2002) 'Microbial siderophore-mediated transport' *Biochem Soc Trans*. 30: 691-6.

Wiegand, I., Hilpert, K., Hancock, R. E. (2008). 'Agar and broth dilution methods to determine the minimal inhibitory concentration (MIC) of antimicrobial substances'. *Nat Protoc*, 3:163-192.

Wittman, R, Hu H. (2002). Cadmium exposure and nephropathy in a 28-year-old female metals worker. *Environ Health Perspect*,110:1261-1226.

Wood, J. M., Wang, H.-K. (1983). 'Microbial resistance to heavy metals'. *Environ Sci Technol*, 17: 582A-590A.

Wragg, J. (2009) 'BGS guidance material 102'. *Ironstone Soil, Certificate of Analysis:* British geological survey, IR/09/006.

Wang, L. K., Vaccari, D. A., Li, Y., Shammas, N. K. (2005). 'Chemical precipitation', Physicochemical treatment processes. Springer: 141-197.

Wu, C. H., Wood, T. K., Mulchandani, A., Chen, W. (2006). 'Engineering plant-microbe symbiosis for rhizoremediation of heavy metals'. *Appl Environ Microbiol*, 72: 1129-1134.

Wu, Y., Guo, Z., Zhang, W., Tan, Q., Zhang, L., Ge, X., Chen, M. (2016). 'Quantitative relationship between cadmium uptake and the kinetics of phytochelatin induction by cadmium in a marine diatom'. *Sci Rep*, 6: 35935.

Wu, H., Wu, Q., Wu, G., Gu, Q., Wei, L. (2016) 'Cd-resistant strains of *B. cereus* S5 with endurance capacity and their capacities for cadmium removal from cadmium-polluted water'. *PloS one*, 11: e0151479.

Wu, J., Kamal, N., Hao, H., Liu, Z., Qian, C., Shao, Y., Zhong, X., Xu, B. (2019) *'Endophytic Bacillus megaterium* BM18-2 mutated for cadmium accumulation and improving plant growth in Hybrid Pennisetum'. *Biotechnol.Rep*:e00374.

Xia, Q., Peng, C., Lamb, D., Mallavarapu, M., Naidu, R., Ng, J. C. (2016). 'Bioaccessibility of arsenic and cadmium assessed for in vitro bioaccessibility in spiked soils and their interaction during the Unified BARGE Method (UBM) extraction'. *Chemosphere*. 147:444-450.

Xie, J.-J., Yuan, C.-G., Xie, J., Shen, Y.-W., He, K.-Q., Zhang, K.-G. (2019). 'Speciation and bioaccessibility of heavy metals in PM2. 5 in Baoding city, China'. *Environ. Pollut*, 252: 336-343.

Xing, W., Zhao, Q., Scheckel, K. G., Zheng, L., Li, L. (2019). 'Inhalation bioaccessibility of Cd, Cu, Pb and Zn and speciation of Pb in particulate matter fractions from areas with different pollution characteristics in Henan Province, China'. *Ecotoxicol Environ Saf*, 175:192-200.

Xiao, X., Han, X., Wang, L.-G., Long, F., Ma, X.-L., Xu, C.-C., Ma, X.-B., Wang, C.-X. & Liu, Z.-Y. (2020) 'Anaerobically photoreductive degradation by CdS nanocrystal: Biofabrication process and bioelectron-driven reaction coupled with *Shewanella oneidensis* MR-1'. *Biochem Eng J*, 154:107466.

Xu, C., He, S., Liu, Y., Zhang, W., Lu, D. (2017) 'Bioadsorption and biostabilization of cadmium by *Enterobacter cloacae* TU'. *Chemosphere*,173: 622-629.

Xu, J., Zhu, L.-Y., Shen, H., Zhang, H.-M., Jia, X.-B., Yan, R., Li, S.-L., Xu, H.-X. (2012) 'A critical view on spike recovery for accuracy evaluation of analytical method for medicinal herbs'. *Journal of pharm bio anal*, 62: 210-215.

Xu, L., Cui, H., Zheng, X., Zhu, Z., Liang, J., Zhou, J. (2016) 'Immobilization of copper and cadmium by hydroxyapatite combined with phytoextraction and changes in microbial community structure in a smelter-impacted soil'. *RSC Advances*, 6:103955-103964.

Yan, G. and Viraraghavan, T. (2003). 'Heavy-metal removal from aqueous solution by fungus *Mucor rouxii*'. *Water Res*, 37: 4486-4496.

Yang, C.-F., Liu, S.-H., Su, Y.-M., Chen, Y.-R., Lin, C.-W., Lin, K.-L. (2019a) 'Bioremediation capability evaluation of benzene and sulfolane contaminated groundwater: Determination of bioremediation parameters'. *Sci Total Environ*, 648: 811-818.

Yang, L., Wen, T., Wang, L., Miki, T., Bai, H., Lu, X., Yu, H., Nagasaka, T. (2019b) 'The stability of the compounds formed in the process of removal Pb (II), Cu (II) and Cd (II) by steelmaking slag in an acidic aqueous solution'. *J Environ Manage*. 231: 41-48.

Yee, N., Fowle, D. A., Ferris, F. G. (2004). 'A Donnan potential model for metal sorption onto *Bacillus subtilis*'. *Geochim Cosmochim Acta*, 68: 3657-3664.

Yilmaz, E. I., Ensari, N. (2005) 'Cadmium biosorption by *Bacillus circulans* strain EB1'. *World J Microbiol Biotechnol*, 21: 777-779.

Yu, G., Saha, U., Kozak, L., Huang, P. (2006). 'Kinetics of cadmium adsorption on aluminum precipitation products formed under the influence of tannate'. *Geochim Cosmochim Acta*, 70: 5134-5145.

Yu, Z., Huang, J., Hu, L., Zhang, W., Lo, I. M. (2019). 'Effects of geochemical conditions, surface modification, and arsenic (As) loadings on As release from As-loaded nano zero-valent iron in simulated groundwater'. *Water Sci Technol*, 5: 28-38.

Yuan, X.-w., Xie, X.-h., Fan, F.-x., Zhu, W.-x., Na, L., Liu, J.-s. (2013) 'Effects of mutation on a new strain *Leptospirillum ferriphilum* YXW and bioleaching of gold ore'. *T Nonferr Metal Soc*, 23: 2751-2758.

Zazzali, I., Calvo, T. R. A., Ruíz-Henestrosa, V. M. P., Santagapita, P. R., Perullini, M. (2019) 'Effects of pH, extrusion tip size and storage protocol on the structural properties of Ca (II)-alginate beads'. *Carbohydrate Polymers*, 206:749-756.

Zajkoska, P., Rebroš, M., Rosenberg, M. (2013). 'Biocatalysis with immobilized Escherichia coli'. *Appl Microbiol Biotechnol*, 97: 1441-1455.

Zhai, Q., Xiao, Y., Zhao, J., Tian, F., Zhang, H., Narbad, A., Chen, W. (2017) 'Identification of key proteins and pathways in cadmium tolerance of *Lactobacillus plantarum* strains by proteomic analysis'. *Sci Rep*, 7:1182-1187.

Zhang, C., Tao, Y., Li, S., Ke, T., Wang, P., Wei, S., Chen, L. (2019a). 'Bioremediation of cadmium-trichlorfon co-contaminated soil by Indian mustard (*Brassica juncea*) associated with the trichlorfon-degrading microbe *Aspergillus sydowii*: Related physiological responses and soil enzyme activities'.*Ecotoxicol Environ Saf*, 1097:1-8.

Zhang, J., Li, Q., Zeng, Y., Zhang, J., Lu, G., Dang, Z., Guo, C. (2019b). 'Bioaccumulation and distribution of cadmium by *Burkholderia cepacia* GYP1 under oligotrophic condition and mechanism analysis at proteome level'. *Ecotoxicol Environ Saf*, 176: 162-169.

Zhang, W., Cheng, J.-H., Xian, Q.-S., Cui, J.-F., Tang, X.-Y., Wang, G.-X. (2019). 'Dynamics and sources of colloids in shallow groundwater in lowland wells and fracture flow in sloping farmland'. *Water Res*, 156: 252-263.

Zhao, X., Wang, X., Liu, B., Xie, G., Xing, D. (2018) 'Characterization of manganese oxidation by *Brevibacillus* at different ecological conditions'. *Chemosphere*, 205:553-558.

Zhdanov, S. I. (1985). 'Sulfur, Selenium, Tellurium, and Polonium', *In*: AJ Bard, R. Parsons and J. Jordan (eds.) Standard potentials in aqueous solution, Dekker, New York:93-126.

Zheng, L., Dang, Z., Yi, X., Zhang, H. (2010). 'Equilibrium and kinetic studies of adsorption of Cd (II) from aqueous solution using modified corn stalk'. *J Hazard Mater*, 176: 650-656.

Zheng, L., Peng, D., Meng, P. (2019). 'Corncob-supported aluminium-manganese binary oxide composite enhanced removal of cadmium ions'. *Colloids Surf A Physicochem Eng Asp*, 561:109-119.

Zheng, L., Yang, Y., Meng, P., Peng, D. (2019). 'Absorption of cadmium (II) via sulfur-chelating based cellulose: Characterization, isotherm models and their error analysis'. *Carbohydr Polym*, 209:38-50.

Żur, J., Wojcieszyńska, D., Guzik, U. (2016). 'Metabolic responses of bacterial cells to immobilization'. *Molecules*, 21: 958.

Zhng, X., Chen, L., Chen, M., Chen, J., Li, X. (2019). 'Functional metagenomics to mine soil microbiome for novel cadmium resistance genetic determinants'. *Pedosphere*, 29: 298-310.

Zhou, W., Wang, J., Shen, B., Hou, W., Zhang, Y. (2009). 'Biosorption of copper (II) and cadmium (II) by a novel exopolysaccharide secreted from deep-sea mesophilic bacterium'. *Colloids Surf B*, 72: 295-302.

Zhou, G., Yang, H., Zhou, H., Wang, C., Fu, F., Yu, Y., Lu, X., Tian, Y. (2016). 'Complete genome sequence of the *Streptomyces* sp. strain CdTB01, a bacterium tolerant to cadmium'*. J Biotechnol*, 229: 42-43

Ziagova, M., Dimitriadis, G., Aslanidou, D., Papaioannou, X., Tzannetaki, E. L., Liakopoulou-Kyriakides, M. (2007). 'Comparative study of Cd (II) and Cr (VI) biosorption on *Staphylococcus xylosus* and *Pseudomonas* sp. in single and binary mixtures'. *Bioresour Technol*, 98: 2859-2865.

Zou, A.-M., Chen, M.-L., Shu, Y., Yang, M., Wang, J.-H. (2007). 'Biological cell-sorption for separation/preconcentration of ultra-trace cadmium in a sequential injection system with detection by electrothermal atomic absorption spectrometry'. *J Anal At Spectrom*, 22: 39.